

Proteome analyses for the characterization of
the ADAM17^{ex/ex} hypomorphic mouse model



DISSERTATION

zur Erlangung des akademischen Grades
Doctor rerum naturalium
der Mathematisch-Naturwissenschaftlichen Fakultät
an der Christian-Albrechts-Universität zu Kiel

eingereicht von

Benjamin John Schönbeck

Kiel

2014

Referee: Prof. Dr. Ottmar J. Janssen

Co-Referee: Prof. Dr. Dr. Thomas C.G. Bosch

Date of oral examination: September 29th, 2014

Acceptance for publication: September 29th, 2014

gez. Prof. Dr. Wolfgang Duschl, Dekan

Scientific knowledge advances haltingly
and is stimulated by contention and doubt.

Claude Lévi-Strauss

Table of Contents

LIST OF ABBREVIATIONS	VI
1 INTRODUCTION	1
1.1 PROTEOLYSIS – AN IRREVERSIBLE POST-TRANSLATIONAL MODIFICATION	1
1.1.1 PROTEASES AND PEPTIDASES	1
1.1.2 REACTION MECHANISM OF METALLOPROTEASES	3
1.2 ECTODOMAIN SHEDDING	4
1.3 THE <u>A</u> DISINTEGRIN <u>AND</u> <u>M</u> ETALLOPROTEASES (ADAMs)	5
1.4 A DISINTEGRIN AND METALLOPROTEASE 17 (ADAM17)	6
1.4.1 ADAM17 – DOMAIN STRUCTURE	7
1.4.2 BIOSYNTHESIS, MATURATION AND TRAFFICKING OF ADAM17	9
1.4.3 REGULATION AND ACTIVITY OF ADAM17	10
1.4.4 THE ADAM17 DEGRADOME	12
1.4.5 ADAM17 IN HEALTH AND DISEASE	15
1.4.6 EXPERIMENTAL SYSTEMS IN ADAM17 RESEARCH	16
1.4.7 THE MURINE HYPOMORPHIC ADAM17 ^{EX/EX} MODEL	18
2 AIM OF THIS THESIS	20
3 MATERIALS	21
3.1 CELLS	21
3.2 ANTIBODIES	21
3.3 REAGENTS, BUFFERS AND MEDIA	22
3.3.1 CELL BIOLOGY	22
3.3.2 IMMUNOFLUORESCENCE	23
3.3.3 ELISA	23
3.3.4 MOLECULAR BIOLOGY	24
3.3.5 CELL LYSIS BUFFERS	24
3.3.6 PROTEIN BIOCHEMISTRY	25
3.3.7 TWO-DIMENSIONAL GEL ELECTROPHORESIS (2D-IEF/SDS-PAGE)	27
3.3.8 2D-CTAB/SDS-PAGE	30
3.3.9 MALDI-ToF/ToF	31
3.3.10 BUFFERS AND REAGENTS FOR PREPARATIONS OF ECM PROTEINS	31
3.3.11 LECTIN-MEDIATED PRECIPITATION OF PROTEINS	32

Table of Contents	ii
3.4 CONSUMABLES	33
3.4.1 GENERAL LABORATORY CONSUMABLES	33
3.4.2 KITS	34
3.5 LABORATORY EQUIPMENT	34
3.5.1 GENERAL LABORATORY EQUIPMENT	34
3.5.2 GEL-BASED PROTEOMICS AND MASS SPECTROMETRY	35
3.6 SOFTWARE AND WEB SERVICES	35
3.6.1 SOFTWARE	35
3.6.2 WEB SERVICES	35
4 METHODS	37
4.1 CELL CULTURE	37
4.1.1 CULTIVATION OF MAMMALIAN CELLS	37
4.1.2 CRYOPRESERVATION OF CELLS	38
4.1.3 DETERMINATING CELL NUMBER AND VIABILITY OF CULTURED CELLS	38
4.2 SAMPLE PREPARATION TECHNIQUES	38
4.2.1 PREPARATION OF MURINE, BONE MARROW –DERIVED MACROPHAGES	38
4.2.2 PREPARATION OF WHOLE CELL LYSATES	39
4.2.3 ENRICHMENT OF PROTEINS FROM CELL CULTURE SUPERNATANTS	39
4.2.4 PREPARATION OF PLASMA MEMBRANE PROTEINS	41
4.2.5 ENRICHMENT OF ECM PROTEINS FROM CELLS AND TISSUES	42
4.2.6 BIOTINYLATION	43
4.2.7 CELL-SURFACE LABELING BY FLUORESCENT DYES	44
4.2.8 PREPARATION OF NUCLEAR PROTEINS FROM CULTURED CELLS	44
4.2.9 DETERMINATION OF PROTEIN CONTENT	44
4.3 ENZYME-LINKED IMMUNOSORBENT ASSAY (ELISA)	44
4.4 CONFOCAL LASER SCANNING MICROSCOPY (CLSM)	44
4.5 GEL-BASED PROTEOMIC APPROACHES	45
4.5.1 SDS-PAGE	45
4.5.2 MMP ZYMOGRAPHY	46
4.5.3 2D-IEF/SDS-PAGE	47
4.5.4 2D-CTAB/SDS-PAGE	50
4.5.5 WESTERN BLOT	52
4.5.6 SLOTBLOT	53
4.6 MASS SPECTROMETRY	54
5 RESULTS	57

Table of Contents	III
5.1 DECREASED SHEDDING ACTIVITY IN ADAM17^{EX/EX} MEF CELLS	57
5.2 PROTEOMIC ANALYSES OF MEF CELL CULTURE SUPERNATANTS	59
5.2.1 PROOF OF PRINCIPLE – ANALYSIS OF SHEDDING BY 2D-DIGE	59
5.2.2 IMPROVED PROTEIN ENRICHMENT BY WGA-MEDIATED PRECIPITATION	61
5.3 CHANGES IN MEF CELL SUPERNATANTS	62
5.3.1 ALTERED LEVELS OF PROTEIN FRAGMENTS IN MEF 1#1 CELL SUPERNATANTS	62
5.3.2 ALTERED PROTEIN SECRETION FROM ADAM17 ^{EX/EX} MEF CELLS	67
5.4 ADAM17 – A MODULATOR OF THE PROTEASE WEB?	72
5.4.1 REDUCED BMP-1 PROTEIN LEVELS IN ADAM17 ^{EX/EX} MEF CELL SUPERNATANTS	72
5.4.2 ADAM17 – A PUTATIVE MODULATOR OF MEF CELL MMP ACTIVITY?	73
5.4.3 ADAM17 AFFECTS PROTEASE INTERACTING PROTEINS	76
5.5 ADAM17-MEDIATED CHANGES OF INTRACELLULAR PROTEINS	78
5.5.1 INCREASED CELLULAR TYPE-I COLLAGEN LEVELS	79
5.5.2 ADAM17 AFFECTS MEMBERS OF THE COFILIN/ADF-FAMILY	80
5.5.3 INCREASED ANNEXIN LEVELS IN ADAM17 ^{EX/EX} MEF CELLS	82
5.6 NETWORK ANALYSIS	83
5.6.1 “THE EXTRACELLULAR NETWORK” OF IDENTIFIED PROTEINS	83
5.6.2 THE EXTENDED NETWORK ANALYSIS	84
5.7 MEF CELLS AND ALTERNATIVE CELLULAR SYSTEMS	85
5.7.1 DIFFERENCES BETWEEN DIFFERENT MEF CELL LINES	85
5.7.2 MURINE EMBRYONIC FIBROBLASTS	89
5.7.3 ALTERNATIVE CELLULAR SYSTEMS AND APPROACHES	89
5.8 EXPERIMENTAL GEL-BASED PROTEOMICS	90
5.8.1 ENRICHMENT OF EXTRACELLULAR MATRIX PROTEINS	90
5.8.2 PLASMA MEMBRANE PROTEOMICS	91
5.8.3 CELL-SURFACE LABELING STRATEGIES	95
6 DISCUSSION	98
6.1 COMPARISON OF THE PROTEIN CONTENT OF MEF CELLS	98
6.2 INDICATIONS FOR SHEDDING	100
6.2.1 ADAM17 – A POTENTIAL REGULATOR OF COLLAGEN MATURATION AND TURNOVER?	102
6.2.2 PERLECAN – A NOVEL ADAM17 SUBSTRATE IN MURINE CELLS?	105
6.3 ADAM17 – A MODULATOR OF THE PROTEASE WEB?	106
6.3.1 THE PROTEASE WEB	106
6.3.2 ADAM17 WITHIN THE PROTEASE WEB	107
6.4 ADAM17-DEPENDENT SECRETOME	109

Table of Contents	IV	
6.5	INTRACELLULAR EFFECTS OF ADAM17 IN MEF CELLS	110
6.5.1	INCREASED COFILIN-1 PHOSPHORYLATION IN WILD-TYPE MEF CELLS	110
6.5.2	INCREASED INTRACELLULAR ANNEXIN LEVELS IN ADAM17 ^{EX/EX} MEF CELLS	111
6.6	METHOD DEVELOPMENT AND LIMITATIONS	111
6.6.1	SHEDDOME AND SECRETOME ANALYSIS BY 2D-DIGE	111
6.6.2	GENERAL LIMITATIONS OF 2D GE	112
6.6.3	SECRETOME AND SHEDDING ANALYSES BY MS APPROACHES	113
6.6.4	DISADVANTAGES OF ADAM17 IN DEGRADOMIC STUDIES	114
6.6.5	STUDYING PLASMA MEMBRANE PROTEINS OF MEF CELLS	114
6.6.6	THE EXTRACELLULAR MATRIX (ECM)	117
6.7	LIMITATIONS OF THE ADAM17^{EX/EX} MEF SYSTEM	117
7	SUMMARY	120
8	ZUSAMMENFASSUNG	121
9	BIBLIOGRAPHY	122
10	ADDENDUM	140
10.1	DIGE145 – SUPERNATANT ANALYSIS	141
10.2	DIGE150 – SUPERNATANT ANALYSIS	142
10.2.1	GEL 12595	142
10.2.2	GEL 12722	143
10.3	DIGE153 – SUPERNATANT ANALYSIS	144
10.4	DIGE169 – SUPERNATANT ANALYSIS	145
10.4.1	GEL 68572	145
10.4.2	GEL 68573	146
10.4.3	GEL 68574	147
10.5	DIGE172 – SUPERNATANT ANALYSIS	148
10.5.1	GEL 68917	148
10.5.2	GEL 68918	149
10.5.3	GEL 68919	150
10.6	DIGE182 – SUPERNATANT ANALYSIS	151
10.7	DIGE158 – ANALYSIS OF WHOLE-CELL LYSATES	152
10.7.1	GEL 76295	152
10.7.2	GEL 76296	153
10.7.3	GEL 76297	154

Table of Contents	V
10.8 DIGE160 – ANALYSIS OF WHOLE-CELL LYSATES	155
10.8.1 GEL 76300	155
10.8.2 GEL 76301	156
10.9 DIGE184 – ANALYSIS OF ECM FROM CULTURED MEF CELLS	157
10.10 CTAB-DIGE: TWO-PHASE SYSTEM	158
10.11 CTAB-DIGE: GIANT PLASMA MEMBRANE VESICLES	159
10.12 CTAB-DIGE: TWO-PHASE SYSTEM AND CONCAVALIN A	160
<u>11 ACKNOWLEDGEMENT</u>	<u>161</u>
<u>12 CURRICULUM VITAE</u>	<u>163</u>
<u>13 LIST OF PUBLICATION</u>	<u>165</u>
13.1 AFFILIATED WORKS	165
13.2 MEETING CONTRIBUTIONS	165
<u>14 EIDESSTATTLICHE ERKLÄRUNG</u>	<u>166</u>

List of Abbreviations

Besides standard units of the *Système international d'unités* (SI), symbols for chemical elements and the one-letter-code for amino acids, the following abbreviations are used in this thesis:

16-BAC	benzylhexadecyldimethylammonium chloride
2D	two-dimensional
2D-DiGE	two-dimensional difference gel electrophoresis
aa	amino acids
ABC	ammonium bicarbonate
ACE2	angiotensin-converting enzyme 2
ADAM	A Disintegrin And Metalloprotease
ADAMTS	ADAM with thrombospondin motif
AEBSF	4-(2-Aminoethyl) benzenesulfonyl fluoride hydrochloride
ALCAM	activated leukocyte cell adhesion molecule
Anxa	annexin
APLP-2	amyloid-like protein 2
APP	amyloid precursor proteins
APS	ammonium persulfate
AREG	amphiregulin
BAC.1-2F5	murine macrophage cell line
BB-94	batimastat
BM	basal membrane
BMP	bone morphogenic protein
BSA	bovine serum albumine
C	cytoplasm
C-terminal	carboxy-terminal
C/I	constitutive/induced
C1-rA	C1 subcomponent rA
C1-sA	C1 subcomponent sA
C4.4A	Ly6/PLAUR domain-containing protein 3 precursor
CA9	carbonic anhydrase 9
CathB	cathepsin B
CAU	Christian-Albrechts-Universität zu Kiel; Kiel University
CD	cluster of differentiation
cDNA	complementary DNA
CHCA	α -Cyano-4-hydroxycinnamic acid

CHO	chinese hamster ovary
CLSM	confocal laser scanning microscopy
CO1A1	type-I collagen α_1 chain
CO1A2	type-I collagen α_2 chain
CO3A1	type-III collagen α_1 chain
CO4A1	type-IV collagen α_1 chain
CO4A2	type-IV collagen α_2 chain
CO6A1	type-VI collagen α_1 chain
CO6A2	type-VI collagen α_2 chain
ConA	Concanavalin A
COS	monkey kidney-derived fibroblast
COX	cyclooxygenase
CPP	C-terminal propeptide
CS	cytoskeleton
CS3CL1	fractalkine
CTAB	Cetyl trimethylammonium bromide
CUB	C1r/C1s, UEGF, BMP1
CV1	monkey kidney cell line
CytB	cystatin B
CytC	cystatin C
Da	Dalton
DAPI	4',6-diamidino-2-phenylindole
DLL-1	Delta-like protein 1
DMEM	Dulbecco's Modified Eagle's Medium
DMSO	dimethyl sulfoxide
DNA	deoxyribonucleic acid
DOC	deoxycholate
DSS	dextran sulfate
e.g.	example given
ECL	enhanced chemiluminescence light
ECM	extracellular matrix
ECM-1	Extracellular matrix protein 1
EDTA	Ethylenediaminetetraacetic acid
EGF	epidermal growth factor
EGF-R	epidermal growth factor receptor
EGTA	ethylene glycol tetraacetic acid
ELISA	enzyme-linked immunosorbent assay
EpCAM	epithelial cell adhesion molecule
EPCR	endothelial protein C receptor
ER	endoplasmic reticulum
EREG	epiregulin

ERK	extracellular signal-regulated kinase
<i>et al.</i>	<i>et alia</i> = and others
EXITS	exon induced translational stop
FaDu	human epithelial squamous carcinoma cell line
FBS	fetal bovine serum
Fig.	figure
FLT3L	Fms-related tyrosine kinase 3 ligand
FSTL-1	follistatin-related protein 1
G	Golgi apparatus
G3PDH	Glyceraldehyde 3-phosphate dehydrogenase
GDN	glia-derived nexin
GHR	growth hormone receptor
GI	ADAM10 inhibitor GI254023X
GP	envelope glycoprotein
GPI	glycophosphatidylinositol
GPIIb	platelet glycoprotein IIb alpha chain
GPMV	giant plasma membrane vesicle
GPV	glycoprotein V
GPVI	glycoprotein VI
GW	ADAM10/17 inhibitor GW28026X
HB-EGF	heparin-binding epidermal growth factor
HEK293	human embryonic kidney cell line 293
HeLa	Henrietta Lacks cervical carcinoma cells
HEPES	4-(2-hydroxyethyl)-1-piperazineethanesulfonic acid
HER4/ErbB4	receptor tyrosine-protein kinase erbB-4
HES	human embryonic stem cells
HPLC	high pressure liquid chromatography
HRP	horseradish peroxidase
HtrA	High-temperature requirement A serine peptidase 1
HUVEC	human umbilical vein endothelial cells
ICAM-1	intercellular adhesion molecule 1
ICAT	isotope-coded affinity tag
ICD	intracellular domain
IEF	isoelectric focusing
IL	interleukin
IL1RL1	interleukin 1 receptor-like 1
IL6-R	interleukin 6 receptor
IPG	immobilized pH gradient
iTRAQ	Isobaric tags for relative and absolute quantitation
JAM-A	junctional adhesion molecule A
kDa	kilodalton

KMLS-8.3.5.1	murine T cell hybridoma cell line
L	lysosome
LAG-3	lymphocyte activation gene 3 protein
LAMP	lysosome-associated membrane protein
LBC	lower buffer chamber
LC-MS	liquid chromatography-mass spectrometry
LG3	laminin-like globular 3
LIMK1	LIM kinase 1
LNCaP	human prostate adenocarcinoma cell line
LPS	lipopolysaccharide
LRP-1	low-density lipoprotein receptor-related protein 1
LTA	lymphotoxin alpha
M	membrane
m-CSF	murine colony stimulating factor
m-CSF-R	murine colony stimulating factor receptor
m/z	mass-to-charge ratio
M2	macrophage cell line
M6P/IGF2R	mannose-6-phosphate/insulin-like growth factor 2 receptor
MAD-2	mitotic arrest deficient protein 2
MALDI	matrix-assisted laser desorption/ionization
MAPK	mitogen-activated protein kinase
MCF-7	human breast cancer cell line
MEF	murine embryonic fibroblast
MEF 1#1	ADAM17 ^{ex/ex} MEF cell line
MEF 1#3	wild-type MEF cell line
MEF 1#7	wild-type MEF cell line
MEF 1#8	ADAM17 ^{ex/ex} MEF cell line
MEF 2#1	wild-type MEF cell line
MEF 2#8	ADAM17 ^{ex/ex} MEF cell line
MES	2-(<i>N</i> -morpholino)ethanesulfonic acid
MHC	major histocompatibility complex
MICA/B	MHC-class-I-related chain A/B
MMP	matrix metalloprotease
MMPI	MMP inhibitor
mRNA	messenger ribonucleic acid
MT-MMP	membrane-type MMP
MUC-1	mucin-1
MWCO	molecular weight cut-off
M ϕ	macrophage
N	nucleus

N-terminal	amino-terminal
NA	not assigned
NCAM-1	neural cellular adhesion molecule 1
Neuro 2a	neuroblastoma cell line 2a
NIH3T3	murine embryonic fibroblast cell line
NL	non-linear
NP-40	Nonidet P-40
NPR-1	atrial natriuretic peptide receptor 1
NRG1	nezregulin 1
NTR	netrin
OLFL	olfactomedin-like protein
p75NTR	Tumor necrosis factor receptor superfamily member 16
PAGE	polyacrylamide gel electrophoresis
PAI	Plasminogen activator inhibitor
PBS	phosphate buffered saline
PC12	embryonic rat pheochromocytoma cell line
PCOC-1	procollagen C-endopeptidase enhancer 1
PCR	polymerase chain reaction
PDI	protein disulfide isomerase
PEDF	Pigment epithelium-derived factor
PEM	PIPES/EGTA/magnesium
PFA	paraformaldehyde
pH	<i>potentia hydrogenii</i>
PIPES	piperazine-N,N'-bis(2-ethanesulfonic acid)
PKC	protein kinase C
PLK2	Polo-like kinase 2
PLOD	Procollagen-lysine,2-oxoglutarate 5-dioxygenase 1
pM	peripheral membrane
PMA	phorbol-12-myristate-13-acetate
Pmel17	melanocyte protein PMEL
PMSF	phenylmethylsulfonyl fluoride
PMT	photomultiplier tubes
PPAR γ	Peroxisome proliferator-activated receptor gamma
Pref-1	preadipocyte EGF-like protein 1
PRG4	proteoglycan 4
PrPc	prion protein c
pSer	phospho-serine
PTP-LAR	receptor-type tyrosine-protein phosphatase F
PTPH1	protein-tyrosine phosphatase 1
Ptprz	receptor-type tyrosine-protein phosphatase zeta
pTyr	phospho-tyrosine

RAW264.7	macrophage cell line
RBL	rat basophilic leukemia cells
RIP	regulated intramembrane proteolysis
RIPA	radioimmunoprecipitation buffer
RNA	ribonucleic acid
S	secreted
S/N	signal-to-noise ratio
SAP97	synapse-associated protein 97
SDC-1/4	syndecan-1/4
SDS	sodium dodecyl sulfate
SDS-PAGE	sodium dodecyl sulfate polyacrylamide gel electrophoresis
Sema	semaphoring
SH3	Src hology 3
shRNA	small hairpin RNA
SILAC	stable isotope labeling by amino acids in cell culture
siRNA	small interfering RNA
SKOV3	human ovarian carcinoma cell line
SN	supernatant
SORCS-1/3	VPS10 domain-containing receptor SorCS1
SORL-1	sortilin-related receptor 1
SORT-1	sortilin 1
SPARC	secreted protein acidic and rich in cystein
sRFP2	secreted Frizzled-related protein 2
Tab.	Table
TACE	tumor necrosis factor α converting enzyme
TAE	tris/acetate/EDTA
TAILS	terminal amine isotopic labeling of substrates
TBS	tris buffered aline
TEMED	N,N,N',N'-tetramethyldiamide
TGF	transforming growth factor
Th1/Th17	T-helper cell 1/17
Thr	threonine
TIMP	tissue inhibitor of metalloproteases
TLR4	Toll-like receptor 4
TMEFF	Tomoregulin
TNF	tumor necrosis factor
TNF-R	tumor necrosis factor receptor
ToF	time of flight
TRANCE/RANKL	TNF-related activation-induced cytokine
Tris	Tris (hydroxymethyl)-aminoethan

U373	human astrocytoma cell line
UBC	upper buffer chamber
UK S-H	Universitätsklinikum Schleswig-Holstein
UV	ultraviolet
v/v	volume per volume
VCAM-1	vascular adhesion molecule 1
w/v	weight per volume
WB	Western blot
WCL	whole-cell lysate
WGA	wheat germ agglutinin

1 Introduction

1.1 Proteolysis – An irreversible post-translational modification

A variety of post-translational modifications vastly increase the number of differentially acting proteins from a given number of genes. These post-translational modifications include the addition of organic (e.g. glycosylation and acetylation), inorganic (e.g. phosphorylation and hydroxylation) and lipid groups (e.g. prenylation and GPI anchors) or the addition of chemical bonds (e.g. disulfide bonds). In addition, a widely irreversible post-translational modification is the proteolytic processing of proteins, which for instance includes the cleavage of ectodomains from transmembrane precursor proteins [Lothrop *et al.*, 2013].

Proteolytic processing reveals an important mechanism for the regulation of both, inter- and intracellular signaling pathways in an either activatory or inhibitory manner. The release of ectodomains from transmembrane proteins – a process widely referred to as ectodomain shedding – contributes to initiate signaling by releasing ligands or receptors from a given cell. These ectodomains bind to their complementary target structure on the same or on a neighboring cell modulating cellular responses. Thus, released protein fragments not only can act in an autocrine manner on the same cell, but also in a paracrine or even endocrine manner [Wiley *et al.*, 1998; Borrell-Pages *et al.*, 2003]. In addition, shedding often precedes the subsequent processing by membrane-resident proteases (e.g. γ -secretases), which in turn leads to the release of the intracellular domain of the processed protein by regulated intramembrane proteolysis (RIP) [Schroeter *et al.*, 1998; De Strooper *et al.*, 1999].

1.1.1 Proteases and peptidases

At standard conditions, most biochemical processes could not be performed without enzymes. These large biomolecules catalyze biochemical processes by lowering the required activation energy and increasing the reaction rate of biochemical reactions. Proteases and peptidases form the largest family of enzymes in vertebrates [López-Otín & Bond, 2008; Sterchi, 2008]. Moreover, about 2 % of the proteins in all kinds of organisms are peptidases [see <http://merops.sanger.ac.uk>].

In proteolysis, proteases catalyze the enzymatic hydrolysis of internal (endoproteases) or terminal peptide bonds (exoproteases). Considering parameters such as activity, functional groups within the active center and the mechanism of catalysis, the repertoire of cellular proteases can be further divided into five different classes: (I) aspartic proteases, (II) threonine proteases, (III) cysteine proteases, (IV) serine proteases and (V) metalloproteases. In addition, the overall importance of proteolysis is reflected not only within the evolutionary conservation among all kingdoms of life, but also by the genomic complexity of this protein class [Rivera *et al.*, 2010]. So far, the known human proteome contains at least 569 (629 in rats and 644 in mouse) proteases or protease-like proteins and homologs [Puentes *et al.*, 2003]. Most of them either belong to cysteine (150), serine (176) or metalloproteases (194) [Rivera *et al.*, 2010].

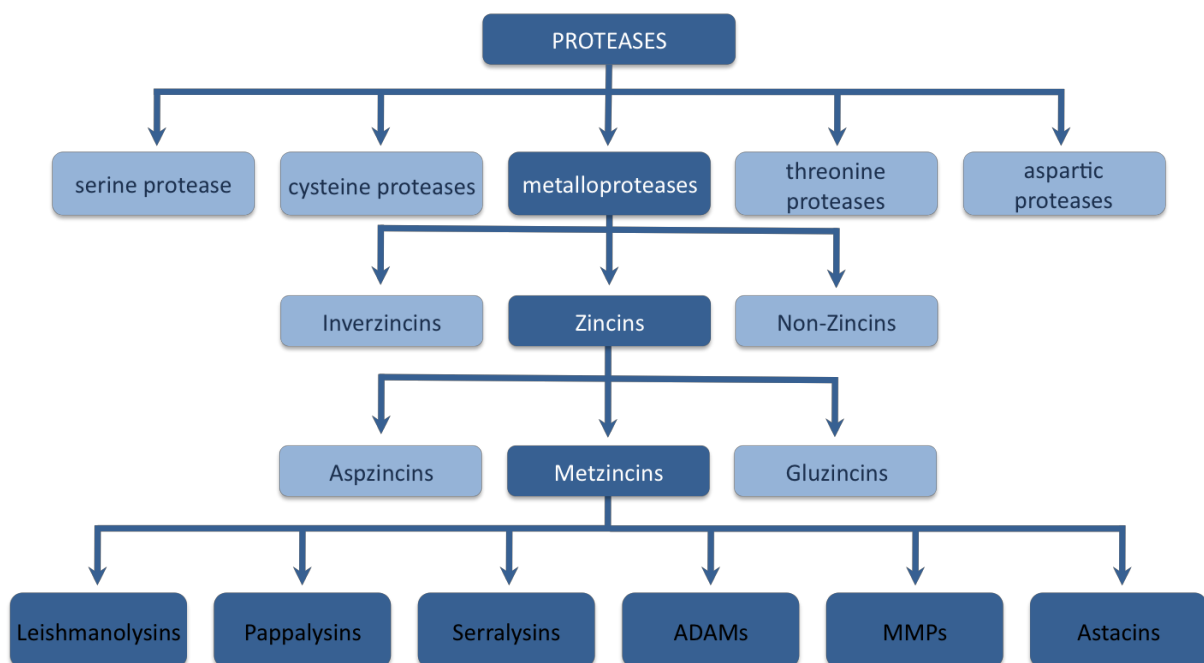


Fig. 1.1: Classes of proteases with a focus on metalloproteases [http://merops.sanger.ac.uk/cgi-bin/clan_index?type=P].

The subgroup of metalloproteases forms the largest group of proteases [Rawlings *et al.*, 2004]. In most cases, they contain one or two divalent zinc cations and share a conserved HEXXH zinc-binding motif. The zinc cations are coordinated at the active site by two histidine residues within an α -helix [Bode *et al.*, 1993]. Most metalloproteases belong to the metzincins superfamily, which is characterized by an elongated HEXXHXXGXXH/D zinc-binding region with a methionine backing and a characteristic three-dimensional structure ("Met Turn") [Bode *et al.*, 1993; Stöcker *et al.*, 1995]. Whereas other groups of metalloproteases show inverted HXXEH zinc binding motifs (inverzincins) or bind other

divalent cations like manganese or cobalt (non-zincins) [Hooper, 1994], the metzincin superfamily comprises the subfamilies of astacins, matrix metalloproteinases (MMPs), adamalysins, serralysins, pappalysins and leishmanalysins. Focusing on metalloproteases, the above figure (Fig. 1.1) provides an overview on the different families of proteases.

1.1.2 Reaction mechanism of metalloproteases

Metalloendopeptidases such as members of the A Disintegrin And Metalloprotease (ADAM) or matrix metalloprotease (MMP) family catalyze the proteolysis of proteins within a hydrolytic reaction. The reaction mechanism of MMPs (MMPs) is depicted in figure 1.2. Thereby, the scissile amide carbonyl group is coordinated to the active-site zinc ion. The carbonyl group is attacked by one water molecule that is coordinated to the zinc ion and hydrogen bound to a conserved glutamic acid residue. The water molecule acts as a proton donor that is transferred to the nitrogen of the scissile amide via the conserved glutamic acid residue. Finally, this proton transfer results in the cleavage of the peptide bond. This process is promoted by the positively charged zinc ion, which stabilizes a negative charge at the carbon atom of the scissile amide. In addition, a conserved alanine residue stabilizes a positive charge distribution at the nitrogen atom of the scissile amide. [Amin and Welsh, 2001; Lovejoy *et al.*, 1994].

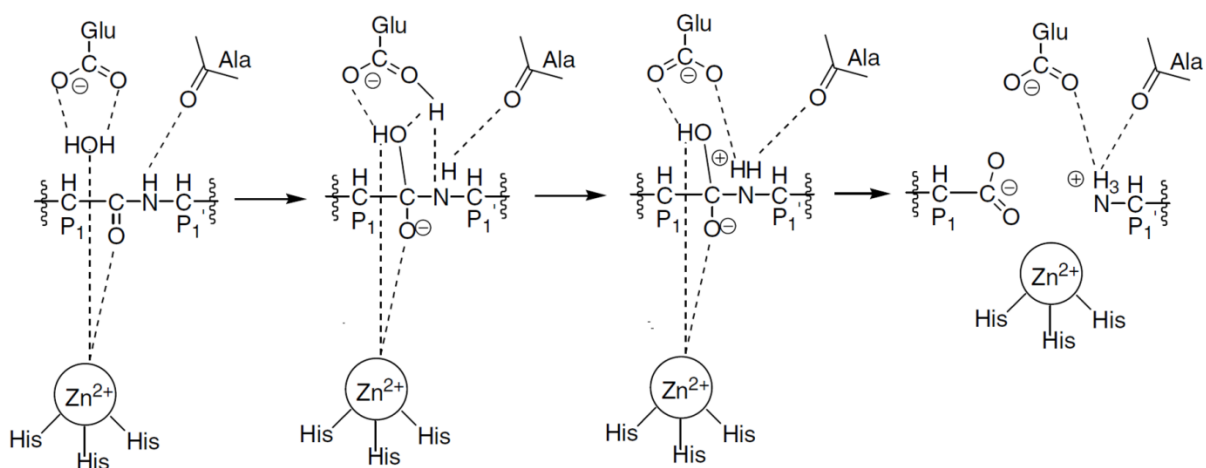


Fig. 1.2: Reaction mechanism of metalloendopeptidases on the example of matrix metalloproteinases (MMPs). This figure has been adapted from Lovejoy and colleagues [Lovejoy *et al.*, 1994]. For detailed information refer to the text.

1.2 Ectodomain shedding

The term ectodomain shedding denotes the proteolytic release of extracellular domains of transmembrane proteins that is mediated by a variety of different proteases at or near the cell surface [Arribas and Borroto, 2002; Ahmad *et al.*, 2006; Brule *et al.*, 2006]. Although basal shedding occurs in non-stimulated cells, it can dramatically be enhanced via different mechanisms, including non-physiologic phorbol ester compounds. As up to two percent of all cell surface molecules can be subjected to ectodomain shedding, these shed ectodomains make up a considerable fraction of soluble mediators [Arribas and Massagué, 1995; Arribas and Borroto, 2002].

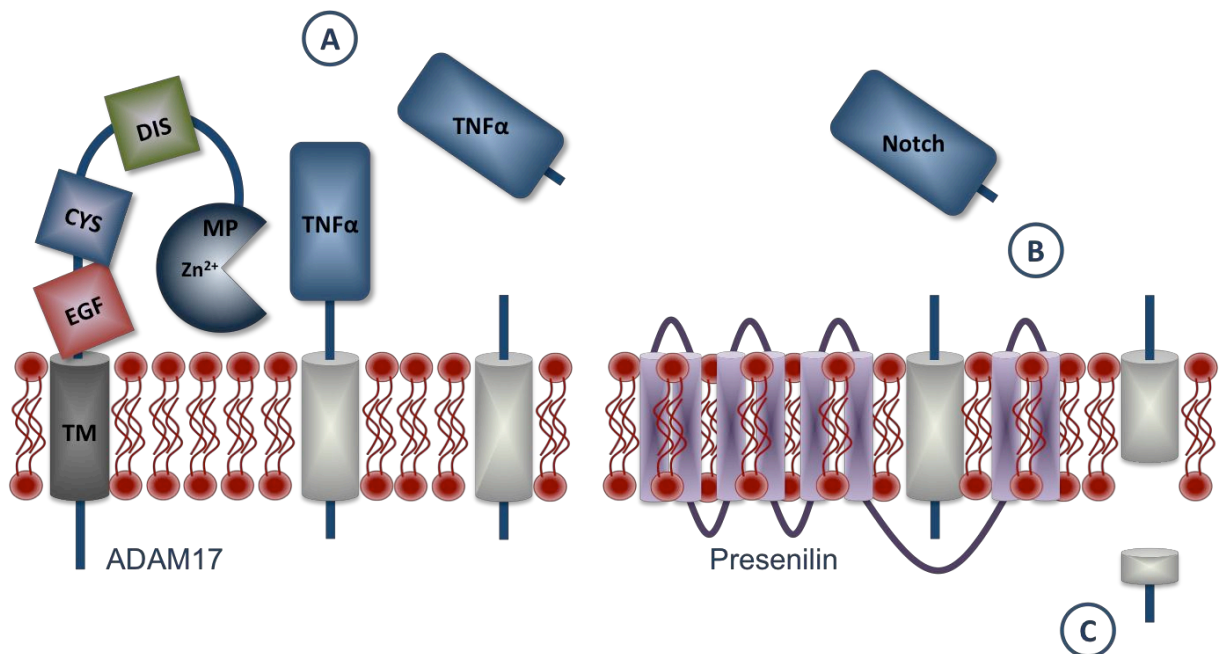


Fig. 1.3: ADAM17-mediated ectodomain shedding and subsequent regulated intramembrane proteolysis. (A) The extracellular domain of TNF α is released by ADAM17-mediated shedding. Proteolytic cleavage occurs in α -position. **(B)** In case of ADAM17- and ADAM10-mediated processing of Notch, the remaining membrane stub is targeted by the γ -secretase presenilin in the process of regulated intramembrane proteolysis (RIP). **(C)** An intracellular fragment of Notch is released into the cytoplasm and can further translocate to the nucleus to mediate gene expression of several genes.

Ectodomain shedding is involved in a variety of cellular processes, including maturation of growth factors or the modulation of membrane receptors and cellular adhesion molecules [Arribas and Borroto, 2003]. Certain growth factors and cytokines, such as members of the TNF and EGF families are synthesized as transmembrane precursor proteins. The extracellular domain of these proteins binds to cognate receptors on the same cell or on other cells. The release of the receptor-binding domain to the extracellular environment is mediated by ectodomain shedding [e.g. Myhre *et al.*, 2004 and Dreymlüller *et al.*, 2012] and

affects subsequent signaling events. As depicted in figure 1.3, proTNF α is matured by ADAM17 [Black *et al.*, 1997; Moss *et al.*, 1997b] and the released extracellular domain can bind to TNF receptors TNF-R_I and TNF-R_{II} on neighboring cells to act in a pro- or antiapoptotic manner or to induce the shedding of these receptors [Ashkenazi and Dixit, 1998; Hehlhans and Pfeffer, 2005]. In addition, ectodomain shedding represents a crucial step in the regulation of cell-cell and cell-matrix interactions, as the extracellular domains of cellular adhesion molecules are mediators of these interactions. One example for shed adhesion molecules is L-selectin, a homing receptor that mediates interactions between lymphocytes and endothelial venules and their migration into peripheral lymph nodes [Gallatin *et al.*, 1983]. In addition, L-selectin also participates in the recruitment of neutrophils into inflamed tissues by mediation of the initial attachment and slow rolling along the vascular endothelium [Springer, 1994; Lawrence *et al.*, 1994]. Shedding of L-selectin can lead to a rapid decrease of surface levels of L-selectin [Kishimoto *et al.*, 1995; Chen *et al.*, 1995], thereby modulating the rolling velocity of neutrophils [Walcheck *et al.*, 1996].

1.3 The A Disintegrin And Metalloproteases (ADAMs)

The A Disintegrin And Metalloproteases (ADAMs) belong to the superfamily of zinc-dependent proteases, also known as metzincins [Stöcker *et al.*, 1995]. They are glycosylated type-I transmembrane and secreted modular proteins with proteolytic and non-proteolytic functions. Due to their proteolytic activity, ADAM proteases play an important role in the regulation of cell adhesion and of ectodomain release of a plethora of cell surface proteins. This protein family was initially established by characterization of metalloproteases from snake venom and from sperm [Wolfsberg *et al.*, 1995a; Wolfsberg *et al.*, 1995b]. Orthologs of ADAM10 and ADAM17 have been identified in many species within the *metazoa*, including *Caenorhabditis elegans* and *Drosophila melanogaster*, via the primitive chordate *Ciona intestinalis* through *Danio rerio* and to the expanded family found in vertebrates [Huxley-Jones *et al.*, 2007]. In addition, ADAM-like sequence motifs have also been discovered in the fission yeast *Schizosaccharomyces pombe* [Nakamura *et al.*, 2004], but are apparently absent in *Saccharomyces cerevisiae* and plants.

Besides, members of the ADAM family have been linked to a variety of different biological processes, including sperm-egg interactions [Blobel *et al.*, 1992], cell fate determinations within the nervous system [Yang *et al.*, 2006], cell migration [Guo *et al.*, 2012; Bakken *et al.*,

2009], axon guidance [Malinverno *et al.*, 2010], muscle development [Coles *et al.*, 2014], cancer progression [for instance reviewed by Murphy, 2008] and immunity.

1.4 A Disintegrin And Metalloprotease 17 (ADAM17)

Among the extended family of ADAMs, ADAM17 was the first ADAM to be implicated in ectodomain shedding by its identification as the **T**NF α **c**onverting **e**nzyme (TACE) [Black *et al.*, 1997; Moss *et al.*, 1997a; Moss *et al.*, 1997b; Black *et al.*, 2003; Moss and Bartsch, 2004]. There, ADAM17 is involved in the orchestration of immunologic and inflammatory responses via activation of proTNF α by ectodomain shedding. Since then, ADAM17 has been established as an important sheddase in mammalian development [Peschon *et al.*, 1998] with an even broader role in adults via the processing of a variety of other substrates, including for instance numerous cytokines and their receptors [Black *et al.*, 1997; Black *et al.*, 2003]. Among others, ectodomain shedding of the cell surface protein Notch is linked to subsequent **r**egulate **i**ntramembrane **p**roteolysis (RIP), which is mediated by the γ -secretase presenilin and generates a nucleus-targeted signal [Schroeter *et al.*, 1998; De Strooper *et al.*, 1999]. ADAM17 is expressed in a variety of tissues including brain, heart, kidney and skeletal muscle [Black *et al.*, 1997]. Meanwhile, the list of ADAM17 substrates contains more than seventy cell-surface proteins, which stresses its physiologic importance. However, the majority of these putative substrates have been evaluated in cell culture approaches and *in vitro* experiments often using non-physiologic stimuli [Gooz, 2010]. Although the *in vivo* relevance of individual ADAM17 cleavage processes still has to be elucidated, the early death of ADAM17 knock-out mice [Peschon *et al.*, 1998] highlights its important physiologic role in organismic development. Further insights into the role of ADAM17 *in vivo* were investigated using the ADAM17 hypomorphic mouse model ADAM17^{ex/ex} [Chalaris *et al.*, 2010], which is described in section 1.4.7 in more detail. Interestingly, looking at phylogenetic trees, ADAM17 only shares limited sequence similarity with other ADAM family members and even with its closest relative ADAM10, sequence similarity is less than 30 % (Fig. 1.4) [Edwards *et al.*, 2008].



Fig. 1.4: Phylogenetic tree of human ADAMs based on protein sequences of the metalloprotease domains. The scale bar represents amino acid substitutions per site. 0.1 represents 10 % of sites having a substitution. This figure has been adapted from Edwards *et al.*, 2008.

1.4.1 ADAM17 – Domain structure

Members of the ADAM subfamily share certain structural similarities, as they contain eight distinct protein subdomains (Fig. 1.5): (I) a N-terminal signal peptide, (II) a pro-domain, (III) a catalytic metalloprotease domain, (IV) a disintegrin-like domain, (V) a cysteine rich-region, (VI) an EGF-like domain, (VII) a transmembrane and (VIII) an intracellular C-terminal region.

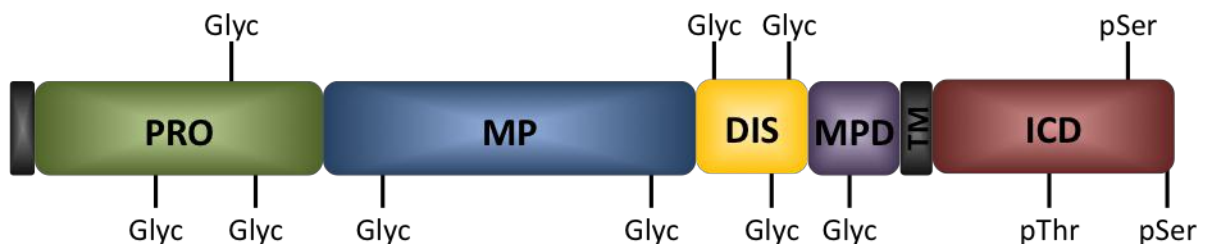


Fig. 1.5: Schematic overview on modular architecture of ADAM17. Different domains are indicated as follows: N-terminal signal peptide (black box), prodomain (PRO), metalloprotease domain (MP), disintegrin-like domain (DIS) membrane proximal domain (MPD), transmembrane region (TM) and intracellular domain (ICD). In addition, putative phosphorylation sites and N-linked glycosylation sites are indicated. Image is based on sequence-dependent domain predictions by the SMART internet platform (smart.embl-heidelberg.de) according to murine ADAM17 protein sequence (NP_033745.4) and on further protein information from www.uniprot.org/uniprot/P78536.

Since only 13 of the 21 human ADAMs are proteolytically active, it is likely that not only the metalloprotease domain, but also other domains contribute to the overall functions of

ADAM proteins. Thus, the prodomain acts in an inhibitory manner on the metalloprotease activity [Moss *et al.*, 2007; Gonzales *et al.*, 2008] and is removed by intracellular pro-protein convertases on the way to the plasma membrane within the secretory pathway [Endres *et al.*, 2003; Seals & Courtneidge, 2003]. In addition, the prodomain is supposed to assist in correct protein folding as an intracellular chaperone [Roghani *et al.*, 1999]. The proteolytic activity is mediated by the metalloprotease domain and determined by a conserved HEXXHXXGXXH motif [Bode *et al.*, 1993]. Three histidine residues and one molecule of water are essential for the coordination of the divalent zinc cation within the active site [Stöcker *et al.*, 1995].

In some cases, the disintegrin-like domain has been shown to be important for interactions with integrins [Bridges *et al.*, 2005], thereby influencing cell-cell contact [Edwards *et al.*, 2008]. For example, cell adhesion is mediated via interactions of the cysteine-rich region with syndecans and fibronectin [Iba *et al.*, 1999]. In addition, the cysteine-rich region, which is part of the disintegrin domain, might also be involved in clustering of different ADAMs [Smith *et al.*, 2002]. Adjacent to the transmembrane region, the EGF-like domain, which is present in most, but not all ADAMs, is thought to mediate the recognition of substrates in co-operation with the disintegrin-like domain [Caescu *et al.*, 2009]. Moreover, this domain seems to be involved in the regulation of the activity of ADAM17, by mediating its multimerization [Lorenzen *et al.*, 2011].

Nevertheless, both, ADAM10 and ADAM17, show an atypical domain structure, as they do not include an EGF-like domain, but an alternate membrane proximal domain (MPD) that replaces the cysteine-rich region and the EGF-like domain [Janes *et al.*, 2005; Takeda, 2008]. Contradictory, the term “EGF-like domain” is often used in ADAM17 literature. At present, the differential nomenclature for certain domains appears to be somehow contradictory within the ADAM17 literature. The hypervariable region of this MPD is placed in close proximity to the active site [Takeda, 2008]. Apparently, this is mediated by a conformational change between a closed and an open form of the MPD due to the activity of associated protein disulfide isomerase [Düsterhöft *et al.*, 2013].

The C-terminal cytoplasmic tail or intracellular region varies in length between different ADAMs, but mostly contains one or more proline-rich stretches that are supposed to interact with Src homology 3 (SH3) domain-containing signaling molecules [compare

<http://uniprot.org/uniprot/Q9Z0F8>]. In addition, the intracellular region of ADAM17 contains several putative phosphorylation sites that might influence recruitment or activation of ADAMs [compare <http://uniprot.org/uniprot/Q9Z0F8>]. Furthermore, yeast two-hybrid screens elucidated several intracellular binding-partners for ADAM17, including the mitotic arrest deficient 2 protein (MAD2) [Nelson *et al.*, 1999], the protein-tyrosine phosphatase PTPH1 [Zheng *et al.*, 2002] and the synapse-associated protein 97 (SAP97) [Peiretti *et al.*, 2003b].

1.4.2 Biosynthesis, maturation and trafficking of ADAM17

The *Adam17* gene is located on chromosome two in humans and on chromosome twelve in mice [Yamazaki *et al.*, 1999]. ADAM17 mRNA was found in many tissues, implicating a ubiquitous and constitutive expression similar to housekeeping genes. Nevertheless, differences in ADAM17 mRNA levels were later detected in different tissues, developmental stages and diseases [Black *et al.*, 1997; Arribas and Borroto, 2003].

Protein synthesis occurs at the rough endoplasmic reticulum, followed by subsequent removal of the N-terminal signal peptide (Fig. 1.6 C). The initial activity of the resulting proADAM17 molecule is inhibited during the translation process by its prodomain [Gonzales *et al.*, 2004; Li *et al.*, 2009]. Thus, proADAM17 translocates to the trans-Golgi compartment (Fig. 1.6 D), where zymogen maturation by proteolytic removal of the prodomain is mediated by the proprotein convertase furin (Fig. 1.6 E) [Schlöndorff *et al.*, 2000; Srour *et al.*, 2003]. The transport of ADAM17 from endoplasmic reticulum through the Golgi compartment has been shown to be dependent on iRhom2 that acts as a cargo receptor specifically on ADAM17 in macrophages [McIlwain *et al.*, 2012; Lichtenthaler, 2012]. In contrast to other metalloproteases, the cysteine switch mechanism does not seem to be relevant for ADAM17 activity [Leonard *et al.*, 2005]. In addition, further maturation of ADAM17 includes N-linked glycosylation [Peiretti *et al.*, 2003a], which leads to the mature 130 kDa form. Although data regarding phosphorylation of ADAM17 are contradictory in terms of shedding activity [Gooz, 2010], ERK-dependent phosphorylation of Thr735 has been shown to be necessary the entry into the secretory pathway [Soond *et al.*, 2005]. Of note, a mechanistic concept of ADAM17 intracellular trafficking in different cell types is still missing [Gooz, 2010]. Moreover, the intracellular distribution of ADAM17 in different cell types also remains enigmatic. Although active ADAM17 predominately appears at the cell-surface

(Fig. 1.6 I), the majority of ADAM17 seems to be localized within the perinuclear compartment (Fig. 1.6 F) [Schlöndorff *et al.*, 2000].

Of note, in hydroxamate inhibitor treated macrophages, TNF α also appeared to be localized in an intracellular compartment [McGeehan *et al.*, 1994], possible intracellular actions of ADAM17 are still matter of debate [Schlöndorff *et al.*, 2000].

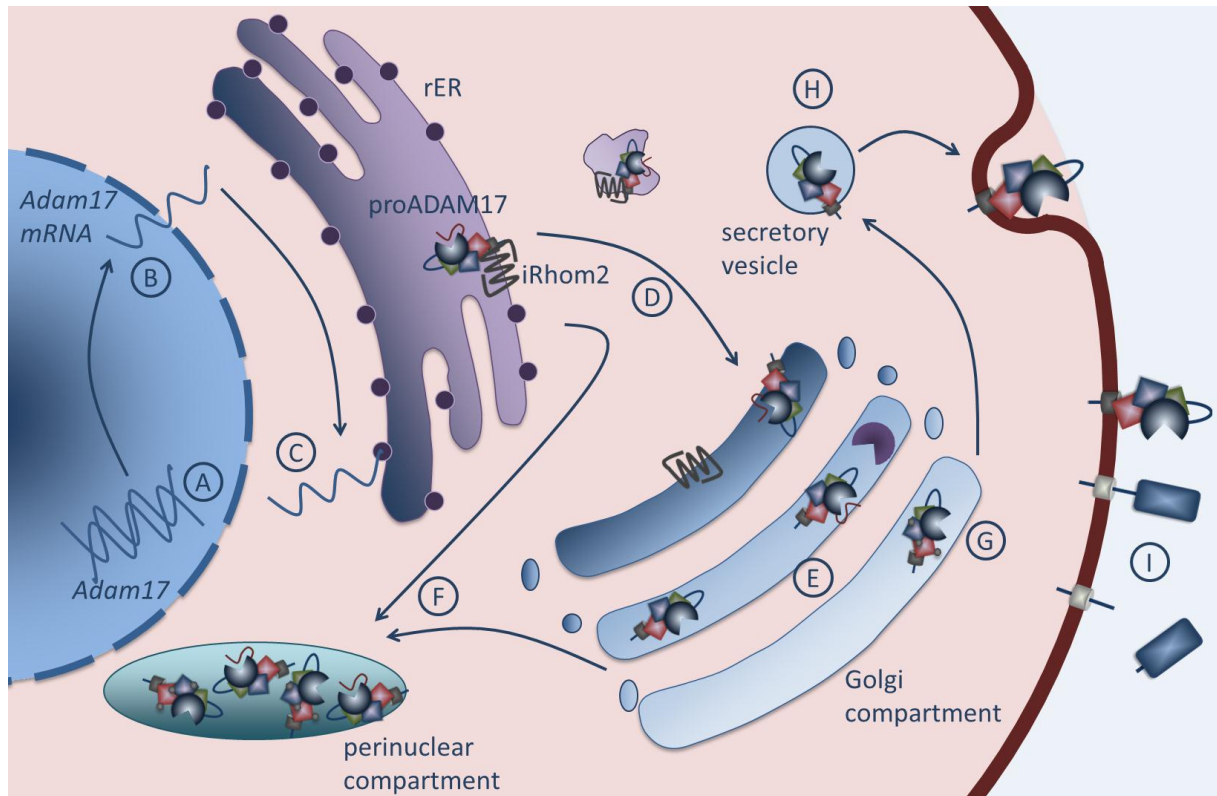


Fig. 1.6: Biosynthesis, maturation and intracellular trafficking of ADAM17. (A) Regulation of *Adam17* gene activity. (B) Expression of the *Adam17* gene and export of *Adam17* mRNA into the cytoplasm. (C) Translation of proADAM17 at the rough endoplasmic reticulum (rER). The immature proADAM17 molecule is released into the lumen of the ER and the signal peptide is removed. (D) Intracellular trafficking from rER to the Golgi compartment (cis) is mediated by the cargo receptor iRhom2. (E) Maturation of proADAM17 by proteolytic removal of the pro-domain by furin. (F) Possible intracellular storage of ADAM17 within a perinuclear compartment. (G) Glycosylation of the processed ADAM17 molecule within the trans-Golgi network. (H) Transport of mature ADAM17 to the plasma membrane via the secretory pathway. (I) ADAM17-mediated release of the ectodomain of a transmembrane substrate by ectodomain shedding.

1.4.3 Regulation and activity of ADAM17

Despite TIMP-3, which is known to be a native inhibitor of ADAM17 [Amour *et al.*, 1998], not much is known about the physiologic regulation of the activity of ADAM17. The phorbol ester “Phorbol-12-myristat-13-acetate” (PMA) is a strong, non-physiologic activator of protein kinase C (PKC) [Myers *et al.*, 1985], and in turn leads to increased shedding activity [Arribas and Borroto, 2002]. Although the intracellular region of ADAM17 contains putative

p38 MAPK and PKC phosphorylation sites [Gechtman *et al.*, 1999; Díaz-Rodríguez *et al.*, 1999], a loss of this intracellular region does not lead to a reduced susceptibility to PMA-induced shedding [Reddy *et al.*, 2000; Le Gall *et al.*, 2010]. Thus, it was concluded that the intracellular region does not play a role for PMA-induced shedding, which also might imply an activation of ADAM17 independent from intracellular signaling pathways. Contradictory, inhibition of ADAM17-mediated shedding via blocking PKC and ERK has been reported [Xu & Derynck, 2010]. Moreover, investigations on ADAM10-mediated shedding of CD44 and ADAM17-mediated shedding of NRG1 indicate a predominant function of the substrates regarding control and specificity of shedding [Dang *et al.*, 2013]. A missing consensus cleavage site and the inhibition of ADAM17-mediated shedding by antibodies directed against different ADAM17 substrates [Hansen *et al.*, 2004] implicate structural aspects of the substrates to be important for the recognition by the protease. In addition, PMA-induced increase of ADAM17 shedding activity seems to be mediated by activation of extracellular protein disulfide isomerases (PDIs) [Willems *et al.*, 2010; Düsterhöft *et al.*, 2013]. Thus, PMA is supposed to lead to a production of reactive oxygen species (ROS), which inactivate PDIs and stabilize the active conformation of the ADAM17 membrane proximal domain via changes in disulfide bonds [Düsterhöft *et al.*, 2013]. Furthermore, ADAM17 is located within lipid rafts [Tellier *et al.*, 2006] and ADAM17-mediated shedding can be increased by depletion of cholesterol [Matthews *et al.*, 2003].

The majority of endogenous ADAM17 molecules are not present at the plasma membrane, but stored intracellularly within the perinuclear compartment [Schlöndorff *et al.*, 2000]. Phosphorylation of Thr735 is mediated by p38 MAPK and leads to the translocation of intracellular ADAM17 to the plasma membrane [Soond *et al.*, 2005; Xu & Derynck, 2010]. Recently, phosphorylation of ADAM17 at Ser794 by the acidophilic polo-like kinase 2 (PLK2) was shown to modulate the ADAM17 activity in case of shedding of TNF α and TNF-R [Schwarz *et al.*, 2013]. Alternate mechanisms of activation of ADAM17-mediated shedding have been reported to occur via Toll-like receptor activation in case of CD62L [Morrison *et al.*, 2010] and TNF-R_I [Yu *et al.*, 2011]. In addition, apoptosis has also been shown to influence the ADAM17-mediated shedding of CD62L [Wang *et al.*, 2010] and human IL-6R [Chalaris *et al.*, 2007].

1.4.4 The ADAM17 degradome

A large number of substrates have been described for ADAM17. As summarized in table 1.1, the reported degradome includes growth factors and cytokines, cell-surface receptors, adhesion molecules and other cell-surface proteins. The big diversity of substrates and their involvement in different cellular processes underscores the general importance of this protease [Pruessmeyer and Ludwig, 2008].

Tab. 1.1.: The reported degradome of ADAM17.

	substrate	constitutive or Induced	investigated system	stimulus/inhibitor	reference
Cytokines & Growth factors	AREG	I	ADAM17 ^{ΔZn/ΔZn} keratinocytes	PMA, recombinant ADAM17	Sunnarborg <i>et al.</i> , 2002
	CSF-1	I	ADAM17 ^{-/-} MEF	PMA	Horiuchi <i>et al.</i> , 2007
	CX3CL1	C/I	HUVECs; NIH3T3	PMA, GM6001	Garton <i>et al.</i> , 2001
	DLL1	C/I	COS-7	PMA	Dyczynska <i>et al.</i> , 2007
	epigen	C/I	COS-7	PMA, BB94, GW, GI	Sahin & Blobel, 2007
	EREG	I	A17 ^{-/-} MEF	PMA	Sahin <i>et al.</i> , 2004
	HB-EGF	I	A17 ^{-/-} MEF, M2 cells	PMA, APMA	Merlos-Suárez <i>et al.</i> , 2001
	Jagged	C/I	HEK, CaSki	shRNA, PMA, Ilomastat	Parr-Sturgess <i>et al.</i> , 2010
	KL-1	C/I	A17 ^{-/-} MEF	PMA	Kawaguchi <i>et al.</i> , 2007
	KL-2	C/I	A17 ^{-/-} MEF	PMA	Kawaguchi <i>et al.</i> , 2007
	LAG-3	C/I	OTII murine transgenic T cells	PMA, TAPI	Li <i>et al.</i> , 2007
	LTA	C	human Th1, Th17 cells	---	Young <i>et al.</i> , 2010
	MICA	I	C1R, HeLa	PMA, MMPI III, GW, GI	Waldhauer <i>et al.</i> , 2008
	MICB	C/I	U373, CV1	PMA, BB94, TIMPs, siRNA	Boutet <i>et al.</i> , 2009
	NRG-1	C/I	CHO, HeLa, A17 ^{ΔZn/ΔZn} MEF	PMA	Montero <i>et al.</i> , 2000
	Pref-1	I	COS cells	PMA, GM6001	Wang <i>et al.</i> , 2006
	Sema4D	I	platelets	PMA, thrombin, collagen	Zhu <i>et al.</i> , 2007
	TGFα	C/I	A17 ^{ΔZn/ΔZn} MEF	PMA	Peschon <i>et al.</i> , 1998
	TMEFF2	I	HEK293, CHO, LNCaPs	PMA, GM6001	Ali & Knäuper, 2007
	TNFα	I		PMA, LPS, glutamate	Moss <i>et al.</i> , 1997; Black <i>et al.</i> , 1997
TRANCE/RANKL	I	COS-7, HEK293, KMLS-8.3.5.1	PMA	Lum <i>et al.</i> , 1999	

cell-surface receptors	ACE2	I	HEK-ACE cells	PMA, TAPI, GM6001; GW, GI, TIMP-3	Lambert <i>et al.</i> , 2005
	CD30	I	Karpas 299 lymphoma cells	PMA	Hansen <i>et al.</i> , 2004
	CD40	I	B cells	α -CD40	Contin <i>et al.</i> , 2003
	CD89	I	HEK293T, CHO, RBL	PMA, GM6001, EDTA	Peng <i>et al.</i> , 2010
	CD91/LRP1	C	brain, CSF	---	Liu <i>et al.</i> , 2009
	EPCR	(C?)/I	HUVECS, EC2-EPCR	PMA, TIMPs, siRNA	Qu <i>et al.</i> , 2007
	FLT3L	C/I	COS-7, TACE/Mx1 murine serum	PMA	Horiuchi <i>et al.</i> , 2009
	GPIba	(C?)/I	A17 ^{ΔZn/ΔZn} murine platelets	PMA, TAPI	Bergmeier <i>et al.</i> , 2004
	GPV	I	A17 ^{ΔZn/ΔZn} murine platelets	PMA, CRP, thrombin	Rabie <i>et al.</i> , 2005
	GPVI	C/I	A17 ^{-/-} platelets	PMA, GM6001	Bender <i>et al.</i> , 2010
	GHR	C/I	HEK-293 (rbGHR infected)	PMA	Wang <i>et al.</i> , 2002
	HER4/ErbB4	I	A17 ^{-/-} MEF cells	PMA	Rio <i>et al.</i> , 2000
	IL-1 receptor-II	I			Reddy <i>et al.</i> , 2000
	IL-15 receptor- α	C, I	Renal Cancer Cells	PVN, GW, GI	Kahawam <i>et al.</i> 2009
	IL-6 receptor	C/I	ADAM17 ^{-/-} MEF cells	PMA	Althoff <i>et al.</i> , 2000
	KDR, VEGFR2	C/I	COS-7, ADAM17 ^{-/-} MEF cells	PMA	Swendeman <i>et al.</i> , 2008
	M6P/IGF2R	C	HUVECs	siRNA, GM6001	Leksa <i>et al.</i> , 2011
	M-CSFR	I	BAC.1-2F5	PMA, LPS, EDTA	Rovida <i>et al.</i> , 2001
	Notch1	I	A17 ^{-/-} monocytes	PMA	Brou <i>et al.</i> , 2000
	NPR	I	Neurons, Purkinje cells	TAPI2, PMA	Cho <i>et al.</i> , 2008
	p75NTR	C/I	A17 ^{-/-} CHO, A17 ^{-/-} MEF	PMA	Weskamp <i>et al.</i> , 2004
	PTP-LAR	I	ADAM17 ^{ΔZn/ΔZn} fibroblasts	PMA	Ruhe <i>et al.</i> , 2006
	Ptprz	C/I	A17 ^{-/-}	PMA, A17 GM6001	Chow <i>et al.</i> , 2008
	SDC1	C/I	ECV304, A549	PMA	Pruessmeyer <i>et al.</i> , 2010
	SDC4	C/I	ECV304, A549	PMA	Pruessmeyer <i>et al.</i> , 2010
	SORCS1	C/I	transfected CHO cells	PMA	Hermey <i>et al.</i> , 2006
	SORCS3	C/I	transfected CHO cells	PMA	Hermey <i>et al.</i> , 2006
	SORL1	I	A17 ^{-/-} CHO	PMA	Guo <i>et al.</i> , 2002
	SORT1	I	transfected CHO cells	PMA	Hermey <i>et al.</i> , 2006
	TNF-R _I	I	A17 ^{ΔZn/ΔZn} EC2	PMA	Reddy <i>et al.</i> , 2000
TNF-R _{II}	I			Peschon <i>et al.</i> , 1998	

	trkA (NGFA)	I	trkA transfected PC12 and CHO cells	PMA	Díaz-Rodríguez <i>et al.</i> , 1999
adhesion molecules	ALCAM	C	CHO/M2 cells	BB-94	Bech-Serra <i>et al.</i> , 2006
	CD44	C/I	OVMz, SKOV3ip	PMA, APMA	Stoek <i>et al.</i> , 2006
	CD62L				Peschon <i>et al.</i> , 1998
	Collagen XVII	(C?)/I	human keratinocytes, murine ADAM17 ^{ΔZn/ΔZn} keratinocytes	PMA, various MP inhibitors	Franzke <i>et al.</i> , 2002
	Desmoglein-2	C	CHO/M2 cells	BB-94	Bech-Serra <i>et al.</i> , 2006
	EpCAM	C	FaDu	siRNA,	Maetzel <i>et al.</i> , 2009
	ICAM-1	C/I	HEK293 _{ICAM1}	TIMP-3, PMA, siRNA	Tsakadze <i>et al.</i> , 2006
	JAM-A	C/I	HEK293, A17 ^{-/-} MEFs	PMA, GW, GI	Koenen <i>et al.</i> , 2009
	L1-CAM	C/I	A17 ^{-/-} EC2 cells	GW, GI, PMA	Maretzky <i>et al.</i> , 2005b
	NCAM-1	C	Neuro 2a, CHO, A17 ^{-/-} MEFs	GM6001	Kalus <i>et al.</i> , 2006
	Nectin-4	C/I	CHO	GM6001, TAPI-1, PMA, TIMPs	Fabre-Lafay <i>et al.</i> , 2005
	VCAM-1	I	NIH3T3 _{VCAM1}	PMA	Garton <i>et al.</i> , 2003
others	APLP2	C	SH-SY5Y	siRNA, insulin, IGF-1	Jacobsen <i>et al.</i> , 2010
	APP	I	ADAM17 ^{-/-} MEFs	PMA, IC3	Buxbaum <i>et al.</i> , 1998
	C4.4A	C	MCF	siRNA	Esselens <i>et al.</i> , 2008
	CA9	C/I	CGL3 cells	PMA, BB-94	Zatovicova <i>et al.</i> , 2005
	CD163	I	HEK293	PMA, TIMP-3	Etzerodt <i>et al.</i> , 2010
	GP	C	RK-13 cells	TAPI-1, ...	Dolnik <i>et al.</i> , 2004
	Klotho	C/I	COS-7	Insulin, TIMP-3	Chen <i>et al.</i> , 2007
	Mepripin-β	I	Transfected COS-1 cells	PMA	Hahn <i>et al.</i> , 2003
	MUC-1	C/I	HES cells	PMA	Thathiah <i>et al.</i> , 2003
	Pmel17	C	B16-F0 melanoma cells	TAPI-2, siRNA	Kummer <i>et al.</i> , 2009
	PrPc	C	A17 ^{-/-} MEFs, A17 HEK293	---	Vincent <i>et al.</i> , 2001
	Vasorin	C	MCF-7 cells	BB-94	Malapeira <i>et al.</i> , 2010

However, one has to keep in mind that many of the known substrates have been identified in a variety of different cellular systems and by different experimental approaches [Gooz, 2010]. For instance, shedding of HB-EGF has been investigated in ADAM17 knock-out MEF cells in presence of PMA [Sunnarborg *et al.*, 2002]. Semaphorin 4D has been identified as PMA-induced substrates in platelets derived from TACE^{ΔZn/ΔZn} mice [Zhu *et al.*, 2007]. ACE2 was identified as an ADAM17 substrate in ACE2-transfected HEK293 cells, treated with PMA and different metalloprotease inhibitors [Lambert *et al.*, 2005]. In addition, CHO cells have

been transfected with human protein sequences, to elucidate ADAM17-mediated shedding of SORCS1 and SORCS3 in presence and absence of PMA [Hermey *et al.*, 2006]. As an exception, the group of Joaquin Arribas identified several substrates of ADAM10 and ADAM17 on tumor-derived cell lines, treated with BB-94 or ADAM17 RNAi, renouncing the use of PMA [Bech-Serra *et al.*, 2006; Esselens *et al.*, 2008; Malapeira *et al.*, 2010]. Moreover, they identified Desmoglein-2 as an ADAM substrate in a 2D-DiGE approach on cell culture supernatant proteins [Bech-Serra *et al.*, 2006].

1.4.5 ADAM17 in health and disease

Although ADAM10 and ADAM17 have a rather bad reputation for promoting pro-inflammatory signaling events (e.g. shedding of TNF α , IL-6 and IL-15R), they also exert protective effects in neuronal differentiation, regeneration and neurodegeneration (e.g. APP processing, shedding of N-cadherin and ephrins). Thus, ADAM17 can take good and bad roles in health and disease, depending on the substrates and their specific functions [Pruessmeyer and Ludwig, 2008].

Upregulation of ADAM17 on various levels of its biosynthetic pathway has been reported to play an important role in a variety of diseases, especially in cancer. Thus, ADAM17 appears to be over-expressed on protein level in human breast cancer [Santiago-Josefat *et al.*, 2007], leading to an increased maturation of proTGF α by increased shedding [Borrell-Pages *et al.*, 2003; Kenny and Bissell, 2007]. Thus, increased shedding of TGF α is associated with tumor progression and metastasis [McGowen *et al.*, 2008]. Moreover, by upregulation of ADAM17 in synovial cells, ADAM17 contributes to rheumatoid arthritis in association with HIF-1 expression [Charbonneau *et al.*, 2007]. In the case of multiple sclerosis, ADAM17 is upregulated in blood vessels, macrophages and astrocytes [Plumb *et al.*, 2006]. Finally, in response to LDL, monocytes from diabetic patients also show increased levels of ADAM17 in contrast to non-diabetic control individuals [Worley *et al.*, 2007].

Increased levels of ADAM17 are also associated with various inflammatory diseases. Thus, ADAM17 levels are elevated in whole cartilage and chondrocytes in patients with osteoarthritis [Patel *et al.*, 1998; Amin, 1999] and in synovial tissues of patients with rheumatoid arthritis [Ohta *et al.*, 2001]. As mentioned, ADAM17 modulates the adherence of leukocytes by shedding of L-Selectin [Peschon *et al.*, 1998] in macrophages [Wang *et al.*,

2009b; Condon *et al.*, 2001]. Furthermore, ADAM17 modulates leukocyte migration, attachment and diapedesis by shedding of CX3CL1/Fractalkine [Garton *et al.*, 2001], V-CAM [Garton *et al.*, 2003], ICAM-1 [Tsakadze *et al.*, 2006] and JAM-1 [Koenen *et al.*, 2009]. The natural inhibitor TIMP-3 has been reported to act in a balancing manner on ADAM17 activity during inflammatory responses as evidenced from TIMP3^{-/-} mice [Mahmoodi *et al.*, 2005; Smookler *et al.*, 2006; Sahebjam *et al.*, 2007]. In contrast to these findings, ADAM17-mediated shedding of CSF-1 from activated macrophages [Rovida *et al.*, 2001], as well as IL-15R α [Kahawam *et al.*, 2009] and IL-6R α [Marin *et al.*, 2002] also implicate an anti-inflammatory role of ADAM17 [Gooz, 2010].

Regarding Alzheimer's disease, together with ADAM9 and ADAM10, ADAM17 is discussed as an α -secretase on the amyloid precursor protein (APP). Thereby, the balance of the APP metabolism is altered to the non-amyloidogenic pathway, which prevents the outcome of Alzheimer's disease [Allinson *et al.*, 2003].

In addition, ADAM17 has also been reported to contribute in a variety of other diseases including sepsis [Horiuchi *et al.*, 2007], inflammatory bowel disease [Cesaro *et al.*, 2009], psoriasis [Moriyama *et al.*, 2004; Kawaguchi *et al.*, 2005; Guinea-Viniegra *et al.*, 2009], multiple sclerosis [Seifert *et al.*, 2002], angiogenesis [Rundhaug, 2005], atherosclerosis [Canault *et al.*, 2006a], diabetes [Togashi *et al.*, 2002] and nephropathy [Dell *et al.*, 2001; Nemo *et al.*, 2005; Kassiri *et al.*, 2009].

1.4.6 Experimental systems in ADAM17 research

In contrast to other proteases (e.g. caspases), ADAM17 does not seem to prefer a defined consensus cleavage site. Although ADAM17 shows a preference for certain amino acid compositions of its substrates, structural aspects of both, ADAM17 and its substrates, as well as membrane proximity seem to have a crucial influence on shedding activity [e.g. White, 2003]. However, these aspects preclude possibilities for identification of unknown ADAM17 substrates that have been used in degradome studies for caspases [compare Lee *et al.*, 2004; Jang *et al.*, 2008] or matrix metalloproteases [compare Bajor *et al.*, 2012]. This includes *in silico* approaches, targeting consensus cleavage sites and *in vitro* approaches like treating complex protein extracts with recombinant proteases.

Several approaches have been used to study the effects of different ADAMs, including knock-down by siRNA or shRNA, increase or decrease of ADAM activity by using different, more or less specific and effective stimuli and inhibitors. However, especially investigations on ADAM10 and ADAM17 have predominantly been made with *in vitro* approaches, as a knock-out of both ADAM10 [Hartmann *et al.*, 2002] and ADAM17 [Zhao *et al.*, 2001] is lethal at embryonic or perinatal developmental stages.

Widely distributed among ADAM research are experiments based on stimulating or inhibiting protease activity using more or less specific compounds. Among these compounds, the phorbol ester PMA is a predominant stimulus, although it is neither physiologic, nor specific for ADAM17 [Gooz, 2010]. An overview on the compounds, most commonly used in metalloprotease research is given in table 1.2.

Tab. 1.2.: Overview on inhibitors and stimuli used in metalloproteases research.

compound	stimulus / inhibitor	way of action	specificity	natural	reference
TPA (=PMA)	stimulus	PKC activation	none	no	Castagna <i>et al.</i> , 1982
ionomycin	stimulus	Ca ²⁺ ionophore	none	no	e.g. Le Gall <i>et al.</i> , 2009
GI254023X	inhibitor	blocking catalytic site	ADAM10	no	Hoettecke <i>et al.</i> , 2010
GW280264X	inhibitor	blocking catalytic site	ADAM10 and ADAM17	no	
Marimastat	inhibitor	mimicking natural MMPI peptides	broad-spectrum MMP	no	Millar <i>et al.</i> , 1998
Batimastat	inhibitor	mimicking natural MMPI peptides	broad-spectrum MMP	no	Steinman <i>et al.</i> , 1998
BzATP	stimulus	activation of P2X7 receptor	ADAM10/17 activator	no	Le Gall <i>et al.</i> , 2009
LPS	stimulus	cell activation via TLR4	none	yes	---
TAPI	inhibitor	blocking catalytic site	ADAM17 and MMPs	no	Mohler <i>et al.</i> , 1994
TIMP3	inhibitor	blocking catalytic site	ADAM17, ADAM10, MMPs	yes	Uria <i>et al.</i> , 1994

However, a variety of overexpression experiments have been performed. Interestingly, cloning of the human ADAM17 gene was not possible for years and human cells have been transfected with ADAM17 overexpression constructs originating from *Mus musculus*, *Rattus norvegicus*, *Gallus gallus* or *Bos tauris*. These experiments are disputable, as the ADAM17 sheddome of different species have been reported to be similar, but not identical [e.g. Garbers *et al.*, 2011]. Moreover, transfected ADAM17 appeared to be processed differentially than its endogenous counterpart [Borroto *et al.*, 2003], indicating that

transfection experiments are also inadequate to study the endogenous situation [Goetz, 2010].

1.4.7 The murine hypomorphic ADAM17^{ex/ex} model

Previously, in the Institute for Biochemistry, a hypomorphic mouse model, showing barely detectable levels of ADAM17 in all tissues has been established [Chalaris *et al.*, 2009]. Briefly, an additional exon, which starts with an in-frame stop codon, has been inserted into the ADAM17 encoding gene sequence (Fig. 1.7 A).

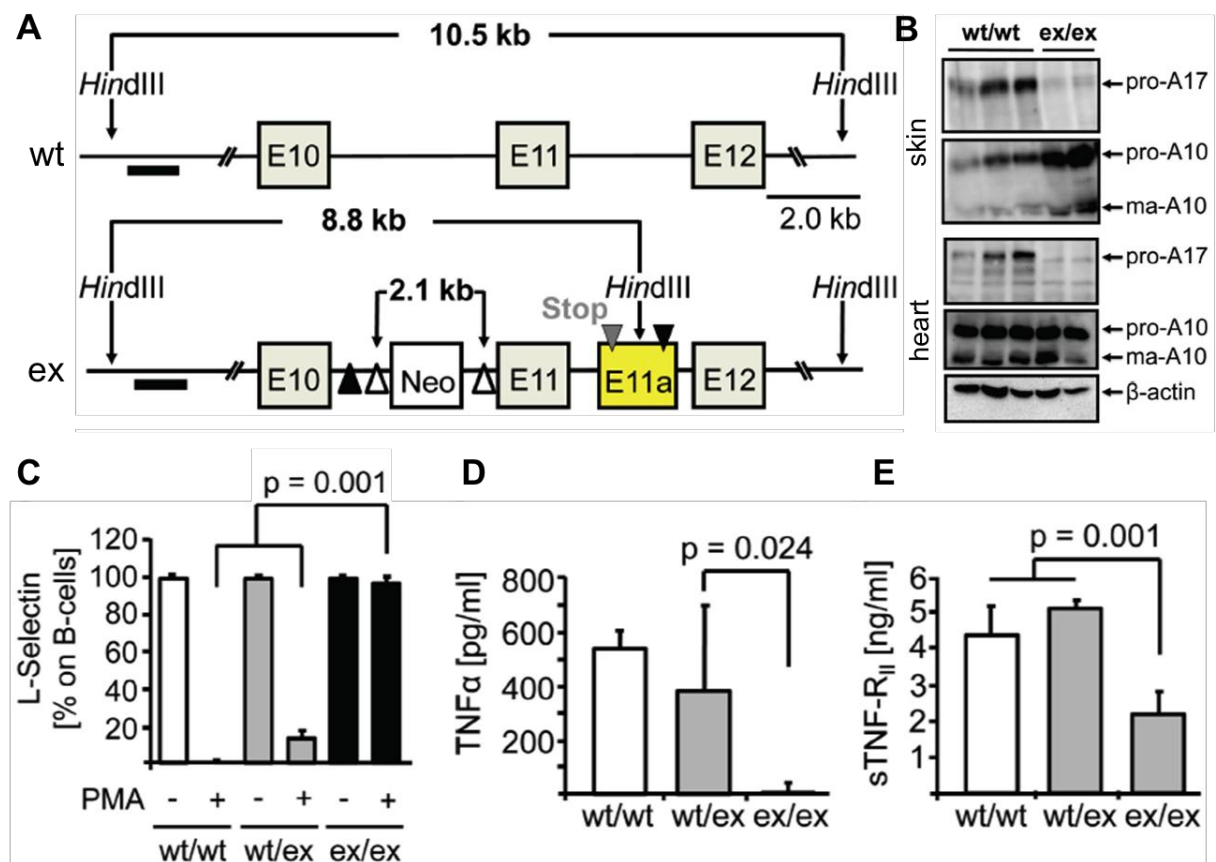


Fig. 1.7: The ADAM17 hypomorphic mouse model (ADAM17^{ex/ex}). **(A)** Scheme for targeting the ADAM17 gene by the Exon Induced Translational Stop (EXITS) strategy. Open arrowheads denote FLP recombinase sites, and LoxP sites are indicated by closed arrowheads. The altered allele contains an artificial exon starting with an in-frame translational stop codon placed downstream of exon 11. The artificial exon (E11a, yellow) containing the stop codon is flanked by noncanonical splice donor and acceptor sites. **(B)** ADAM10 and ADAM17 Western blots of tissue samples from skin and heart. **(C)** Shedding of L-selectin from B cells. **(D)** Shedding of proTNFα from spleen cells. **(E)** Serum levels of sTNF-R_{II}. Figures were taken and rearranged from Chalaris *et al.*, 2010.

The exon induced translational stop (EXITS) strategy leads to a severe decrease in ADAM17 protein levels, as 95 % of cellular mRNA includes the additional exon, leading to a precocious abrogation of the translation process. Therefore, cells and tissues derived from ADAM17^{ex/ex} mice only show very low ADAM17 protein levels (Fig. 1.7 B). In contrast to ADAM17^{-/-} mice,

ADAM17^{ex/ex} mice are viable and fertile, but show severe defects in a variety of tissues, including heart, eyes, skin and hair, similar to TGF α ^{-/-} mice [Chalaris *et al.*, 2010]. Moreover, a clear reductions in ADAM17-mediated shedding of L-selectin, TNF α and TNF-R_{II} could be observed (Fig. 1.7 C – E) and a decrease in ADAM17-maturated amphiregulin EGF receptor ligands might be responsible for the reduced milk duct development in female individuals as well as for the increased susceptibility to DSS-induced colitis [Chalaris *et al.*, 2010]. As already mentioned, the reported ADAM17 degradome was investigated using divers cellular systems and different experimental approaches [Gooz, 2010]. Thus, the ADAM17^{ex/ex} hypomorphic mouse system might be a potent tool to study the effects of a loss of ADAM17 activity *in vivo*.

The elucidation of ADAM17-dependent, proteome-wide changes in cells and tissues of wild-type and ADAM17^{ex/ex} mice using an unbiased, gel-based proteomic approach was the major aim of this project. At initial stages of this project, murine embryonic fibroblasts (MEFs) from wild-type and ADAM17^{ex/ex} mice were available and used to adapt and enhance suitable approaches for this proteomic study prior to the investigation of the effects of ADAM17 in tissue-derived cell. In case of cultured cells, ectodomain shedding leads to the accumulation of shed protein fragments within the supernatant of cultured cells. Thus, a variety of recent studies analyzed metalloprotease-dependent alterations of cell culture supernatant proteins by gel-based proteomic approaches, including two-dimensional difference gel electrophoresis (2D-DiGE). For instance, supernatant proteins of PMA-treated DRM ADAM17^{-/-} enriched by lectin-mediated precipitation revealed several substrates of ADAM17 including the “macrophage colony stimulating factor 1” (M-CSF-1) and the “interleukin-6 receptor” (IL-6R) [Guo *et al.*, 2002]. In addition, ADAM17-dependent alterations of desmoglein-2 shedding were observed in breast cancer cells, treated with broad-spectrum metalloprotease inhibitors by 2D-DiGE [Bech-Serra *et al.*, 2006].

2 Aim of this thesis

The general aim of this work was the characterization of ADAM17-dependent, proteome-wide changes in cells and tissues upon loss of ADAM17 activity in an unbiased proteomic approach. Specifically, the following questions were to be addressed.

- (I) Do MEF cells from wild-type and ADAM17^{ex/ex} mice differ in their capacity to release cell surface proteins?
- (II) Which proteins are differentially shed or secreted in the presence or absence of ADAM17?
- (III) Is this model based on the analysis of murine embryonic fibroblasts suited to analyze the ADAM17 sheddome?

Based on the initial analyses of culture supernatants from MEF populations, a proof of principle for the methodological approach was required to address whether or not the 2D-DiGE strategy would allow the detection of known ADAM17 substrates.

- (IV) Can one detect differential processing of TNF α in wild-type and ADAM17^{ex/ex} MEF cells following overexpression of an established substrate?

Moreover, as part of the Z2 unit of the SFB877, method development was one of the major tasks of the project, especially regarding the enrichment of plasma membrane proteins or the analysis of extracellular matrix proteins by electrophoresis.

- (V) How to enrich plasma membrane-associated proteins prior to 2D-DiGE analyses?
- (VI) Could lectins be used to enrich glycosylated plasma membrane proteins?
- (VII) Which electrophoresis protocols are suited for the analysis of membrane proteins in combination with differential fluorescence labelling?

3 Materials

3.1 Cells

Most experiments were performed on wild-type (MEF 1#3, 1#7, 2#1) and ADAM17^{ex/ex} (MEF 1#1, 1#8, 2#8) murine embryonic fibroblasts (MEFs). These cells were generated and kindly provided by Dr. Athena Chalaris (Institute for Biochemistry, CAU Kiel). MEF cells were routinely cultured in MEF-10 medium (DMEM medium, supplemented with 1 % (v/v) penicillin/streptomycin, 2 mM L-glutamine, 110 mg/ml sodium pyruvate and 10 % (v/v) FBS).

3.2 Antibodies

The following table (Tab. 3.1) summarizes all antibodies that have been used within this work. In addition, information about working concentrations, epitopes, manufacturers and application are also provided.

Tab. 3.1: Overview on used antibodies.

antibody	clone	origin	concentration [mg/ml]	application	dilution	manufacturer
Annexin A2	---	rabbit	1.00	WB	1:1000	abcam
Bip/GRP78	40	mouse	0.25	WB	1:250	BD
BMP-1	---	rabbit	0.20	WB	1:500	Santa Cruz
Cathepsin B	---	rat	1.0	WB	1:1000	R&D
Cofilin	D3F9	rabbit	1.0	WB	1:1000	CellSignaling
COL1 α 1 (C-Pro)	LF-41	rabbit	1.00	WB	1:1000	Fisher <i>et al.</i> , 1989a
COL1 α 1 (C-telo)	LF-68	rabbit	1.00	WB	1:1000	Bernstein <i>et al.</i> , 1995b
COX IV	F-8	mouse	0.20	WB	1:1000	Santa Cruz
ECM-1	H-300	rabbit	0.20	WB	1:250	Santa Cruz
Fibronectin	IST-9	mouse	0.20	WB	1:500	Santa Cruz
Flotilin-2	29	mouse	0.25	WB	1:1000	BD
Galectin-3	9C4	mouse	0.20	WB	1:500	SantaCruz
GAPDH	6C5	rabbit	0.25	WB	1:2000	Trevigen
HtrA1	---	rabbit	0.25	WB	1:500	biorbyt

Integrin α 2	H-293	rabbit	0.20	WB	1:500	Santa Cruz
LAMP-1	25	mouse	0.25	WB	1:500	BD
mADAM10	10.2	rabbit	1.00	WB	1:1000	AG Chalaris
mADAM17	18.2	rabbit	1.00	WB, CLSM	1:1000	AG Chalaris
mADAM17	10.1	rabbit	1.00	WB, CLSM	1:1000	AG Chalaris
MMP-2		rabbit	0.20	WB	1:500	Santa Cruz
Mouse IgG2a, HRP-linked	IgG2a	rabbit	1.00	WB	1:10000	Cell Signaling
Nucleolin	- - -	rabbit	1.00	WB	1:1000	Abcam
Nucleophosmin	EP1848Y	rabbit	1.00	WB	1:1000	Abcam
pCofilin	S3	rabbit	1.00	WB	1:1000	CellSignaling
pCofilin (Ser3)	S3	rabbit	1.00	WB	1:1000	Cell Signaling
PCPE-1	7A11/1	mouse	0.20	WB	1:250	Santa Cruz
Periostin	H-300	rabbit	0.20	WB	1:250	Santa Cruz
Perlecan		rat	0.20	WB	1:500	Santa Cruz
Pro-COL1A1	A-17	goat	0.20	WB	1:500	Santa Cruz
Rabbit IgG, HRP-linked	IgG	mouse	1.00	WB	1:5000	Cell Signaling
Rat IgG, HRP-linked	IgG	rabbit	1.00	WB	1:5000	Cell Signaling
Vimentin	RV202		1.00	WB	1:1000	Abcam
Vinculin	SPM227	mouse	0.20	WB	1:1000	Abcam
β -actin	- - -	rabbit	0.25	WB	1:1000	Cell Signaling

3.3 Reagents, buffers and media

3.3.1 Cell biology

DMEM medium

L-glutamine (200 mM)

FBS (heat-inactivated and sterilized by filtration)

penicillin/streptomycin (10^4 U / 10^4 μ g/ml)

Trypsin/EDTA (0.5 % / 0.2 % (w/v))

PBS

sodium pyruvate (110 mg/l)

Biochrom AG, Berlin, GER

Biochrom AG, Berlin, GER

Invitrogen, Carlsbad, USA

Biochrom AG, Berlin, GER

Biochrom AG, Berlin, GER

Biochrom AG, Berlin, GER

Sigma-Aldrich, St. Luis, USA

3.3.4 Molecular biology

polymerase chain reaction:

DreamTaq polymerase
dNTPs
customized oligonucleotides

Thermo Scientific, Karlsruhe, GER
Thermo Scientific, Karlsruhe, GER
MWG Biotech, Ebersberg, GER

agarose electrophoresis:

agarose
ethidium bromide
50x TAE buffer
242 g/l Tris
5.7 % (v/v) glacial acetic acid
50 mM EDTA, pH 8.0
1 kb DNA ladder

Invitrogen, Carlsbad, USA
Carl Roth, Karlsruhe, GER
Merck KGaA, Darmstadt, GER
Carl Roth, Karlsruhe, GER
Merck KGaA, Darmstadt, GER
New England Biolabs, Ipswich, USA

3.3.5 Cell lysis buffers

NP40 lysis buffer:

1 % (v/v) Nonidet[®] P40
20 mM tris base
150 mM NaCl
2 µg/ml aprotinin
2 µg/ml leupeptin
1 mM PMSF
1 mM Na₃VO₄
10 mM NaF
1 mM Na₂P₂O₇
2 µg/ml pepstatin A

Sigma-Aldrich, St. Luis, USA
Merck KGaA, Darmstadt, GER
Merck KGaA, Darmstadt, GER
Sigma-Aldrich, St. Luis, USA
Sigma-Aldrich, St. Luis, USA
Sigma-Aldrich, St. Luis, USA
Merck KGaA, Darmstadt, GER
Sigma-Aldrich, St. Luis, USA
Sigma-Aldrich, St. Luis, USA
Sigma-Aldrich, St. Luis, USA

RIPA Lysis Buffer:

1 % (v/v) Nonidet[®] 40
50 mM tris base
150 mM NaCl
1 % (w/v) DOC
2 % (w/v) SDS
2 µg/ml aprotinin
2 µg/ml leupeptin
1 mM PMSF
1 mM Na₃VO₄
10 mM NaF
1 mM Na₂P₂O₇
2 µg/ml pepstatin A

Sigma-Aldrich, St. Luis, USA
Merck KGaA, Darmstadt, GER
Merck KGaA, Darmstadt, GER
Sigma-Aldrich, St. Luis, USA
Sigma-Aldrich, St. Luis, USA
Sigma-Aldrich, St. Luis, USA
Sigma-Aldrich, St. Luis, USA
Sigma-Aldrich, St. Luis, USA
Merck KGaA, Darmstadt, GER
Sigma-Aldrich, St. Luis, USA
Sigma-Aldrich, St. Luis, USA
Sigma-Aldrich, St. Luis, USA

DOC Lysis Buffer:

2 % (v/v) DOC
20 mM tris base
2 mM EDTA

Sigma-Aldrich, St. Luis, USA
Merck KGaA, Darmstadt, GER
Merck KGaA, Darmstadt, GER

2 mM iodoacetamide	GE Healthcare, Uppsala, SWE
2 µg/ml aprotinin	Sigma-Aldrich, St. Luis, USA
2 µg/ml leupeptin	Sigma-Aldrich, St. Luis, USA
1 mM PMSF	Sigma-Aldrich, St. Luis, USA
1 mM Na ₃ VO ₄	Merck KGaA, Darmstadt, GER
10 mM NaF	Sigma-Aldrich, St. Luis, USA
1 mM Na ₂ P ₂ O ₇	Sigma-Aldrich, St. Luis, USA
2 µg/ml pepstatin A	Sigma-Aldrich, St. Luis, USA

2D lysis buffer:

7 M urea	GE Healthcare, Uppsala, SWE
2 M thiourea	GE Healthcare, Uppsala, SWE
4 % (w/v) CHAPS	Merck KGaA, Darmstadt, GER
30 mM tris base	Merck KGaA, Darmstadt, GER

Solution adjusted to pH 8.5 prior to supplement of CHAPS. Buffer was stored at -20 °C until use and was supplemented with Roche Complete Protease Inhibitor.

3.3.6 Protein biochemistry

Bradford reagent Thermo Scientific, Karlsruhe, GER

3x reducing sample buffer (Protean II system):

6 % (w/v) SDS	Merck KGaA, Darmstadt, GER
30 % (v/v) glycerol	Merck KGaA, Darmstadt, GER
200 mM tris base, pH 6.8	Merck KGaA, Darmstadt, GER
2 % (v/v) 2-mercaptoethanol	Merck KGaA, Darmstadt, GER
0.005 % (w/v) bromophenol blue	Merck KGaA, Darmstadt, GER

15 % SDS running gel (Protean II system):

15.0 ml 30 % acrylamide/0.8 % bisacrylamide	Carl Roth, Karlsruhe, GER
11.2 ml 1 M tris base, pH 8.8	Merck KGaA, Darmstadt, GER
0.3 ml 10 % (w/v) SDS	SERVA, Heidelberg, GER
3.7 ml <i>aqua ad injectabilia</i>	Braun, Meslungen, GER
0.1 ml 20 % (w/v) APS	Merck KGaA, Darmstadt
0.02 ml TEMED	GE Healthcare, Uppsala, SWE

12.5 % SDS running gel (Protean II system):

12.5 ml 30 % acrylamide/0.8 % bisacrylamide	Carl Roth, Karlsruhe, GER
11.2 ml 1 M tris base, pH 8.8	Merck KGaA, Darmstadt, GER
0.3 ml 10 % (w/v) SDS	SERVA, HEIDELBERG, GER
6.2 ml <i>aqua ad injectabilia</i>	Braun, Meslungen, GER
0.1 ml 20 % (w/v) APS	Merck KGaA, Darmstadt
0.02 ml TEMED	GE Healthcare, Uppsala, SWE

10 % SDS running gel (Protean II system):

10.0 ml 30 % acrylamide/0.8 % bisacrylamide	Carl Roth, Karlsruhe, GER
11.2 ml 1 M tris base, pH 8.8	Merck KGaA, Darmstadt, GER
0.3 ml 10 % (w/v) SDS	SERVA, Heidelberg, GER

8.7 ml <i>aqua ad injectabilia</i>	Braun, Meslungen, GER
0.1 ml 20 % (w/v) APS	Merck KGaA, Darmstadt
0.02 ml TEMED	GE Healthcare, Uppsala, SWE
<u>4 % SDS stacking gel (Protean II system):</u>	
1.67 ml 30 % acrylamide/0.8 % bisacrylamide	Carl Roth, Karlsruhe, GER
1.25 ml 1 M tris base, pH 6.8	Merck KGaA, Darmstadt, GER
0.1 ml 10 % (w/v) SDS	SERVA, Heidelberg, GER
7.0 ml <i>aqua ad injectabilia</i>	Braun, Meslungen, GER
0.05 ml 20 % (w/v) APS	Merck KGaA, Darmstadt
0.01 ml TEMED	GE Healthcare, Uppsala, SWE
<u>10x SDS running buffer (Protean II system):</u>	
30.3 g/l tris base	Merck KGaA, Darmstadt, GER
144.0 g/l glycine	Carl Roth, Karlsruhe, GER
1.0 g/l SDS	Merck KGaA, Darmstadt, GER
Low-Range Standard	Bio-Rad, Hercules, USA
Precision Plus Protein All Blue Standard	Bio-Rad, Hercules, USA
NuPAGE [®] LDS sample buffer (4x)	Invitrogen, Carlsbad, USA
NuPAGE [®] MES SDS running buffer (20x)	Invitrogen, Carlsbad, USA
DTT (0.85 M in sterile water)	Serva, Heidelberg, GER
<u>Coomassie staining solution:</u>	
100.0 g/l NH ₄ Cl	Carl Roth, Karlsruhe, GER
10 % (v/v) H ₃ PO ₄	Carl Roth, Karlsruhe, GER
20 % (v/v) methanol	Carl Roth, Karlsruhe, GER
1.2 g/l Coomassie Brilliant Blue (G-250)	Sigma-Aldrich, St. Luis, USA
<u>Coomassie destaining solution:</u>	
10 % (v/v) ethanol (96 %)	Carl Roth, Karlsruhe, GER
2 % (v/v) H ₃ PO ₄	Carl Roth, Karlsruhe, GER
<u>Western transfer buffer:</u>	
25 mM tris base	Merck KGaA, Darmstadt, GER
192 mM glycine	Merck KGaA, Darmstadt, GER
20 % (v/v) methanol	Carl Roth, Karlsruhe, GER
0.015 % (w/v) SDS	Merck KGaA, Darmstadt, GER
Ponceau S staining solution	Sigma-Aldrich, St. Luis, USA
<u>TBS (pH 7.5):</u>	
10 mM tris base	Merck KGaA, Darmstadt, GER
150 mM NaCl	Carl Roth, Karlsruhe, GER

TBS-T:

10 mM tris base	Merck KGaA, Darmstadt, GER
150 mM NaCl	Carl Roth, Karlsruhe, GER
0.05 % (v/v) Tween-20	Merck KGaA, Darmstadt, GER

Western blocking solution A:

100 mM tris base	Merck KGaA, Darmstadt, GER
2.2 % (w/v) NaCl	Carl Roth, Karlsruhe, GER
0.01 % (w/v) NaN ₃	Merck KGaA, Darmstadt, GER
5 % (w/v) BSA	Serva, Heidelberg, GER

Western blocking solution B:

10 mM tris base	Merck KGaA, Darmstadt, GER
150 mM NaCl	Carl Roth, Karlsruhe, GER
0.05 % (v/v) Tween-20	Merck KGaA, Darmstadt, GER
5 % (w/v) dry milk	Granovita, Lüneburg, GER

Stripping solution:

62.5 mM tris base, pH 8.8	Merck KGaA, Darmstadt, GER
2 % (v/v) 2-mercaptoethanol	Merck KGaA, Darmstadt, GER
6.9 % (w/v) SDS	Serva, Heidelberg, GER

ECL™ detection reagent

GE Healthcare, Buckinghamshire, UK

Zymography buffer I:

2.5 % (v/v) Triton X-100	Merck KGaA, Darmstadt, GER
<i>Aqua iniectionabilia</i>	Braun, Meslungen, GER

Zymography buffer II:

50 mM tris base	Merck KGaA, Darmstadt, GER
150 mM NaCl	Carl Roth, Karlsruhe, GER
10 mM CaCl ₂	Carl Roth, Karlsruhe, GER
5 mM NaN ₃	Carl Roth, Karlsruhe, GER
<i>Aqua iniectionabilia</i>	Braun, Meslungen, GER

Adjust pH to 7.8 by addition of concentrated hydrochloric acid.

3.3.7 Two-dimensional gel electrophoresis (2D-IEF/SDS-PAGE)10 % SDS running gel (2nd dimension):

15.0 ml 30 % acrylamide/0.8 % bisacrylamide	Carl Roth, Karlsruhe, GER
11.2 ml 1.5 M tris base, pH 8.8	Merck KGaA, Darmstadt, GER
0.3 ml 10 % (w/v) SDS	SERVA, Heidelberg, GER
3.7 ml <i>aqua ad iniectionabilia</i>	Braun, Meslungen, GER
0.1 ml 20 % (w/v) APS	Merck KGaA, Darmstadt
0.02 ml TEMED	GE Healthcare, Uppsala, SWE

12.5 % SDS running gels (2nd dimension):

15.0 ml 30 % acrylamide/0.8 % bisacrylamide	Carl Roth, Karlsruhe, GER
11.2 ml 1.5 M tris base, pH 8.8	Merck KGaA, Darmstadt, GER
0.3 ml 10 % (w/v) SDS	SERVA, Heidelberg, GER
3.7 ml <i>aqua ad injectabilia</i>	Braun, Meslungen, GER
0.1 ml 20 % (w/v) APS	Merck KGaA, Darmstadt
0.02 ml TEMED	GE Healthcare, Uppsala, SWE

2D lysis buffer:

7 M urea	GE Healthcare, Uppsala, SWE
2 M thiourea	GE Healthcare, Uppsala, SWE
4 % (w/v) CHAPS	Merck KGaA, Darmstadt, GER
30 mM tris base	Merck KGaA, Darmstadt, GER

Solution adjusted to pH 8.5 prior to supplement of CHAPS. Buffer was stored at -20 °C until use and was supplemented with Roche Complete Protease Inhibitor.

2D-DiGE Sample Buffer:

7 M urea	GE Healthcare, Uppsala, SWE
2 M thiourea	GE Healthcare, Uppsala, SWE
4 % (w/v) CHAPS	Merck KGaA, Darmstadt, GER

Solution was stored at -20 °C until use and supplemented with:

2 % (w/v) DTT	Serva, Heidelberg, GER
2 % (v/v) IPG buffer	GE Healthcare, Uppsala, SWE

2D-SDS Running Buffer (10-fold solution):

250 mM tris base	Merck KGaA, Darmstadt, GER
1.92 M glycine	Merck KGaA, Darmstadt, GER
0.1 % (w/v) SDS	Merck KGaA, Darmstadt, GER

APS solution:

ammonium persulfate	Merck KGaA, Darmstadt, GER
<i>Aqua iniectabilia</i>	Braun, Meslungen, GER

Solution is stored as 1 ml aliquots at -20 °C until use.

Displacing Solution:

25 % (v/v) tris base (1.5 M, pH 8.8)	Merck KGaA, Darmstadt, GER
50 % (v/v) glycerol (98 %)	Carl Roth, Karlsruhe, GER
0.005 % (w/v) bromophenol blue	GE Healthcare, Uppsala, SWE
25 % (v/v) <i>aqua ad injectabilia</i>	Braun, Meslungen, GER

This solution is stored at 4°C until use.

Equilibration Solution:

5 % (v/v) tris base (1.5 M, pH 8.8)	Merck KGaA, Darmstadt, GER
-------------------------------------	----------------------------

6 M urea	Carl Roth, Karlsruhe, GER
30 % (v/v) glycerol (98 %)	Carl Roth, Karlsruhe, GER
2 % (w/v) SDS	SERVA, Heidelberg, GER
0.005 % (w/v) bromophenol blue	GE Healthcare, Uppsala, SWE
<i>ad 100 ml aqua ad injectabilia</i>	Braun, Meslungen, GER

This solution is stored as 10 ml aliquots at 4 °C. Prior to use, two aliquots are supplemented with 100 mg dithiotreitol or 250 mg iodoacetamide, respectively.

Flamingo™ fixation buffer:

40 % (v/v) ethanol (99 %, undenatured)	Carl Roth, Karlsruhe, GER
10 % (v/v) acetic acid (100 %)	Carl Roth, Karlsruhe, GER
50 % (v/v) <i>aqua ad injectabilia</i>	Braun, Meslungen, GER

Flamingo™ staining solution:

10 % (v/v) Flamingo™ Fluorescent Gel Stain (10x)	Bio-Rad, Hercules, USA
90 % (v/v) <i>aqua ad injectabilia</i>	Braun, Meslungen, GER

Lower Chamber Buffer (LBC buffer):

25 mM tris base	Merck KGaA, Darmstadt, GER
0.192 M glycine	Merck KGaA, Darmstadt, GER
0.01 % (w/v) SDS	Merck KGaA, Darmstadt, GER

LBC buffer is made from 10x 2D-SDS running buffer by dilution in a one to ten ratio.

Low-melting agarose:

0.5 % (w/v) low-melting agarose	Thermo Scientific
0.005 % (w/v) bromophenol blue	GE Healthcare, Uppsala, SWE

Components are suspended in UCB-buffer, brought to a final volume of 20 ml and heated in a microwave oven until agarose is completely solved. Low-melting agarose mixture is stored at 4 °C until use.

Lysin Solution:

L-lysine	SERVA, Heidelberg, GER
----------	------------------------

1.5 M Tris Solution:

1.5 M tris base	Merck KGaA, Darmstadt, GER
-----------------	----------------------------

Tris base is solved in 700 ml of *Aqua iniectabilia* and pH is adjusted to 8.8 by addition of an appropriate amount of 37 % hydrochloric acid solution. Finally, volume is adjusted to 1000 ml and the solution is stored at 4 °C until use.

Upper Chamber Buffer (UCB buffer):

50 mM tris base	Merck KGaA, Darmstadt, GER
0.384 M glycine	Merck KGaA, Darmstadt, GER
0.02 % (w/v) SDS	Merck KGaA, Darmstadt, GER

UCB buffer is made from 10x 2D-SDS running buffer by dilution in a one to five ratio.

3.3.8 2D-CTAB/SDS-PAGE

CTAB Gel Buffer I:

300 mM KH₂PO₄

Carl Roth, Karlsruhe, GER

Substance is dissolved in 350 ml *Aqua iniectionabilis* and pH is adjusted to 2.1 by adding an appropriate amount of phosphoric acid (85 %).

CTAB Gel Buffer II:

500 mM KH₂PO₄

Carl Roth, Karlsruhe, GER

Substance is dissolved in 350 ml *Aqua iniectionabilis* and pH is adjusted to 4.1 by adding an appropriate amount of phosphoric acid.

CTAB Running Buffer:

0.192 M glycine

Merck KGaA, Darmstadt, GER

50 mM H₃PO₄

Carl Roth, Karlsruhe, GER

0.25 % CTAB

Carl Roth, Karlsruhe, GER

CTAB Sample Buffer:

4.5 M urea

Carl Roth, Karlsruhe, GER

10 % CTAB

Carl Roth, Karlsruhe, GER

15 % (v/v) glycerol (98 %)

Carl Roth, Karlsruhe, GER

0.005 % (w/v) Pyronine Y

Sigma-Aldrich, St. Luis, USA

Mix urea, CTAB and glycerole with 4 ml of *Aqua iniectionabilis*. Carefully heat the paste-like mixture in a microwave oven, until it is completely dissolved. Add DTT and Pyronin Y and bring the solution to a final volume of 10 ml. Store this 2-fold sample buffer at 60 °C until use.

CTAB/SDS-Equilibration Buffer:

2 % (w/v) SDS

Serva, Heidelberg, GER

1 M tris, pH 6.8

Merck KGaA, Darmstadt, GER

10 % (v/v) glycerol (98 %)

Carl Roth, Karlsruhe, GER

0.005 % (w/v) bromophenol blue

Sigma-Aldrich, St. Luis, USA

CTAB stacking gel (4 %):

1 g urea

Carl Roth, Karlsruhe, GER

1.76 ml 30 % acrylamide/0.8 % bisacrylamide

Carl Roth, Karlsruhe, GER

1.1 ml Gel B (2 % bisacrylamide)

Carl Roth, Karlsruhe, GER

2.5 ml CTAB gel buffer II

0.7 ml 25 mM CTAB

Carl Roth, Karlsruhe, GER

1.0 ml 80 mM L-ascorbic acid

Carl Roth, Karlsruhe, GER

80 µl 10 mM iron (II) sulfate

Carl Roth, Karlsruhe, GER

aqua ad iniectionabilis ad 10 ml

Braun, Meslungen, GER

5 µl 37 % hydrogen peroxide

Carl Roth, Karlsruhe, GER

CTAB separation gel (8 %):

7.2 g urea

Carl Roth, Karlsruhe, GER

10.0 ml 30 % acrylamide/0.8 % bisacrylamide

Carl Roth, Karlsruhe, GER

1.0 ml Gel B (2 % bisacrylamide)

Carl Roth, Karlsruhe, GER

10.0 ml CTAB gel buffer II	
5.0 ml 25 mM CTAB	Carl Roth, Karlsruhe, GER
2.5 ml 80 mM L-ascorbic acid	Carl Roth, Karlsruhe, GER
80 µl 10 mM iron (II) sulfate	Carl Roth, Karlsruhe, GER
<i>aqua ad injectabilia</i> ad 40 ml	Braun, Meslungen, GER
5 µl 37 % hydrogen peroxide	Carl Roth, Karlsruhe, GER

3.3.9 MALDI-ToF/ToF

1 M ABC Stock Solution:

1 M (NH ₄)HCO ₃	Carl Roth, Karlsruhe, GER
water (HPLC Gradient Grade)	Carl Roth, Karlsruhe, GER

250 mM ABC Stock Solution:

250 mM (NH ₄)HCO ₃	Carl Roth, Karlsruhe, GER
water (HPLC Gradient Grade)	Carl Roth, Karlsruhe, GER

Digester Solution 1:

50 % (v/v) methanol	Carl Roth, Karlsruhe, GER
50 mM (NH ₄)HCO ₃ (from 1 M stock)	Carl Roth, Karlsruhe, GER
50 % (v/v) water (HPLC Gradient Grade)	Carl Roth, Karlsruhe, GER

Digester Solution 2:

50 % (v/v) acetonitrile (with 0.1 % TFA)	Carl Roth, Karlsruhe, GER
50 % (v/v) water (HPLC Gradient Grade)	Carl Roth, Karlsruhe, GER

Solvent A:

65 % (v/v) acetonitrile (with 0.1 % TFA)	Carl Roth, Karlsruhe, GER
35 % (v/v) water (with 0.1 % TFA)	Carl Roth, Karlsruhe, GER

Lyophilized CHCA MALDI Matrix (LaserBio Labs, Sophia-Antipolis Cedex, FRA) is solved in 1.66 ml of Solvent A.

Trypsin solution:

10 µg/ml trypsin	Serva, Heidelberg, GER
25 mM (NH ₄)HCO ₃ (from 250 mM stock)	Carl Roth, Karlsruhe, GER

Lyophilized trypsin is dissolved in 2.5 ml of a 25 mM ABC solution, sonicated within a waterbath and immediately used for sample processing.

3.3.10 Buffers and reagents for Preparations of ECM Proteins

T-ECM-1 (Low-Salt ECM Buffer):

0.5 M sodium chloride	Carl Roth, Karlsruhe, GER
10 mM tris base	Carl Roth, Karlsruhe, GER

Dissolve components in 200 ml *Aqua iniectabilia*, adjust pH to 7.5 and bring the solution to a final volume of 250 ml. Solution has to be stored at 4 °C until use. Prior to use, protease inhibitors were freshly added.

3.4 Consumables

3.4.1 General laboratory consumables

Agarose-bound Wheat Germ Agglutinin	Vector Labs, Burlingame, USA
Amicon® Filter Unit (20 ml, 100 kDa MWCO)	Millipore, Darmstadt, GER
cell culture dish, 10 cm	Becton Dickinson, Heidelberg, GER
cell culture dish, 20 mm	NUNC, Roskilde, DK
cell culture plate (6-, 12-, 24-, 96-wells)	Sarstedt, Nümbrecht, GER
cell scraper	Sarstedt, Nümbrecht, GER
centrifugation tube (15 ml, 50 ml)	Sarstedt, Nümbrecht, GER
colibri tips	Kisker Biotech, Steinfurt, GER
Concanavalin A (biotinylated)	Sigma-Aldrich, München, GER
coverslips	Carl Roth, Karlsruhe, GER
CryoTube™	NUNC, Roskilde, DK
Falcon Tubes (15, 50 ml)	Greiner, Frickenhausen, GER
Feather® scalpels	Feather, Osaka, JPN
glass slide	Carl Roth, Karlsruhe, GER
Hyperfilm™ ECL chemiluminescence film	GE Healthcare, Buckinghamshire, UK
Microlance® syringe	Becton Dickinson, Heidelberg, GER
Microlance® syringe needles (20-gauge)	Becton Dickinson, Rutherford, USA
Micropipette filter tips (10, 100, 200, 1000 µl)	Sarstedt AG, Nümbrecht, GER
Micropipettes (2.5, 10, 20, 100, 200, 1000 µl)	Eppendorf, Hamburg, GER
Multichannel Pipette Tips	Mettler-Toledo, Gießen, GER
NuPAGE™ 4-12% Bis-Tris (10 well, 1.5 mm)	Life Technologies
NuPAGE™ 4-12% Bis-Tris (15 well, 1.5 mm)	Life Technologies
object slide	Carl Roth, Karlsruhe, GER
Optitran® (0.2 µm)	GE Healthcare, Uppsala, SWE
Optitran® (0.45 µm)	GE Healthcare, Uppsala, SWE
Parafilm®	Pechiney Plastic Packaging, USA
Pasteur pipet	Hecht, Sondheim, GER
PMA (10 ng/ml)	Sigma-Aldrich, München, GER
reaction tubes (0.5 ml, 1.5 ml, 2.0 ml)	Sarstedt, Nümbrecht, GER
Reaction Tubes (250, 500, 1500, 2000 µl)	Sarstedt AG, Nümbrecht, GER
Serologic Pipettes (5, 10, 25, 50 ml)	Greiner, Frickenhausen, GER
spectroscopic cuvettes	Sarstedt, Nümbrecht, GER
sterile filter (0.22 µm, 0.445 µm)	GE Healthcare, Uppsala, SWE
sterile filter (0.22 µm, 500 ml)	Millipore, Billerica, USA
Streptavidin magnetic beads	Sigma-Aldrich, München, GER
syringe filters (0.22 and 0.45 µm)	Sartorius, Göttingen, GER
syringes (1 ml, 10 ml, 50 ml)	Braun, Meslungen, GER
Ultra-Clear™ centrifugation tubes, 11-60 mm	Beckman Coulter, Krefeld, GER
Ultra-Clear™ centrifugation tubes, 16-102 mm	Beckman Coulter, Krefeld, GER
VivaSpin® 20 (3 kDa MWCO)	GE Healthcare, Buckinghamshire, UK
VivaSpin® 500 (3 kDa MWCO)	GE Healthcare, Buckinghamshire, UK
Whatman paper	Millipor, Billerica, USA
Zeba Desalting Columns (500 µl, 7 kDa MWCO)	Thermo Scientific, Schwerte, GER

3.4.2 Kits

2D CleanUp Kit	GE Healthcare, Uppsala, SWE
Amersham ECL Western Blotting Detection Reagents	GE Healthcare, Buckinghamshire, UK
CyDye™ DIGE Fluor Labeling Kit (5 nM)	GE Healthcare, Uppsala, SWE
DeStreak Rehydration Solution	GE Healthcare, Uppsala, SWE
Membrane Protein Extraction Kit	PromoKine, Heidelberg, GER
Mycoprobe® Mycoplasma detection kit	R&D, Wiesbaden, GER
NE-PER™ Nuclear & Cytoplasmic Extraction Reagent	Thermo Scientific, Schwerte, GER

3.5 Laboratory equipment

3.5.1 General laboratory equipment

Avanti J-25.1 ultracentrifuge	Beckman Coulter, Fullerton, USA
Axioskop	Carl Zeiss, Jena, GER
Axiovert 10	Carl Zeiss, Jena, GER
Biofuge 15R	Heraeus, Osterrode, GER
Branson Sonifier 450	Branson, Danbury, USA
calibrated densitometric gel scanner GS-800	Bio-Rad, Hercules, USA
CO ₂ -humidified, water jacketed incubator	Forma Scientific, Marietta, USA
Confocal FL-1000	Olympus, Hamburg, GER
Cryo preservation tank	Cryotherm, Euteneuen, GER
Developing machine Curix60	Agfa, Mortael, BE
Dounce homogenizers	Braun, Meslungen, GER
Eppendorf® Centrifuge 5415C	Eppendorf, Hamburg, GER
Eppendorf® Centrifuge 5417R	Eppendorf, Hamburg, GER
film cassettes	GE Healthcare, Buckinghamshire, UK
Fridge/freezer combination (+4 °C / -20 °C)	Liebherr, Bieberach, GER
heating block	Techne, Wertheim, GER
Infinite® M200 Microplate Reader	Tecan, Durham, USA
inverse light microscope	Carl Zeiss, Jena, GER
LaminAir® - Laminar flow hoods	Heraeus, Osterrode, GER
Laser scanning microscope LSM 510 Meta	Carl Zeiss, Jena, GER
Megafuge 10	Heraeus, Osterrode, GER
microwave oven	Bosch, Gerlingen, GER
Minifold-II SlotBlot system	Schleicher & Schüll, Dassel, GER
NanoDrop™ ND-1000	Thermo Scientific, Schwerte, GER
Neubauer hemocytometer	Fischer, Frankfurt, GER
pH meter	WTW, Weilheim, GER
Pipetting Aid <i>accu-jet pro</i>	Brand, Wertheim, GER
Power Supply 200/300	Bio-Rad, Hercules, USA
Protean® II electrophoresis chamber	Bio-Rad, Hercules, USA
rocking device	Fröbel, Lindau, GER
shaking incubator	GFL, Burgwedel, GER
shaking water bath	GFL, Burgwedel, GER
SmartSpec™ 3000 spectrophotometer	Bio-Rad, Hercules, USA

ThermoMixer®	Eppendorf, Hamburg, GER
Trans-Blot® Transfer Tank	Bio-Rad, Hercules, GER
Ultracentrifuge TLA-100	Beckman Coulter, Hrefeld, GER
Ultracentrifuge XL-100	Beckman Coulter, Krefeld, GER
UV documentation system	INTAS, Göttingen, GER
Varifuge 3.0R	Heraeus, Osterrode, GER
Vortex-Genie 2	Scientific Industries, Bohemia, USA
Weighing machine	Sartorius, Göttingen, GER
Weighing machine (special accuracy)	Sartorius, Göttingen, GER

3.5.2 Gel-based proteomics and mass spectrometry

4800 Plus MALDI-ToF/ToF™ Analyzer	AB Sciex, Framingham, USA
automatic multichannel pipette (250 µl)	Mettler-Toledo, Gießen, GER
equilibration chamber	GE Healthcare, Uppsala, SWE
Ettan Dalt six	GE Healthcare, Uppsala, SWE
Ettan Digester	GE Healthcare, Uppsala, SWE
Ettan IPGphor	GE Healthcare, Uppsala, SWE
Ettan Spotpicker	GE Healthcare, Uppsala, SWE
gel caster (for six gels)	GE Healthcare, Uppsala, SWE
OPTI-TOF 384 MALDI grid	AB Sciex, Framingham, USA
rehydration chamber	GE Healthcare, Uppsala, SWE
TyphoonTRIO laser scanner	GE Healthcare, Uppsala, SWE
Ultrasonic bath	Branson, Danbury, USA

3.6 Software and Web Services

3.6.1 Software

DeCyder™ 2D software 7.2	GE Healthcare, Uppsala, SWE
Ettan Digester control software	GE Healthcare, Uppsala, SWE
Ettan Spot Picker control software	GE Healthcare, Uppsala, SWE
ImageMaster 2D Platinum 7.0	GE Healthcare, Uppsala, SWE
ImageQuant TL 7.0	GE Healthcare, Uppsala, SWE
Infinite® 200 PRO	Tecan, Durham, USA
IPGphor 3 control software	GE Healthcare, Uppsala, SWE
MS Office 2011 (Word, Excel, PowerPoint)	Microsoft, Redmond, USA
TyphoonTRIO control software	GE Healthcare, Uppsala, SWE

3.6.2 Web Services

ExPASy pI/MW tool	http://web.expasy.org/compute_pi/
National Center for Biotechnology Information	http://ncbi.nlm.nih.gov/
SMART domain prediction tool	http://smart.embl-heidelberg.de/

STRING 9.1

<http://string-db.org>

UniProt Protein Knowledgebase

<http://uniprot.org>

4 Methods

4.1 Cell culture

4.1.1 Cultivation of mammalian cells

Cells were routinely cultured at 37 °C in a humidified atmosphere with 5 % carbon dioxide.

Cell culture media, used for different cell lines are listed in table 4.1.

Tab. 4.1: Cell culture media

cell line	medium	composition		used for ...
		substance	amount	
murine embryonic fibroblasts (MEF)	MEF-10	DMEM sodium pyruvate L-glutamine FBS Penicillin/Streptomycin	110 mg/ml 2 mM 10 % (v/v) 1 % (v/v)	cultivation
	MEF-0	DMEM sodium pyruvate L-glutamine Penicillin/Streptomycin	110 mg/ml 2 mM 1 % (v/v)	washing, supernatant analyses
	MEF-ECM	DMEM ascorbic acid sodium pyruvate L-glutamine FBS Penicillin/Streptomycin	10 nM 110 mg/ml 2 mM 10 % (v/v) 1 % (v/v)	cultivation
macrophages (MΦ)	MΦ-10	DMEM sodium pyruvate L-glutamine FBS Penicillin/Streptomycin HEPES rm m-CSF	110 mg/ml 2 mM 10 % (v/v) 1 % (v/v) 10 mM 40 ng/ml	differentiation, cultivation
	MΦ-0	DMEM sodium pyruvate L-glutamine Penicillin/Streptomycin HEPES rm m-CSF	110 mg/ml 2 mM 1 % (v/v) 10 mM 40 ng/ml	washing, supernatant analyses

For standard cultivation of murine embryonic fibroblasts (MEFs), cells were detached by trypsin-containing PBS for 5 min at room temperature. Cells were transferred into fresh medium and harvested by centrifugation for 5 min at 500 xg and room temperature. The pelleted cells were resuspended in 1 ml of fresh culture medium and passaged in a 1:10 or 1:5 ratio. Possible contaminations by mycoplasmas were excluded periodically using a PCR-based mycoplasma detection kit.

4.1.2 Cryopreservation of cells

Long-term storage of stable cell lines (e.g. murine embryonic fibroblasts) was carried out by cryopreservation in liquid nitrogen. Prior to cryopreservation, cells were harvested, counted and washed with fresh culture medium. Afterwards, cells were pelleted by centrifugation for 5 min at 500 xg and room temperature and re-suspended in an appropriate volume of cryo-medium, which is normal growth medium containing additional 20 % (v/v) of FBS and 10 % (v/v) DMSO. Immediately, cells were transferred into 1 ml cryo tubes and stored at -80°C for short periods before transfer into liquid nitrogen.

4.1.3 Determinating cell number and viability of cultured cells

Cells were counted using standard Neubauer hemocytometer. Thereto, 10 μl of the cell suspension was mixed with 90 μl of trypan blue or eosin red before counting.

4.2 Sample preparation techniques

4.2.1 Preparation of murine, bone marrow –derived macrophages

Anesthetized mice were killed by cervical dislocation and *Os femoris* and *Os tibia* from both legs were prepared by dissection. Bones were cleaned from remaining tissues and kept on ice in culture medium on ice. Bone marrow was obtained after cutting the joint ends and the sockets of the bones, respectively. The red bone marrow was rinsed into a sterile sieve using a 20-gauge needle and fresh M Φ -0 medium to obtain a single cell suspension. The cells were then pelleted by centrifugation for 10 min at 300 xg and 4°C , resuspended in 7 ml M Φ -10 medium, transferred into a coated cell culture plate and incubated for 24 h at standard culture conditions.

Then, the monocyte-containing culture supernatant was removed and discarded. The adherent cells were detached with 10 ml of fresh MΦ-0 medium, centrifuged for 10 min at 300 xg and 4 °C, resuspended in 1 ml of fresh MΦ-10 medium and counted. 1×10^7 cells were transferred into a coated cell culture plate with 7 ml of MΦ-10 medium.

Differentiation of macrophages was performed for 48 h under standard culture conditions, followed by additional 72 h after supplementing 7 ml of fresh MΦ-10 medium. Differentiated macrophages were harvested by accutase and used for respective experiments.

4.2.2 Preparation of whole cell lysates

In order to analyze proteins from whole cell lysates by SDS-PAGE and subsequent Western blot analyses, 2.5×10^6 cells were harvested and washed three times with PBS. Cells were centrifuged for 5 min at 500 xg and room temperature, re-suspended in an appropriate volume of NP40 or RIPA lysis buffer and kept on ice for 20 minutes. Cellular debris was removed by centrifugation for 10 min at 15.000 xg and 4 °C and the supernatant was collected for further processing or storage at -20 °C. In case of 2D-DiGE analyses, whole cell lysates were produced using 2D Lysis Buffer.

4.2.3 Enrichment of proteins from cell culture supernatants

4.2.3.1 Enrichment of proteins using centrifugal filter units

In a first series of experiments, proteins from cell culture supernatants were enriched by reduction of the sample volume, using Vivaspin 500 centrifugal filter units with a 3 kDa molecular weight cut-off (GE Healthcare). Briefly, $2 \cdot 10^8$ cells per cell line were seeded on ten 20 cm cell culture dishes and incubated overnight at standard culture conditions. Afterwards, the supernatants were removed and the cells were washed three times with MEF-0 medium before adding fresh MEF-0 medium for another 48 h of incubation. Two hours before harvesting the cell culture supernatant, 10 nM of the phorbol ester PMA was added. The cell culture supernatants were harvested and detached cells were removed by centrifugation for 10 min at 1,500 xg and 4 °C. Cleared supernatants were supplemented with protease inhibitors and the volume was reduced by centrifugal filter units (3 kDa MWCO). For subsequent 2D-DiGE analyses, remaining medium was exchanged against 2D

lysis buffer, using Zeba Spin Desalting Columns (7 kDa MWCO, Thermo Scientific) following the manufacturer's instructions.

4.2.3.2 Precipitation of glycosylated proteins by wheat germ agglutinin

In order to enrich secreted or shed membrane proteins from cell culture supernatants, proteins were precipitated using WGA-agarose beads. This procedure was introduced as a means for the identification of shed cell-surface proteins by metalloproteases [Guo *et al.*, 2002] and, more specifically for the identification of Desmoglein-2 as a substrate of ADAM10 [Bech-Serra *et al.*, 2010]. This approach is based on the fact that most cell-surface proteins contain one or more carbohydrate groups and released cell-surface proteins are thus likely to be highly glycosylated. WGA is a lectin from *Triticum vulgare* and binds N-acetyl-D-glycosamines and sialic acids that are common to many secreted and membrane glycoproteins of mammalian cells.

For the preparation of proteins from cell culture supernatants of MEF cells from wild-type or ADAM17^{ex/ex} mice, 2×10^8 cells per cell line were placed in ten cell culture dishes (20 cm). After incubation for 12 h at 37 °C and 5 % CO₂, cells were washed twice with MEF-0 medium and finally covered with 15 ml of MEF-0 medium. After incubation for 46 h at 37 °C and 5 % CO₂, cells were exposed to 10 nM PMA and for additional two hours. Subsequently, cell culture supernatants were harvested and centrifuged at 1000 xg and 4 °C for 10 min to remove cellular debris. Supernatants were carefully transferred into fresh tubes with protease inhibitors and stored on ice. Washed WGA-agarose beads were added to the supernatants (200 µl to 100 ml supernatant) and incubated for 16 h at 4 °C. WGA-agarose beads were centrifuged at 4,000 xg and 4 °C and transferred to a fresh 1.5 ml reaction tube. Precipitated proteins were eluted with WGA elution buffer for 2 h, rotating at 4 °C. Finally, WGA-agarose beads were collected by centrifugation at 15,000 xg and 4 °C for 5 minutes. The supernatant contained the eluted proteins and the volume was reduced to 100 µl using VivaSpin 500 centrifugal filter units (3 kDa MWCO). Proteins were cleaned up using the 2D CleanUp Kit and subjected to two-dimensional differential gel electrophoresis. In case of Western blot analyses, respective aliquots for separation of proteins by SDS-PAGE were taken from the concentrated sample.

4.2.4 Preparation of plasma membrane proteins

4.2.4.1 Preparation of plasma membrane proteins by a “two-phase system”

In order to address a potential regulation of membrane proteins, plasma membrane proteins were enriched using the Plasma Membrane Extraction Kit (PromoKine). The extraction was performed according to manufacturer’s instructions. Putative membrane fractions were resuspended in 2D lysis buffer for subjection to 2D-CTAB/SDS-DiGE or in DOC lysis buffer for subjection to WGA-mediated precipitation.

4.2.4.2 Formation of Giant Plasma Membrane Vesicles (GPMVs)

For the formation of GPMVs, 10^7 MEF cells were seeded into 20 cm cell culture plate and incubated overnight at standard conditions. Cell culture medium was discarded and cells were washed with pre-warmed GPMV wash buffer, twice. Cells were covered with 10 ml pre-warmed, TPA-containing GPMV blebbing buffer and incubated for 2 h at 37 °C and gentle agitation. Supernatant was harvested, transferred to a 50 ml reaction tube and underlaid with GPMV sucrose buffer. After centrifugation for 30 min at 500 xg and 4 °C, the upper phase was transferred into Ultra-Clear® centrifugation tubes and centrifuged for one hour at 100,000 xg and 4 °C. GPMVs were resuspended in PBS and sonicated. After centrifugation for 30 min at 25,000 xg and 4 °C, GPMV debris was resuspended in 2D lysis buffer and subjected to further proteomic analysis.

4.2.4.3 Combination of a “two-phase system” and ConA-mediated precipitation

Another strategy for plasma membrane protein enrichment was a combined approach of the two-phase system and Concanavalin A-mediated lectin precipitation. Thus, putative membrane fractions were generated as described before (see section 4.2.4.1) and were resuspended in ConA binding buffer. Biotinylated ConA was linked to streptavidine-magnetic beads as described elsewhere [Lee *et al.*, 2008] and transferred to the sample. After incubation for 16 h at 4 °C, Con A-bound proteins were harvested by magnets and eluted by incubation in ConA elution buffer for 2 h at 4 °C. Con A-magnetic beads were removed and proteins were precipitated using the 2D CleanUp Kit. Precipitated proteins were resolubilized in 2D lysis buffer overnight at 4 °C and subjected to 2D-CTAB/SDS-DiGE.

4.2.5 Enrichment of ECM proteins from cells and tissues

4.2.5.1 Preparation of ECM proteins from cultured cells

In order to identify and verify potential differences in the extracellular matrix (ECM) composition of wild-type and ADAM17^{ex/ex} MEF cells, enrichment of ECM from these cells was performed as described elsewhere [Cukierman *et al.*, 2001]. Briefly, 3×10^6 MEF cells were seeded into four 20-cm cell culture dishes. Cells were cultured for 17 days under standard culture condition, changing MEF-ECM medium every third day. Afterwards, the medium was removed and discarded. Cells were twice rinsed with 5 ml pre-warmed PBS, covered with 5 ml of pre-warmed ECM extraction buffer (C-ECM) and incubated for 5 to 10 minutes at 37 °C to lyse the cells. After addition of 10 ml ice-cold PBS, supernatant was removed and cell culture plates were washed two times with cold PBS. Finally, supernatant was removed completely and the remaining ECM was harvested in 2D lysis buffer using a cell scraper. After desalting, the sample was immediately subjected to 2D-DiGE analysis.

4.2.5.2 Adapted protocol for the preparation of ECM proteins from cultured cells

In order to optimize the enrichment of ECM proteins from cultured MEF cells, decellularization was linked to WGA-mediated precipitation. Thus, ECM enrichment was performed as described before. Putative ECM proteins were transferred into WGA wash buffer and supplemented with WGA-agarose beads. Proteins were harvested and processed as described in section 4.2.3.2.

4.2.5.3 Preparation of ECM Proteins from Murine Tissues

In order to verify potential differences in extracellular matrix composition between wild-type and ADAM17^{ex/ex} phenotype *in vivo*, different organs were dissected from wild-type and ADAM17^{ex/ex} mice. Several protocols have been published for enrichment of ECM proteins from different tissues. The procedure used here combines protocols for cartilage matrix preparation for 2D-DiGE analyses [Wilson and Bateman, 2008] and for preparation of cardiac ECM for subsequent mass spectrometrical analyses [de Castro Brás *et al.*, 2013]. Therefore, mice were sacrificed by cervical dislocation and dissected immediately. Heart, lung, spleen, kidneys, liver, colon, intestine and parts of the skin were removed, washed three times in sterile and ice-cold PBS and were stored at -80 °C for 24 h. For preparation of ECM, organs

were thawed and cut into smaller pieces. Organs were incubated in high-salt extraction buffer (T-ECM-1) for 40 h at 4 °C. Afterwards, the solution was aspirated, tissues were washed once with isosmotic decellularization buffer (T-ECM-2) and incubated in fresh T-ECM-2 for 24 to 48 h at room temperature. After removing the liquid from each sample, the remaining tissues were carefully washed with deionized water and further incubated in guanidine extraction buffer (T-ECM-3) for 48 h at 4 °C and 800 rpm. For further sample processing, tissue debris was removed by centrifugation for 15 min at 10,000 *xg* and 4 °C. The supernatants were transferred into centrifugal filter units with 3 kDa MWCO and sample volume was reduced to 200 µl by centrifugation at 15,000 *xg* and 4 °C. Finally, proteins were precipitated using the 2D CleanUp Kit (GE Healthcare), resuspended in 2D lysis buffer and subjected to 2D-DiGE analysis or Western blot analysis, respectively.

4.2.5.4 Adapted protocol for the enrichment of ECM proteins

In order to increase the amount of extracted ECM components by the previous described decellularization protocol, this procedure was amended by enrichment of glycosylated proteins, using WGA-agarose beads. Therefore, decellularization and ECM enrichment was performed as described in section 4.2.5.3 and ethanol-precipitated proteins were dissolved in WGA Wash Buffer. The samples were then supplemented with 50 µl of stirred WGA-agarose bead solution and incubated for 16 h at 4 °C on an over-head incubator. Afterwards, WGA-agarose beads were harvested and bound proteins were eluted as described previously (see section 4.2.3.2). Again, the sample volume was reduced by centrifugal filter units (3 kDa MWCO) to a final volume of 100 µl and proteins were precipitated using the 2D CleanUp Kit. Finally, proteins were re-suspended in 2D Lysis Buffer for subsequent measurement of protein concentration.

4.2.6 Biotinylation

Enrichment of putative membrane fractions for screening analyses was also performed by biotinylation. Thus, the Pierce Cell Surface Protein Isolation Kit (Thermo Scientific) was used, following manufacturers instructions. Eluted proteins were precipitated using the 2D CleanUp Kit and resuspended in 2D lysis buffer for further analysis.

4.2.7 Cell-surface labeling by fluorescent dyes

Similar to biotinylation, cell-surface proteins in some cases can also be labeled by fluorescent dyes (e.g. CyDye's). Cell-surface labeling was performed as described elsewhere [Mayrhofer *et al.*, 2006].

4.2.8 Preparation of nuclear proteins from cultured cells

Nuclear proteins were enriched using the NE-PER Nuclear Protein Extraction Kit (Pierce), following the manufacturer's instructions. Prior to subsequent analyses by 2D-DiGE or SDS-PAGE, the enrichment of nuclear proteins was analyzed by Western blot analyses.

4.2.9 Determination of protein content

Protein concentrations were determined using a Bradford Assay (Thermo Scientific), following the manufacturer's instructions [Bradford, 1976]. Briefly, 5 μ l of protein sample were supplemented with 995 μ l of Coomassie (Bradford) Protein Assay Reagent (Thermo Scientific) and incubated for 15 min at room temperature. Absorbance was measured with a SmartSpec™ 3000 spectrophotometer (Bio-Rad) and protein concentration was calculated *in silico* using a straight calibration line.

4.3 Enzyme-linked immunosorbent assay (ELISA)

In order to measure the concentration of shed fragments of known ADAM17 substrates (sTNF α , sTNF-R_I and sTNF-R_{II}) in the supernatant of wild-type and ADAM17^{ex/ex} MEF cells, the colorimetric enzyme-linked immunosorbent assay (ELISA) was. For each soluble fragment, a specific DuoSet ELISA Development Kit (R&D Systems, Minneapolis, USA) was used according to manufacturer's instructions. Finally, absorption of the samples was detected using the Tecan® ELISA plate reader.

4.4 Confocal laser scanning microscopy (CLSM)

Cover slips were incubated for 15 min in concentrated hydrochloric acid at room temperature. Hydrochloric acid was removed and cover slips were washed twice with ultra pure water and once with 70 % ethanol. Finally, cover slips were dried over night at 180 °C

and sterilized. For confocal imaging of MEF cells, cover slips were transferred into sterile 12-well plates and labeled with poly-L-lysine for 30 min at 37 °C. Coated cover slips were washed three times with sterile PBS and 10^5 MEF cells were seeded per well and cultured overnight. After stimulation with TPA for two hours, cell culture medium was removed and cells were washed twice with sterile PBS. Cells were fixed with 3 % PFA/PEM buffer for 5 min at room temperature, followed by 10 min of incubation in 3 % PFA/borate buffer. For staining of intracellular proteins, cells were permeabilized by incubation in 1 % Triton X-100 in PBS for 15 min. Cells were washed three times with PBS and free aldehyde groups were reduced by incubating the cells twice for 10 min in sodium borohydride solution. Again, cells were washed three times with PBS, followed by blocking of unspecific binding sites by 1 % BAS/PBS for one hour at room temperature. Primary antibodies were diluted in 60 μ l of blocking solution and spotted on a piece of Parafilm®. The cells on the cover slip were placed in the antibody solution and incubated over night at 4 °C. Subsequently, cells were washed twice with PBS and incubated with the secondary antibody for one hour at room temperature. Finally, cells were washed with ultra pure water and were placed on an object slide containing 14 μ l mounting medium with DAPI. After one hour of incubation at room temperature, samples were stored at 4 °C until imaging using the Olympus FV-1000 confocal microscope. Images were processed using the FluoView Viewer software.

4.5 Gel-based proteomic approaches

4.5.1 SDS-PAGE

The sodium dodecyl sulfate polyacrylamide gel electrophoresis (SDS-PAGE) is an electrophoretic separation technique for the analysis and separation of protein mixtures according to their molecular masses. As the migration of a protein within an electric field (mobile phase) and a polyacrylamide gel (stationary phase) does not only depend on the molecular weight, but also on intramolecular charge distributions, the anionic detergent sodium dodecyl sulfate (SDS) is used to circumvent inhomogeneous charge distribution. In an SDS solution, proteins are covered by a homogeneous negative charge and electrophoretic separation solely depends on the molecular weight. In addition, reduction of disulfide bonds by DTT or β -mercaptoethanol can lead to enhanced protein separation. In

the context of this work, SDS-PAGE was performed in three different systems: (I) NuPAGE[®], (II) Protean II and (III) Ettan DALTsix.

NuPAGE[®]:

This system includes preformed 4 – 12 % gradient gels and a MES buffer system. Prior to separation, 8 – 10 µg of a protein mixture were supplemented with a corresponding volume of 4-fold NuPAGE[®] LDS Sample Buffer and DTT. Finally, the sample volume was brought to 30 µl and the protein mixture was denatured for 5 min at 95 °C. The electrophoretic separation was performed by applying a current of 200 V until the dye front reached the bottom of the gel.

Protean II:

In contrast to the NuPAGE[®] system, the Protean II system allows the adaption of the acrylamide concentration to the particular needs of the analysis. In the context of this work, this system has been used for a variety of analyses, including (I) one-dimensional separation of proteins prior to subsequent Western blot analyses, (II) separation of proteins upon isoelectric focusing and (III) separation of proteins upon CTAB-PAGE in the first dimension.

Ettan DALTsix system:

In order to achieve a higher degree of comparability of different separations of protein samples by 2D-DIGE, the Ettan DALTsix system was used for second dimension separation of proteins in 2D-IEF/SDS approaches. In contrast to the Protean II system six different gels were made in a row by using the DALTsix Gel Caster (GE Healthcare). Glass plates were cleaned with an aqueous solution of 2 % SDS and ultrapure water. In addition, dry plates were cleaned with a duster to remove particles of dust and placed in the gel caster. Finally, the gel solution was poured into the gel caster and displacing solution was added. A film of ultrapure water on top of the gels was used to create a smooth surface. Gel composition is summarized in section 3.3.7.

4.5.2 MMP zymography

In order to investigate changes in MMP activity in ADAM17^{ex/ex} MEF cells a zymography assay was performed, as described by previously [Toth *et al.*, 2012] with slight modifications. Briefly, a 12.5 % SDS separation, containing 0.2 mg/ml gelatin (for MMP-2 and MMP-9) or casein (for MMP-3) was prepared. Protein samples from cell culture were combined with

SDS sample buffer without reducing agents and boiling of the sample. The samples were separated by SDS-PAGE, until the bromophenol blue front reached the end of the gel. SDS was removed from the zymography gels by incubation in zymography buffer I for 45 min at room temperature. Digestion of the incorporated MMP substrates was performed by incubation in zymography buffer II for 20 h at 37 °C. Finally, MMP activity was detected by staining the gel with Coomassie staining solution and subsequent destaining.

4.5.3 2D-IEF/SDS-PAGE

In the context of unbiased, gel-based proteomic approaches, the resolution of separated protein mixtures can be increased by two-dimensional techniques. In case of the 2D-IEF/SDS-PAGE, the electrophoretic separation of protein mixtures is performed by isoelectric focusing according to the isoelectric point (pI) of a given protein within a preformed pH gradient, followed by a separation via SDS-PAGE [O'Farrell, 1979]. Despite the increased resolution of this two-dimensional technique, the comparability of two different proteomes separated in different gels was often problematic. An increase in resolution and comparability was achieved by the 2D-DiGE technique [Ünlü *et al.*, 1997]. This approach uses different weight-matched fluorochromes (CyDyes™) for covalent fluorescent labeling of protein mixtures prior to two-dimensional separation. Differentially labeled protein mixtures can then be combined and separated in a single gel (Fig. 4.1).

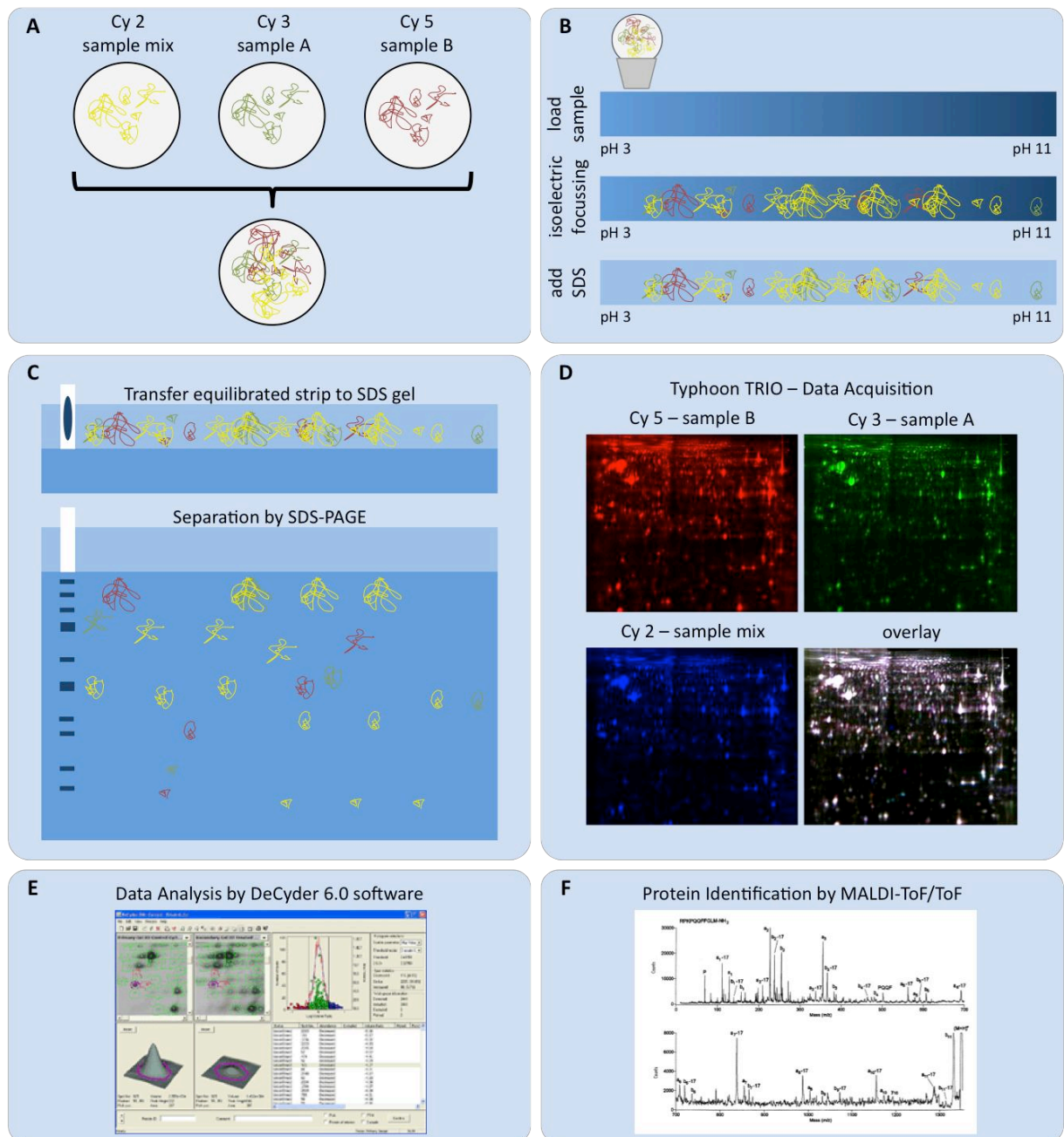


Fig. 4.1: Overview on 2D-IEF/SDS-DiGE workflow. (A) Sample Labelling: Prepared protein samples, which have to be compared are differentially labelled by fluorescent dyes (Cy3 and Cy5). In addition, a mixture of both samples is labelled by Cy2 for subsequent statistic evaluations. After stopping the labelling, all three samples mixtures are combined. (B) First Dimension: After rehydration of the IPG strip, the prepared sample is applied to the IPG strip and separation of proteins by isoelectric focussing is performed. The IPG strip is equilibrated to SDS-PAGE conditions and proteins are reduced and alkylated. (C) Second Dimension: The equilibrated IPG strip is transferred on top of SDS gel and proteins are separated according to their molecular weight by SDS-PAGE. (D) Data Acquisition: Fluorescence of differentially labelled and separated proteins is detected by Typhoon TRIO laser scanner. (E) Data Analyses: Differences in protein levels between both samples are calculated by DeCyder 6.5 software. (F) Protein Identification: Finally, Proteins of interest are selected and processed for subsequent identification by MALDI-ToF/ToF.

4.5.3.1 Isoelectric focussing (first dimension)

Rehydrated DryStrips were placed on the ceramic tray of an IPGphor device and a cup was placed onto the acidic part of the strip. Both, the acidic and the alkaline ends were covered

with wet paper wicks on which the electrodes were placed. In order to prevent dehydration of the DryStrip, the strips and the whole ceramic tray were covered with DryStrip Cover Fluid. Separation of proteins was performed according to a standard program reaching up to 65 kVh by limiting the amperage to 75 μ A per strip (see Fig. 4.2).

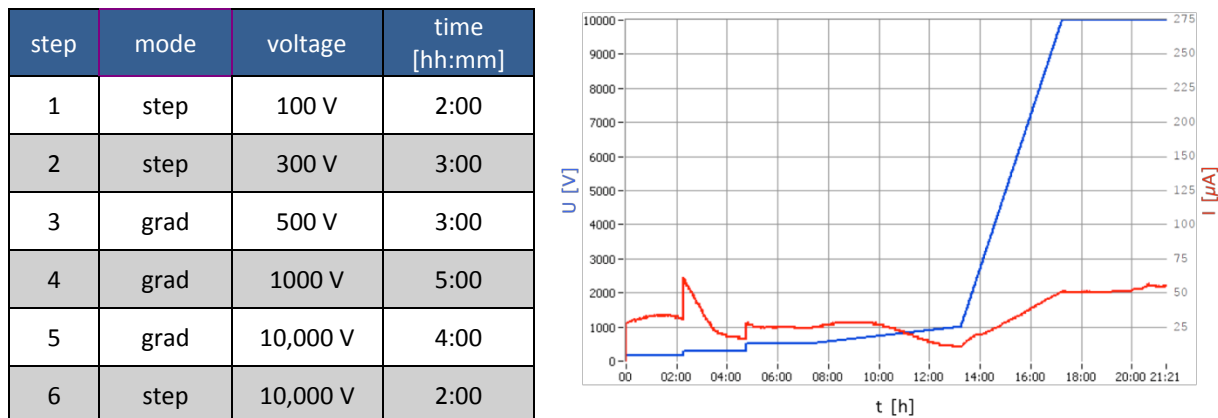


Fig. 4.2: Parameters and progression curve of both, voltage and amperage, during isoelectric focussing of proteins on a 24-cm IPGstrip (3-11 NL), using the Ettan IPGphor3 device.

4.5.3.2 SDS-PAGE (second dimension)

Second dimension separation of isoelectrically focused proteins was routinely performed using the Ettan DALTsix system. Briefly, strips were equilibrated to SDS-PAGE conditions with concurrent reduction and alkylation of proteins at room temperature for 15 minutes with DTT and iodoacetamide, respectively. Strips were washed with 2-fold running buffer, transferred on top of a SDS-PAGE gel and fixed with 0.5% low melting agarose in 2-fold running buffer. Separation by molecular weight was performed at 24 mA per gel until the bromophenol blue front reached the bottom end of the gel.

4.5.3.3 Visualization of CyDye-labelled proteins

In order to detect and quantify differences in protein levels of proteins separated by 2D-DIGE, glass plates were cleaned with ultrapure water. The glass plates were placed on Typhoon Trio laser scanner, using appropriate spacers. As the DeCyder 2D Analysis Software (GE Healthcare) requires fluorescence data that do not exceed 100,000 relative fluorescent units, prescans were performed with a resolution of 1000 microns for adaption of correct PMT values. Finally, different CyDyeTM fluorescence's were scanned with a resolution of 100 microns according to the settings depicted in table 4.2.

Tab. 4.2.: Overview on Typhoon TRIO laser settings for the detection of protein, labeled by CyDye's.

CyDye™	emission filter	laser
Cy5	670 BP 30	red (633 nm)
Cy3	580 BP 30	green (532 nm)
Cy2	520 BP 40	blue (488 nm)

In principle, the detected fluorescence intensities can dynamically be correlated to the amount of proteins. Individual scan images of different fluorescence's (Cy5, Cy3 and Cy2) were opened with the Differential In-gel Analysis (DIA) program of the DeCyder 2D Analysis Software package (GE Healthcare). Different criteria, e.g. fluorescence intensity, slope and area were used for selection of spots for subsequent *in silico* analysis of protein abundances. Different fold-change values of individual protein spots were used to calculate a threshold, which indicates certain protein spots to be differentially regulated.

4.5.3.4 Selection of proteins of interest for subsequent MS analysis

Proteins that appeared to be differentially abundant were selected for subsequent identification by MALDI-ToF/ToF analysis. As the in-gel migration of labelled proteins might slightly differ from that of non-labelled proteins [REF], gels were fixed with Flamingo™ Fixing Solution for at least 3 hours at room temperature, followed by an additional 12 hours of incubation within Flamingo™ staining solution (Bio-Rad). After removal of the staining solution, gels were washed twice with ultrapure water for 20 minutes at room temperature and gels were placed on a cellulose membrane. Prior to imaging of proteins using the TyphoonTRIO Variable Mode Imager (GE Healthcare) with the Cy3 emission filter settings, the cellulose membrane was dried on paper towels for at least 30 minutes in the dark. Fluorescence data were processed using the ImageQuant TL 7.0 software and proteins of interest were marked within a pick list that was created by selecting spots of interest within the ImageMaster 2D Platinum 7.0 software (GE Healthcare). Finally, the gel was placed into the EttanPicker unit and selected proteins were picked automatically and transferred into 96-well plates.

4.5.4 2D-CTAB/SDS-PAGE

Conventional 2D-IEF/SDS-PAGE combines isoelectric focusing of proteins according to their isoelectric point and a subsequent, mass-related separation by SDS-PAGE. Due to their

increased hydrophobicity, integral membrane proteins, especially those containing more than one transmembrane domain, can only hardly be separated by this approach. Alternative two-dimensional electrophoretic approaches for analytical and semi-preparative separations of membrane proteins therefore use cationic detergents such as benzyldimethyl-*n*-hexadecylammoniumchloride (16-BAC) [Harbingers *et al.*, 1996] or cethyltrimoniumbromide (CTAB) [Macfarlane *et al.*, 1989] to increase the resolution of membrane proteins. In contrast to 2D-IEF/SDS-PAGE, 2D-CTAB/SDS-PAGE combines two mass-related separations within two different gels using two different buffer systems and detergents. First, proteins are separated by a cationic CTAB polyacrylamide gel electrophoresis (CTAB-PAGE) at low pH. Second, proteins are transferred to an anionic SDS polyacrylamide gel electrophoresis (SDS-PAGE) at alkaline pH. In both cases, the particular detergent covers intramolecular charge distributions and protein separated is carried out according to their molecular weight (see Fig. 4.3). The approach that was used in the present work was recently published for the characterization of membrane components of *Plasmodium falciparum*-infected erythrocytes [Philipp *et al.*, 2012]. Related to the 2D-DiGE approach [Ünlü *et al.*, 1997], separation of different protein samples within one gel is also possible, as the usage of CyDyes™ is compatible with the 2D-CTAB/SDS system [Helling *et al.*, 2006]. Within this thesis, 2D-CTAB/SDS-DiGE was used to separate membrane proteins enriched from both wild-type and ADAM17^{ex/ex} MEF cell surfaces by different approaches.

At the beginning of this project, separation of proteins by 2D-CTAB/SDS-PAGE was shown to be compatible with a variety of different lysis buffers for protein sample preparation, including NP40 and 2D lysis buffer (data not shown). If performed as a 2D-CTAB/SDS-DiGE, protein samples were cleaned up with the 2D CleanUp-Kit and were solubilized in 2D lysis buffer. Differential labelling of proteins was performed as described before.

The separation gel of the first dimension is prepared at least twelve hours before separation of proteins. All components, except CTAB and hydrogen peroxide are mixed vigorously until the urea is completely dissolved. Then, CTAB and hydrogen peroxide are added and the solution is mixed vigorously, again. The stacking gel is poured into a prepared gel caster, using 1 mm spacers, and overlaid with 2 ml of pure ethanol. After 15 min, ethanol is removed, gels are flushed with pure water and covered with CTAB Storage Solution for overnight storage at 4 °C. For proper polymerization of the stacking gel, the solution has to

be vortexed vigorously for 30 seconds. Finally, the solution can be poured on top of the separation gel, using a 10-well comb for formation of sample pockets.

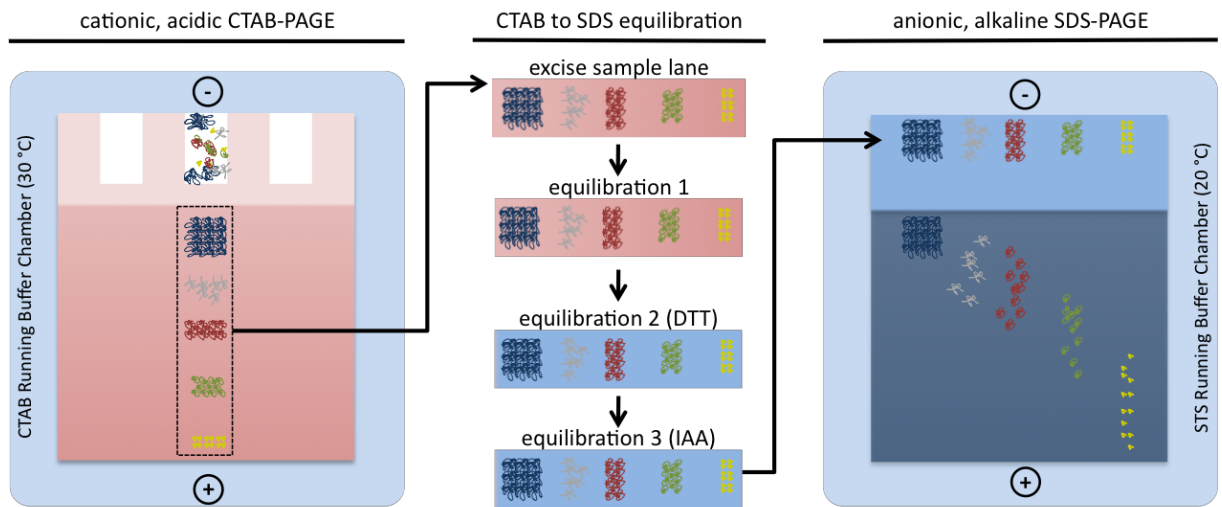


Fig. 4.3.: Schematic overview on 2D-CTAB/SDS-PAGE. Proteins, denatured by an CTAB-containing sample buffer are separated by CTAB-PAGE at 30 °C. Sample lanes are excised and equilibrated to SDS-PAGE conditions by incubation in CTAB/SDS equilibration buffer. In addition, disulfide bonds are reduced and alkylated by DTT and iodoacetamide, respectively. Finally, equilibrated sample lane is transferred onto an SDS gel and proteins are separated at room temperature.

For second dimension separation, sample lanes were excised and equilibrated in 20 ml of CTAB/SDS equilibration buffer for 15 min, followed by two additional incubation steps in the presence of 100 mM DTT (15 minutes) and 250 mM iodoacetamide (15 minutes).

For the SDS-PAGE in the second dimension, a 12.5 % gel was used, which was overlaid with a 1 cm stacking gel. The equilibrated gel strips were placed on top of the SDS stacking gel and fixed with 0.5 % Gel Fixing Solution. In addition, protein markers were placed next to the fixed gel strips. Separation of proteins was performed at 125 V per gel, until the bromophenol blue front reached the bottom end of the gel.

4.5.5 Western blot

Following in-gel electrophoresis, proteins were transferred to nitrocellulose membranes. Transfers were performed as wet blots in Western blot transfer buffer for 2 h at 150 V and 4 °C (Protean II system) or for 1 h at 100 V and 4 °C (NuPAGE® system). A schematic overview on the assembly of a Western blot cassette is shown in figure 4.4.

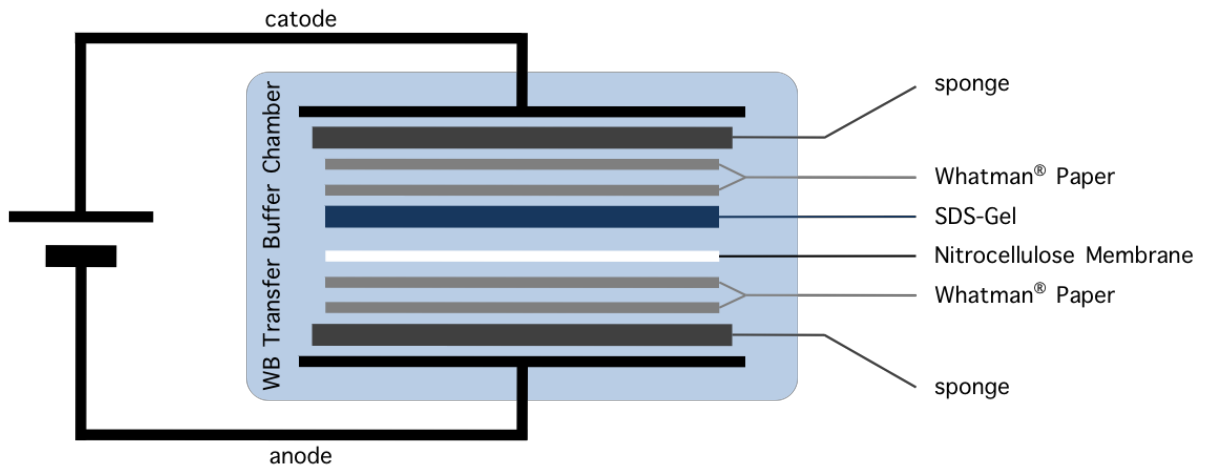


Fig. 4.4: Assembly of a Western blot cassette. Transfer of proteins from SDS gel onto a nitrocellulose membrane is performed by electrophoresis within transfer buffer at 4 °C with proteins migrating from anode to cathode due to covering by SDS. Between the Western blot clip, the SDS gel, which is in close contact to the nitrocellulose membrane, is surrounded by two layers of Whatman® paper and a sponge. Formation of air bubbles between all layers has to be avoided for proper transfer of proteins.

After blotting of proteins, transfer was monitored by Ponceau S staining for 5 min at room temperature. Afterwards, destaining was performed by incubation in TBS for 5 min at room temperature. Nitrocellulose membranes were blocked by WB Blocking Buffer I or WB Blocking Buffer II for one hour at room temperature. Membranes were washed with WB Wash Buffer and incubated with a primary antibody against a protein of interest over night at 4 °C. Afterwards, membranes were washed with WB Wash Buffer for 10 min and the HRP-tagged secondary antibody, which is directed against the Fc part of the primary antibody, was applied for 45 min at room temperature. The membrane was washed three times with WB Wash Buffer for 10 min, each, and chemiluminescence substrate (ECL) was applied for one minute. Finally, the chemiluminescence was detected using Amersham Hyperfilms ECL (GE Healthcare), which were developed in a Curix 60 device (Agfa).

4.5.6 SlotBlot

SlotBlot analysis was performed for proteins enriched from cell culture supernatants by centrifugal filter units and whole-cell lysates. Protein samples were transferred onto nitrocellulose membranes by vacuum using the Minifold II Slot Blot System (Schleicher & Schüll). Immunodetection of transferred proteins was performed as described for Western blot analyses (see section 4.5.5).

4.6 Mass Spectrometry

In case of top-down proteomic approaches, proteins of interest that were separated by 2D-DiGE were analyzed by mass spectrometry. This analytical approach records molecular weights of sample molecules that have been converted into electrically charged particles by ionization. The molecular weight of ionized sample molecules is determined upon their migration within an electromagnetic field according to their mass:charge ratio (m/z). All protein identifications of proteins separated by 2D-DiGE were performed by MALDI-ToF/ToF analysis by Bart van den Berg and Tomas Koudelka at the laboratory of Prof. Dr. Andreas Tholey (Institute for Experimental Medicine, UK S-H Kiel), using a 4800 Plus MALDI-ToF/ToFTM Analyzer from AB Sciex.

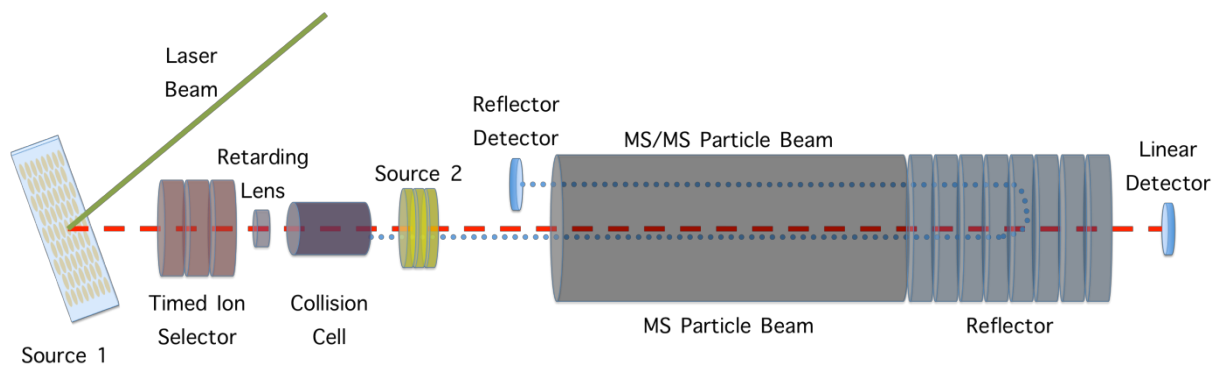


Fig. 4.5.: Schematic overview on the inside structure and particle flow of an MALDI-ToF/ToF device. For further information, refer to the text below.

Briefly, peptides are embedded into a MALDI-compatible matrix (e.g. α -cyano-4-hydroxycinnamic acid) and placed onto a MALDI spot grid. By applying a high-energy laser beam to the sample, ionized peptides are produced. These ionized peptides fly through the highly evacuated MALDI chamber and its magnetic field. Finally, peptides are detected at the linear detector and linked to a measured time of flight (ToF). In case of tandem mass spectrometry, specific ionized peptides are selected for reflection by a magnetic reflector. The single peptides within this generated MS/MS particle beam can be detected at the reflector detector. Again, the detected peptides are linked to a time of flight value. The combination of the MS- and MS/MS-derived ToF-values leads to an enhanced accuracy for peptide identification. Identification of detected peptides is performed *in silico* by linking the measured ToF values to theoretical ToF values, derived from protein databases [compare ...].

4.6.1.1 Sample preparation

Picked protein spots were washed according to the following settings by the EttanDigester (GE Healthcare; see Tab. 4.6). Afterwards, washed gel pieces were processed immediately or covered with acetonitrile for storage at -80 °C.

Prior to in-gel tryptic digestion, gel pieces were washed two times with pure water and three times with 50 mM ammonium bicarbonate in 50 % methanol for 20 min, each. Finally, gel spots were dehydrated with 70 % acetonitrile for 20 min.

For preparation of 384 protein spots for analysis by MALDI-ToF/ToF 50 µg of trypsin, were solved in 5 ml of a 25 mM ammonium bicarbonate solution. 10 µl of this trypsin solution was added to each picked protein spot and incubated for 10 minutes at 4 °C. Then, another 10 µl of the 25 mM ammonium bicarbonate solution were added to each protein spot and tryptic digestion was performed for 12 h at 37 °C.

Digestion was stopped by addition of 20 µl of acetonitrile containing 0.1 % (v/v) trifluoroacetic acid. After 15 minutes of incubation in an ultrasonic bath, supernatants were transferred into a clean, U-shaped 96-well plate and the remaining protein spots were covered with 20 µl of acetonitrile containing 0.1 % (v/v) trifluoroacetic acid. After additional 15 minutes of incubation at room temperature, the supernatants were combined. Evaporation of the collected supernatants was performed in a SpeedVac® concentrator under medium heat conditions for approximately 45 minutes.

Lyophilized α -cyano-4-hydroxycinnamic acid (CHCA, LaserBio Labs) was solved in Solvent A to reach a final concentration of 5 mg/ml. Each protein spot was solved within 0.8 µl of the CHCA matrix solution and was transferred onto a MALDI spot grid for subsequent analysis.

4.6.1.2 MALDI-ToF/ToF analytical parameters

In case of identifying proteins that were selected from 2D gels, MALDI-TOF/TOF was performed at the group of Prof. Dr. Andreas Tholey at the Institute for Experimental Medicine by Bart van den Berg and Tomas Koudelka. Briefly, spectra were acquired on an AB SCIEX MALDI-TOF/TOF 5800 (AB SCIEX) mass spectrometer in positive ion mode. For MS measurements 1600 to 2000 shots were accumulated in the mass range of 800 - 4000 m/z . Default calibration was performed using 4800 Proteomics Analyzer Standards Kit, while MS

measurements were calibrated internally using trypsin, matrix and contaminant peaks (842.509, 877.034 and 2807.315 Da) and smoothed using a FFT Poisson-Denoise algorithm.

Precursor selection for MS/MS analysis was achieved using the 4000 Series Explorer Software (AB SCIEX) with acquisition of the 20 most intense precursors ($S/N > 20$) beginning with the strongest first. All MS/MS spectra were acquired with 1 kV collision energy at ambient air pressure (CID medium: 1.25×10^{-6} Torr) using 3000 laser shots. MS/MS post processing involved smoothing using the Savitsky-Golay algorithm with 7 points across the peak and a polynomial order of 4.

For peptide identification, MALDI-TOF/TOF MS/MS raw files were searched using AB SCIEX GPS software (Version 3.6, build 332) with the following pre-filter settings: only peaks within a mass range from 60 Da to the precursor mass minus 35 Da and S/N ratio above 10 were used. Spectra were searched with Mascot (version 2.2.04, Matrix Science, London, U.K) against the Swissprot database using either *Mus musculus* (16 345 sequences) or *Homo sapiens* as a taxonomy filter (20 254 sequences) and the following parameter settings: precursor tolerance, 30 to 50 ppm; MSMS tol, 0.3 to 0.5 Da; max missed cleavages 2. Oxidation (M) was set as a variable modification, while carbamidomethylation (C) was set as a fixed modification. Proteins were considered identified when either 2 peptides were identified with a confidence interval $\geq 99\%$ ($p < 0.01$) or 3 peptides $\geq 95\%$ ($p < 0.05$) [Tomas Koudelka, personal communication].

5 Results

This section summarizes the observed changes in ADAM17-dependent proteome and sub-proteome compositions that were identified by gel-based approaches. The presented differentially regulated proteins only represent a small portion of the overall identified proteins. All indicated 2D-DiGE images are included in the addendum of this thesis. The information on individual protein spots (e.g. MALDI-ToF/ToF data and fold-change values when using differential electrophoresis) are available in separated files on the enclosed digital data carrier.

5.1 Decreased shedding activity in ADAM17^{ex/ex} MEF cells

At the beginning of this thesis, a hypomorphic mouse model (ADAM17^{ex/ex}) was introduced as a putative tool for the analysis of the effects of reduced ADAM17 activity *in vivo* [Chalaris *et al.*, 2010]. Murine embryonic fibroblasts (MEFs) from wild-type (MEF 1#3) and ADAM17^{ex/ex} (MEF 1#1) mice and were provided by Athena Chalaris (Institute for Biochemistry, CAU Kiel) for initial proteomic analysis. For further experiments (section 5.7), two additional pairs of wild-type (MEF 1#7 and MEF 2#1) and ADAM17^{ex/ex} (MEF 1#8 and MEF 2#8) MEF cells became available.

The ADAM17 status in the provided MEF cells was routinely monitored by Western blotting for ADAM17. Immunodetection of ADAM17 in different MEF cell lysates confirmed the ADAM17^{ex/ex}-dependent reduction of both, the ADAM17 pro-form (130 kDa) (Fig. 5.1 A) and the mature form (100 kDa, Fig. 5.1 B). In contrast, ADAM10 protein levels were not affected (Fig. 5.1 C). Shedding activity of wild-type and ADAM17^{ex/ex} MEF cells was monitored by ELISA, targeting the soluble and shed fragments of TNF α (Fig. 5.1 D) and TNF-R₁ (Fig. 5.1 E). The loss of ADAM17 activity led to decreased shedding of both substrates from all tested ADAM17^{ex/ex} MEF cell lines. In addition, shedding activity was enhanced upon treatment with the phorbol ester TPA (Fig. 5.1 D and E, dark blue bars) in contrast to non-stimulated MEF cells (Fig. 5.1 D and E, light blue bars). Of note, because the addition of ionomycin resulted in significant cell death, only TPA was used for MEF cell stimulation.

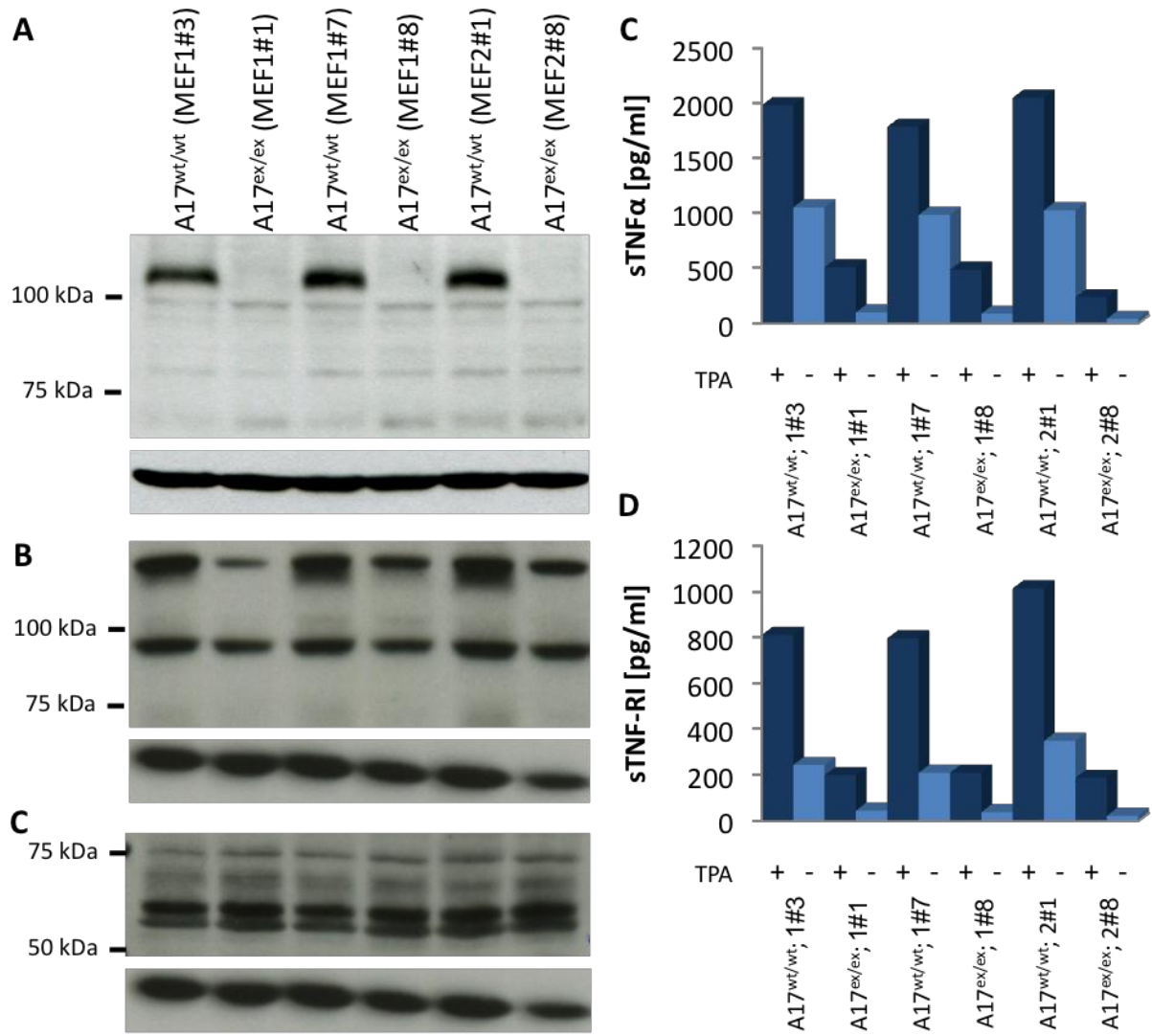


Fig. 5.1: Reduced ADAM17 levels in ADAM17^{ex/ex} MEF cells lead to reduced shedding activity. Protein levels of both, (A) ADAM17 and (B) ADAM10 were checked routinely by immunodetection in whole-cell lysates of TPA-treated MEF cells. Proteins were separated by 12.5 SDS-PAGE prior to transfer to a nitrocellulose membrane. Shedding activity was monitored by detection of soluble TNF α (C) and TNF-R₁ (D) in cell culture supernatants of unstimulated and TPA-treated MEF cells.

In addition, the subcellular localization of ADAM17 in wild-type and ADAM17^{ex/ex} MEF cells was monitored by confocal microscopy, using the available anti-mADAM17 antibody clone 18.2 (Fig. 5.2). In ADAM17^{ex/ex} MEF cells, decreased levels of ADAM17 were seen at the cell-surface and within the cell. Interestingly, the majority of the cellular ADAM17 content was not located at the plasma membrane, but within a perinuclear compartment. In addition, specific fluorescent signals were also detected within the nuclei of both, wild-type and ADAM17^{ex/ex} MEF cells.

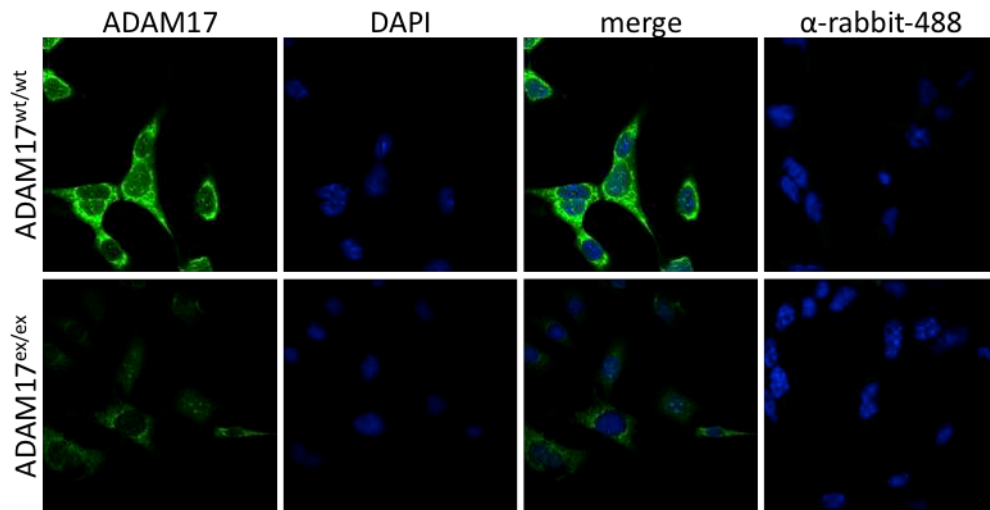


Fig. 5.2: Reduced intracellular and cell-surface ADAM17 levels in ADAM17^{ex/ex} MEF cells. Wild-type and ADAM17^{ex/ex} MEF cells were grown on poly-L-lysine coated coverslip and immunostained for ADAM17 using the 18.2 antibody against the extracellular region of ADAM17. Images show ADAM17 staining (ADAM17), the nucleus (DAPI), an overlay of both pictures (merge) and a staining with the secondary antibody alone.

5.2 Proteomic analyses of MEF cell culture supernatants

5.2.1 Proof of principle – Analysis of shedding by 2D-DiGE

Based on the assumption that ADAM17 primarily acts as a plasma membrane-located sheddase, the starting point of this project was the characterization of the ADAM17-dependent MEF cell sheddome. To this end, proteins from cell culture supernatants of MEF cells had to be enriched for a subsequent separation by 2D-DiGE.

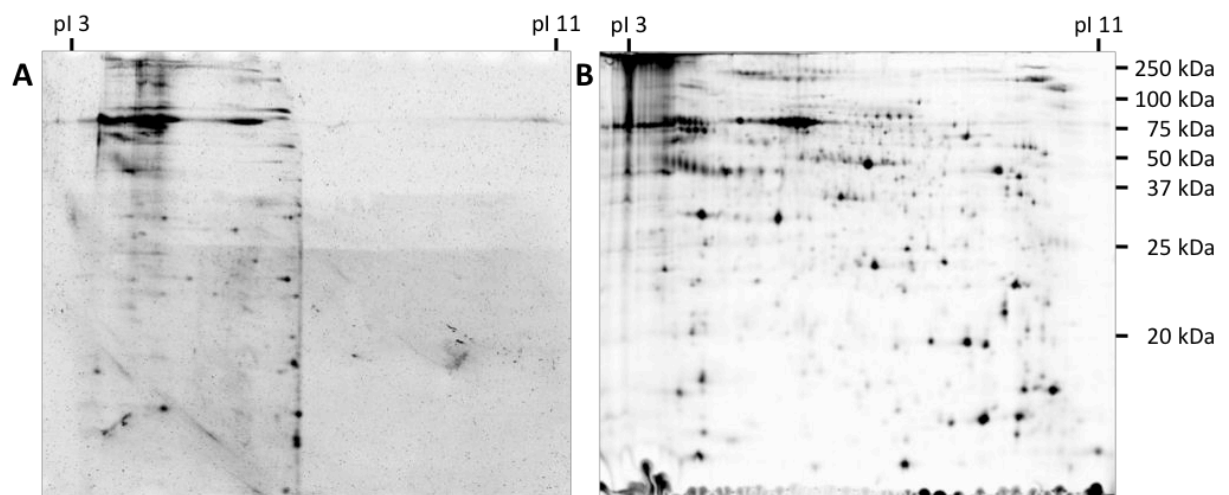


Fig. 5.3: Different resolution of enriched supernatant samples by two-dimensional electrophoresis. Proteins from MEF cell culture supernatants were enriched by precipitation with 85 % ammonium sulfate (A) or using centrifugal filter units (B). Proteins were separated by two-dimensional gel electrophoresis on a 24 cm 3-11NL IPG strip, followed by SDS-PAGE. Proteins were stained by FlamingoTM fluorescent gel stain. Images were captured by the TyphoonTRIO device.

Initially, proteins from conditioned cell culture media were thus enriched by protein ammonium sulfate precipitation. Although sufficient amounts of protein were precipitated, re-solubilization was mostly incomplete and led to impaired protein separation by two-dimensional gel electrophoresis (Fig. 5.3 A). In contrast, the enrichment of supernatant proteins using centrifugal filter unit, resulted in a decent resolution on 2D (Fig. 5.3 B).

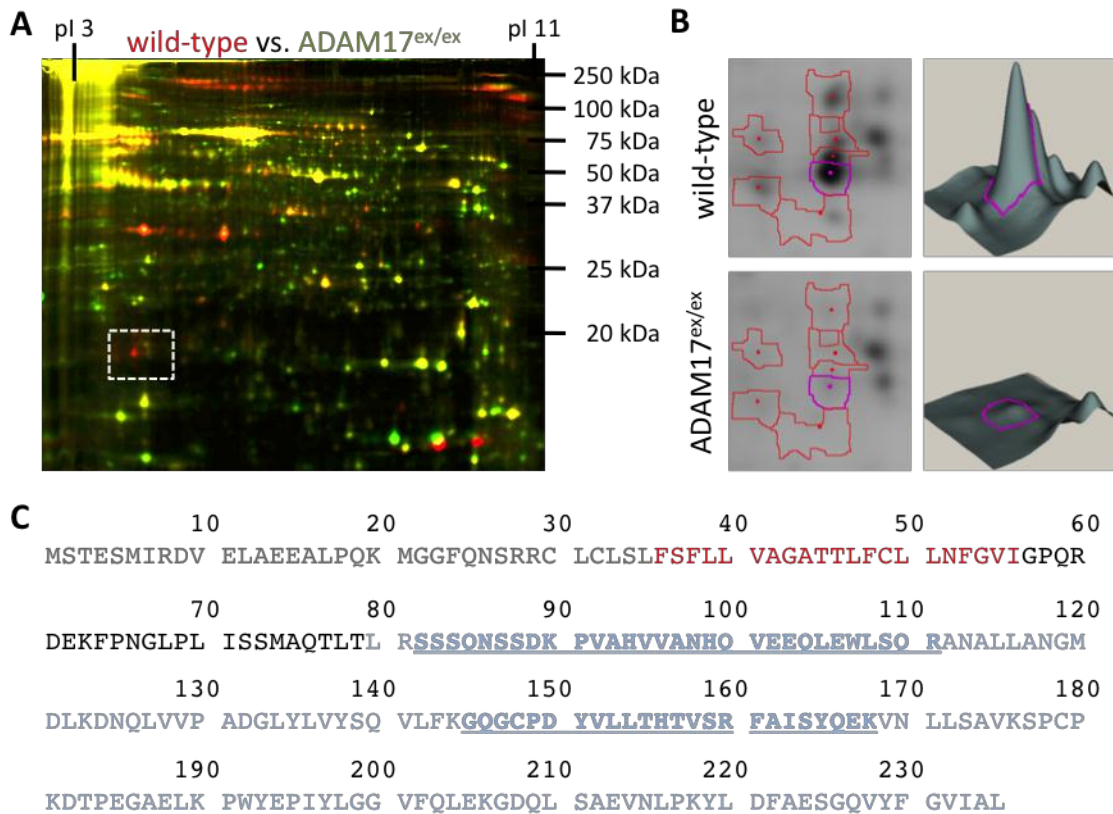


Fig. 5.4: Reduced levels of sTNF α in supernatants of TNF α -overexpressing ADAM17^{ex/ex} MEF cells. (A) Pseudo-colored 2D-DiGE image of separated proteins from cell culture supernatants of TNF α -overexpressing wild-type (Cy5, red) and ADAM17^{ex/ex} (Cy3, green) MEF cells. Proteins were separated on 24 cm 3-11NL IPG strips, followed by a SDS-PAGE. The white box indicates protein spots, identified as TNF α . (B) Enlarged, single-colored section of the boxed area (part A) and 3D fluorescence histograms of the putative TNF α spots in wild-type (upper panel) and ADAM17^{ex/ex} MEF cell supernatants (lower panel) as integrated by the DeCyder 2D software. (C) The protein sequence of the full-length TNF α molecule comprises an intracellular domain (gray), a transmembrane region (red) and an extracellular region (black and light blue). Light blue sequence represents the soluble TNF α form. Bold and underlined letters indicate high confident MALDI-ToF/ToF-derived sequence coverage.

Unfortunately, the initial supernatant-based sheddome analyses did not reveal indications for major changes in ADAM17-mediated ectodomain shedding. Therefore, a proof-of-principle experiment needed to be performed, using TNF α -transfected variants of the wild-type (MEF 1#3^{mTNF α}) and ADAM17^{ex/ex} (MEF 1#1^{mTNF α}) MEF cells. As before, proteins were enriched by centrifugation and analyzed by 2D-DiGE. As detailed in figure 5.4, at a molecular weight of approximately 17 kDa and an isoelectric point of 4.5 (Fig. 5.4 A, white box), a group of protein spots was drastically (14.9-fold) reduced in ADAM17^{ex/ex} MEF cell

supernatants (Fig. 5.4 B). The subsequent analysis of these differentially regulated protein spots by MALDI-ToF/ToF identified them as TNF α . Of note, the observed reduction of the molecular weight of the 25 kDa proTNF α and the sequence coverage in mass spectrometry confirmed the reduced TNF α shedding in ADAM17^{ex/ex} MEF cells. All detected peptides were located within the soluble TNF α region (Fig. 5.4 C). This result clearly demonstrated that 2D-DiGE experiments are suited for the analysis of alterations in ectodomain shedding.

5.2.2 Improved protein enrichment by WGA-mediated precipitation

According to the proof-of-principle experiment, 2D-DiGE appeared to be a suitable approach for the analysis of cell culture supernatants and for the detection of ADAM17-mediated changes in ectodomain shedding. Nevertheless, 2D-DiGE analyses of samples enriched by centrifugal filter units revealed changes in protein cleavage and secretion (see below), but did not point to evident ADAM17-mediated shedding events. Moreover, the identification of the enriched proteins only revealed a rather low abundance of secreted or cell-surface proteins. In order to increase the enrichment of cell-surface, shed and secreted proteins from cell culture supernatants, agarose-bound wheat germ agglutinin (WGA) was chosen for lectin-mediated protein enrichment. Wheat germ agglutinin contains a variety of closely related isolectins that specifically bind to N-acetyl-D-glucosamine and to sialic acid.

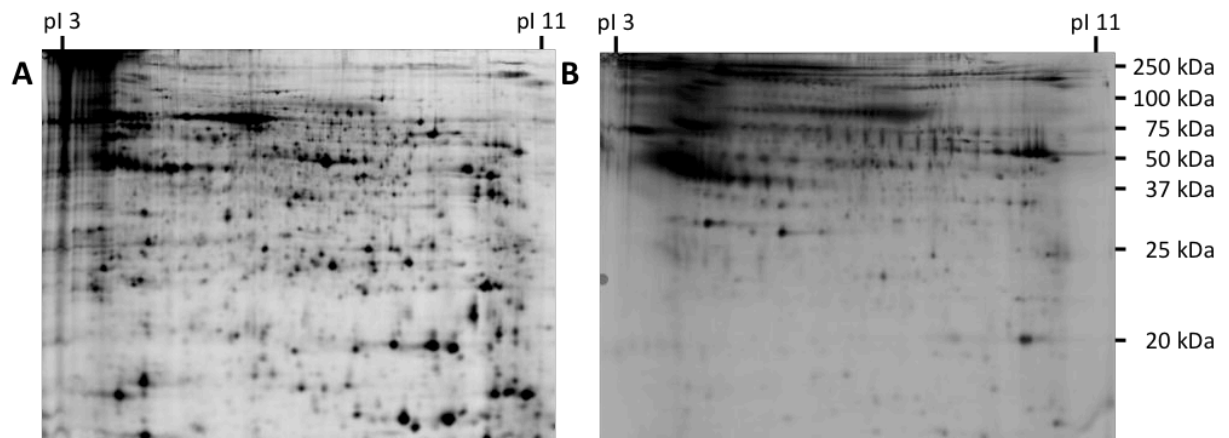


Fig. 5.5: Reduced sample complexity of supernatant samples, derived by WGA-mediated precipitation. Proteins were either enriched by centrifugal filter units (A) or by WGA-mediated precipitation (B). Proteins were separated on 24 cm 3-11NL IPG strip, followed by SDS-PAGE. Proteins were stained with FlamingoTM fluorescent gel stain.

As the majority of cell-surface and secreted proteins of mammalian cells are highly glycosylated by sialic acid or terminal N-acetyl-D-glucosamine [e.g. reviewed by Gahmberg and Tolvanen, 1996], WGA was chosen for purification of cell culture supernatant proteins. An initial experiment using cell culture supernatants of TPA-treated wild-type (MEF 1#3) and

ADAM17^{ex/ex} (MEF 1#1) MEF cells led to a decrease of sample complexity in comparison to samples enriched by centrifugal size exclusion and indicated a reduced number of detectable protein spots (Fig. 5.5). More importantly, WGA-mediated protein precipitation also led to an increased enrichment of surface or secreted proteins.

Notably, two-dimensional separation of WGA-enriched supernatant proteins in many cases led to reduced protein resolution of high molecular proteins at lower isoelectric points. This could be circumvented by deglycosylation of the enriched proteins, unfortunately accompanied by decreased protein information following mass spectrometry.

5.3 Changes in MEF cell supernatants

Overall, seven 2D-DiGE analyses of wild-type (MEF 1#3) and ADAM17^{ex/ex} (MEF 1#1) MEF cell supernatant proteins were performed. These analyses revealed that several protein fragments and full-length proteins differed in their abundance upon reduced ADAM17 activity.

5.3.1 Altered levels of protein fragments in MEF 1#1 cell supernatants

Overall, fourteen protein fragments were identified that showed reduced or increased protein levels in 2D-DiGE analyses of MEF cell supernatants (Tab. 5.1).

The 30 kDa fragments of the **type-I collagen α_1** (CO1A1) and **α_2 chains** (CO1A2) and a 25 kDa fragment of **perlecan** (PGBM) were identified in several independent experiments. Further results on these proteins will be presented separately (sections 5.3.1.1 and 5.3.1.2).

In addition, decreased protein levels were seen for the C-terminal propeptide of the **type-III collagen chain α_1** (CO3A1) in supernatants of TNF α -overexpressing ADAM17^{ex/ex} MEF cells. As observed for the type-I collagen propeptides, MALDI-ToF/ToF-derived sequence coverage revealed three peptides with high confidence that were located within the C-terminal propeptide of CO3A1.

The 151 kDa proteoglycan **lubricin** (PRG4) was identified from a protein spot with a molecular weight of 11 kDa and an isoelectric point of 9. Elevated lubricin fragment levels were found in supernatants of untransfected and TNF α -overexpressing ADAM17^{ex/ex} MEF cells. This protein fragment was identified in three independent analyses and showed increased protein levels (1.5-fold to 1.9-fold) in TNF α -overexpressing MEF cells. In

supernatants of untransfected ADAM17^{ex/ex} MEF cells, the fragment was increased by 3.85-fold. Here, the protein was identified with four peptides, located between aa956 and aa1033, which represents the “proteoglycan-4 C-terminal part” (<http://uniprot.org/uniprot/Q9JM99>).

Tab. 5.1: Differentially regulated proteins identified by 2D-DiGE analyses of MEF cell culture supernatant proteins, enriched by centrifugal filter units (CFU) and WGA-mediated precipitation (WGA). Protein fold-change values are based on DeCyder 2D software calculations. Results from seven independent experiments are summarized. Underlined fold-change values indicate spots that were not identified by MS analyses in a given experiment, but showed the same in-gel localization as identified spots from other experiments. Theoretical protein data (pI_{Lit} and MW_{Lit}) are listed according to the ExpASY pI/MW tool web service (http://web.expasy.org/compute_pi/). Observed protein data (pI_{Obs} and MW_{Obs}) were estimated by approximation. Information about subcellular distribution was searched from <http://uniprot.org> and according to the corresponding accession number. Subcellular distribution is indicated as follows: secreted (S), extracellular matrix (EM), basal membrane (BM), plasma membrane (M). Please note: samples separated in DiGE150 were proteins from TNF α -overexpressing MEF cells.

Experiment	Protein ID	fold-change values (wild-type \rightarrow ADAM17 ^{ex/ex})													
		C1RA_LC	C1SA_LC	Cadherin-2	CO1A1_CPP	CO1A2_CPP	CO3A1_CPP	Cystatin-C	IL1RL1	Lumican	NCAM-1	PCOC-1	PGBM_LG3	PRG4_CTF	sTNF α
CFU	145				-2.52	-2.11							-1.78		
	150a			-2.33	-4.72	-5.62		-2.90					-2.89	1.51	-14.8
	150b			-2.41	-6.15	-6.49	-6.04	-3.40					-3.01	1.93	-6.64
WGA	153				-1.81	-2.28			2.35			-5.82			
	169		-1.23		-1.42	-1.57							-2.88		
	172	-2.71	-3.27											3.85	
	182								2.91	-1.96	-1.69				
pI_{LIT}	5.44	4.96	4.61	5.65	9.27	6.11	8.50	8.50	6	5	8.63	5.88	8.66	5.01	
MW_{LIT}	80.0	76.9	99.8	138	130	139	20	64.8	38	120	47.6	405	116	25.9	
pI_{Obs}	6	8	4.5	5	5.5	5	8	8.5	5.5	5	5.5	5.5	9.5	5	
MW_{Obs}	30	30	20	30	30	30	15	40	35	105	30	25	10	15	
Distribution	S	S	M/S	S/EM	S/EM	S/EM	M/S	M/S	S/EM	M	S	S/EM	S	M/S	
Accession	Q8CG16	18CG14	P15116	P11087	Q01149	P08121	P21460	P14719	P51885	P13595	Q69318	Q05793	Q9JM99	P06804	

The differential analyses of culture supernatants also revealed several proteases and protease interacting proteins to be altered in ADAM17^{ex/ex} MEF cell supernatants (see section 5.4). Reduced protein levels of the extracellular **serine protease C1 subcomponents C1r-A** and **C1s-A** were observed in WGA-enriched ADAM17^{ex/ex} MEF cell supernatants. These fragments showed a 2.7- and 3.3-fold lower abundance in ADAM17^{ex/ex} MEF cells. All peptides detected by MALDI-ToF/ToF are located between aa463 and aa767 (C1r-A;

<http://www.uniprot.org/uniprot/Q8CG16>) and aa438 and aa636 (C1s-A; <http://www.uniprot.org/uniprot/Q8CG14>), representing the light chains of these proteins. Moreover, in supernatants of TNF α -overexpressing ADAM17^{ex/ex} MEF cells lower amounts of a 15 kDa form of the cysteine protease **cystatin-C** were detected. In contrast, the 20 kDa form was slightly elevated (compare Tab. 5.2). Finally, the 50 kDa **procollagen C-endopeptidase enhancer** (PCOC-1) was identified in one single experiment as a 30 kDa fragment. MALDI-ToF/ToF-derived sequence coverage was located within the 35 kDa CUB1-CUB2-region (<http://uniprot.org/uniprot/Q61398>).

Only a few proteins that were identified as protein fragments contain transmembrane domains that seem to be a crucial characteristic of ADAM substrates [White, 2003]. This includes **TNF α** that was only identified from TNF α -overexpressing MEF cells. The 99 kDa **cadherin-2** is a known substrate of the metalloprotease ADAM10 [Reiss *et al.*, 2005] and was decreased in a 15 to 20 kDa fragment with peptides at aa69 to aa91 and aa68 to aa91. According to the available protein domain information for cadherin-2 (<http://uniprot.org/uniprot/P15116>), these peptides are located within the N-terminal propeptide. In addition, several supernatant analyses revealed an increased release of the **interleukin-1 receptor-like protein 1** (IL1RL1). This 65 kDa transmembrane protein was identified in several independent experiments as a 40 kDa fragment. Finally, the 120 kDa transmembrane **neural cellular adhesion molecule 1** (NCAM-1) was already mentioned as a known ADAM17 substrate. The 2D-DiGE analysis of deglycosylated supernatant proteins, enriched by WGA-mediated precipitation revealed a 100 kDa fragment to be reduced by 1.69-fold in ADAM17^{ex/ex} MEF cell supernatants.

5.3.1.1 Reduced levels of the type-I collagen C-terminal propeptides

As already mentioned, fragments of the type-I collagen α_1 and α_2 chains were reproducibly reduced in ADAM17^{ex/ex} MEF cell supernatants. Figure 5.6 A depicts the C-terminal propeptide spots in a 2D-DiGE image of WGA-enriched cell culture supernatant proteins (DIGE169). The protein spots with a molecular weight of approximately 30 kDa were identified as the 138 kDa collagen alpha-1 (I) chain (Fig. 5.6 A, red arrow) and the 130 kDa collagen alpha-2 (I) chain (Fig. 5.6 A, white arrow), respectively. Calculation of the changes in protein levels revealed a decrease by approximately 2.5-fold (Fig. 5.6 B), but these values varied between different 2D-DiGE analyses (compare Tab. 5.1). Interestingly, the impaired release of these protein fragments from TNF α -overexpressing ADAM17^{ex/ex} MEF cells was

even more prominent, showing a decrease by approximately 6-fold (compare Tab. 5.1, DIGE150).

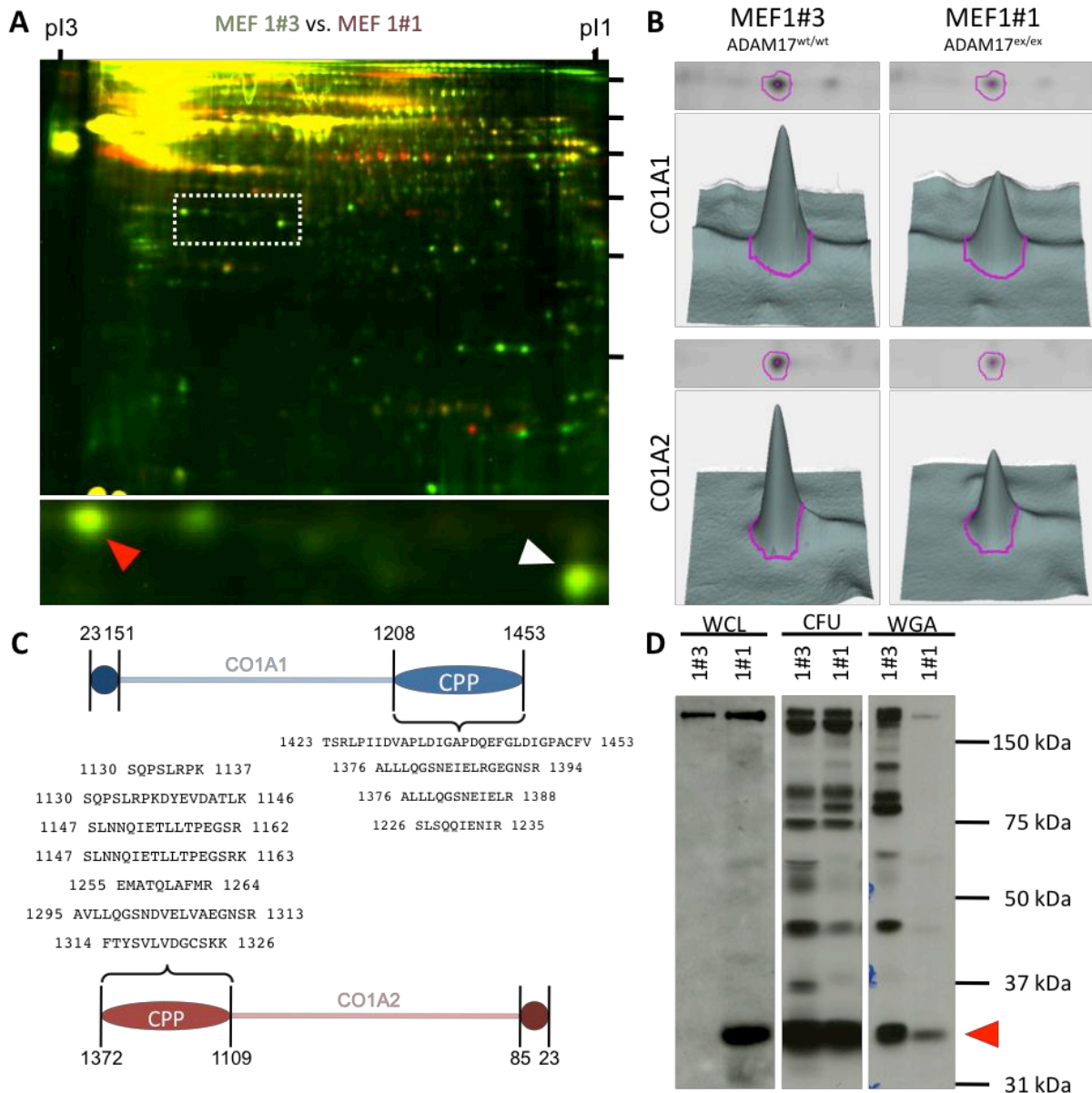


Fig. 5.6: Reduced release of the type-I collagen C-terminal propeptides from ADAM17^{ex/ex} MEF cells. (A) Pseudo-colored 2D-DiGE image of MEF cell culture supernatant proteins enriched from wild-type (Cy3, green) and ADAM17^{ex/ex} MEF cells (Cy5, red) by WGA-mediated precipitation. Proteins were separated on a 24 cm 3-11NL IPG strip, followed by SDS-PAGE. The image was recorded using a TyphoonTRIO device and processed with ImageQuant TL software. Protein spots, identified as the type-I collagen chains α_1 (red arrow) and α_2 (white arrow) C-terminal propeptides are indicated in the enlarged section below. (B) Fluorescence intensities of the observed protein spots in wild-type (left panel) and ADAM17^{ex/ex} MEF cells (right panel), as calculated by DeCyder 2D software (Version 7.2). (C) Schematic overview on localization of the MALDI-ToF/ToF-identified peptide sequences within the full-length type-I collagen α_1 and α_2 chain sequence. Numbers indicate starting and ending amino acid (compare <http://uniprot.org/uniprot/P11087> and <http://uniprot.org/uniprot/Q01149>). Peptide sequences are presented by the one letter code. (D) Immunodetection of type-I collagen α_1 chain fragments in whole-cell lysates (WCL) and supernatant samples, enriched by centrifugal filter units (CFU) and WGA-mediated precipitation (WGA).

The MALDI-ToF/ToF-derived sequence coverage clearly demonstrated that the indicated collagen molecules represent the C-terminal propeptide regions (Fig. 5.6 C). Immunodetection of the C-terminal propeptide in samples enriched by centrifugal filter units yielded a very intense signal at low exposure times (Fig. 5.6 D, center panel). However, this was not seen in WGA-precipitated samples (Fig. 5.6 D, right panel).

In summary, the Western blot analyses confirmed the reduced levels of the C-terminal propeptide of the collagen alpha-1 (I) chain in ADAM17^{ex/ex} MEF cell culture supernatants. In contrast, a high molecular form of the type-I collagen (>250 kDa) was increased in ADAM17^{ex/ex} MEF cell whole-cell lysates (Fig. 5.6 D, left panel). Interestingly, immunodetection of type-I collagen via the C-terminal propeptide also revealed a variety of collagen fragments which were increased in wild-type MEF cell supernatants.

5.3.1.2 Reduced levels of the LG3 peptide of perlecan in ADAM17^{ex/ex} supernatants

Another protein fragment with a molecular weight of approximately 25 kDa and an isoelectric point of 5 was identified as the 405 kDa basement heparane sulfate proteoglycan core protein (perlecan, Fig. 5.7 A, white arrow). Protein levels of this protein fragment appeared to be reduced in cell culture supernatants of ADAM17^{ex/ex} MEF cells by 2.89-fold (Fig. 5.7 B). This protein was identified by MALDI-ToF/ToF with two highly confident peptide sequences (aa3514 to aa3707 of the full-length perlecan molecule), which indicates the LG3 peptide (compare <http://uniprot.org/uniprot/Q05793>). Unfortunately, Western blot analysis targeting the perlecan C-terminal region of MEF cell-derived protein samples did not deliver any additional information. Thus, the protein samples were further fractionated using centrifugal filter units (100 kDa MWCO) into a <100 kDa and a >100 kDa fraction and subjected to SlotBlot analysis (Fig. 5.7 C). As depicted, the SlotBlot analysis confirmed the reduced perlecan levels within the <100 kDa fraction of ADAM17^{ex/ex} MEF cell-derived supernatants (Fig. 5.7 C, SN, <100kDa). In contrast, whole-cell lysates showed increased perlecan levels within the >100 kDa fraction derived from ADAM17^{ex/ex} MEF cell lysates (Fig. 5.7 C, WCL, >100kDa). Interestingly, small amounts of a shorter perlecan fragment were also observed in whole-cell lysates of MEF 1#1.

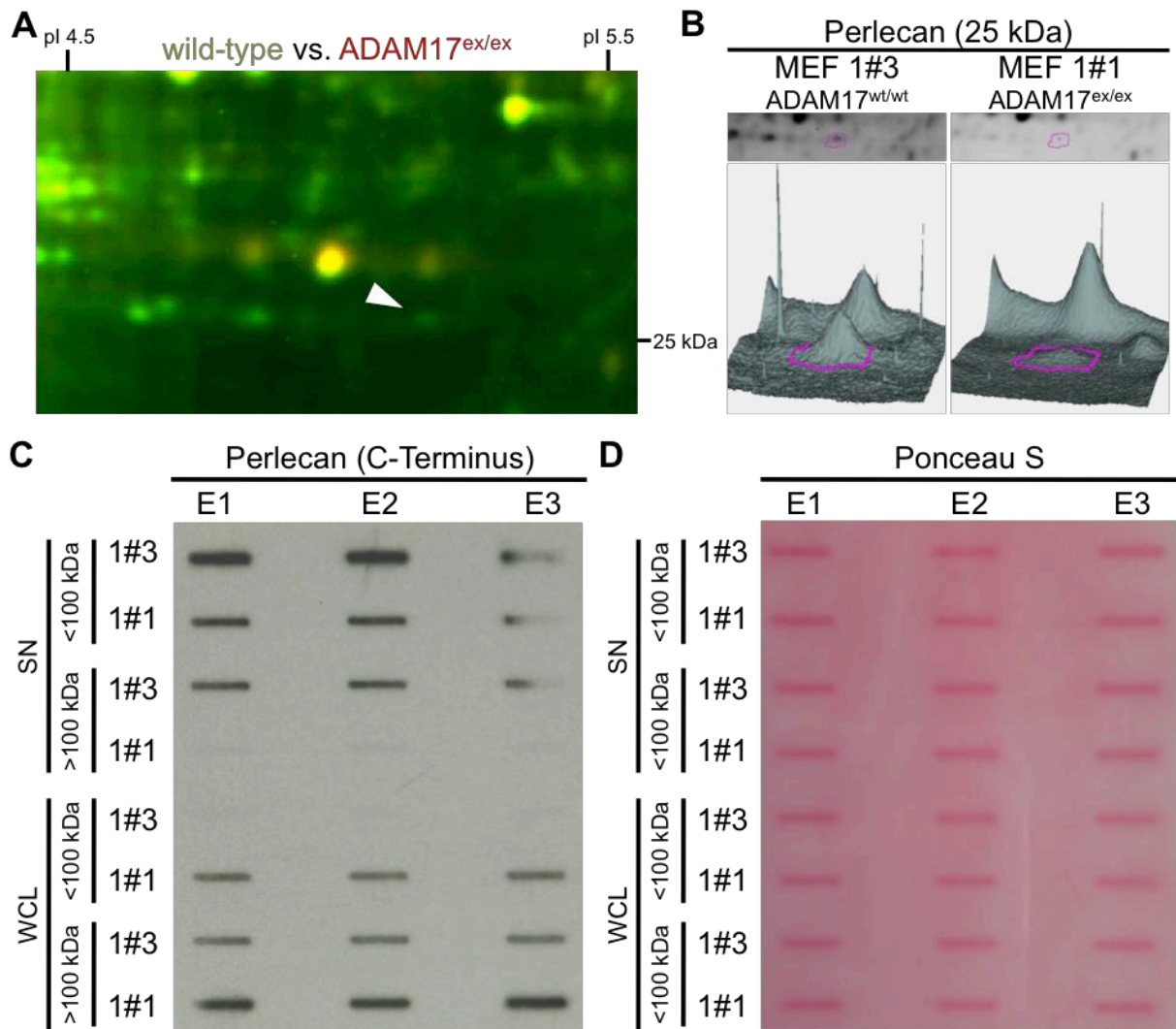


Fig. 5.7: Reduced generation of the perlecan LG3 peptide in *ADAM17^{ex/ex}* MEF cells. (A) Pseudo-colored 2D-DiGE image section of wild-type (Cy3, green) and *ADAM17^{ex/ex}* (Cy5; red) MEF cell-derived cell culture supernatant proteins, enriched by centrifugal filter units. Proteins were separated on a 24 cm 3-11NL IPG strip, followed by SDS-PAGE. The image was recorded using the TyphoonTRIO laser scanner and processed by the ImageQuant TL software. The protein spot identified as the perlecan LG3 peptide is indicated (white arrow). (B) Fluorescence intensities of the observed protein spot in wild-type (left panel) and *ADAM17^{ex/ex}* MEF cells, as calculated by DeCyder 2D software (Version 7.2). (C) Immunodetection of the C-terminal region of perlecan by SlotBlot analysis of fractionized (<100 kDa and >100 kDa) cell culture supernatants (SN) and whole-cell lysates. (D) Equal protein amount loading was monitored by Ponceau S staining.

5.3.2 Altered protein secretion from *ADAM17^{ex/ex}* MEF cells

The analyses of MEF cell-derived cell culture supernatants not only revealed a variety of differentially abundant protein fragments, but also changes in the representation of several full-length proteins. Out of approximately 400 different identified proteins, around 70 proteins were supposed to be secreted into the cell culture supernatant. Fold-change values of differentially regulated secreted proteins, derived from seven independent 2D-DiGE analyses are summarized in table 5.2. Of note, the proteins included in the table only represent a selection from all identified proteins.

Tab. 5.2: Differentially regulated proteins within MEF cell culture supernatants, enriched by centrifugal filter units (CFU) or WGA-mediated precipitation (WGA). Fold-change values based on DeCyder 2D software (Version 7.2) calculations as given. Results from seven independent approaches are summarized. Underlined fold-change values indicate spots that were not identified by MS analyses in the given experiment, but were annotated according to the localization in other experiments. Information about the subcellular distribution were taken from <http://uniprot.org> based on the corresponding accession number and are indicated as follows: secreted (S), extracellular matrix (ECM), basal membrane (BM), plasma membrane (M). Please note: samples separated in DiGE150 were proteins from TNF α -overexpressing MEF cells.

Experiment Protein ID	145	150a	150b	153	169	172	182	Locus	Accession
TNF α		-14.7	-6.64					M/S	P06804
CO1A1_FL			-8.12		-1.55			S/ECM	P11087
B2MG		-10.5	-7.48					S	P01887
PCOC-1 (35 kDa)				-5.82				S	Q61398
PXDN						-5.14		S/ECM	Q3UQ28
CFAH						-3.33	-5.65	S	P06909
Cysatatin-B					-4.39			C	Q62426
BGAL					-4.36			L	P23780
PAFA	-1.45		-2.85					S	Q60936
CO1A2_FL		-5.26	-3.15					S/ECM	Q01149
CO5A1_FL	-1.64	-6.2	-4.76					S/ECM	O88207
GST Ω 1	-1.68	-1.76			-8.66			C	O09131
CO1A1_CPP	-2.52	-7.83	-6.15	-1.81	-1.85			S/ECM	P11087
Transgelin	-2.02				-5.66			C	P37804
CO1A2_CPP	-2.11	-5.62	-6.49	-2.28	-1.57			S/ECM	Q01149
CO1A1_FL	-1.9	-4.3	-4.48					S/ECM	P11087
CO1A2_FL		-2.73	-3.97					S/ECM	Q01149
Cystatin-C		-2.90	-3.40					S	P21460
CO3A1_CPP			-6.04					S/ECM	P08121
Fascin					-2.84			C/CS	Q61553
Galectin-3		-1.19		-2.02	-2.45			S/ECM	P16110
TIMP-1	-3.01	-2.76	-2.53					S	P12032
Moesin					-2.65			pM	P26041
Perlecan_LG3	-1.78	-2.89	-3.01		-2.89			S/BM	Q05793
Galectin-1	-2.01				-3.22			S/ECM	P16045
PAI		-2.61						S	P22777
CO6A1_FL						-2.73	-2.38	S/ECM	Q04857
CO6A2_FL						-3.03	-1.95	S/ECM	Q02788
ILGBP4	-2.48							S	Q80W15
Cadherin-2_CP		-2.33	-2.41					M/S	P15116
MRC2							-2.28	M	Q64449

Fibulin-1					-1.14	-4.32	1.23	S/ECM	Q08879
Neogenin					-2.02			M	P97798
Lumican							-1.96	S/ECM	P51885
Peroxiredoxin-1	-1.78							C	P35700
TCTP	-1.25	-1.15			-2.87			C	P63028
NCAM-1							-1.69	M/S	P13595
PPIC	-2.43	-1.27			-1.29			C	P30412
CO4A2_FL						-1.66		S/BM	P08122
Periostin					-1.64	-1.57		S/ECM	Q62009
Mimecan						-1.60		S/ECM	Q62000
HtrA1				-1.09	-2.07			S; C	Q9R118
HSP7C					-1.49			S; M	P63017
OLFL-1					-1.45				
Gelsolin	-1.29							C; S	P13020
C1-sA					-1.23	-3.27		S	Q8CG14
OLFL-3					-1.26	-2.02	-1.53	S	Q8BK62
C1-rA					-1.17	-2.71		S	Q8CG16
Peroxiredoxin-6	1.52				-3.81			C	O08709
Renin receptor	-1.81	1.08			-2.54			M	Q9CYN9
PPIA	-1.50	-1.49			-2.83			C; S	P17742
TIMP-2	1.77	-1.98	-1.06		-1.43			S	P25785
Peroxiredoxin-2	1.54				-2.71			C	Q61171
PCOC-1		1.09		1.34	1.24			S	Q61398
Serpin H1			1.42	1.21	1.49			ER	P19324
Vimentin	1.17	1.64						C	P20152
Thioredoxin		1.42						N; C; S	P10639
Cathepsin B	1.34			1.44	1.78			L; S	P10605
Cystatin-C		1.34	1.67					S	P21460
PLOD-1					1.57			ER; pM	Q9R0E2
PDI	1.60							ER; M	P09103
Vasorin					1.93			M	Q9CZT5
MMP-2				1.33	2.62			S/ECM	P33434
Peroxiredoxin-1	3.31		1.58				1.5	C	P35700
PRG4_CP		1.51	1.93			3.85		S	Q9JM99
FSTL-1				2.04	3.78	2.33	2.09	S	Q62356
PLTP					2.87			S	P55065
B4GT1					3.02			S	P15535
ECM-1				2.48	1.86	3.43	1.55	S/ECM	Q61508

Fibulin-3					3.30			S/ECM	Q8BPB5
MMP-3		3.26	3.62					S/ECM	P28862
PEDF					4.06			S	P97298
alpha-Enolase	1.52							C; M	P17182
IL1RL1				2.35				M; S	P14719
sFRP2		3.26	2.18		5.25			S	P97299
Glia-derived nexin					9.84			S	Q07235
B2MG		29.11	21.63		5.25			S	P01887

Although a large number of differentially abundant proteins were identified from analyses of MEF cell culture supernatants, individual analyses did not deliver consistent data sets. Some proteins were only identified from samples enriched by centrifugal filter units (e.g. cystatin-C) or WGA-mediated precipitation (e.g. ECM-1), respectively. Although, several secreted proteins showed altered protein levels in ADAM17^{ex/ex} MEF cell culture supernatants, there was no common direction of the alterations. Whereas some proteins (e.g. ECM-1 and Fstl-1) were increased within ADAM17^{ex/ex} MEF cell supernatants, others were decreased (e.g. Olf1-1). Notably, the rather prominent group of ECM proteins, mainly represented by various types of collagens, showed reduced protein levels in ADAM17^{ex/ex} MEF cell supernatants.

In summary, the analyses of cell culture supernatants by 2D-DiGE pointed to a variety of changes in protein secretion, but also delivered incomplete data sets.

5.3.2.1 Reduced levels of full-length type-I collagen molecules in ADAM17^{ex/ex} supernatants

Reduced levels of the type-I collagen C-terminal propeptides in ADAM17^{ex/ex} MEF cell supernatants were highlighted in section 5.3.1.1. However, the analyses of MEF cell culture supernatants also revealed changed protein levels for various full-length collagen chains, which were mostly reduced within ADAM17^{ex/ex} MEF cell supernatants. As summarized in table 5.2, this not only includes type-I collagen molecules, but also type-IV, type-V and type-VI collagen chains. Unfortunately, antibodies for verification of these findings were not available (except for the already mentioned type-I collagen α_1 chain antibody). Reduced full-length type-I collagen protein spots were observed at two different molecular masses of about 150 and 120 kDa (compare Fig. 5.8 A and the corresponding fold-change values in Tab. 5.2).

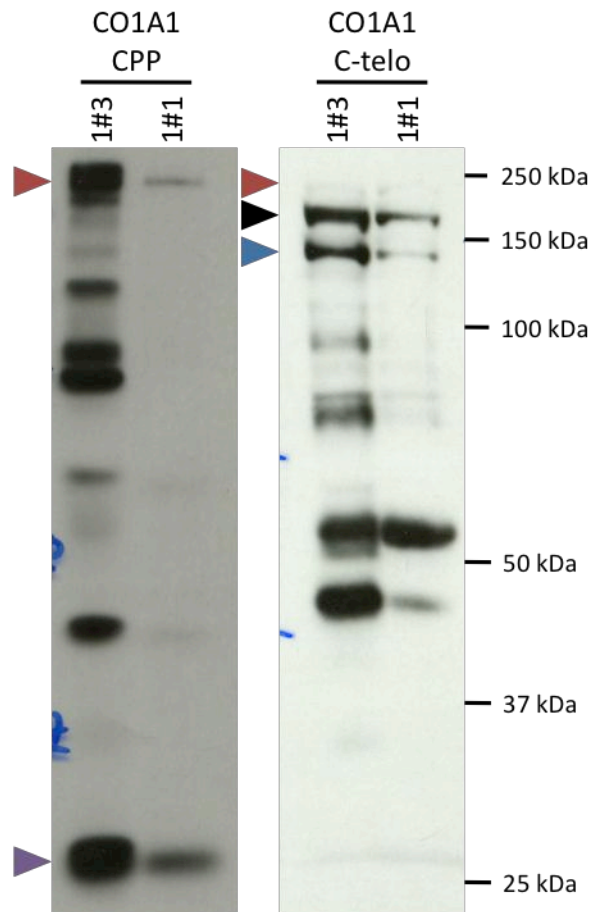


Fig. 5.8: Reduced levels of type-I collagen α_1 protein bands in ADAM17^{ex/ex} MEF cell supernatants. Cell culture supernatant proteins, enriched by WGA-mediated precipitation were separated by SDS-PAGE (12.5 %) and transferred onto a nitrocellulose membrane. Type-I collagen α_1 chain was targeted via its C-terminal propeptide (CO1A1 CPP) and its C-terminal telo-peptide (CO1A1 C-telo) by antibodies LF-41 and LF-68, respectively.

At least for the type-I collagen α_1 chain, these findings were confirmed by Western blot analyses via the C-terminal propeptide (Fig. 5.8 B; left panel) and the C-terminal telo-peptide (Fig. 5.8 B, right panel). In addition to the 30 kDa CO1A1 C-terminal propeptide (Fig. 5.8, CO1A1 CPP, purple arrow) also a high molecular weight form of type-I collagen of approximately 250 kDa was decreased in ADAM17^{ex/ex} MEF cell supernatants (Fig. 5.8, CO1A1 CPP, red arrow). Moreover, type-I collagen α_1 chain molecules, targeted via their C-terminal telo-peptide (Fig. 5.8 B, CO1A1 C-telo), revealed decreased levels of two protein bands with molecular weights of approximately 200 kDa (Fig. 5.8 B, black arrow) and of 130 kDa (Fig. 5.8 B; blue arrow). The cell culture supernatant of wild-type MEF cells contained a variety of further protein fragments that were specifically detected by the used antibodies.

5.4 ADAM17 – A modulator of the protease web?

Tab. 5.3: Differentially regulated proteases, protease inhibitors and protease enhancers identified by 2D-DiGE analyses from MEF cell culture supernatant proteins, enriched by centrifugal filter units (CFU) or WGA-mediated precipitation (WGA). Protein fold-change values base on DeCyder 2D software (Version 7.2) calculations. Results from seven independent experiments are summarized. Information upon subcellular distribution was taken from <http://uniprot.org> and the corresponding accession number and are indicated as follows: secreted (S), extracellular matrix (ECM), basal membrane (BM), plasma membrane (M). Please note: samples separated in DiGE150 were proteins from TNF α -overexpressing MEF cells.

Protein ID		Experiment	145	150a	150b	153	169	172	182	Locus	Accession
fold-change values (wild-type \rightarrow ADAM17 ^{ex/ex})	Proteases	BMP-1						-1.58	-1.59	S/ECM	P98063
		Cathepsin B	1.34			1.44	1.78			L/S	P10605
		HtrA1					-1.09	-2.07		S; C	Q9R118
		MMP-2				1.33	2.62			S/ECM	P33434
		MMP-3		3.79	3.62					S/ECM	P28862
	PE	OLFL3				-2.74	-1.26	-2.02	-1.53	S	Q8BK62
		PCOC-1		1.31		1.34	1.24			S	Q61398
	Protease inhibitors	SFRP2		3.26	2.18		5.28			S	P97299
		Cystatin-B					-4.39			C; S	Q62426
		Cystatin-C		-2.9	-3.4					S	P21460
		Cystatin-C		1.43	1.67					S	P21460
		ECM-1				2.48		3.43	1.55	S/ECM	Q61508
		GDN					9.84			S	Q07235
		PAI		-2.61						S	P22777
		PEDF					4.06			S	P97298
Serpin H1					1.42	1.21	1.49		ER	P19324	
TIMP1			-3.01	-4.18	-2.53				S	P12032	
TIMP2		1.77	-1.98	-1.05		-1.43		S	P25785		

A third group of differentially abundant proteins, identified from MEF cell culture supernatants is represented by proteases and protease interacting proteins. As summarized in table 5.3, these protease-associated proteins included matrix metalloproteases (MMPs), tissue inhibitors of metalloproteases (TIMPs), serpin family proteins (e.g. serpin H1, glia-derived nexin 1) and cystein protease inhibitors (cystatins).

5.4.1 Reduced BMP-1 protein levels in ADAM17^{ex/ex} MEF cell supernatants

Within two analyses of supernatant proteins, enriched by WGA-mediated precipitation, the procollagen C-proteinase BMP-1 showed reduced protein levels in ADAM17^{ex/ex} MEF cell

supernatants. Western blot analysis of wild-type and ADAM17^{ex/ex} MEF cell-derived supernatant proteins confirmed these findings (Fig. 5.9, left panel). In contrast, immunodetection of BMP-1 within MEF cell-derived whole-cell lysates showed increased protein levels within the wild-type MEF cell samples (Fig. 5.9, right panel). Of note, another pro-collagenase, Meprin β , was not detectable in MEF cell samples by various anti-mMeprin- β antibodies.

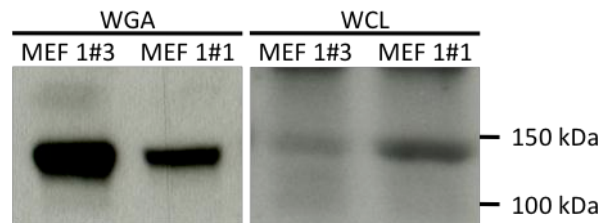


Fig. 5.9: Altered protein levels of the procollagen C-proteinase BMP-1. Whole-cell lysates (WCL) and WGA-precipitated supernatant proteins (WGA) were separated by SDS-PAGE, using a 4-12% pre-cast gradient gel. Separated proteins were transferred onto a nitrocellulose membrane and stained for BMP-1.

5.4.2 ADAM17 – A putative modulator of MEF cell MMP activity?

The matrix metalloproteases MMP-2 and MMP-3 showed elevated protein levels in ADAM17^{ex/ex} MEF cell supernatants (Tab. 5.3, MMP2 and MMP3). Unfortunately, suitable antibodies were not available for further analyses. Thus, putative changes in MMP activity were assayed by gelatin and casein zymography using cell culture supernatant proteins enriched by centrifugal filter units without protease inhibitor treatment.

5.4.2.1 Impaired gelatinolytic activity of ADAM17^{ex/ex} MEF cell supernatants

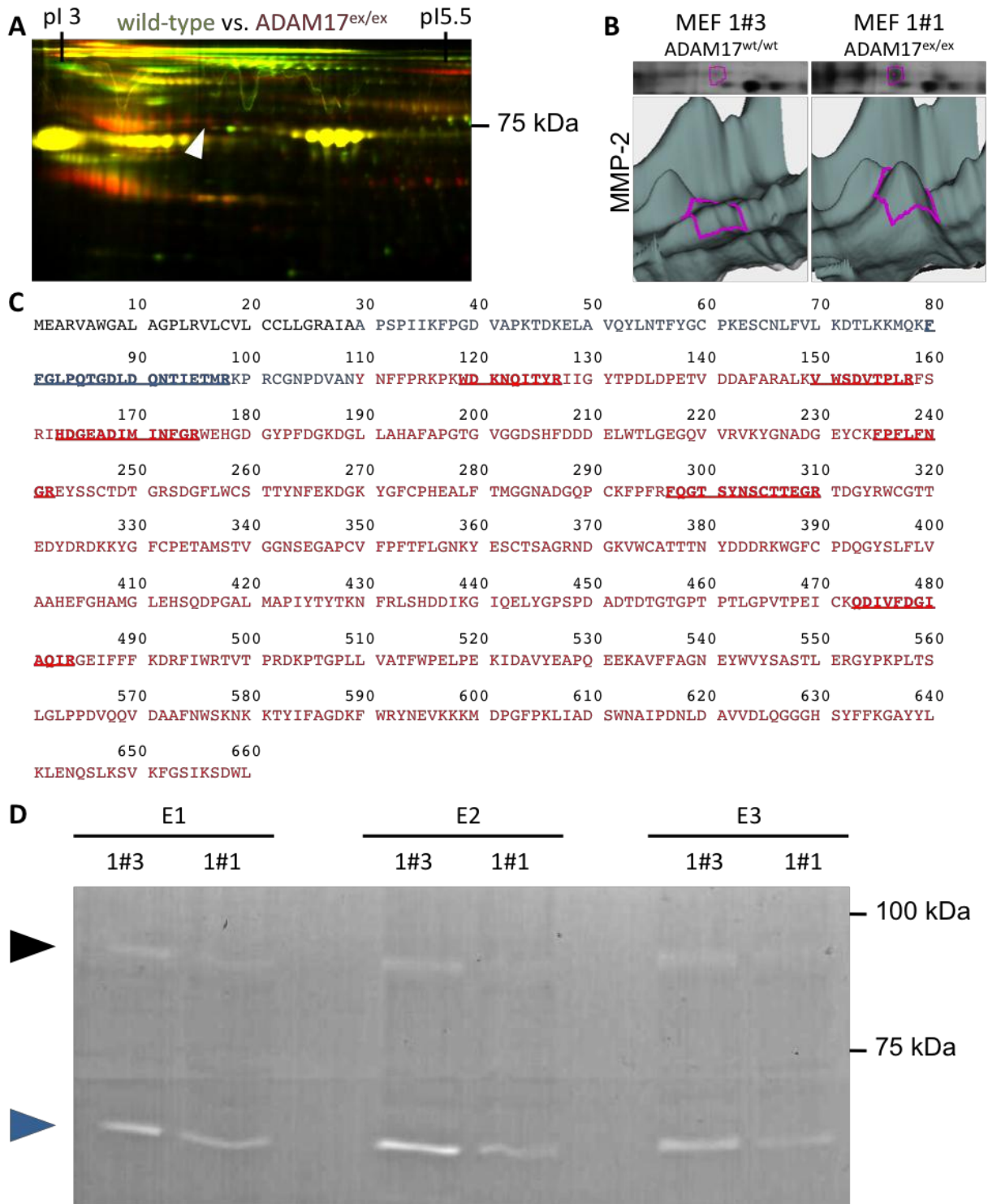


Fig. 5.10: Impaired gelatinolytic activity of ADAM17^{ex/ex} MEF cell culture supernatants. (A) Pseudo-colored image section of MEF cell culture supernatants proteins, separated by 2D-DiGE. Proteins from MEF cells were enriched by WGA-precipitation and differentially labeled by Cy3 (MEF 1#3, green) and Cy5 (MEF 1#1, red). Proteins were separated on a 24 cm 3-11NL IPG strip, followed by SDS-PAGE. (B) Fluorescence intensities of MMP-2 protein levels in wild-type and ADAM17^{ex/ex} MEF cells. (C) MALDI-ToF/ToF-derived sequence coverage of the full-length proMMP-2 sequence consisting of the signal peptide (black), a propeptide (light blue) and the MMP-2 region (red). Underlined regions indicate peptides identified by MALDI-ToF/ToF. (D) Gelatinolytic activity at approximately 92 kDa (black arrow) and 63 kDa (blue arrow) within wild-type and ADAM17^{ex/ex} MEF cell culture supernatants. Proteins were separated on a 12.5% polyacrylamide gel, containing 2 mg/ml gelatin. Cleared protein bands represent gelatin degradation after 20 h of incubation.

As indicated in figure 5.10, high confident peptides, identified by MALDI-ToF/ToF analysis were also located within the MMP-2 propeptide (Fig. 5.10 C). However, the gelatin zymogram of wild-type MEF cell culture supernatants revealed two distinct and clear protein bands at approximately 92 kDa (Fig. 5.10 D, black arrow) and at approximately 63 kDa (Fig. 5.10 D, blue arrow). In both cases, gelatinolytic activity was reduced in ADAM17^{ex/ex} MEF cell culture supernatants.

5.4.2.2 Impaired caseinolytic activity within ADAM17^{ex/ex} MEF cell supernatants

In addition to MMP-2, one 2D-DiGE analysis also revealed increased protein levels of matrix metalloprotease 3 (MMP-3) in supernatants of TNF α -overexpressing ADAM17^{ex/ex} MEF cells. As indicated in figure 5.11 A, the observed protein spot was elevated by approximately 3.8-fold (Fig. 5.11 B). Moreover, the localization of MMP-3 above the 50 kDa marker implicated that this protein spot represents the immature proMMP-3 form. This was supported by the MALDI-ToF/ToF derived sequence coverage, as some peptides within the MMP-3 pro-domain were identified (Fig. 5.11 C). Although less sensitive, casein zymography is more suitable for the detection of MMP-3 activity, compared to gelatin zymography.

As shown in figure 5.11, the casein zymogram of wild-type MEF cell culture supernatants revealed two distinct and clear protein bands below (Fig. 5.11 D, blue arrow) and above the 50 kDa marker (Fig. 5.11 D, black arrow). Whereas the <50 kDa form is increased in wild-type samples, the >50 kDa signal appeared to be slightly increased within ADAM17^{ex/ex} MEF cell supernatants.

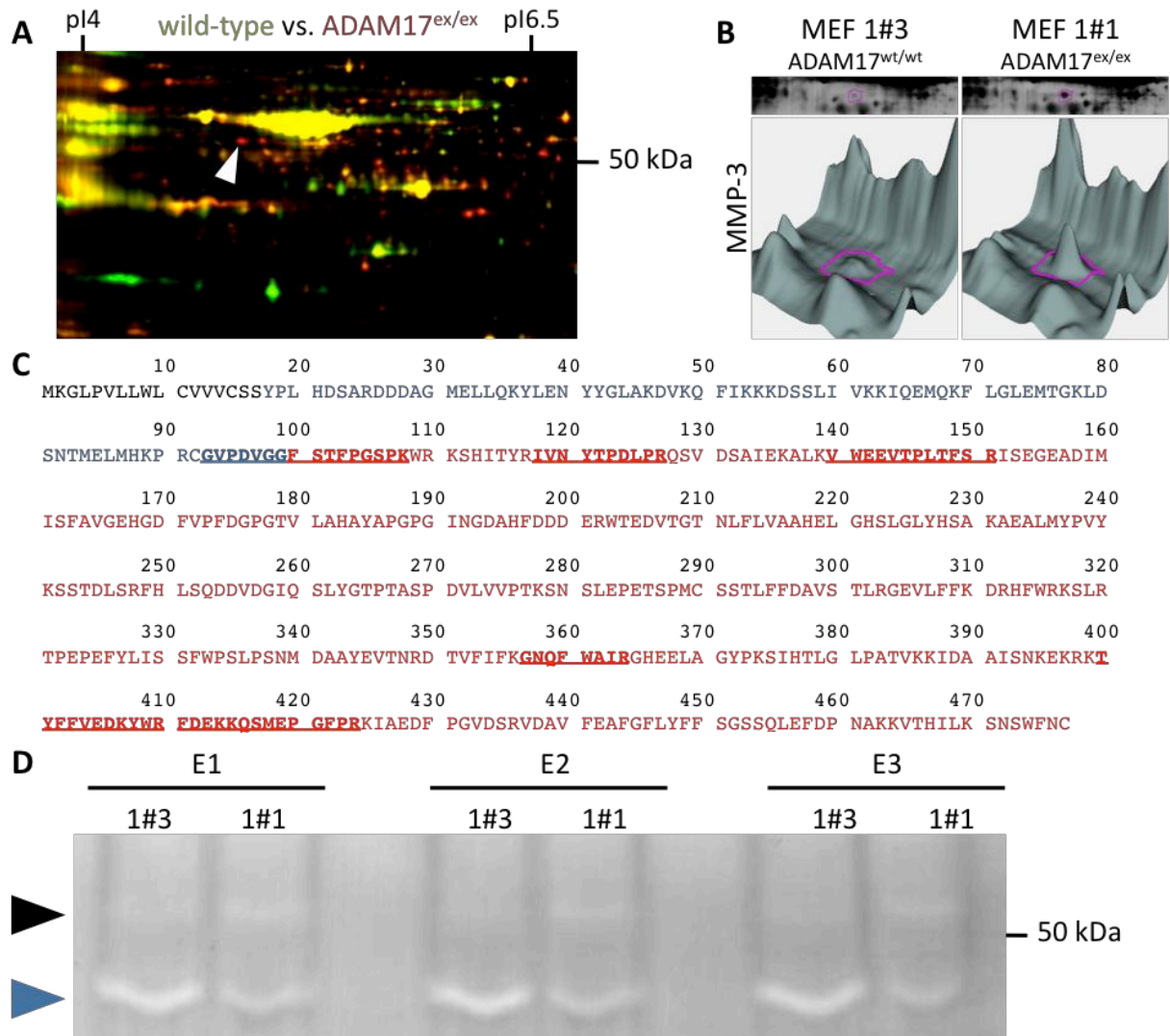


Fig. 5.11: Impaired MMP-3 caseinolytic activity of *ADAM17^{ex/ex}* MEF cell supernatants. (A) Pseudo-colored image section of MEF cell culture supernatants proteins, separated by 2D-DiGE. Proteins from TNF α -overexpressing MEF cells were enriched by centrifugal filter units and differentially labeled by Cy5 (MEF 1#3) and Cy3 (MEF 1#1). Proteins were separated on a 24 cm 3-11NL IPG strip, followed by SDS-PAGE. (B) Fluorescence intensities of MMP-3 protein levels in wild-type and *ADAM17^{ex/ex}* MEF cells. (C) MALDI-ToF/ToF-derived sequence coverage of the full-length proMMP-3 sequence consisting of the signal peptide (black), a propeptide (light blue) and the MMP-3 region (red). Underlined regions indicate peptides identified by MALDI-ToF/ToF. (D) Caseinolytic activity above (black arrow) and below the 50 kDa marker (blue arrow) within wild-type and *ADAM17^{ex/ex}* MEF cell culture supernatants. Proteins were separated on a 12.5 % polyacrylamide gel, containing 2 mg/ml casein. Cleared protein bands represent casein degradation after 20 h of incubation.

5.4.3 ADAM17 affects protease interacting proteins

As mentioned before, analyzed cell culture supernatants not only showed altered protein levels for different protease, but also for protease interacting proteins, including protease inhibitors and protease enhancer molecules.

5.4.3.1 Reduced TIMP-1 and TIMP-2 levels within ADAM17^{ex/ex} MEF cells

Tissue inhibitors of metalloproteases (TIMP) proteins are physiological inhibitors of matrix metalloproteases and other metalloproteases via their characteristic netrin-like (NTR) domain [Williamson *et al.*, 2008]. Analyses of supernatants from TNF α -overexpressing ADAM17^{ex/ex} MEF cells showed reduced levels of TIMP-1 (Fig. 5.12 A, white arrow and B, upper panel) and TIMP-2 (Fig. 5.12 A, red arrow and B, lower panel).

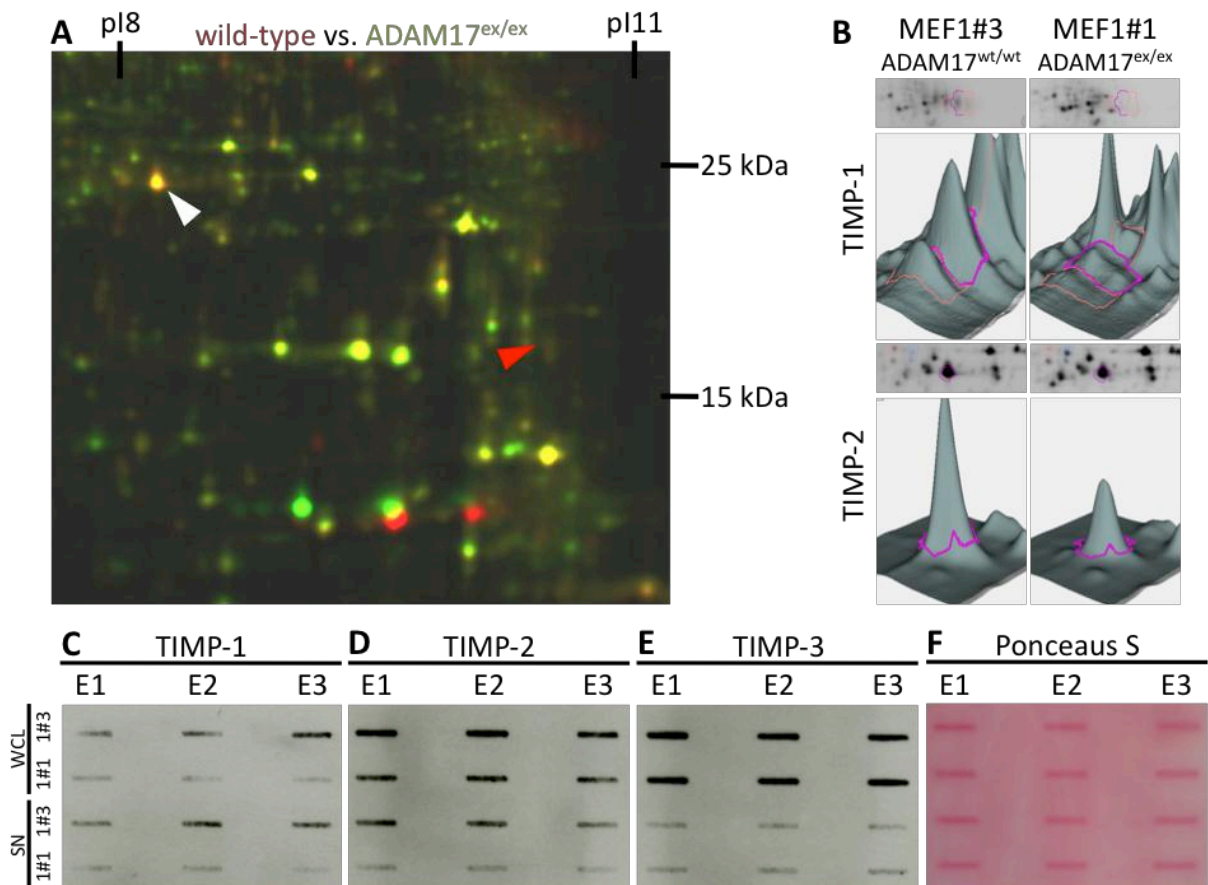


Fig. 5.12: Reduced cellular and extracellular TIMP-1 and TIMP-2 protein levels in ADAM17^{ex/ex} MEF cells. (A) Pseudo-colored 2D-DiGE image section of separated TNF α -overexpressing MEF cell culture supernatant proteins, enriched by centrifugal filter units. Samples were differentially labeled by Cy3 (ADAM17^{ex/ex}, green) and Cy5 (wild-type, red) and separated on a 24 cm 3-11NL IPG strip, followed by SDS-PAGE. (B) Fluorescence intensities of TIMP-1 (upper panel) and TIMP-2 (lower panel) in the supernatant of wild-type (left panel) and ADAM17^{ex/ex} MEF cells (right panel). (C) SlotBlot analyses of TIMP-1, TIMP-2 and TIMP-3 in whole-cell lysates (WCL) and concentrated cell culture supernatants (SN). Equal protein amount loading was monitored by Ponceau S staining.

Unfortunately, the available antibodies yielded poor results in case of Western blot analyses. Thus, supernatants and whole-cell lysates were subjected to immunodetection of TIMP-1, TIMP-2, and TIMP-3 by SlotBlot analyses. As shown, SlotBlot analyses confirmed the observed reduction of TIMP-1 (Fig. 5.12 C; SN) and TIMP-2 (Fig. 5.12 D; SN) in ADAM17^{ex/ex} MEF cell supernatants. Moreover, ADAM17^{ex/ex} MEF whole-cell lysates also showed reduced TIMP-1 (Fig. 5.12 C; WCL), and TIMP-2 (Fig. 5.12 D; WCL) protein levels. In contrast, TIMP-3

protein levels were comparable in wild-type and ADAM17^{ex/ex} MEF cell supernatants and lysates.

5.5 ADAM17-mediated changes of intracellular proteins

During the analyses of cell culture supernatant proteins not only secreted and cell-surface proteins were identified, but also a variety of intracellular proteins. Also, the described alterations concerning type-I collagen levels indicated that other proteins might be affected by the absence of ADAM17. To address this, whole-cell lysates were analyzed for putative changes in relation to the ADAM17^{ex/ex} phenotype. Whole-cell lysates were generated in five independent biological replicate approaches and separated in two 2D-DiGE experiments. Notably, the five biological replicates resulted in five very similar gels with similar overall resolutions and detectable protein changes. Fold-change values for selected differentially abundant proteins are summarized in table 5.4.

Tab. 5.4: Differentially regulated proteins from MEF cell-derived whole-cell lysates. Protein fold-change values are depicted for several identified proteins, as calculated by the DeCyder 2D software after separation of differentially labeled whole-cell lysates proteins by 2D-DiGE. Each column represents values from one out of five independent 2D-DiGE analyses. Fold-change values are indicated and highlighted by different colors. Underlined fold-change value indicate that this spot was observed but not identified by MALDI-ToF/ToF analyses from the corresponding sample, but showed the same localization as protein spots identified within other analyses. Information on subcellular distributions (Sub. Loc.) were taken from <http://uniprot.org> and the corresponding accession number (Acc. No.) and are indicated as follows: extracellular matrix (ECM), secreted (S), mitochondrium (Mi), nucleus (N), lysosome (L), plasma membrane (PM), basal membrane (BM), endoplasmic reticulum (ER), cytoskeleton (CS).

Protein ID	DIGE158			DIGE160		Acc. No.	Sub. Loc.
	E1	E2	E3	E4	E5		
Argininosuccinate synthase	2,98	5,97	1,7		2,78	P16460	MI
Collagen alpha-1 (I) chain	4,68	2,66	2,45	2,64	3,9	P11087	S/ECM
Latexin	2,87	2,78	3,59			P70202	C
SPARC	1,21	2,43	3,93			P07214	S, ECM
T-complex protein subunit zeta	2,28	2,54	2,5	2,09	3,1	P80317	C
Cartilage-associated protein	2,38	2,33	2,46			Q9CYD3	S/ECM
Gelsolin	2,53	2,38	2,58	2,23	2,07	P13020	C; S
Prolyl 4-hydroxylase subunit alpha-1	1,98	1,76	2,64	2,2	2,06	Q60715	ER
Galectin-3	1,65	2,13	2,22			P16110	C; N; S
Prelamin-A/C	1,76	1,89	1,68	1,95	2,15	P48678	N
Vimentin	1,88		1,82	1,88	1,94	P20152	C
Biglycan	2,28	1,47	1,64			P28653	S/ECM
Annexin A3	1,87	1,83	1,8	1,63	1,85	O35639	M
Vinculin	1,65	1,93	1,95		1,54	Q64727	C; M
Serpin H1	1,66	1,66	1,68	2,09	1,74	P19324	ER
Septin-7	1,94	1,66	1,61		1,73	O55131	C
Protein disulfide isomerase A3	1,91	1,77			1,52	P27773	ER
Ezrin	1,84	1,66	1,65	1,59	1,81	P26040	C;CS;PM
PLOD-3	1,39	1,85	1,88	1,46	1,88	Q9R0E1	ER

Moesin		1,7	1,67	1,91	1,48	P26041	M
Septin-11	1,66	1,66	1,64			Q8C1B7	C
Protein disulfide isomerase	1,65	1,77	1,73	1,55	1,53	P09103	ER; M
Follistatin-related protein 1		1,57	1,7			Q62356	S, ECM
Destrin	1,81	1,13	1,77	1,58		Q9R0P5	C/CS
Ras suppressor protein 1	1,78	1,45	1,71	1,38	1,15	Q01730	
Annexin A5	1,47	1,48	1,78	1,23		P48036	S, ECM
Annexin A1	1,39	1,48	1,37	1,54	1,61	P10107	N;C;BM
Mitogen-activated kinase 1	1,36	1,36	1,52	1,48	1,58	P63085	C/CS; N
Annexin A2	1,48	1,34	1,63	1,58	1,26	P07356	S/BM
PLOD-1	1,39	1,19	1,7			Q9R0E2	ER
Calpain small subunit	1,41	1,3	1,42		1,38	O88456	C; M
Peptidyl-prolyl cis-trans isomerase A	1,29	1,15	1,34	1,46	1,25	P17742	C; S
SERPIN B6				1,24	1,32	Q60854	C
Peroxiredoxin-1	1,18	1,26	1,26	1,26	1,32	P35700	C
LIM and SH3 domains protein 1	1,36	1,1	1,4	1,14	1,18	Q61792	C/CS
Cofilin-1	1,09	1,08	1,01	1,04	1,11	P18760	N;C;pM
Peroxiredoxin-2	-1,36	-1,68	-1,51	-1,37	-1,44	Q61171	C
Peroxiredoxin-6	-1,63	-1,52	-1,51	-1,45	-1,34	O08709	C; L
Annexin A1	-1,36	-1,41	-1,51	-1,52	-1,7	P10107	N;C; BM
ER resident protein 29	-1,61	-1,6	-1,26	0	-1,61	P57759	ER
Stress-induced phosphoprotein 1		-1,73	-1,21	-1,63	-1,64	Q60864	C; N
HNRP A2/B1	-1,31	-2,06	-1,38	-1,46	-1,61	P49312	N; C
Lon protease homolog, mitochondrial		-1,69	-1,5	-1,65	-1,65	Q8CGK3	MI
Cystatin B	-3,6	-1,27	-1,32	-1,51	-1,41	Q62426	C
Elongation factor 2	-1,88	-1,95		-1,95	-1,64	P58252	C
Inorganic pyrophosphatase	-1,89	-2,23	-1,79		-1,59	Q9D819	C
T-complex protein ξ	-2,25	-1,91	-2,09	-1,62	-1,53	P80317	C
Destrin	-1,36	-1,72	-1,31	-2,67	-3,47	Q9R0P5	C/CS
GST omega-1	-3,22		-3,08	-2,66	-2,8	O09131	C
pCofilin-1	-3,6	-3,87	-3,07	-4,34	-4,79	P18760	N;C; pM

As expected, most identified proteins were annotated to be located intracellularly, e.g. cofilin-1 and mitogen activated kinase. However, several proteins are normally secreted or comprise the extracellular matrix. For example, type-I collagen was observed with increased protein levels in ADAM17^{ex/ex} whole-cell lysates, in contrast to its decreased protein levels in ADAM17^{ex/ex} MEF cell supernatants. Thus, to some extent, the whole-cell lysate analysis might be complementary to the described supernatant analysis.

5.5.1 Increased cellular type-I collagen levels

In contrast to reduced full-length type-I collagen α_1 and α_2 chain protein levels in ADAM17^{ex/ex} MEF cell supernatants, ADAM17^{ex/ex} MEF cell whole-cell lysates revealed increased levels of both type-I collagens with molecular weights of 200 and 130 kDa (Fig. 5.13 A). When MEF cell-derived whole-cell lysates were subjected to Western blot

analysis, detection of the type-I collagen α_1 chain via its C-terminal propeptide confirmed increased protein levels of a 250 kDa form of type-I collagen within ADAM17^{ex/ex} MEF cell lysates (Fig. 5.13 B, CO1A1_CPP; red arrow). In addition, immunodetection of the type-I collagen α_1 chain via its C-terminal telo-peptide (Fig. 5.13 B, CO1A1_C-telo) also showed increased protein levels of the 250 kDa collagen (Fig. 5.13 B, CO1A1_C-telo, red arrow). In contrast, increased levels of a 200 kDa and 130 kDa fragment were seen in wild-type whole-cell lysates (Fig. 5.13 B, CO1A1_C-telo, black and blue arrow).

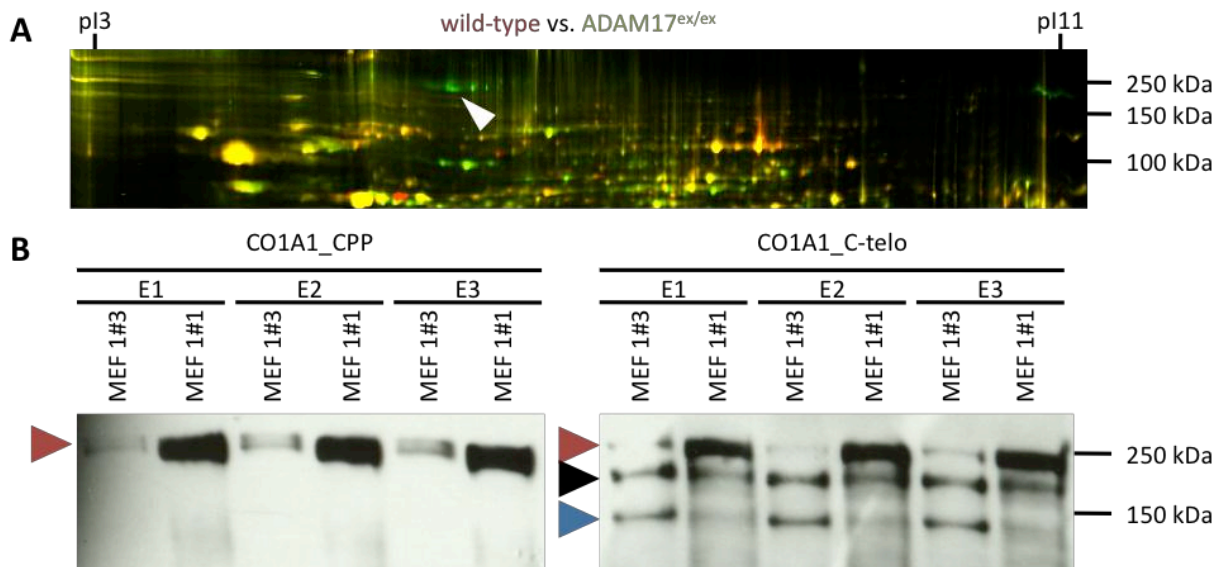


Fig. 5.13: Reduced type-I collagen α_1 chain fragment levels in ADAM17^{ex/ex} MEF cell whole-cell lysates. (A) Pseudo-colored 2D-DiGE image of differentially labeled wild-type (Cy5, red) and ADAM17^{ex/ex} MEF cell (Cy3, green) whole-cell. Proteins were separated on a 24 cm 3-11NL IPG strip followed by SDS-PAGE. Identified type-I collagen α_1 chain molecules is indicated (white arrow). (B) Immunodetection of the type-I collagen α_1 chain in wild-type (1#3) and ADAM17^{ex/ex} MEF cell whole-cell lysates via the C-terminal propeptide (CO1A1_CPP) and the C-terminal telo-peptide, respectively. Specific collagen signals at 250 kDa (red arrow), 200 kDa (black arrow) and 130 kDa (blue arrow) are indicated.

5.5.2 ADAM17 affects members of the Cofilin/ADF-family

5.5.2.1 Altered Cofilin-1 phosphorylation in ADAM17^{ex/ex} MEF cells

Among the various intracellular proteins, the 2D-DiGE analyses of whole-cell lysates of revealed two different protein spots that were identified as cofilin-1. Both cofilin-1 protein spots were located at a molecular of approximately 20 kDa, and were segregated during isoelectric focusing (compare Fig. 5.13 A). In addition, the spots were inversely regulated (Fig. 5.14 B). Whereas the cofilin-1 protein spot with at pI8 (Fig. 5.14 A, white arrow) showed equal or slightly increased protein levels in wild-type and ADAM17^{ex/ex} MEF cells (Fig. 5.14 A, white arrow), the cofilin-1 spot pI6.5 (Fig. 5.14 A, red arrow) was clearly reduced in

ADAM17^{ex/ex} cells. Two-dimensional Western blot analysis using a pan-cofilin-1 antibody confirmed both spots to be cofilin-1 (Fig. 5.14 C and D). The analysis also confirmed the reduced cofilin-1 levels at pI6.5.

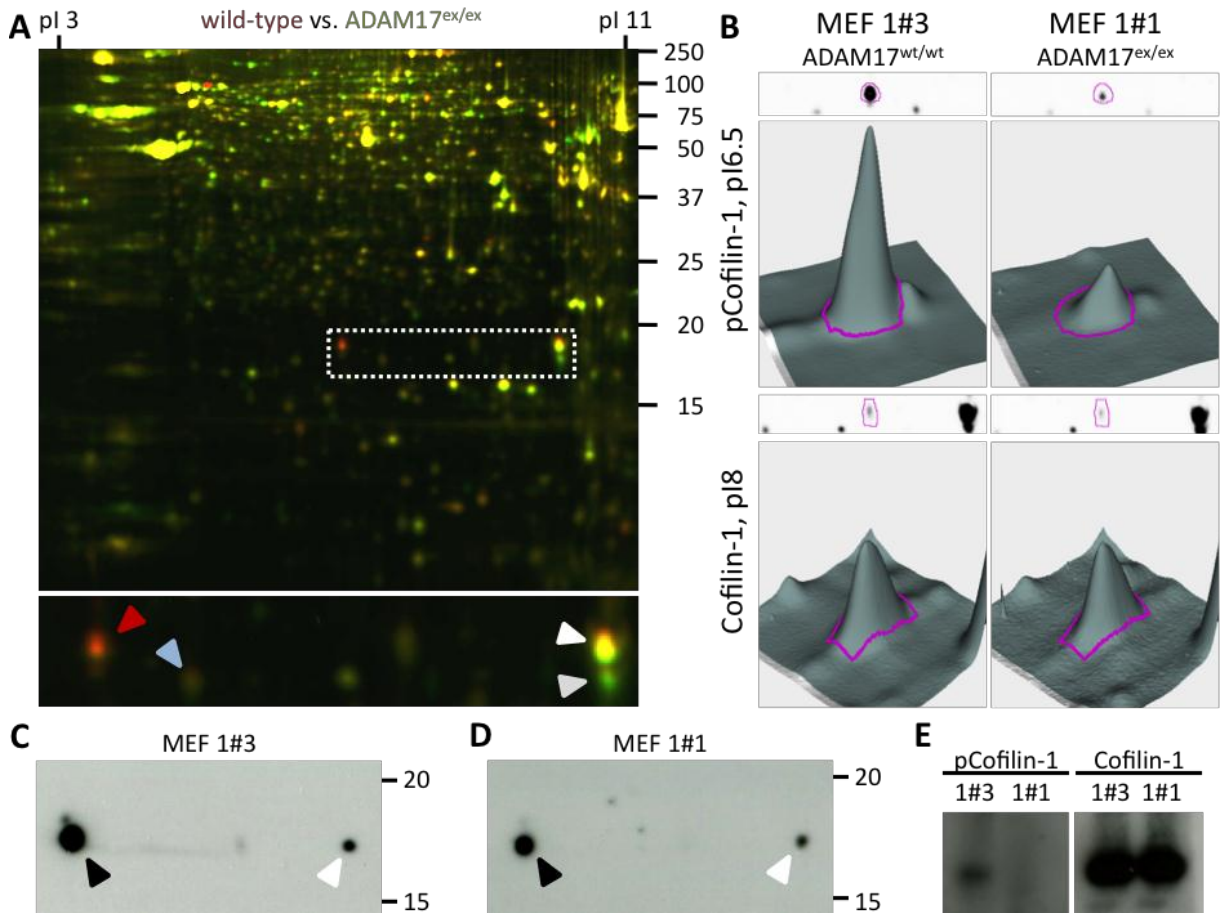


Fig. 5.14: Reduced cofilin-1 phosphorylation in ADAM17^{ex/ex} MEF cells. (A) Pseudo-colored 2D-DiGE image of differentially labeled wild-type (Cy5, red) and ADAM17^{ex/ex} MEF cell (Cy3, green) whole-cell lysate proteins. Proteins were separated on a 24 cm 3-11NL IPG strip followed by SDS-PAGE. The white dashed box indicates the cofilin-1 region and is enlarged in the lower panel. Protein spots, identified as phospho-cofilin-1 (red arrow) and non-phosphorylated cofilin-1 (white arrow) are indicated. Light blue and gray arrows indicate destrin protein spots (refer to section 5.5.2.2). (B) Fluorescence intensities of the phospho-cofilin-1 (upper panel) and the non-phosphorylated cofilin-1 spot (lower panel) in wild-type (MEF 1#3, left panel) and ADAM17^{ex/ex} MEF cells (MEF 1#1, right panel) were calculated using the DeCyder 2D software. Cofilin-1 protein identity was confirmed by immunodetection of two-dimensionally separated (C) wild-type and (D) ADAM17^{ex/ex} MEF cell lysates by a general anti-cofilin-1 antibody. Cofilin-1 spots at pI6.5 (black arrow) and pI8 (white arrow) are indicated. (E) Immunodetection of MEF cell lysates, separated by a 12.5 % SDS-PAGE and subsequent transfer onto a nitrocellulose membrane via a general anti-cofilin-1 antibody (right panel) and a anti-phospho-cofilin-1 specific antibody (left panel).

In addition, detection of cofilin-1 via a Ser3 phospho-specific antibody (Fig. 5.14 E, left panel) confirmed reduced phospho-cofilin-1 protein levels in ADAM17^{ex/ex} MEF cells. In contrast, immunodetection of cofilin-1 by the general antibody showed no differences between wild-type and ADAM17^{ex/ex} MEF cells.

5.5.2.2 Inverse regulation of two different destrin protein spots

In proximity to the observed cofilin-1 protein spots, two protein spots were identified as destrin, another member of the cofilin/ADF protein family. As observed for cofilin-1, the destrin spot at pI8 (Fig. 5.14 A, light blue arrow) appeared to be slightly increased or not altered, whereas the destrin spot at pI6.5 was lower upon reduction of ADAM17 activity (Fig. 5.14 A, grey arrow).

5.5.3 Increased Annexin levels in ADAM17^{ex/ex} MEF cells

The annexin family of Ca²⁺-dependent membrane/phospholipid binding proteins was represented by four different members: Anxa1, Anxa2, Anxa3 and Anxa5.

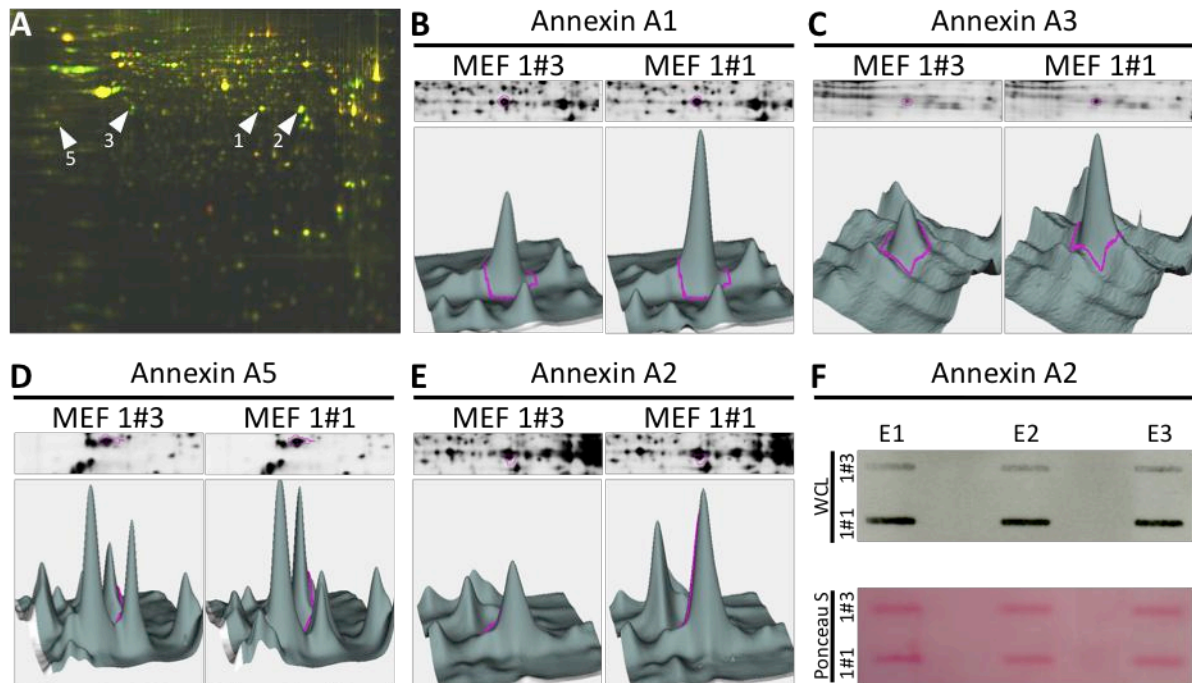


Fig. 5.15: Increased cellular protein levels of various annexin family members in ADAM17^{ex/ex} MEF cells. (A) Pseudo-colored 2D-DiGE image of differentially labeled wild-type (Cy5, red) and ADAM17^{ex/ex} MEF cell (Cy3, green) whole-cell lysate proteins. Proteins were separated on a 24 cm 3-11NL IPG strip followed by SDS-PAGE. Numbered arrows indicated positions of (1) annexin A1, (2) annexin A2, (3) annexin A3 and (5) annexin A4. Fluorescence intensities for (B) annexin A1, (C) annexin A3, (D) annexin A5 and (E) annexin A2 were calculated using the DeCyder 2D software. (F) Immunodetection of annexin A2 in wild-type (1#3) and ADAM17^{ex/ex} MEF cell lysates by SlotBlot analysis. Sampling of equal protein amounts was monitored by Ponceau S staining (lower panel). Equal protein amount loading was monitored by Ponceau S staining.

All proteins were elevated in whole-cell lysates of ADAM17^{ex/ex} MEF cells by approximately 1.5-fold in average (see table 5.4 for details). Figure 5.15 A summarizes information about the protein spots that were identified as annexins in representative 2D-DiGE image of separated proteins from MEF whole-cell lysates. Fluorescence intensities are shown for Annexin A1 (Fig. 5.15 B), Annexin A2 (Fig. 5.15 E), Annexin A3 (Fig. 5.15 C) and Annexin A5

(Fig. 5.15 D). The increased protein levels of Annexin A2 were verified by SlotBlot analyses of whole-cell lysates, derived from three independent experiments (Fig. 5.15 F).

5.6 Network analysis

The performed analyses revealed a variety of differentially affected proteins upon loss of ADAM17 proteolytic activity. In order to identify putative protein interactions, that might give insights into the role of ADAM17 on the affected proteins, an *in silico* network analysis was performed. To this end, selected proteins were analysed for putative and known protein interactions using the STRING 9.1 web service (<http://string-db.org>) at medium confidence settings.

5.6.1 “The extracellular network” of identified proteins

First, differentially regulated proteins identified from cell culture supernatants were included into the network analysis, which is shown in figure 5.16. The predicted network revealed two major clusters that are comprised by the majority of proteins, included in the analysis: (I) metalloproteases and tissue inhibitors of metalloproteases and (II) members of the collagen protein family. As a metalloprotease, ADAM17 was placed into the first cluster and showed interactions with TIMP-3 and its main substrate TNF α . Interestingly, TNF α shows a confident interaction with the over-expressed glia-derived nexin (Serpine-2). In addition, slight interactions with TIMP-2 and matrix metalloproteases MMP-2, MMP-3, MMP-9 and MMP-14 were predicted. However, the predominant interactions within this cluster were observed between the different MMP family members and the TIMP proteins. These proteins also showed weak interactions with cathepsin B and ECM-1. The matrix metalloprotease 2 (MMP-2) represents a linkage knot between the two major clusters and showed interactions with various collagen molecules. All included proteins showed high confident protein interaction with each other. In addition, type-I and type-III collagens were predicted to interact with serpin H1 and BMP-1, but were also linked to a smaller third cluster that contained a variety of intracellular collagen modifying proteins (e.g. PLOD-1 and PLOD-3). The basement heparan sulfate proteoglycan core protein was also placed into this third cluster and showed weak interactions with BMP-1. In contrast, other observed proteins (e.g. IL1RL1 and proteoglycan-4) showed no direct interactions with one of the three

observed clusters. In summary, except for some tissue inhibitors of metalloproteases and matrix metalloproteases, there is no predicted protein interaction with ADAM17.

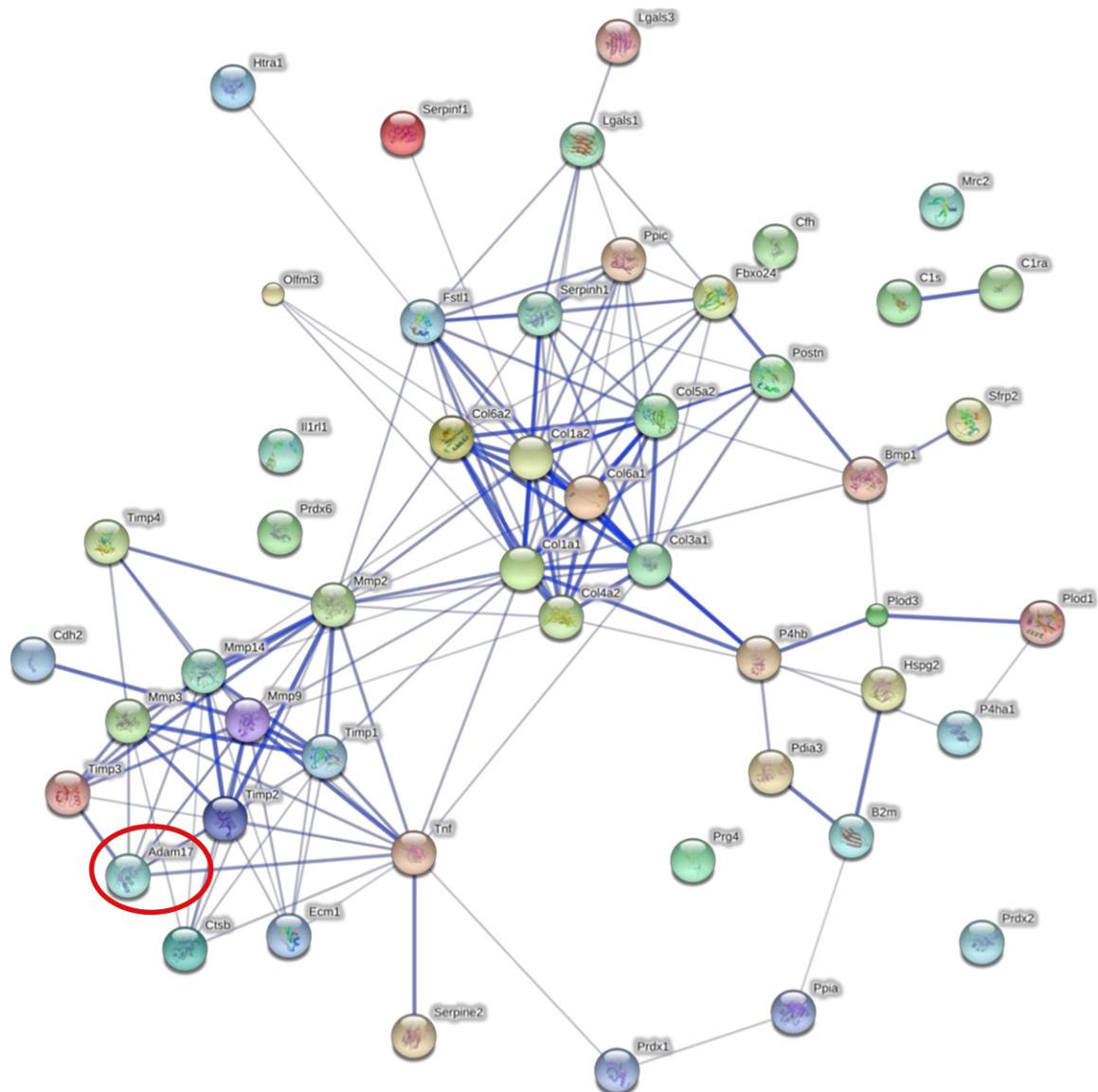


Fig. 5.16: Known and predicted interactions of proteins, differentially regulated in ADAM17^{ex/ex} MEF cell supernatants. This *in silico* analysis was performed using the STRING 9.1 web service (<http://string-db.org>; Snel *et al.*, 2000). Position of ADAM17 is highlighted.

5.6.2 The extended network analysis

The performed analyses also revealed a variety of intracellular changes. Thus, these intracellular proteins were introduced into the network analysis. The confidence view of the predicted protein interactions is shown in figure 5.17. Including the intracellular proteins into this analysis, only slightly changed the complete network. Matrix metalloproteases and TIMPs and collagens still comprised two major clusters of this network. In addition, a third big cluster, including the annexin proteins and cytoskeletal proteins (e.g. ezrin and vimentin) appeared.

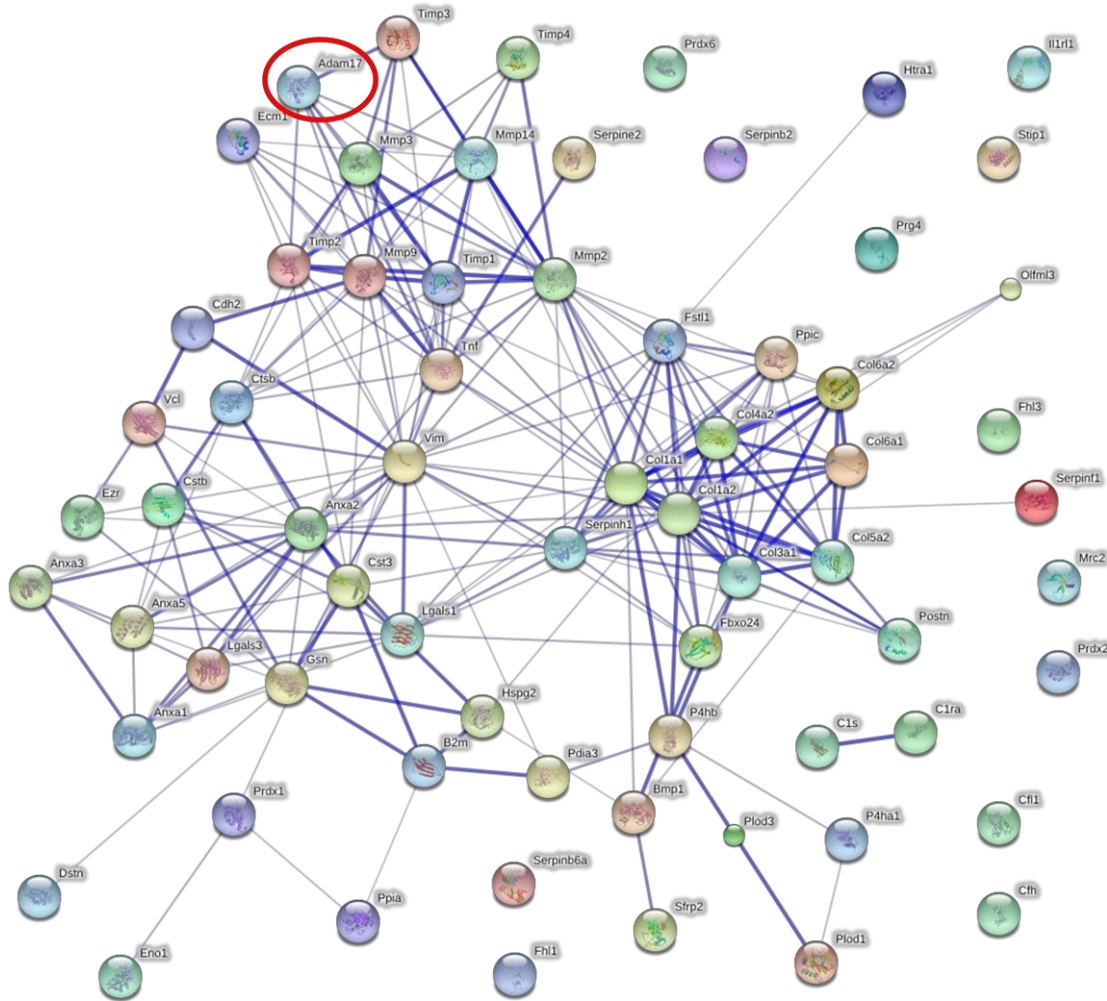


Fig. 5.17: Known and predicted protein interactions of proteins, differentially regulated in ADAM17^{ex/ex} MEF cell supernatants and whole-cell lysates. This *in silico* analysis was performed using the STRING 9.1 web service (<http://string-db.org>; Snel *et al.*, 2000). Position of ADAM17 is highlighted.

This cluster is linked to the small cluster, including perlecan and the collagen modifying proteins via gelsolin and to the MMP and TIMP cluster via cadherin-2. Thus, the extended network analysis did not provoke major changes if compared to the first predicted network, but elucidated another, intracellular network cluster. Especially direct interactions of these proteins with ADAM17 were not shown.

5.7 MEF cells and alternative cellular systems

5.7.1 Differences between different MEF cell lines

Unfortunately, murine embryonic fibroblasts, derived from wild-type and ADAM17^{ex/ex} mice were the only cellular samples of the ADAM17^{ex/ex} system, available for the performed proteomic analysis. As already mentioned, at later stages, two additional sets of wild-type

(MEF 1#7 and MEF 2#1) and ADAM17^{ex/ex} MEF cells (MEF 1#8 and MEF 2#8) were generated and included in the sheddome/secretome analysis. According to the Western blot analysis for ADAM17 protein levels and to the ELISA analysis for alterations in TNF α and TNF-R_I shedding, these cells did not differ from the MEF cell pair used for the experiments described so far (Fig. 5.1 A, D and E). However, the analysis of cell culture supernatants, derived from wild-type and ADAM17^{ex/ex} MEF cells by WGA precipitation revealed major differences between the different MEF cell pairs (compare Tab. 5.5).

Tab. 5.5: Differences in protein levels of differentially regulated cell culture supernatant proteins of three different sets of wild-type and ADAM17^{ex/ex} MEF cell. Proteins of wild-type (MEF 1#3, 1#7 and 2#1) and ADAM17^{ex/ex} MEF cells (MEF 1#1, 1#8 and 2#8) were enriched by WGA-mediated precipitation and separated by 2D-DiGE using a sample mix, labeled with Cy2 as an internal standard. Indicated protein intensities were calculated by the DeCyder 2D software. Underlined values indicate fold-changes for proteins that were not identified by MALDI-ToF/ToF from the corresponding gel, but were matched with protein spots from one of the other gels by the DyCyder 2D software. Information regarding subcellular distribution was taken from <http://uniprot.org> and the corresponding accession number.

Protein ID	Accession No	Subc. Loc	DIGE169		
			68572 1#3 vs. 1#1	68573 1#7 vs. 1#8	68574 2#1 vs. 2#8
Antithrombin III	P32261	S	<u>1,23</u>	-1,64	<u>-1,21</u>
B4GT1	P15535	G; S	2,05	<u>-1,51</u>	<u>1,62</u>
BGAL	P23780	L	-4,36		
C1s-A	Q8CG16	S	<u>-1,17</u>	<u>1,03</u>	1,99
C1s-A	Q8CG14	S	<u>-1,23</u>	<u>2,49</u>	-1,14
C3	P01027	S	<u>-1,44</u>	<u>-6,35</u>	<u>1,3</u>
CO1A1_CPP	P11087	S/ECM	-1,85	<u>2,02</u>	-1,42
CO1A1_FL	P11087	S/ECM	<u>-1,55</u>	<u>1,17</u>	-1,96
CO1A2_FL	Q01149	S/ECM	<u>-3,59</u>		<u>-1,96</u>
CO1A2_CPP	Q01149	S/ECM	-1,57	4,14	-2,78
Cathepsin B	P10605	L; S	1,71	<u>2,46</u>	-2,5
Cystatin-B	Q26426	C	4,4	<u>-2,34</u>	
ECM-1	Q61508	S/ECM	<u>1,86</u>	3,38	1,38
Fascin	Q61553	C	-2,84	<u>-1,01</u>	<u>1,41</u>
Fibulin1	Q08879	S/ECM	<u>-1,14</u>	4,43	<u>-2,43</u>
Fibulin3	Q8BPB5	S/ECM	<u>3,3</u>	19,5	<u>-2,92</u>
fibronectin			<u>1,36</u>	1,06	
FSTL-1	P32261	S	3,78	<u>2,16</u>	<u>-3,29</u>
GDN	Q07235	S	<u>6,76</u>		<u>-8,34</u>
GDN	Q07235	S	9,84		
GST A4	P24472	C	-2,67	-1,44	
GST Ω 1	O09131	C	<u>-8,66</u>		<u>1,85</u>
HSP7C	P63017	C; N; M	<u>-1,49</u>	<u>-1,4</u>	<u>4,18</u>
HtrA1	Q9R118	C; S	-1,09	<u>1,15</u>	-1,01
Galectin-1	P16045	S/ECM	<u>-3,24</u>	<u>1,09</u>	2,7
Galectin-3	P16110	C; N; S	-2,45	<u>2,29</u>	<u>2,85</u>
MMP-2	P33434	S/ECM; C; N	<u>2,65</u>	-1,88	<u>-1,61</u>
Neogenin	P97798	M	<u>-2,02</u>	-4,15	3,06
PCOC-1	Q61398	S	1,24	1,37	2,18

PEDF	P97298	S	4,06	<u>1,27</u>	
Perlecan_LG3	Q05793	S/BM	-2,89	-2,97	
PLOD-1	Q9R0E2	ER	<u>1,57</u>	4,79	<u>1,38</u>
Phospholipid transfer protein	P55065	S	2,87	-1,1	<u>-1,07</u>
Phospholipid transfer protein	P55065	S	2,65		<u>-1,61</u>
Phospholipid transfer protein	P55065	S	<u>4,48</u>	14,77	<u>-1,71</u>
Periostin	Q62009	G; S/ECM	<u>-1,64</u>		<u>-3,89</u>
PPIA	P17742	C; S	-2,84	<u>-2,6</u>	5,23
PPIC	P30412	C	-1,3		
Peroxiredoxin-1	P35700	C		<u>-2,4</u>	
Peroxiredoxin-2	Q61171	C	-2,71	-2,51	2,89
Peroxiredoxin-6	O08709	C	<u>-3,81</u>	<u>-3,73</u>	
Sulfhydryl oxidase 1	Q8BND5	M; S	<u>1,83</u>	4,13	<u>1,17</u>
Renin receptor	Q9CYN9	M	-2,55		
Sulfated glycoprotein 1	Q61207	S	<u>3,99</u>		-2,59
Serpin H1	P19324	ER	<u>1,21</u>	<u>1,73</u>	<u>-4,28</u>
sFRP2	P97299	S	5,25	<u>4,82</u>	<u>-5,9</u>
sFRP2	P97299	S	11,06	<u>5,17</u>	<u>-1,83</u>
Translationally-controlled tumor protein	P63028	C	-2,87	-4,83	<u>4,01</u>
TIMP-2	P25785	S	1,17	-4,69	1,14
Vasorin	Q9CZT5	M	<u>1,93</u>		-1,34

As indicated by the color-coding, only a few proteins, such as ECM-1 and FSTL-1 showed a consistent regulation in all three sets of cells. For many other proteins, at least one set yielded no or an inverted pattern of regulation.

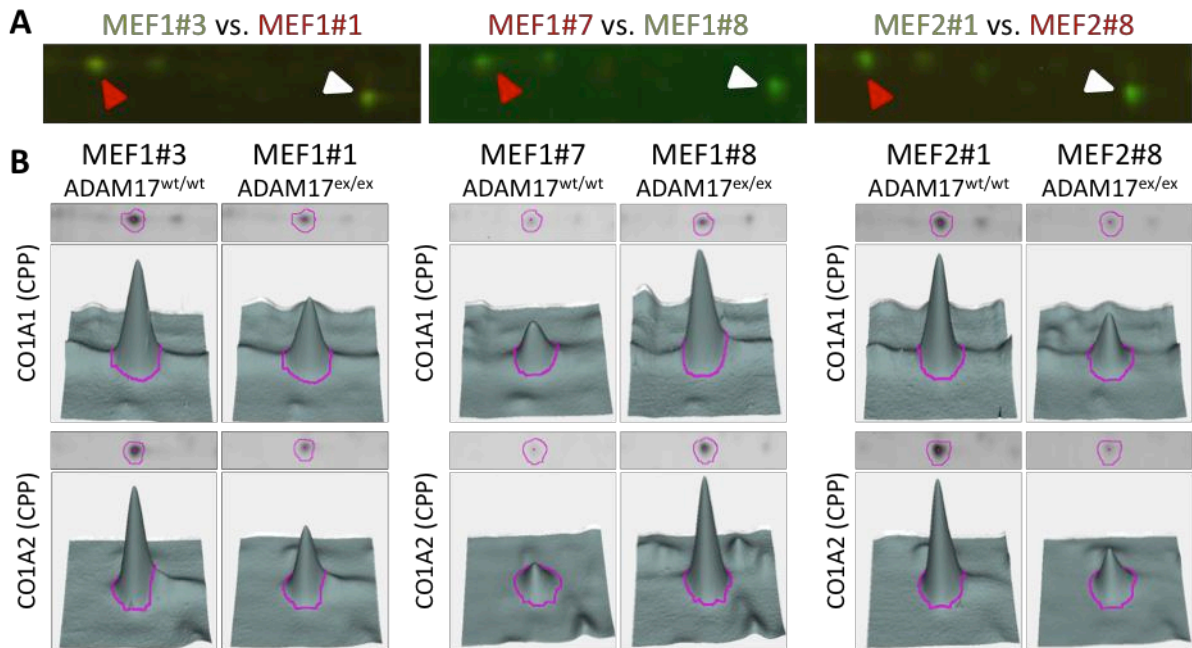


Fig. 5.18: Different type-I collagen C-terminal propeptide levels in supernatants of ADAM17^{ex/ex} MEF cell line MEF 1#1, MEF 1#8 and MEF 2#8. (A) Pseudo-colored 2D-DiGE image sections of differentially labeled MEF cell culture supernatant proteins, enriched by WGA-mediated precipitation. Proteins were separated on a 24 cm 3-11NL IPG strip, followed by SDS-PAGE. Protein spots identified as the type-I collagen α_1 (red arrow) and α_2 (white arrow) chain C-terminal propeptides are indicated. (B) Fluorescence intensities of the identified type-I collagen C-terminal propeptides from each cell line, as calculated by the DeCyder 2D software.

As an example the full-length forms and C-terminal propeptides of both type-I collagen chains α_1 and α_2 are shown in figure 5.18. Whereas the fluorescence intensities of the two fragments showed reduced levels in supernatants of the ADAM17^{ex/ex} cell lines MEF 1#1 (Fig. 5.18 B, left panel) and MEF 2#8 (Fig. 5.18 B, right panel), the ADAM17^{ex/ex} MEF cell line MEF 1#8 showed elevated levels of these protein fragments (Fig. 5.18 B, center panel) at the same position.

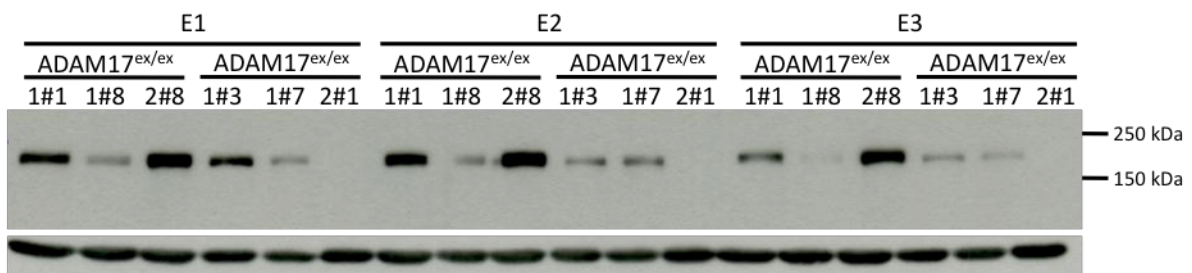


Fig. 5.19: Immunodetection of full-length type-I collagen α_1 chain via the C-terminal propeptide. MEF cell-derived whole-cell lysates were generated in three independent approaches and separated by SDS-PAGE. After protein transfer onto a nitrocellulose membrane, the type-I collagen α_1 chain was targeted via a specific antibody against its C-terminal propeptide.

In addition, detection of the type-I collagen α_1 chain via its C-terminal propeptide in MEF cell-derived whole-cell lysates also revealed inverted levels of the full-length, cell-bound

type-I collagen. As shown (Fig. 5.19), increased collagen levels could be observed in ADAM17^{ex/ex} MEF cell lines MEF 1#1 and MEF 2#8, but were decreased in MEF 1#8 cells.

However, so far, only two analyses of supernatant proteins included these additional cell lines. Notably, further verifications of these findings by Western blot analyses led to contradictory results. For instance, detection of the type-I collagen C-terminal propeptide showed reduced levels in MEF 1#8 (ADAM17^{ex/ex}) and MEF 2#1 (wild-type) cells. Merely, the MEF 1#1 (ADAM17^{ex/ex}) and MEF 1#3 (wild-type) always showed the same picture in subsequent analyses.

5.7.2 Murine embryonic fibroblasts

Besides the observed discrepancies between the different analyzed MEF cell pairs, the use of these MEF cells also impeded several efforts to verify the observed protein level alterations by Western blot analyses. Several antibodies, although recommended and verified for the use with murine samples did not deliver any results if applied to MEF cell-derived samples. For example, the use of an anti-Meprin- β that has been successfully applied by the group of Prof. Dr. Becker-Pauly for different murine tissue samples, did not deliver any signals in MEF cell-derived samples. In addition, an anti-MMP-2 that apparently worked in NIH3T3 cells did not work on MEF cell-derived samples.

5.7.3 Alternative cellular systems and approaches

Within this project, alternative cellular systems were investigated. Besides MEF cells, bone marrow-derived macrophages were derived from wild-type and ADAM17^{ex/ex} mice. After initial studies had been performed, the low number of available macrophages could not be compensated by the use of additional animals, since most animals were required for other projects. In cooperation with Gerina Vollmers, intestinal cells were harvested and cultured, but these cells showed insufficient proliferative capacities. A non-small lung cell cancer cell line, stably transfected with ADAM17 shRNA was provided by Keisuke Yamamoto, but also only showed too less proliferation to reach cell numbers as regarded for the planned experiments.

Finally, ECM extraction techniques from whole murine tissues were adapted, but could not be tested at tissues, derived from ADAM17^{ex/ex} mice, since there were no animals provided.

Thus, the observed changes in MEF cell secretion, MMP activity and collagen cleavage could not be confirmed in other tissues or *in vivo*.

5.8 Experimental gel-based proteomics

As part of Z2 proteomics platform of the collaborative research center 877, the adaption of suitable methods for proteomic profiling of the ADAM17^{ex/ex} MEF cell system was also part of this project. This section briefly summarizes a selection of efforts to analyse the MEF cell subproteoms.

5.8.1 Enrichment of extracellular matrix proteins

According to the subcellular distribution of the observed proteins within cell culture supernatants, some of these proteins comprise the extracellular matrix of cells and tissues.

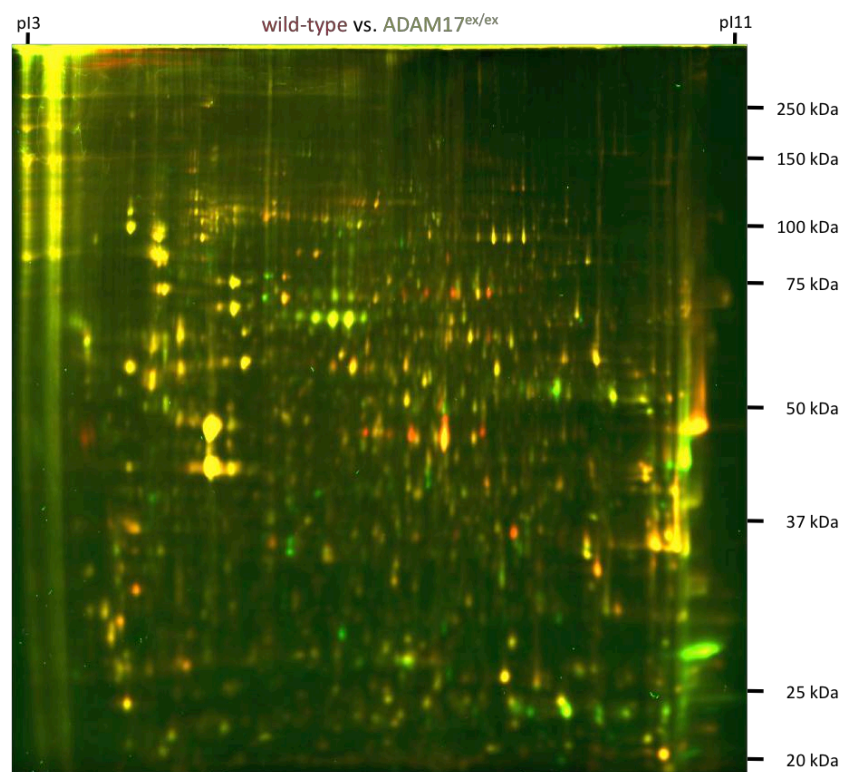


Fig. 5.20: Separation of a putative ECM fraction by 2D-DiGE. Pseudo-colored 2D-DiGE image, of putative ECM fractions from wild-type (Cy5, red) and ADAM17^{ex/ex} MEF cells (Cy3, green). Proteins were separated on a 24 cm 3-11NL IPG strip, followed by SDS-PAGE.

Cultured MEF cells were subjected to ECM preparation, following decellularization protocols as described. Subsequently, enriched ECM fractions were subjected to 2D-DiGE analysis. A representative 2D-DiGE image is shown in figure 5.20, demonstrating the high resolution of

the extracted protein fraction. However, out of 60 protein spots, differentially regulated by at least 1.5-fold, there was only small number of cell-surface proteins detected (compare list of identified proteins in section 10.7). In contrast, a variety of identified proteins originated from the nucleus. Among the differentially regulated proteins, the serine protease HtrA1 appeared to be very prominent, as this protease was identified from several protein spots. Protein levels of both, HtrA1 forms with a molecular weight of 50 kDa and at 30 kDa were strongly reduced in enriched ECM samples of ADAM17^{ex/ex} MEF cells. These findings are in line with reduced HtrA1 levels in ADAM17^{ex/ex} MEF cell supernatants. In addition, members A1 and A5 of the already mentioned Annexin family of proteins also appeared to be increased within these samples.

However, only a few known ECM proteins were identified from these experiments. Especially collagens were not detected from the enriched ECM fractions. Efforts for further purification of ECM proteins, e.g. by the use of WGA-mediated precipitation, only yielded insufficient amounts of protein. Thus, known protocols for the enrichment of ECM fractions from cultured cells did not work on MEF cells.

5.8.2 Plasma membrane proteomics

In case of ectodomain shedding, ADAM proteases are thought to primarily act at the plasma membrane. Thus, alterations in ADAM17-mediated shedding upon the ADAM17^{ex/ex} phenotype could also be targeted via changes in protein levels of plasma membrane proteins. Unfortunately, gel-based plasma membrane proteomics is a challenging endeavor in terms of sample preparation and compatibility with two-dimensional gel-based separation techniques. Various enrichment techniques were selected for proper purification of plasma membrane proteins and subsequent analysis by 2D-CTAB/SDS-DiGE. This section summarizes the different efforts.

5.8.2.1 The “Two-phase system”

Manufacturers of commercially available kits claim to be able to enrich plasma membrane proteins to a high extent. Thus, the plasma membrane extraction kit (PromoKine) was chosen and the resulting sample was subjected to 2D-CTAB/SDS-DiGE.

Western blot analyses targeting integrin α_2 (Fig. 5.21 A) and GA3PDH (Fig. 5.21 B) that are commonly used for monitoring of plasma membrane protein enrichment implicated an

enrichment of membrane proteins. Moreover, integrin α_2 showed reduced levels in ADAM17^{ex/ex} MEF cell membrane fractions. However, two-dimensional separation of these putative membrane fractions by 2D-CTAB/SDS-DiGE always led to unproper protein resolution (compare Fig. 5.21 C). Besides, protein identification by MALDI-ToF/ToF (see list of identified proteins in section 10.10) revealed cytoplasmic proteins or proteins from other intracellular compartments to be present within this putative membrane fraction (Fig. 5.21 D).

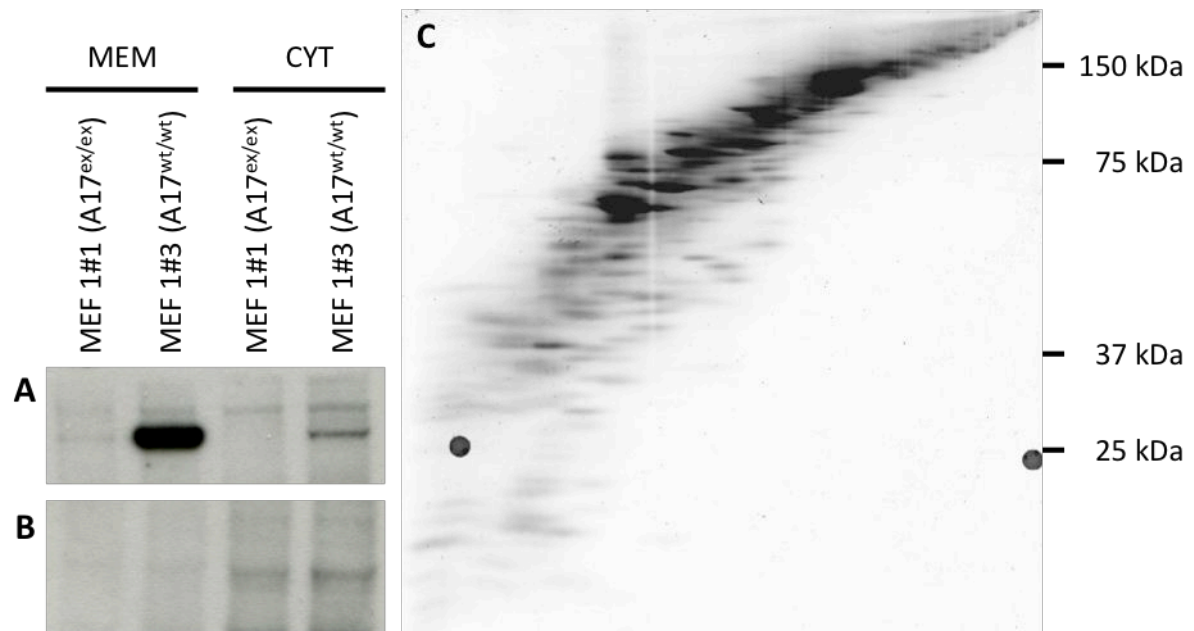


Fig. 5.21: Incomplete enrichment of plasma membrane proteins by two-phase systems. Protein enrichment was monitored by targeting **(A)** integrin α_2 (150 kDa) and **(B)** GA3PDH (37 kDa) by Western blot analysis in cytoplasmic (CYT) and membrane fractions (MEM). **(C)** Putative plasma membrane proteins from wild-type MEF cells were separated by 2D-CTAB/SDS-PAGE.

5.8.2.2 GPMV-derived plasma membrane proteins

Giant plasma membrane vesicles (GPMVs) represent a rather exotic way of plasma membrane protein enrichment. Originally, this system was used for the characterization of lipid rafts and membrane dynamics [Sezgin *et al.*, 2012], but might also be a suitable tool for general plasma membrane protein enrichment. Treatment of wild-type (Fig. 5.22 A, black arrows) and ADAM17^{ex/ex} MEF cells (Fig. 5.22 B, black arrows) with DTT and calcium ions induced the constriction of GPMVs from MEF cell plasma membranes.

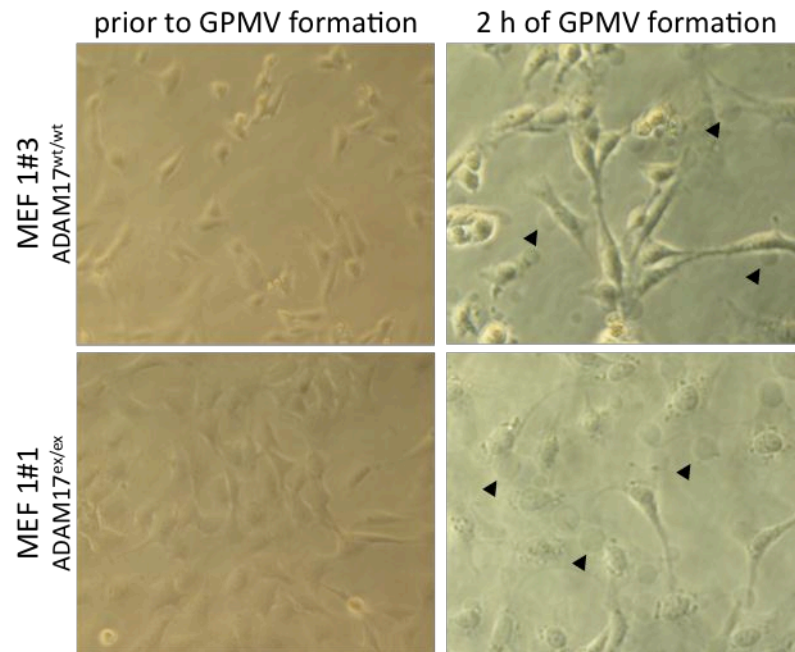


Fig. 5.22: Constriction of giant plasma membrane vesicles (GPMVs) MEF cells. Exemplified light microscopy images of wild-type (upper panel) and ADAM17^{ex/ex} MEF cells (lower panel), prior to induction of GPMV formation (left panel) and after 2 h of GPMV formation (right panel, black arrows).

Collected GPMVs were lysed and monitored for efficiency of non-plasma membrane protein depletion by immunodetection of the lysosomal marker LAMP-1, the mitochondrial marker COX IV and the plasma membrane marker flotilin-1 (Fig. 5.23). In contrast to LAMP-1 and COX IV, only flotilin-1 appeared in protein samples generated from harvested GPMVs (Fig. 5.23, pel). Thus, samples were subjected to two-dimensional separation by 2D-CTAB/SDS-DiGE.

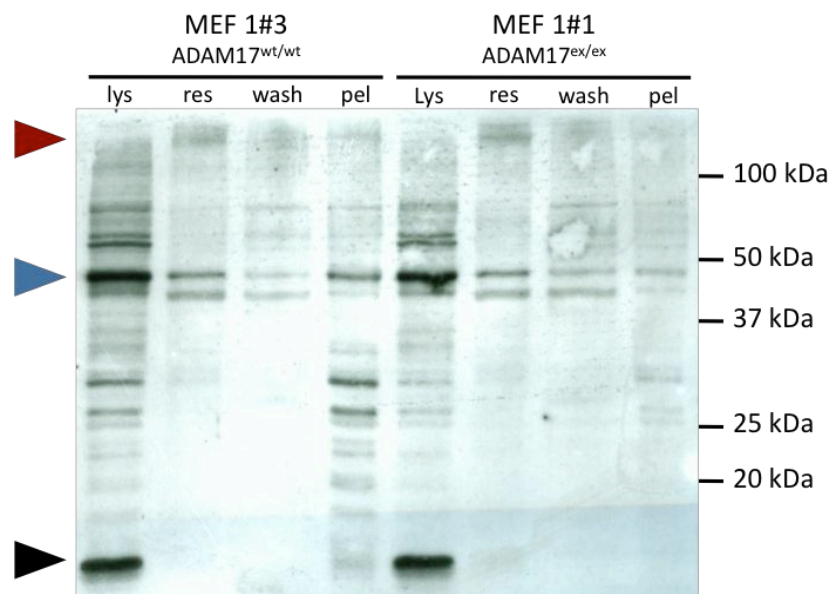


Fig. 5.23: Monitoring of GPMV protein purity.

Although compatible with the 2D-CTAB/SDS-PAGE, separation of GPMV-derived always resulted in a poor protein resolution and showed only few differentially regulated protein spots (Fig. 5.24).

Moreover, subsequent identification of separated proteins only delivered intracellular proteins, including actin and cofilin and peptidyl-prolyl cis-trans isomerases. Modifications of the sample preparation procedure, e.g. using sponin or digitonin treatment in combination with extensive washing steps, did not further increase the purity of membrane proteins.

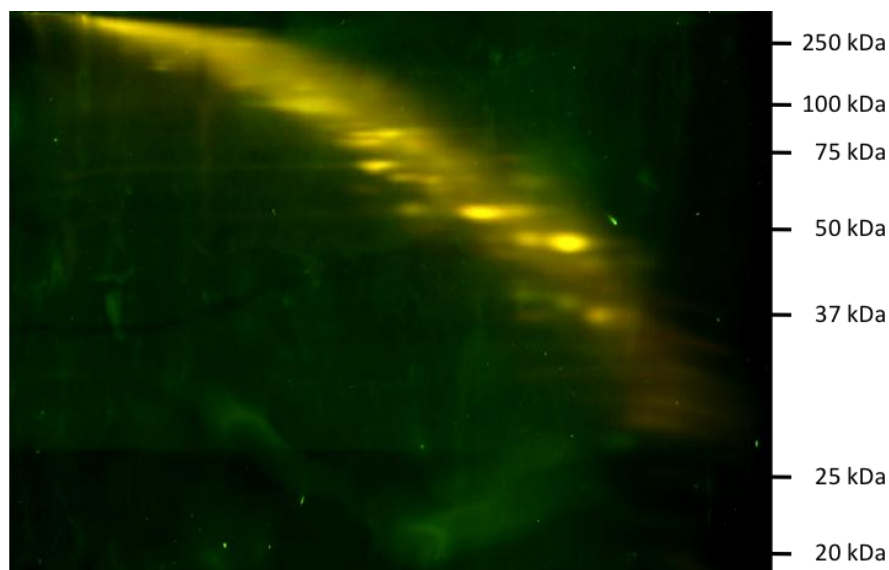


Fig. 5.24: Separation of GPMV-derived proteins by 2D-CTAB/SDS-DiGE. Pseudo-colored image of differentially-labeled wild-type (Cy3, green) and ADAM17^{ex/ex} (Cy5, red) MEF cell-derived GPMV proteins. Proteins were separated by a 8 % CTAB-PAGE, followed by a 10 % SDS-PAGE.

5.8.2.3 Two-phase system, linked to lectin-mediated precipitation

Lectin-mediated precipitation of proteins has already been used to reduce undesired intracellular proteins from cell culture supernatant samples. Thus, another approach for the enrichment of plasma membrane proteins was the combined use of a two-phase separation system and subsequent lectin-mediated precipitation. The putative membrane fractions were differentially labeled and subjected to 2D-CTAB/SDS-DiGE. In contrast to previous separations, a higher protein resolution was achieved (compare Fig. 5.25).

However, although several analyses were performed, objectively there was no significantly increased enrichment of membrane proteins as most proteins were annotated as cytoplasmic (e.g. actin and heat shock proteins), endoplasmic reticulum-derived (e.g. calnexin) or cytoskeletal (e.g. tubulin and vimentin) origin.

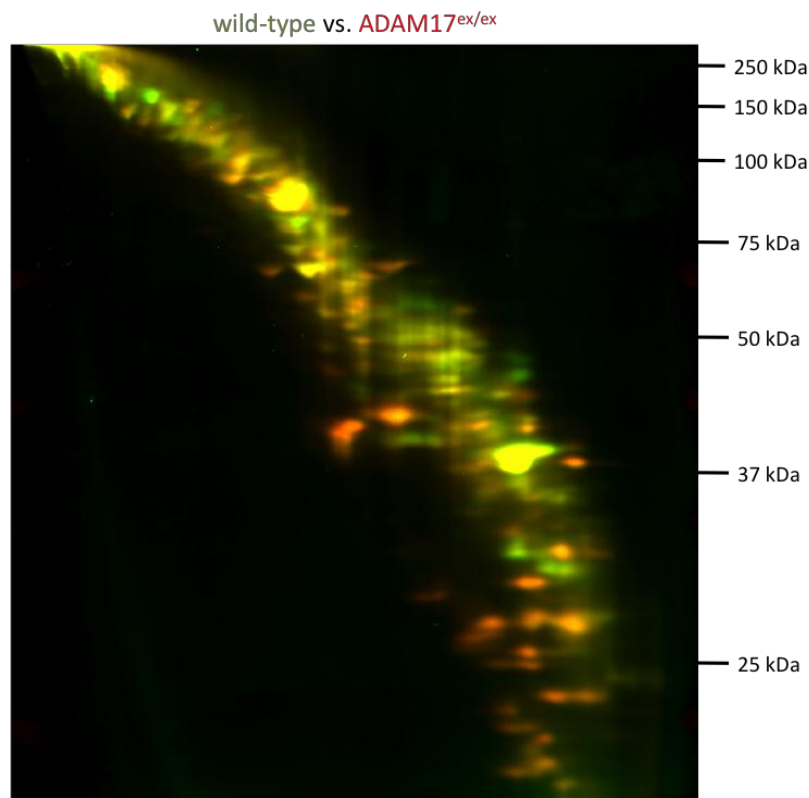


Fig. 5.25: 2D-CTAB/SDS-DiGE separation of putative membrane fractions derived from wild-type and *ADAM17^{ex/ex}* MEF cell by combination of a two-phase system and ConA-mediated precipitation. Samples were differentially labeled by Cy3 (wild-type, green) and Cy5 (*ADAM17^{ex/ex}*, red), respectively. Proteins were separated by an 8 % CTAB-PAGE, followed by a 12.5 % SDS-PAGE.

In summary, although different approaches were used for enrichment of plasma membrane proteins from wild-type and *ADAM17^{ex/ex}* MEF cells, none of the used experimental settings generated a protein sample that led to a significant increase of the plasma membrane fraction. Thus, the effect of the *ADAM17* knock-down on the MEF cell membrane proteome remains unknown.

5.8.3 Cell-surface labeling strategies

Besides extraction of membrane or extracellular matrix by subcellular fractionation, alternative techniques use directed labeling of cell-surface proteins and subsequent separation of a whole-cell lysate-like sample. Two different approaches were also applied on MEF cell samples and are presented below.

5.8.3.1 Biotinylation of cell-surface proteins

Biotinylation is a common approach for enrichment of cell-surface proteins and is mostly for subsequent one-dimensional in-gel separation. However, wild-type MEF cells (MEF 1#3)

were used for biotinylation of cell-surface proteins using a commercially available kit. Subsequently, proteins were extracted by 2D lysis buffer and separated by 2D-CTAB/SDS-PAGE (Fig. 5.26 A). In addition, whole-cell lysates were generated using 2D lysis buffer and subjected to 2D-CTAB/SDS-PAGE, too (Fig. 5.26 B). Unfortunately, both gels show no clear differences between biotinylated samples and whole-cell lysates. Apparently, the employed biotinylation protocol did not lead to an enrichment of cell-surface proteins for subsequent two-dimensional analysis.

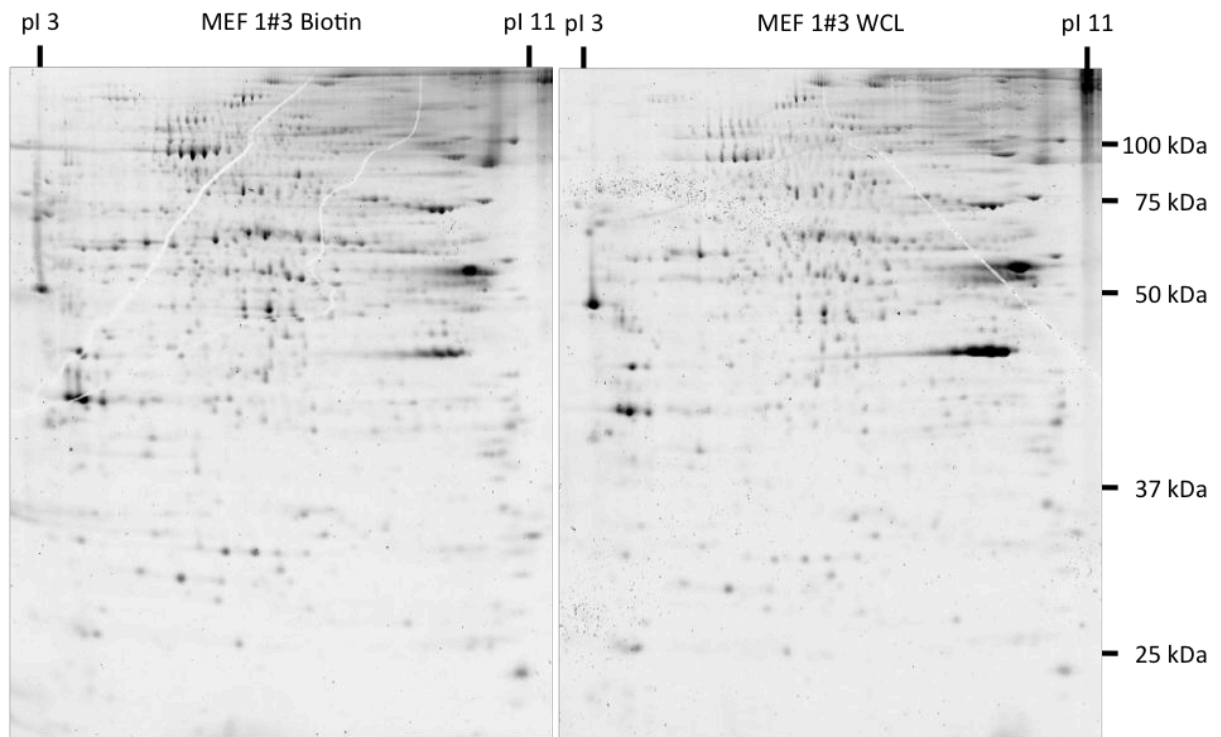


Fig. 5.26: Cell-surface biotinylation of wild-type (MEF 1#3) MEF cells. Two-dimensional gelelectrophoresis of putative cell-surface proteins enriched by biotinylation (left panel) and whole-cell lysates (right panel). Samples were separated on separate gels using 13 cm 3-11NL IPG strips prior to SDS-PAGE. Proteins were visualized via Flamingo™ Fluorescent Gel stain solution.

5.8.3.2 Cell-surface labeling using fluorescent dyes

An alternate approach uses fluorescent dyes for directed labeling of cell-surface proteins. The general protocol of cell-surface-labeling using fluorescent dyes is also based on an expected limitation of endocytosis at 4 °C. In addition, CyDyes™ also bind to lysyl residues via a NHS ester connection.

Cultured wild-type MEF cells (MEF 1#3) were labeled by Cy3 and subsequently lysed in 2D lysis buffer. In addition, a second set of MEF 1#3 cells was lysed in 2D lysis buffer and the generated whole-cell lysate was labeled by Cy5. Finally, both samples were combined and

subjected to 2D-CTAB/SDS-PAGE. Again, there was no apparent difference between both samples regarding the visualized sample complexity, indicating that the CyDyes penetrated the MEF cell membrane and also stained intracellular proteins (Fig. 5.27).

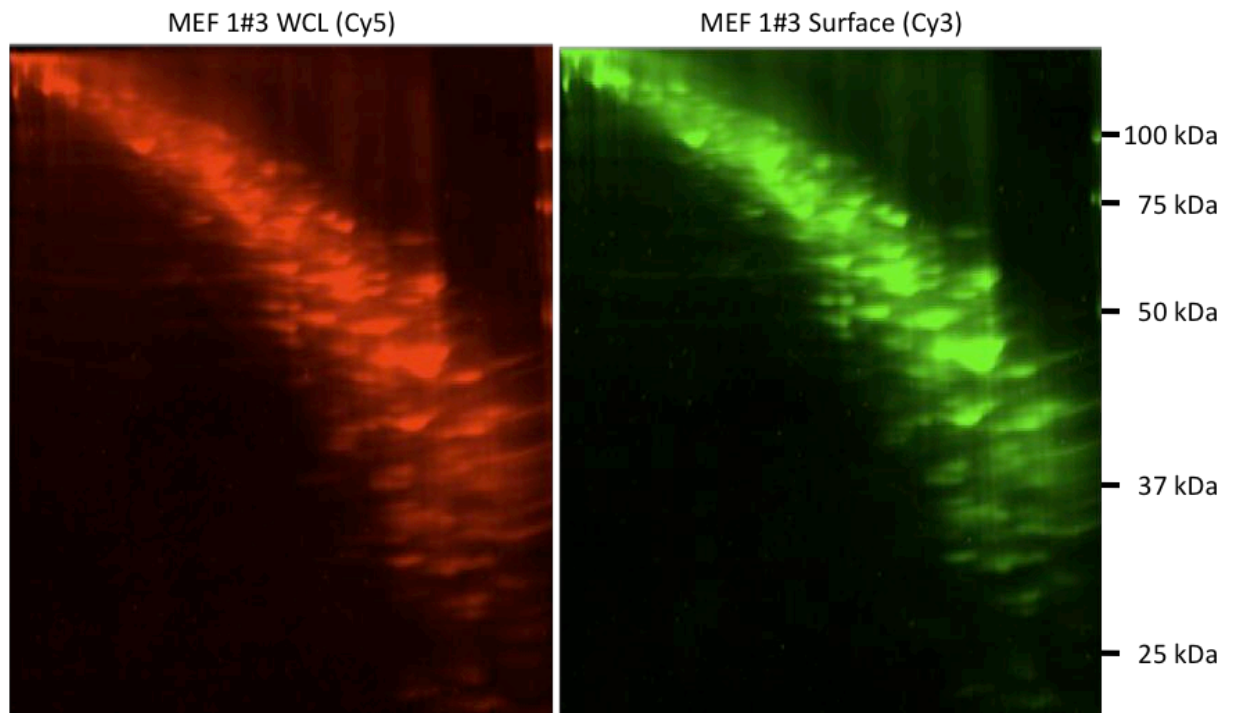


Fig. 5.27: Cell-surface labeling of wild-type (MEF 1#3) MEF cells using fluorescent dyes. MEF cells were labeled prior to generation of MEF cell-whole lysates by Cy5 (left panel) or after generation of a whole-cell lysate by Cy3 (right panel). Both samples were combined and separated by 2D-CTAB/SDS-PAGE.

6 Discussion

Based on a large number of *in vitro* and *in vivo* studies, it became apparent that ADAM17 is implicated in the irreversible processing of numerous growth factors, cytokines, adhesion proteins and their corresponding receptors. If the shedding of one or the other substrate is impaired or altered, this might be associated with pathological disturbances of cell or tissue homeostasis [e.g. Arribas and Esselens, 2009; Gooz, 2010]. In this present work, we addressed the role of ADAM17 in the processing of known and unknown substrates in MEF cells isolated from ADAM17^{ex/ex} mice as compared to wild-type MEF cells by a gel-based proteomic approach. To date, only a few studies were published that have addressed the global sheddome of ADAM17 [e.g. Guo *et al.*, 2002; Bech-Serra *et al.*, 2006; Kawahara *et al.*, 2014]. In general, proteomic approaches have been hampered by the fact that sheddome analyses depend of the cellular source and that the direct comparison of ADAM17 knock-out versus wild-type cells is rather impossible except for embryonic fibroblast, bone marrow-derived macrophages and cancer cell lines. Thus, the usage of hypomorphic mice opened the way to possibly circumvent this problem. Nonetheless, it turned out that the performed analyses only provide few indications for ADAM17-mediated shedding. Instead, reduced ADAM17 activity in ADAM17^{ex/ex} mice is associated with various protein alterations that point to a rather complex regulation of the protease web around ADAM17.

6.1 Comparison of the protein content of wild-type and ADAM17^{ex/ex} MEF cells

Overall, more than seventy different substrates are supposed to be shed by ADAM17 [Pruessmeyer and Ludwig, 2009; Saftig and Reiss, 2011; Scheller *et al.*, 2011]. The first identified substrate was TNF α [Black *et al.*, 1997; Moss *et al.*, 1997]. Therefore, ADAM17 was initially termed TNF α -converting enzyme (TACE). Based on the broad substrate specificity, ADAM17 and its closest relative ADAM10 have been implicated in the regulation of numerous pathways during development, neurogenesis, tissue homeostasis and tumor formation [e.g. reviewed in Edwards *et al.*, 2007; Pruessmeyer and Ludwig, 2009; Gooz, 2010].

In order to get insights into the substrate patterns in a given cell type in the presence or absence of ADAM17, the complete knock-out of ADAM17 in mice, which is associated with embryonic lethality, has clear limitations regarding the available cellular material [Peschon *et al.*, 1998]. To circumvent this issue, ADAM17 hypomorphic (ADAM17^{ex/ex}) mice were regarded as a more suitable model since these mice are viable and fertile [Chalaris *et al.*, 2010]. In fact, ADAM17^{ex/ex} mice have been examined to address the effect of very low expression of ADAM17 in various disease models including intestinal inflammation [Chalaris *et al.*, 2010] and lung cancer progression [Stevanović, 2014]. However, the availability of cells and tissues from ADAM17^{ex/ex} mice was still a major limitation for the outcome of this project. Thus, the prime idea was to initially investigate proteomic alterations in the context of murine embryonic fibroblasts (MEF cells) and to run follow-up experiments on various other cell types including bone marrow-derived macrophages and tissue-derived cells.

Assuming that ADAM17 acts as a plasma membrane-associated sheddase, cleaved substrates should be enriched to some extent in cell culture supernatants. Thus, the first experiments were performed to enrich proteins from MEF cell culture supernatants, to separate them by two-dimensional gel electrophoresis and to look for differences in the supernatants of wild-type and ADAM17^{ex/ex} MEF cell supernatants by applying differential labeling. Nonetheless, the first 2D-DiGE experiments indicated that there are differences in the released proteins, but there are not many putative substrates that could be identified by this approach. In order to prove that the 2D-DiGE approach might be suitable in general for this purpose, we compared supernatant proteins from wild-type and ADAM17^{ex/ex} MEF cells upon transfection with the cognate ADAM17 substrate TNF α . In this case, the 2D-DiGE analysis followed by protein identification of altered protein spots by mass spectrometry, clearly revealed an impaired TNF α processing in ADAM17^{ex/ex} MEF cells. Thus, the processed TNF α was detected in wild-type MEF cells with a 14-fold higher abundance.

Although this experiment clearly proved that the gel-based proteomic approach is suitable to detect forced alterations, it also revealed that other constitutively or inducibly shed substrates might not be detected due to sensitivity problems. Notably, supernatants of wild-type and ADAM17^{ex/ex} MEF cells were routinely checked for TNF α cleavage by ELISA as a standard procedure to verify the correct phenotype. Although these analyses indicate that

TNF α is also processed in untransfected MEF cells, it did not prove that other substrates are also available for shedding in this cellular system.

6.2 Indications for shedding

Besides identifying TNF α as an ADAM17 substrate in wild-type MEF cells, there were only few indications for an ADAM17-related shedding of other proteins. In wild-type MEF cells, the relative abundance of a 15 kDa TNF α fragment was increased 14-fold, whereas a putative 100 kDa fragment of NCAM-1 was 1.69-fold increased and a 15 kDa cadherin-2 fragment was 2.3-fold increased (section 5.3.1; Tab. 5.1). In addition, a 25 kDa fragment of perlecan and 30 kDa fragments of the type-I collagen α_1 and α_2 chains showed approximately 2.5-fold decreased protein levels in ADAM17^{ex/ex} MEF cells. Light chains of the C1 subcomponents C1r-A and C1r-S were 3-fold increased in wild-type supernatants, as were 15 kDa fragments of cystatin-C. A 35 kDa fragment of the procollagen C-endopeptidase enhancer 1 was 5.8-fold decreased in ADAM17^{ex/ex} supernatants. In contrast, a 40 kDa fragment of IL1RL1 and a 11 kDa fragment of lubricin were increased in ADAM17^{ex/ex} MEF cell supernatants.

Besides the already mentioned ADAM17 substrate **TNF α** [Black *et al.*, 1997], only **NCAM-1** has been reported to be a substrate of ADAM17 by Kalus and colleagues [Kalus *et al.*, 2006]. In this case, the generation of the predominant soluble 110 kDa form of NCAM-1 [e.g. He *et al.*, 1986; Sadoul *et al.*, 1986] from crude membrane fractions of murine brain was monitored *in vitro* in presence and absence of chelating EDTA [Kalus *et al.*, 2006]. Finally, the role of ADAM17 in NCAM-1 processing was proven in murine neuroblastoma cells (Neuro 2a) upon GM 6001 treatment and in ADAM17-deficient fibroblast [Kalus *et al.*, 2006].

In addition, most of the identified protein fragments lack a designated transmembrane domain, which seems to be crucial for ADAM17-mediated substrate cleavage [White, 2003]. This might implicate an indirect effect of ADAM17. Indeed, all proteins that fall into this category might be substrates of other proteases. For example, we noted an increase of the **type-I collagen α_1 and α_2 chain propeptides** and the **perlecan LG3 peptide** in wild-type MEF cell supernatants. Only recently, however, meprin β has been identified as the prominent C- and N-procollagenase for type-I and type-III collagens [Broder *et al.*, 2013]. Interestingly, the astacin family metalloprotease “bone morphogenic protein 1” (BMP-1) was reduced 1.59-

fold in ADAM17^{ex/ex} MEF cell supernatants. BMP-1 also mediates type-I and type-III C-terminal propeptide cleavage [Kessler *et al.*, 1995]. Moreover, although perlecan contains several putative cleavage sites for other proteases [Farach-Carson and Carson, 2007], so far, the observed LG3 was only reported to be released by BMP-1 cleavage [Gonzales *et al.*, 2005]. In addition, we detected decreased levels of a 36 kDa fragment of the **procollagen C-endopeptidase enhancer 1** (PCOC-1) in supernatants of ADAM17^{ex/ex} MEF cells. Apparently, the generation of this fragment is required for BMP-1-mediated C-procollagen maturation [Hulmes *et al.*, 1997].

The transmembrane adhesion molecule **cadherin-2** was discussed as a substrate of ADAM10, before [Reiss *et al.*, 2005]. Like other cadherins, cadherin-2 is synthesized as a precursor protein with an N-terminal prodomain. The removal of the prodomain, which is mediated by intracellular furin or other proprotein convertases [Ozawa and Kemmler, 1990], is crucial for its adhesive function [Koch *et al.*, 2004]. However, since we observed reduced levels of the propeptide in supernatants of TNF α -overexpressing ADAM17^{ex/ex} MEF cells, an effect of ADAM17 on maturation of this transmembrane protein cannot be excluded.

The cysteine protease inhibitor **cystatin-C** was detected as a 15 kDa fragment that was reduced in ADAM17^{ex/ex} MEF cell supernatants. According to the literature, cystatin-C is degraded by MMP-2 and MMP-9 [Prudova *et al.*, 2010]. Both MMPs, however showed reduced activity in ADAM17^{ex/ex} MEF cell supernatants. Thus, the lower abundance of the cystatin-C cleavage product might be an indirect effect due to ADAM17-mediated regulation of MMPs. Also the light chains of the **C1 subcomponents C1r-A and C1s-A** were reduced in ADAM17^{ex/ex} MEF cell supernatants. Both serine proteases show major characteristics with other proteases of the complement system [Sim and Laich, 2000]. Interestingly, zymogenic C1s-A is matured by active C1r-A prior to processing of C2 and C4 [Gál *et al.*, 2002]. Moreover, C1r-A was recently described as another target of MMP-2 [Prudova *et al.* 2010].

In contrast, an 11 kDa fragment of the 225 kDa proteoglycan **lubricin** (PRG4) was increased in supernatants of ADAM17^{ex/ex} MEF cells. It has been reported that the removal of this C-terminal part is mediated by a subtilisin-like proprotein convertase [Rhee *et al.*, 2005]. Of note, increased protein levels were also observed for the **interleukin-1-like related protein 1** (IL1RL1). This protein is supposed to exist as a transmembrane protein or as a secreted

protein, which is dependent on gene expression, but not on post-translational modification [Rössler *et al.*, 1995].

Taken together, a variety of differentially abundant proteins or protein fragments were detected in supernatants of ADAM17^{ex/ex} versus wild-type MEF cells. However, in most cases, a direct proteolysis by ADAM17 seems unlikely, since most of these proteins are not classical transmembrane proteins and are documented targets of other proteases. This again strengthens the notion that in MEF cells ADAM17 might influence the activity of other proteases rather than releasing numerous substrates into the cell culture supernatant.

6.2.1 ADAM17 – A potential regulator of collagen maturation and turnover?

6.2.1.1 Reduced type-I collagen maturation in ADAM17^{ex/ex} MEF cells

Among the different protein fragments that were reduced in ADAM17^{ex/ex} MEF cell supernatants, the C-terminal propeptides of the type-I collagen α_1 and α_2 chains were amongst the most prominent ones. Type-I, -II and -III collagens represent the major fibrillar components of the extracellular matrix. Fibrillar collagens are synthesized as precursor proteins (procollagens) containing N- and C-terminal propeptides and are released into the extracellular matrix. The proteolytic removal of the propeptides is a crucial step in collagen maturation, including collagen fiber assembly. Thus, collagen maturation is essential for its regulated deposition and for ECM structure and morphogenesis [Kühn, 1987; Kadler *et al.*, 2000; Hulmes, 2002; Canty and Kadler, 2005; Hulmes, 2008].

The reduced levels of the C-terminal type-I collagen propeptide might thus implicate impaired type-I collagen maturation in ADAM17^{ex/ex} MEF cells. This is supported by findings from MEF cell-derived whole-cell lysates that showed increased levels of procollagen at 250 kDa in ADAM17^{ex/ex} samples. Moreover, if targeted with an antibody directed against the C-terminal type-I collagen telo-peptide, fragments at approximately 200 and 130 kDa show increased levels in wild-type MEF cell samples. These fragments are correlated with C- and N-terminal collagen maturation [e.g. Broder *et al.*, 2013]. However, except for type-XIII, -XVII, -XXIII and -XXV collagen, collagens lack a transmembrane region, implicating that the C-terminal propeptide might not be processed by the plasma membrane-associated ADAM17.

It has proposed that ADAM-related proteases such as ADAMTS-2, -3 and -14 are involved in N-terminal procollagen maturation, whereas the C-terminal propeptide is removed by BMP-1 and related tolloid-like proteases [Kessler *et al.*, 1995; Sarras, 1996; Colige *et al.*, 2002; Hopkins *et al.*, 2007; Moali *et al.*, 2005; Moali and Hulmes, 2012]. In line with the reduced C-terminal type-I collagen maturation, ADAM17^{ex/ex} MEF cell supernatants contained reduced levels of BMP-1 levels indicating that reduced C-terminal collagen maturation might be due to reduced C-procollagenase activity. In addition, various protease enhancer molecules promote BMP-1 activity in a substrate dependent manner [Vadon-Le Goff *et al.*, 2011]. For instance, **periostin** (that was also reduced in ADAM17^{ex/ex} MEF cell supernatants) is involved in BMP-1-mediated proteolytic activation of lysyl oxidase [Maruhashi *et al.*, 2010] and the BMP-1 C-procollagenase activity is supported by the **procollagen C-endoprotease enhancer I** (PCOC-1) [Moali *et al.*, 2005]. Notably, a 36 kDa fragment of PCOC-1 [Hulmes *et al.*, 1997] was found to be reduced in supernatants of TNF α -overexpressing ADAM17^{ex/ex} MEF cells. Here, it is already reported that the proteolytic cleavage of the PCOC-1 netrin-like (NTR) domain is mediated by MMP-2 [Dean and Overall, 2007], which is also reduced in ADAM17^{ex/ex} MEF cell supernatants. However, it has also been suggested that the full-length form of PCOC-1 displays BMP-1 enhancing activity by binding to the type-I collagen C-terminal propeptide via its two CUB domains [Ricard-Blum *et al.*, 2002] and to BMP-1 via its NTR domain [Bekhouche *et al.*, 2010]. As the full-length form of PCOC-1 only showed moderate protein alterations in ADAM17^{ex/ex} supernatants, reduced BMP-1 levels might be more relevant for the observed reduced C-terminal collagen maturation.

Moreover, in the postulated protease web, ADAM17 might mediate the maturation of the astacin family metalloprotease meprin β by shedding in a PMA-dependent manner [Hahn *et al.*, 2003]. Recently, meprin β has been described as an important mediator of C- and N-terminal type-I and type-III collagen maturation [Broder *et al.*, 2013]. Unfortunately, a direct effect of meprin β could not be investigated in more detail, since the available antibodies did not yield reliable results in MEF cell samples. Moreover, there is no direct evidence for the presence of meprin β in MEF cells [Prof. Dr. Becker-Pauly, personal communication].

6.2.1.2 Reduced collagen fragmentation in ADAM17^{ex/ex} MEF cells

The analysis of cell culture supernatants not only revealed reduced C-terminal type-I collagen maturation, but also a reduced release of smaller type-I collagen fragments with

different molecular weights (e.g. a three-quarter fragment (90 kDa) of the type-I collagen molecule). In general, degradation of collagen is important for remodelling of the extracellular matrix and for growth and development [reviewed by Cox and Erler, 2011]. It has been proposed that collagen degradation can occur intra- and extracellularly [Sodek and Overall, 1988; Everts *et al.*, 1996]. Fragmentation of collagens is a regulated process that is mainly orchestrated by matrix metalloproteases during collagen turnover [Fisher *et al.*, 2009]. Initial type-I collagen fragmentation into quarter and three-quarter fragments is mediated by MMP-1 in humans [Janecki *et al.*, 1995; Lee *et al.*, 2006] and by MT-MMP1 (MMP-14) in mice [Holmbeck *et al.*, 1999; Sounni *et al.*, 2005]. The resulting three-quarter and quarter fragments can be further degraded by MMP-2, MMP3 and MMP-9 [López *et al.*, 2010]. In addition, collagen fragments not only indicate collagen degradation, but can also act as biologically active ECM fragments (matrikines). For instance, the glycyl-histidyl-lysine tripeptide (GHL) that is derived from type-I collagen α_2 chains stimulates the synthesis of collagens [Maquart *et al.*, 1988] and induces the expression of MMP-2 by cultured fibroblasts [Siméon *et al.*, 2000]. Moreover, serum levels of the type-I C-terminal propeptide and the C-terminal telo-peptide are used as biomarkers for collagen degradation in cardiac disease [Tziakas *et al.*, 2007; López *et al.*, 2010]. In the present study, Western blot analyses of whole-cell lysates and cell culture supernatants not only pointed to a reduced C-terminal type-I collagen maturation, but also indicated an impaired release of this fragment into the supernatant of ADAM17^{ex/ex} MEF cells. A reduced remodelling of the ADAM17^{ex/ex} MEF cell ECM might contribute to the reduced release of this fragment. In this context, the C-terminal propeptide has been described to mediate TGF β effects in osteoblasts [Mizuno *et al.*, 2000].

In conclusion, the present results suggest that ADAM17 might indirectly influence the maturation and turnover of collagens via modulation of MMP activity, indicating a reduced extracellular matrix remodelling in ADAM17^{ex/ex} MEF cells. Interestingly, the “**secreted protein acidic and rich in cysteine**” (SPARC) is a known mediator of extracellular matrix remodelling [Engel *et al.*, 1987; Funk and Sage, 1991; Lane and Sage, 1994; Murphy-Ullrich *et al.*, 1995]. This protein displayed increased protein levels in ADAM17^{ex/ex} MEF whole-cell lysates and might thus contribute to the reduced ECM remodelling in ADAM17^{ex/ex} MEF cells due to decreased secretion. Similar observations were recently made for ADAM17^{-/-} MEF cells [Kawahara *et al.*, 2014]. Moreover, increased collagen turnover in wild-type MEF cells implicates an enhanced ECM remodeling in an MMP-dependent manner. In line with this,

MMPs are often up-regulated in cancer, thereby leading to progressive destruction of normal ECM and enhanced tumor invasion [Kumar and Weaver, 2009; Cox and Ertler, 2011]. Since ADAM17 activity apparently is also increased in various tumors in comparison to normal tissues [Arribas and Esselens, 2009], the comparison of wild-type and ADAM17^{ex/ex} cells might reflect these phenotypic differences to a certain extent. Along this line, a negative effect of the ADAM17^{ex/ex} background on tumor progression was recently demonstrated, as injection of Lewis lung carcinoma cells led to a reduced tumor burden in ADAM17^{ex/ex} mice [Stavanović, 2014].

6.2.2 Perlecan – A novel ADAM17 substrate in murine cells?

The “**basement heparane-sulfate proteoglycan core protein**” (perlecan) is widely expressed during early development and plays a role in vasculogenesis and tumor angiogenesis [Iozzo *et al.*, 2001; Zhou *et al.*, 2004]. This 400 kDa proteoglycan displays a modular architecture of five subdomains, with a C-terminal, 85 kDa endorepellin domain [Iozzo *et al.*, 1998]. Thereby, the angiostatic activity is mainly located within the laminin-like globular domain 3 (LG3), which forms part of this endorepellin domain [Bix *et al.*, 2004]. In the present study, perlecan was identified as a 26 kDa fragment that correlates in size and peptide sequence to the described LG3 peptide. This fragment showed a 2.9-fold reduced abundance in ADAM17^{ex/ex} MEF cell supernatants. In contrast, according to the performed SlotBlot analyses the perlecan full-length protein levels were increased in ADAM17^{ex/ex} MEF cell whole-cell lysates, indicating a reduced perlecan cleavage in ADAM17^{ex/ex} MEF cells.

The cleavage of perlecan has been studied thoroughly before and several proteases were identified as putative processing enzymes. It was found that MMP-3, MMP-14 and collagenase-1 [Whitelock *et al.*, 1996; d’Ortho *et al.*, 1997], but also MMP-7 [Grindel *et al.*, 2014] are involved in perlecan degradation. However, the aforementioned LG3 peptide is known to be liberated by extracellular BMP-1/tolloid-like metalloproteases [Iozzo *et al.*, 2005], which also showed reduced protein levels in ADAM17^{ex/ex} supernatants. Of note, MMP-2 and MMP-9 are not involved in perlecan processing [Whitelock *et al.*, 1996]. In addition, the endorepellin domain of perlecan interacts with a variety of proteins, including ECM-1 [Mongiati *et al.*, 2003] and $\alpha_1\beta_2$ integrin [Ida-Yonemochi, 2013]. Additional protein interactions between the perlecan N-terminal domains and growth factors and receptors, suggest a dual role of perlecan as a regulator of tumor progression and tumor suppression

via limited proteolysis of the perlecan LG3 peptide [Whitelock *et al.*, 2008]. Again, however, perlecan does not contain a transmembrane domain, suggesting that classical ADAM17 cleavage is unlikely.

Nonetheless, perlecan cleavage has also been found to be altered in the mass spectrometry-based study of the ADAM17-dependent MEF cell secretome [Kawahara *et al.*, 2014]. There the authors observed increased endorepellin levels in wild-type MEF cell supernatants and demonstrated ADAM17-dependent generation of the LG3 fragment *in vitro*. This *in vitro* cleavage assay was performed on recombinant human endorepellin, using recombinant human ADAM17 (aa271 to aa671), lacking the prodomain, the transmembrane region and intracellular domain [Kawahara *et al.*, 2014]. Since, the ADAM17-mediated generation of a 25 kDa fragment was observed, it was concluded that endorepellin might serve as a novel substrate of ADAM17. However, such *in vitro* cleavage assays do not necessarily reflect the *in vivo* situation and various parameters including the temporal and spatial localization of proteases and substrates [Li *et al.*, 2004; Fortelny *et al.*, 2014]. Noteworthy, the mass spectrometry data presented by Kawahara and colleagues also revealed decreased extracellular BMP-1 levels in ADAM17^{-/-} MEF cell supernatants [Kawahara *et al.*, 2014].

6.3 ADAM17 – A modulator of the protease web?

6.3.1 The protease web

“Proteases do not operate alone, but in pathways and amplification cascades with a one way flow of information, or in regulatory circuits where information feeds back. This complexity is increased because of the presence of interacting proteins, receptors, substrates, cleavage products and inhibitors.” [Overall and Dean, 2006].

It was observed that many proteases and protease inhibitors such as “secreted leukocyte protease inhibitor” and cystatins were found to be substrates of MMPs or to be indirectly modulated by MMP activity. For example, fetuin A and cystatin C are able to interact with MMP9 and MMP2, preventing them from autocatalytic degradation [Ray *et al.*, 2003; Chen *et al.*, 2005]. Therefore, it was considered that proteolytic pathways *in vivo* do not act alone, but are part of interconnected proteolytic systems and cascades, the protease web. The net activity of a protease within the protease web therefore depends on the activity of several

associated proteases and inhibitors. Thus, overexpression of proteases can induce unexpected activities of other proteases and inhibition of proteases can lead to effects on unrelated proteases [Overall and Dean, 2006].

Interactions between different proteases have been described before and are well characterized for proteolytic cascades of the complement [e.g. Müller-Eberhardt, 1988] and coagulation system [e.g. Macfarlane, 1964] and for caspase-mediated apoptosis [Thornberry and Lazebnik, 1998; Lincz, 1998]. However, more recent studies on matrix metalloproteases revealed an even higher complexity of these protease interactions. For instance, cysteine and serine proteases that are inhibited by cystatins or serpins remain active upon MMP-mediated cleavage and inactivation of cystatins and serpins [Knäuper *et al.*, 1990; Mast *et al.*, 1991; Dean and Overall, 2007; Auf dem Keller *et al.*, 2013].

Meanwhile, the idea of the protease web has been considered in a variety of different publications, dealing with proteolysis and its role in pathophysiological events such as cancer [Mason and Joyce, 2010]. In addition, *in vitro* and *in cellulo* degradomic studies on protease substrates [Butler and Overall, 2009; Prudova *et al.*, 2010], but also gene expression analysis under reduced or elevated protease inhibitor activities in cancer [Krüger, 2009] strengthened the concept of the protease web. Finally, *in vivo* studies on the impact of reduced or enhanced protease activity (e.g. based on knock-out or overexpression approaches) might lead to indirect effects via “proteolytic side effects” [Fortelny *et al.* 2014]. Thus, alterations of protein abundance observed within this project might not be mediated by ADAM17 directly, but might be affected by ADAM17 as a regulatory protease within the protease web.

6.3.2 ADAM17 within the protease web

A variety of protein fragments and proteases showed altered levels in ADAM17^{ex/ex} MEF cells. Among these changes, the impaired maturation and fragmentation of the type-I collagen chains were rather prominent. In addition, the observed changes in protein secretion included components of the ECM proteome that has been renamed as the matrisome [Naba *et al.*, 2013]. Thus, the observed decrease of extracellular matrix protein levels within a given cell culture might reflect a reduced remodeling of the extracellular matrix due to the reduced activity of ADAM17. Investigations regarding extracellular matrix remodeling in various physiological processes and tissues elucidated matrix

metalloproteinase (MMPs) as important mediators of matrix remodeling [e.g. Vu and Werb, 2000; Löffek *et al.*, 2010]. In line with this, gelatin and casein-based zymographic analyses of MEF cell culture supernatants revealed a reduced activity of MMP-2, MMP-3 and MMP-9. In case of MMP-3 and MMP-2, decreased activity of the mature protein forms in ADAM17^{ex/ex} MEF cells were accompanied by increased protein levels of the correspondent proforms. This might reflect an impaired maturation due to reduced MT-MMP1 (MMP-14) activity, which is known to mediate the maturation of proMMP-2 [Deryugina *et al.*, 2001]. On the other hand, decreased *Mmp2* expression was reported in a model for cardiac remodelling upon knock-down of ADAM17 [Wang *et al.*, 2009]. In addition, the reduced TIMP-2 protein levels in ADAM17^{ex/ex} MEF cells might also affect reduced proMMP-2 maturation, since this physiologic inhibitor is required for MMP-2 maturation by MMP-14 [Stetler-Stevenson *et al.*, 1990; Deryugina *et al.*, 2001]. Reduced MMP-2 activity thus might be modulated on the gene expression and the protein level.

Similarly, impaired MMP-9 activity has also been shown to correlate with an impaired *Mmp9* expression when performing a siRNA-mediated knock-down of ADAM17 in lung epithelial cells [Li *et al.*, 2013]. Again, MMP-9 activity is also regulated on the protein level due to reduced maturation via the MT1-MMP/MMP2 axis [Toth *et al.*, 2003]. In a prostate cancer model, expression of both, MMP-2 and MMP-9 is positively up-regulated in an EGFR-MEK-ERK dependent manner [Xiao *et al.*, 2012]. Besides, the observed ECM-1 protein levels might also affect the reduced MMP-9 activity observed in ADAM17^{ex/ex} MEF cell supernatants, since ECM-1 can inhibit MMP-9 by direct interaction via its C-terminal region [Fujimoto *et al.*, 2006]. In conclusion, the reduced ADAM17 activity in ADAM17^{ex/ex} MEF cells might affect the activity of matrix metalloproteases also via altered gene expression levels. Notably, Kawahara and colleagues observed increased *Mmp2* expression in wild-type MEF cells, but no effect on *Mmp9* expression [Kawahara *et al.*, 2014].

As mentioned before, “**bone morphogenic protein 1**” (BMP-1) was also reduced in ADAM17^{ex/ex} MEF cell supernatants. BMP-1 is an important C-procollagenase for type-I and type-III collagens [Kessler *et al.*, 1986]. This protease and other members of the family of tolloid-like metalloproteases directly effect ECM formation [Hopkins *et al.*, 2007] by acting on fibrillar and non-fibrillar collagens and non-collagenous ECM components such as perlecan [Gonzales *et al.*, 2005] and mimecan [Funderburgh *et al.*, 1997]. Notably, also perlecan and mimecan were found to be less abundant in ADAM17^{ex/ex} MEF cell

supernatants. Moreover, BMP-1 activity is enhanced by the “procollagen C-endopeptidase enhancer 1” (PCOC-1) [Kessler and Adar, 1989] and might be inhibited by the “secreted frizzled-related protein 2” (sFRP2), which conversely displayed increased protein levels in ADAM17^{ex/ex} MEF cell supernatants. At least, murine sFRP2 is capable to inhibit BMP1/TLD-like proteases in *Xenopus* and *Danio rerio* [Lee *et al.*, 2006].

What has been discussed so far strongly argues that studies of the ADAM17-dependent secretome or sheddome seem to be highly affected by “proteolytic side effects” within a complex protease web. This implies that studies of protease-dependent proteome alterations should generally be combined with gene expression profiling to get deeper insights into the role of a certain protease within a specific cellular system.

6.4 ADAM17-dependent secretome

Besides the described proteins, protein fragments, proteases and protease inhibitors, also other full-length proteins were altered in their abundance on reduced ADAM17 activity. Overall 400 different proteins were identified from MEF cell culture supernatants. However, according to available protein information (e.g. on <http://uniprot.org>) only seventy proteins were expected to be present in this fraction. Recently, Naba and colleagues mentioned that available protein information (especially subcellular distribution) is often incomplete [Naba *et al.*, 2012]. Thus, it remains unknown, whether the intracellular protein (e.g. ER proteins PLOD-1 and PLOD-3) are also secreted into the cell culture supernatant or whether this is an artificial effect due to cell death. However, whereas most proteins were rather reduced in ADAM17^{ex/ex} MEF cell supernatants (e.g. various types of collagen), some proteins were also detected with increased levels. For example, the „**follistatin-like protein 1**“ (FSTL-1) and the „**extracellular matrix protein 1**“ (ECM-1) were increased in ADAM17^{ex/ex} supernatants, especially when enriched by WGA precipitation. Interestingly, Kawahara and colleagues also observed increased ECM-1 levels in ADAM17^{-/-} MEF cell supernatants, whereas FSTL-1 levels were decreased [Kawahara *et al.*, 2014]. Whether the increased levels of full-length FSTL-1 observed in the present study are a consequence of enhanced secretion or of reduced cleavage by MMP-2 [Prudova *et al.*, 2004] remains unknown. Interestingly, ECM-1 is known to interact with MMP-9 in an inhibitory manner [Fujimoto *et al.*, 2006]. Notably, FSTL-1 was recently mentioned to modulate expression of collagens and ECM proteoglycans in chondrocytes [Chaly *et al.*, 2014].

It should be stressed that several of the observations detected in ADAM17^{ex/ex} MEF cells are in agreement with the findings reported by Kawahara and colleagues [Kawahara *et al.*, 2014]. This includes various types of collagens, periostin and cadherin-2. Among others, these proteins are involved in proliferation and motility. In fact, ADAM17^{-/-} MEF cells showed reduced migratory capacity that could be partially restored by treatment with conditioned cell culture supernatants from wild-type MEF cells. The reduced proliferation of wild-type is supposed to be mediated by reduced ERK phosphorylation and increased FAK phosphorylation due to altered activity of the transcription factor PPAR γ [Kawahara *et al.*, 2014].

Overall, if compared to the study of Kawahara and colleagues, the ADAM17^{ex/ex} MEF cell secretome shows certain similarities to the secretome of ADAM17^{-/-} MEF cells, but also revealed some inverse protein regulations. Whether these differences are due to the residual ADAM17 activity in ADAM17^{ex/ex} hypomorphic MEF cells or whether they relate to more general problems when investigating MEF cells, remains unknown. Nonetheless, both studies clearly indicate a role of ADAM17 beyond direct substrate shedding.

6.5 Intracellular effects of ADAM17 in MEF cells

As mentioned, ADAM17 might indirectly influence protein secretion and regulate cellular processes via an altered „secretome“ composition. Therefore we also addressed whether reduced ADAM17 activity in ADAM17^{ex/ex} MEF cells also leads to altered levels of intracellular proteins that might be interesting in the context of ADAM17.

6.5.1 Increased cofilin-1 phosphorylation in wild-type MEF cells

Cofilin-1 and destrin are members of the ADF/cofilin family of actin-binding proteins and are potent regulators of actin dynamics [Moon and Drubin, 1995]. Interestingly, we detected a reduced (Ser3) phosphorylation of cofilin-1 in ADAM17^{ex/ex} MEF cells, which might also be the case for destrin. It was reported that the ability of cofilin-1 to bind and depolymerize actin is abolished upon Ser3 phosphorylation [Agnew *et al.*, 1995; Moriyama *et al.*, 1996]. Phosphorylation of cofilin-1 at Ser3 is mediated by „LIM kinase 1“ (LIMK1) [Arber *et al.*, 1998] in a Rac-mediated manner [Yang *et al.*, 1998]. In addition, in neurons, cofilin-1 is also phosphorylated upon reelin signaling [Chai *et al.*, 2009]. Since a direct correlation between

ADAM17 and cofilin-1 is suggested from our present data, this might indicate that ADAM17 is somehow involved in the regulation of actin dynamics.

6.5.2 Increased intracellular annexin levels in ADAM17^{ex/ex} MEF cells

Annexins comprise a family of Ca²⁺-regulated membrane binding proteins that were detected at higher levels in ADAM17^{ex/ex} MEF cell whole-cell lysates and ECM fractions, whereas there were only little indications for annexins in MEF cell supernatants. Interestingly, the recent study on the ADAM17-dependent MEF cell secretome revealed decreased levels of annexins A2 and A5 in ADAM17^{-/-} MEF cell supernatants [Kawahara *et al.*, 2014] suggesting an impaired release/secretion in the absence of ADAM17 activity. Of note, membrane-bound annexin A2 plays a crucial role in ADAM17-mediated ectodomain shedding of EGFR ligands by forming a shedding platform that dictates substrate specificity [Nakayama *et al.*, 2012]. In addition, direct interactions of annexins with ADAM17 were shown in monocytes and colon epithelial cells, where annexin A2 promoted IL-1 β and TPA-induced shedding of TNF α , but not HB-EGF and amphiregulin [Tsukamoto *et al.*, 2013].

6.6 Method development and limitations

6.6.1 Sheddome and secretome analysis by 2D-DiGE

The 2D-DiGE approach has been proven suitable for the detection of shedding events at early stages of this project. However, except for TNF α and NCAM-1, we did not find clear indications for ADAM17-dependent shedding comparing samples derived from ADAM17^{ex/ex} MEF cells and wild-type counterparts. Nonetheless, different gel-based proteomic studies of cell culture supernatants have lead to the identification of several novel metalloprotease substrates.

Gou and colleagues enriched supernatant proteins from bone marrow-derived macrophages that were cultured in presence or absence of the broad-spectrum metalloprotease inhibitor IC-3 by centrifugal filter units. The samples were subjected to classical 2D separations but revealed no indication for metalloprotease-dependent alterations. The enrichment of supernatant proteins by WGA-mediated precipitation and subsequent one-dimensional separation led to the characterization of nine fragments of transmembrane proteins, including IL-6R and L-selectin [Guo *et al.*, 2002]. In a later study, supernatant proteins of

ADAM17-transfected A431 breast cancer cells were analyzed. To this end, cells were cultured in presence or absence of the broad-spectrum metalloprotease inhibitor BB-94 and supernatant samples were again enriched by WGA precipitation. Subsequent analysis of supernatant proteins by 2D-DiGE revealed three candidates (Desmoglein-2, Transferrin Receptor and ALCAM) that appeared to be shed in an ADAM17- or ADAM10-dependent manner [Bech-Serra *et al.*, 2006]. Finally, the analysis of supernatant samples enriched by size exclusion centrifugation from untreated and BB-94-treated transformed macrophages (Raw267.7 cells) revealed the metalloprotease-dependent shedding of M-CSFR, VIP36, Sema4D and MHC class I α chains D and L. In addition, this study pointed to differences between LPS- and PMA-induced shedding [Shirakabe *et al.*, 2013]. Taken together, some shed proteins have been identified by gel-based proteomic approaches, but the identified substrates only reflect a minor portion of the published ADAM17 sheddome.

6.6.2 General limitations of 2D GE

Besides recent advantages like reduced gel-to-gel variation using 2D-DiGE [e.g. Gade *et al.*, 2003] and the possible characterization of protein isoforms [e.g. Poth *et al.*, 2008], there might be a number of possible intrinsic limitations of 2D-based approaches [Chevalier, 2010]. These include the reduced separation capacity for membrane proteins [Luche *et al.*, 2003; Santoni *et al.*, 2000], the separation of high molecular weight proteins [Yokoyama *et al.*, 2009], but also the impaired visualization of low abundant proteins. Low abundant proteins are only rarely seen on 2D-GE images, as their detection is masked by large amounts of (highly) abundant soluble proteins [Patton, 2002; Yamada *et al.*, 2004; Ahmed and Rice, 2005]. In fact, most identified proteins from 2D-based analyses represent highly abundant polypeptides although the low abundant proteins are often considered the more important factors that dictate a given analyzed phenotype [Chevalier, 2010]. Also shed proteins might represent only a minor fraction within cell culture supernatants, if compared to the overall secreted proteins or to intracellular proteins released from dead cells. This notion is supported by the fact that shed TNF α was observed by ELISA in wild-type MEF cell supernatants, but could only be detected in supernatants by the gel-based proteomic analysis of TNF α -overexpressing MEF cells. Therefore, more general limitations of the gel-based approach might be one important reason for the low number of identified shed

proteins in various gel-based analyses [Guo *et al.*, 2002; Bech-Serra *et al.*, 2006; Shirakabe *et al.*, 2013].

6.6.3 Secretome and shedding analyses by MS approaches

As mentioned, the quantification of protein ratios by 2D-DiGE is one of the major advantages of this technique [e.g. Chevalier, 2010]. Thus, this is also valuable for degradomic studies, where differences in protein levels, including protein levels of protease substrates can be quantified. Meanwhile, quantitative proteomics is no longer limited to gel-based analyses, but also available for gel-free, LC-based proteomic approaches [Butler and Overall, 2009]. Degradome samples can be labeled by various mass tags prior to subsequent MS analysis. This includes stable isotope labeling by amino acids in cell culture (SILAC) [Mann, 2006], metabolic ^{18}O labeling, but also isotope-coded affinity tags (ICAT) [Shiio and Aebersold, 2006] and isobaric tags for relative and absolute quantitation (iTRAQ) [Ross *et al.*, 2004]. Recently, the group of Prof. Tholey also performed a LC-MS based cleavage site for the metalloproteases ADAM10 and ADAM17 using proteome-derived peptide libraries [Tucher *et al.*, 2014]. Of note, a variety of label-free analyses were published recently. For instance, Fong and colleagues deciphered the overall sheddome of resting and activated human platelets by LC-MS/MS analysis of one-dimensional platelet supernatant proteins LC-MS/MS in combination with strong cation exchange chromatography. Notably, out of 1049 identified supernatant proteins, 69 proteins contained a transmembrane domain, including some putative substrates of ADAM10 and ADAM17 [Fong *et al.*, 2011]. In addition, Meissner and colleagues characterized the sheddome of TLR4-activated macrophages [Meissner *et al.*, 2013]. Using only 150,000 cells per condition, they identified 775 supernatant proteins including 59 cytokines. For comparison only, the analyses of WGA-enriched supernatant proteins by 2D-DiGE requires 2×10^8 MEF cells.

Another advance in degradomics has been achieved by introducing N-terminomic techniques. This includes terminal amine isotopic labeling of substrates (TAILS) and allows the identification and quantification of substrate degradation. In addition, TAILS and other N-terminomic approaches also reveal information on cleavage sites [Doucet *et al.*, 2008; Kleifeld *et al.*, 2010]. Although mass spectrometry also faces several disadvantage, including the resolution of low abundant proteins [Wasinger *et al.*, 2013], recent studies propagate the use of solely MS-based approaches for degradomic studies. For instance, the MMP-2

degradome was characterized by TAILS, revealing approximately 200 MMP-2 substrates and information on respective cleavage sites [Prudova *et al.*, 2004]. In addition, the co-operative actions of meprin β and ADAM10 were investigated by iTRAQ-TAILS, resulting in 151 shed protein fragments [Jefferson *et al.*, 2013]. Thus, mass spectrometry-based techniques result in significantly higher numbers of identified protein fragments, compared to 2D-DiGE approaches and might be the approach of choice for future degradomic studies.

6.6.4 Disadvantages of ADAM17 in degradomic studies

Degradomics screenings include the comparison of a proteome exposed to the protease of interest and an unexposed proteome [Butler and Overall, 2009]. Such analyses are mostly performed within cell culture system or tissues of wild-type and knock-out animals [e.g. Vaisar *et al.*, 2009; Dean and Overall, 2007; Dean *et al.*, 2007]. However, these approaches are affected by „proteolytic side effects“ in a complex protease web. Another strategy in degradomics includes the exposure of an extracted proteome to a recombinant protease *in vitro*. These strategies led to overall insight into the cleavage capacities of MMP-2 [Kleinfeld *et al.*, 2009] and MMP-14 [Hwang *et al.*, 2004]. Of course, these *in vitro* approaches not necessarily reflect the overall *in vivo* degradome. However, MMPs seem to be more accessible to be studied by various approaches as compared to ADAM17. Complete ADAM17 knock-out mice are not viable [Peschon *et al.*, 1998], thus the ADAM17 degradome has been mostly studied in cell culture systems. However, *in vitro* studies on ADAM17 so far failed due to its poor clonability. Thus, the frequently used recombinant variants of ADAM17 lack several domains [Kawahara *et al.*, 2014] or recombinant expression of ADAM17 in various cells is performed with heterologous proteins. As the membrane placement of ADAM17 is one of the features that dictates its specific proteolytic function [White, 2013], it will be interesting to find out to which extent the derived *in vitro* degradome covers the overall or cell-type specific ADAM17 degradome. Especially, elucidation of cleaved intracellular proteins might change the picture of ADAM17 as a membrane-located sheddase, reflecting the overall intracellular location of ADAM17 [Schlöndorff *et al.*, 2000; Ebsen *et al.*, 2013].

6.6.5 Studying plasma membrane proteins of MEF cells

The problematic resolution of plasma membrane proteins by conventional two-dimensional electrophoresis is one of the major disadvantages of the standard 2D-DiGE approach

[Chevalier, 2010]. To circumvent this issue, alternative two-dimensional techniques were used for the separation, enrichment and visualization of cell-surface proteins. These approaches avoid isoelectric focussing by combining two mass-related separations using two different detergents, e.g. the 16-BAC/SDS-PAGE [Zahedi *et al.*, 2012] or the CTAB/SDS-PAGE [Philipp *et al.*, 2012]. As detailed in the results paragraph, 2D-CTAB/SDS-PAGE has been successfully adapted into the core project and was linked to differential labeling (2D-CTAB/SDS-DiGE). The second major problem for gel-based proteomics is to find a suitable protocol for sample preparation. Several published approaches and commercially available kits for plasma membrane protein extraction propose a pure preparation of this subcellular fraction. As detailed in the results paragraph, several techniques were adapted and applied to MEF cells. This includes the use of a commercially available „two-phase system“ for the separation of plasma membrane fractions and a combined approaches using lectin-mediated precipitation. Monitoring of the purity of the resulted fractions via known marker proteins by Western blot analysis always indicated an enrichment of plasma membrane proteins. However, subsequent separation of these membrane fractions by CTAB/SDS-PAGE resulted in the identification of a few membrane proteins. In contrast, most identified proteins were of intracellular origin. Again, the low number of identified membrane proteins might be due to the limited resolution and detection of low abundant proteins [Chevalier, 2010]. Nonetheless, recent studies showed an improved resolution of enriched plasma membrane proteins. For instance, Philipp and colleagues enriched membrane proteins from *Plasmodium falciparum*-infected erythrocytes to elucidate the mechanism of erythrocyte infection by CTAB/SDS-PAGE and 16-BAC/SDS-PAGE [Philipp *et al.*, 2012]. In this case, hemolytic treatment of erythrocytes leads to the formation of erythrocyte ghosts that represent free erythrocyte membranes and can be harvested easily. Unfortunately, this is a rather unique feature of erythrocytes. In addition, most studies of plasma membrane proteins monitored the protein enrichment via known marker proteins, which implicates purities sufficient for subsequent Western blot analyses. However, there is still a severe difference between enriched and pure membrane fractions. Thus, proteomic investigation of membrane samples might only be enhanced by mass spectrometry-based techniques [Savas *et al.*, 2011].

Recently, giant plasma membrane vesicles (GPMVs) were introduced as a suitable tool to study cholesterol-rich membrane regions and membrane dynamics [Levental *et al.*, 2011].

However, Bauer and colleagues used this approach for the enrichment of membrane proteins mammalian cells [Bauer *et al.*, 2009]. There, digested GPMV proteins were analyzed by LC-MS/MS and displayed a plasma membrane protein content of 93 %. As summarized in the results paragraph, we successfully adapted the protocol for GPMV formation in the context of MEF cells. However, subsequent separation of enriched GPMV proteins resulted in a low resolution of plasma membrane proteins, as predominately actin and other highly abundant intracellular proteins were identified. Unfortunately, several modifications of the original protocol did not increase the resolution of plasma membrane proteins.

Besides subcellular fractionation, cell-surface labelling represents an alternative approach to study alterations of the membrane proteome. Cell-surface labelling is performed on intact cells at low temperature to avoid intracellular uptake of the labeling compound. After saturation of the labelling agent, cells are lysed and subjected to further analysis. The use of biotin-NHS ester compounds is a rather prominent approach for enrichment of cell-surface proteins and subsequent Western blot analysis and has also been used in ADAM research [Horiuchi *et al.*, 2007]. We decided to use a commercially available kit for cell-surface protein extraction from MEF cells prior to protein separation by two-dimensional gel electrophoresis. As displayed in the results paragraph, the generated samples were compatible with two-dimensional separation, but showed no enrichment of certain protein spots as compared to separated whole-cell lysates. Recently, Niehage and colleagues enriched proteins from human mesenchymal stroma cells by biotinylation prior to one-dimensional in-gel separation and subsequent protein identification by LC-MS/MS [Niehage *et al.*, 2011]. There, they identified approximately 200 plasma membrane molecules, including several integrins and cadherins. However, they also displayed limitations of the biotinylation approach as approximately 700 proteins were supposed to be intracellular proteins. Thus, the impurity of samples derived from biotinylation might hamper the resolution of membrane proteins by gel-based approaches.

Also fluorescent CyDyesTM have been proposed for differential labelling of cell-surface proteins [Mayrhofer *et al.*, 2008]. Meanwhile, this approach has been described for various cellular systems, including chinese hamster ovary (CHO) cells [Hagner-McWhirter *et al.*, 2008], undifferentiated murine embryonic stem cells [Nunomura *et al.*, 2005] and gram-positive bacteria [Anaya *et al.*, 2007]. Thus, we applied cell-surface labelling using fluorescent CyDyesTM to wild-type MEF cells. However, subsequent separation of the

labelled sample and a whole-cell lysate by two-dimensional gel electrophoresis showed no differences indicating an uptake of the CyDyes™ by the MEF cells.

In conclusion, different techniques for the enrichment of membrane proteins were applied to MEF cells. Despite an enrichment of membrane proteins according to Western blot analyses, gel-based proteomic analyses revealed only few membrane proteins.

6.6.6 The extracellular matrix (ECM)

As detailed in the results paragraph, the analyses of MEF cell culture supernatants indicated an ADAM17-dependent alteration of ECM remodelling or degradation. In order to verify these findings and to study changes in ECM composition in more detail, we adapted appropriate techniques for ECM protein enrichment. So far, preparation of ECM from cultured MEF cells has not been described, but approaches, based on decellularization and harvesting of remaining ECM are published for other cell, e.g. mesenchymal stromal cells [Harvey *et al.*, 2013]. We successfully adapted the protocol for ECM protein enrichments of Harvey and colleagues and separated the resulting sample by 2D-DiGE. Subsequent protein identification revealed increased levels of various annexins and of the serine protease HtrA1 that also showed reduced levels in ADAM17^{ex/ex} MEF cell supernatants and is involved in fibronectin degradation and MMP regulation [Grau *et al.*, 2005]. In addition, the analyzed samples contained a variety of nuclear proteins, whereas major ECM proteins (e.g. collagens or fibronectin) were not observed. Unfortunately, further enrichment of MEF cell ECM proteins by WGA precipitation only delivered low protein amounts. Of note, an initial experiment for preparation of ECM proteins from murine livers using the “Texas 3-step” approach [de Castro Brás *et al.*, 2013] was performed. Although this experiment only revealed little indications for enriched ECM proteins, a subsequent WGA precipitation might increase the purity of this sample. However, further efforts for ECM preparation were aborted as no ADAM17^{ex/ex} mice were available for this *in vivo* characterization.

6.7 Limitations of the ADAM17^{ex/ex} MEF system

Overall seventy different proteins are supposed to be shed by ADAM17 [reviewed by Gooz, 2009]. As summarized in the introduction various cellular systems and experimental approaches were used to elucidate the ADAM17 sheddome. This includes overexpression,

knock-down and knock-out of ADAM17, but also stimulation and inhibition of metalloprotease activity by various compounds (compare Tab. 1.2). Nonetheless, the characterization of the ADAM17 sheddome in a more context-dependent manner is still missing.

Therefore, we wanted to address the characterization of the context-dependent ADAM17-sheddome using different cells and tissues derived from the ADAM17^{ex/ex} murine model [Chalaris *et al.*, 2010]. At the beginning of this project, wild-type and ADAM17^{ex/ex}-derived MEF cells were available and were used for the adaption of various approaches for the aimed sheddome characterization. As already discussed, gel-based analyses of MEF cell culture supernatants revealed several differentially abundant protein fragments. However, TNF α and NCAM-1 represent the only known ADAM17 substrates identified in this project. Notably, other protein fragments are reported substrates of other proteases and might reflect “proteolytic side effects” via the protease web. In addition, MEF cell supernatants contained a variety of secreted proteins. Thus, intrinsic limitations of the 2D-DiGE approach might be the reason for the low number of identified ADAM17 substrates. On the other hand, ADAM17-mediated shedding might only play a minor role in MEF cell biology.

To address this issue, we also analyzed other ADAM17-deficient cells, including non-small lung cancer cells and cells derived from ADAM17^{ex/ex} mice. As mentioned in the methods section, at least 2×10^8 cells are required to yield sufficient protein amounts subsequent supernatant analysis by 2D-DiGE analysis. Unfortunately, ADAM17 knock-down non-small cell lung cancer cells [Baumgart *et al.*, 2010] showed strongly reduced proliferation as compared to wild-type non-small cell lung cancer cells. If supplemented with exogenous EGF, the proliferation of the ADAM17 knock-down cells was stabilized to a certain extent [Baumgart *et al.*, 2010], but still prevented the generation of necessary amounts of cells. Along this line, reduced proliferation was also observed for primary cell cultures of colon and intestinal cells, derived from ADAM17^{ex/ex} MEF cells. Interestingly, Kawahara and colleagues also showed reduced proliferation of ADAM17^{-/-} MEF cells [Kawahara *et al.*, 2014]. However, ADAM17^{ex/ex} and ADAM17^{-/-} MEF cells did not show a severe reduction of proliferation as compared to the ADAM17^{ex/ex} intestinal cells. Thus, the effect of reduced ADAM17 activity differs between different cell types, indicating a cell-type specific role of this protease. Even more, this substantiates the demand for a more context-dependent (=cell-type specific) evaluation of the ADAM17 sheddome.

Notably, bone marrow-derived macrophages were derived from wild-type and ADAM17^{ex/ex} mice were used for several *ex vivo* studies [e.g. Schwarz *et al.*, 2014]. Initial experiments regarding the sheddome characterization of these cells were also performed and revealed compatibility to the already adapted enrichment techniques. Moreover, derived cell numbers were sufficient for supernatant analyses by 2D-DiGE. Unfortunately, there were not enough mice available for further sheddome and secretome characterizations of these cells.

Finally, *in vivo* studies that rely on the comparison of wild-type and protease knock-out samples (e.g. wild-type versus ADAM17^{ex/ex}) are hampered, as the observed effects might be induced by the removal of the investigated protease [Fortelny *et al.*, 2014]. Thus, the biological system might react to the removal of the protease, leading to altered gene expression profiles of proteases, inhibitors and substrates [Auf dem Keller *et al.* 2013; Krüger, 2009]. In addition, biological consequences of altered substrate cleavage *in vivo*, e.g. cleaved transcription factors [Goulet *et al.*, 2004] or activation or degradation of other proteases and inhibitors [e.g. Dean and Overall, 2007; Auf dem Keller *et al.*, 2013], interfere with the real effect of the reduced activity of the investigated protease. Thus, proteomic studies will not only detect direct effects of a certain protease, but also indirect effects via the interaction of mediators of proteolysis via the protease web [Fortelny *et al.*, 2014]. In line with this, the benefits of the ADAM17^{ex/ex} MEF system might be low, as ADAM17^{-/-} MEF cells are available and were already used for the characterization of various ADAM17 substrates [e.g. Sahin *et al.*, 2004]. However, a direct comparison of supernatant proteins from ADAM17^{ex/ex} and ADAM17^{-/-} MEF cells might help to separate the effects of ADAM17 from “proteolytic side effects”.

7 Summary

The ectodomain shedding of numerous transmembrane proteins by the A Disintegrin And Metalloprotease 17 (ADAM17) governs a variety of physiological and developmental processes. Focusing on murine embryonic fibroblasts (MEFs) of ADAM17^{wt/wt} and ADAM17^{ex/ex} (hypomorphic) mice, we investigated ADAM17-mediated changes in conditioned cell culture supernatants, in membrane preparations and in whole cell lysates using a 2D-DiGE proteomic approach. The detection of high amounts of cleaved TNF α in supernatants of TNF α -overexpressing wild-type but not ADAM17^{ex/ex} MEF cells demonstrated the general suitability of the employed 2D-DiGE approach for the identification of shed protein fragments. Interestingly, the analyses of whole-cell lysates revealed that ADAM17 might also influence intracellular protein levels since a variety of proteins (e.g. annexins) showed altered abundances at reduced levels of ADAM17. From conditioned MEF supernatants, seventy differentially abundant secreted and cell-surface proteins were identified. These included collagens and other extracellular matrix components, several proteases and several protein fragments. Thus, wild-type and ADAM17^{ex/ex} MEF cells clearly differ in their ability to secrete or shed proteins. However, only fourteen different protein fragments were less abundant in ADAM17^{ex/ex} MEF cell supernatants, including only two known ADAM17 substrates (TNF α and NCAM-1). Notably, most full length proteins that were detected as fragments lack a transmembrane region and are thus no *bona fide* ADAM17 substrates. The high amounts of the perlecan LG3 peptide and of the type-I collagen C-terminal propeptide in supernatants of wild-type MEF cells point to a reduced collagen maturation and degradation in ADAM17^{ex/ex} MEF cells. Since we also observed reduced levels of the C-procollagenase “bone morphogenic protein 1” and reduced matrix metalloproteinase activity in ADAM17^{ex/ex} MEF cell culture supernatants, the observed processing of collagen and perlecan might reflect “proteolytic side effects” by other proteases in a complex “protease web”.

8 Zusammenfassung

Die Metalloprotease *A Disintegrin And Metalloprotease 17* (ADAM17) vermittelt das Freisetzen der extrazellulären Domänen verschiedener Transmembranproteine (*ectodomain shedding*) und ist somit an verschiedensten physiologischen und entwicklungsbiologischen Prozessen beteiligt. Mit einem Fokus auf murine embryonale Fibroblasten (MEF) von ADAM17^{wt/wt} und ADAM17^{ex/ex} (hypomorphen) Mäusen haben wir ADAM17-abhängige Veränderungen in konditionierten Zellkulturüberständen, Membranfraktionen und Zelllysaten analysiert. Die Tauglichkeit der verwendeten 2D-DiGE Methode zur Identifizierung von Proteinfragmenten konnte dabei an Kulturüberständen von TNF α -überexprimierenden MEF-Zellen demonstriert werden. Im Gegensatz zu ADAM17^{ex/ex} MEF-Zellen, konnten so in Kulturüberständen von wildtyp MEF-Zellen hohe Mengen an löslichem TNF α beobachtet werden. Darüber hinaus deutete die Analyse von Zelllysaten auch auf intrazelluläre Effekte von ADAM17 hin, da zahlreiche Proteine (z.B. Annexine) veränderte Abundanzen unter reduzierter ADAM17 Aktivität zeigten. Aus konditionierten MEF-Kulturüberständen konnten siebzig differentiell abundante sekretierte und Zelloberflächenproteine identifiziert werden, darunter Kollagene und andere Komponenten der extrazellulären Matrix, verschiedene Proteasen und mehrere Proteinfragmente. Wildtyp und ADAM17^{ex/ex} MEF-Zellen zeigen somit deutliche Unterschiede in Sekretion und *Shedding* von Proteinen. Insgesamt wurden jedoch lediglich vierzehn Proteinfragmente mit veränderter Abundanz in ADAM17^{ex/ex} MEF-Zellen identifiziert, darunter zwei bekannte Substrate von ADAM17 (TNF α und NCAM-1). Interessanter Weise weisen die meisten Proteine, welche als Proteinfragmente identifiziert wurden keine Transmembrandomäne auf und sind somit kein *bona fide* ADAM17 Substrate. Der erhöhte Gehalt an dem Perlecan LG3-Peptid und dem C-terminalen Propeptid des Typ-I Kollagens in wildtyp MEF-Kulturüberständen deutet daneben auf eine Verminderte Reifung und Degradierung von Kollagenen in ADAM17^{ex/ex} MEF-Zellen hin. Da wir außerdem eine reduzierte Abundanz der C-Procollagenase "*bone morphogenic protein 1*" und verminderte Matrixmetalloprotease-Aktivitäten in Kulturüberständen von ADAM17^{ex/ex} MEF-Zellen beobachteten, könnten die beobachtete Veränderung der Kollagen- und Perlecanprozessierung ein "proteolytischer Nebeneffekt" durch andere Proteasen in einem komplexen „proteolytischen Netzwerk“ sein.

9 Bibliography

Agnew BJ, Minamide LS, Bamburg JR (1995) Reactivation of phosphorylated actin depolymerizing factor and identification of the regulatory site. *J Biol Chem*; 270:17582–17587.

Ahmad M, Takino T, Miyamori H, Yoshizaki T, Furukawa M, Sato H (2006) Cleavage of amyloid-beta precursor protein (APP) by membrane-type matrix metalloproteinases. *J Biochem*; 139(3):517-26.

Ahmed N and Rice GE (2005) Strategies for revealing lower abundance proteins in two-dimensional protein maps. *Journal of Chromatography B-Analytical Technologies in the Biomedical and Life Sciences*, 815:39-50.

Ali N and Knaüper V (2007) Phorbol ester-induced shedding of the prostate cancer marker transmembrane protein with epidermal growth factor and two follistatin motifs 2 is mediated by the disintegrin and metalloproteinase-17. *J Biol Chem*; 282(52):37378-88.

Allinson TM, Parkin ET, Turner AJ, Hooper NM (2003) ADAMs family members as amyloid precursor protein alpha-secretases. *J Neurosci Res*; 74(3):342-52.

Althoff K, Reddy P, Voltz N, Rose-John S, Müllberg J (2000) Shedding of interleukin-6 receptor and tumor necrosis factor alpha. Contribution of the stalk sequence to the cleavage pattern of transmembrane proteins. *Eur J Biochem*; 267(9):2624-31.

Amin AR (1999) Regulation of tumor necrosis factor-alpha and tumor necrosis factor converting enzyme in human osteoarthritis. *Osteoarthritis Cartilage*; 7(4):392-4.

Amin EA and Welsh WJ (2001) Three-dimensional quantitative structure-activity relationship (3D-QSAR) models for a novel class of piperazine-based stromelysin-1 (MMP-3) inhibitors: applying a "divide and conquer" strategy. *J Med Chem*; 44(23):3849-55.

Amour A, Slocombe PM, Webster A, Butler M, Knight CG, Smith BJ, Stephens PE, Shelley C, Hutton M, Knäuper V, Docherty AJ, Murphy G (1998) TNF-alpha converting enzyme (TACE) is inhibited by TIMP-3. *FEBS Lett*; 435(1):39-44.

Anaya C, Church N, Lewis JP (2007) Detection and identification of bacterial cell surface proteins by fluorescent labeling. *Proteomics*; 7(2):215-9.

Arber S, Barbayannis FA, Hanser H, Schneider C, Stanyon CA, Bernard O, Caroni P (1998) Regulation of actin dynamics through phosphorylation of cofilin by LIM-kinase. *Nature*; 393(6687):805-9.

Arribas J and Borroto A. (2002) Protein ectodomain shedding. *Chem Rev*; 102(12):4627-38.

Arribas J and Esselens C (2009) ADAM17 as a therapeutic target in multiple diseases. *Curr Pharm Des*; 15(20):2319-35.

Arribas J and Massagué J (1995) Transforming growth factor-alpha and beta-amyloid precursor protein share a secretory mechanism. *J Cell Biol*; 128(3):433-41.

Ashkenazi A and Dixit VM (1998) Death receptors: signaling and modulation. *Science*; 281(5381):1305-8.

Auf dem Keller U, Prudova A, Eckhard U, Fingleton B, Overall CM (2013) Systems-level analysis of proteolytic events in increased vascular permeability and complement activation in skin inflammation. *Sci Signal*; 6: rs2.

Bakken AM, Protack CD, Roztocil E, Nicholl SM, Davies MG. (2009) Cell migration in response to the amino-terminal fragment of urokinase requires epidermal growth factor receptor activation through an ADAM-mediated mechanism. *J Vasc Surg*; 49(5):1296-303.

Bauer B, Davidson M, Orwar O (2009) Proteomic analysis of plasma membrane vesicles. *Angew Chem Int Ed Engl*; 48(9):1656-9.

Bech-Serra JJ, Santiago-Josefat B, Esselens C, Saftig P, Baselga J, Arribas J, Canals F (2006) Proteomic identification of desmoglein 2 and activated leukocyte cell adhesion molecule as substrates of ADAM17 and ADAM10 by difference gel electrophoresis. *Mol Cell Biol*; 26(13):5086-95.

Bender M, Hofmann S, Stegner D, Chalaris A, Bösl M, Braun A, Scheller J, Rose-John S, Nieswandt B (2010) Differentially regulated GPVI ectodomain shedding by multiple platelet-expressed proteinases. *Blood*; 116(17):3347-55.

Bergmeier W, Piffath CL, Cheng G, Dole VS, Zhang Y, von Andrian UH, Wagner DD (2004) Tumor necrosis factor- α -converting enzyme (ADAM17) mediates GPIIb/IIIa shedding from platelets in vitro and in vivo. *Circ Res*; 95(7):677-83.

Bix G, Fu J, Gonzalez E, Macro L, Barker A, Campbell S, Zutter MM, Santoro SA, Kim JK, Höök M, Reed CC and Iozzo RV (2004) Endorepellin causes endothelial cell disassembly of actin cytoskeleton and focal adhesions through α 2 β 1 integrin. *J Cell Biol*; (166) 97–109

Black RA, Doedens JR, Mahimkar R, Johnson R, Guo L, Wallace A, Virca D, Eisenman J, Slack J, Castner B, Sunnarborg SW, Lee DC, Cowling R, Jin G, Charrier K, Peschon JJ, Paxton R (2003) Substrate specificity and inducibility of TACE (tumour necrosis factor α -converting enzyme) revisited: the Ala-Val preference, and induced intrinsic activity. *Biochem Soc Symp*; (70):39-52.

Black RA, Rauch CT, Kozlosky CJ, Peschon JJ, Slack JL, Wolfson MF, Castner BJ, Stocking KL, Reddy P, Srinivasan S, Nelson N, Boiani N, Schooley KA, Gerhart M, Davis R, Fitzner JN, Johnson RS, Paxton RJ, March CJ, Cerretti DP (1997) A metalloproteinase disintegrin that releases tumour-necrosis factor- α from cells. *Nature*;385(6618):729-33.

Blobel CP, Wolfsberg TG, Turck CW, Myles DG, Primakoff P, White JM (1992) A potential fusion peptide and an integrin ligand domain in a protein active in sperm-egg fusion. *Nature*; 356(6366):248-52.

Bode W, Gomis-Rüth FX, Stöckler W (1993) Astacins, serralysins, snake venom and matrix metalloproteinases exhibit identical zinc-binding environments (HEXXHXXGXXH and Met-turn) and topologies and should be grouped into a common family, the 'metzincins'. *FEBS Lett*; 331(1-2):134-40.

Boersema PJ, Geiger T, Wisniewski JR, Mann M (2012) Quantification of the N-glycosylated secretome by super-SILAC during breast cancer progression and in human blood samples. *Mol Cell Proteomics*; 12(1):158-71.

Borrell-Pagès M, Rojo F, Albanell J, Baselga J, Arribas J (2003) TACE is required for the activation of the EGFR by TGF- α in tumors. *EMBO J*; 22(5):1114-24.

Borroto A, Ruiz-Paz S, de la Torre TV, Borrell-Pages M, Merlos-Suarez A, Pandiella A, Blobel CP, Baselga J, Arribas J (2003) Impaired trafficking and activation of tumor necrosis factor- α -converting enzyme in cell mutants defective in protein ectodomain shedding. *J Biol Chem*; 278(28):25933-9. Epub 2003 Apr 24.

Boutet P, Agüera-González S, Atkinson S, Pennington CJ, Edwards DR, Murphy G, Reyburn HT, Valés-Gómez M (2009) Cutting edge: the metalloproteinase ADAM17/TNF- α -converting enzyme regulates proteolytic shedding of the MHC class I-related chain B protein. *J Immunol*; 182(1):49-53.

Bradford MM (1976), Rapid and sensitive method for the quantitation of microgram quantities of protein utilizing the principle of protein-dye binding, *Anal. Biochem.* **72**: 248–254.

Bridges LC, Sheppard D, Bowditch RD (2005) ADAM disintegrin-like domain recognition by the lymphocyte integrins α 4 β 1 and α 4 β 7. *Biochem J*; 387(Pt 1):101-8.

Broder C, Arnold P, Vadon-Le Goff S, Konerding MA, Bahr K, Müller S, Overall CM, Bond JS, Koudelka T, Tholey A, Hulmes DJ, Moali C, Becker-Pauly C (2013) Metalloproteases meprin α and meprin β are C- and N-procollagen proteinases important for collagen assembly and tensile strength. *Proc Natl Acad Sci USA*; 110(35):14219-24.

Brou C, Logeat F, Gupta N, Bessia C, LeBail O, Doedens JR, Cumano A, Roux P, Black RA, Israël A (2000) A novel proteolytic cleavage involved in Notch signaling: the role of the disintegrin-metalloprotease TACE. *Mol Cell*; 5(2):207-16.

Brule S, Charnaux N, Sutton A, Ledoux D, Chaigneau T, Saffar L, Gattegno L (2006) The shedding of syndecan-4 and syndecan-1 from HeLa cells and human primary macrophages is accelerated by SDF-1/CXCL12 and mediated by the matrix metalloproteinase-9. *Glycobiology*; 16(6):488-501.

Butler GS and Overall CM (2009) Updated biological roles for matrix metalloproteinases and new "intracellular" substrates revealed by degradomics. *Biochemistry*; 48: 10830–10845.

Buxbaum JD, Liu KN, Luo Y, Slack JL, Stocking KL, Peschon JJ, Johnson RS, Castner BJ, Cerretti DP, Black RA (1998) Evidence that tumor necrosis factor alpha converting enzyme is involved in regulated alpha-secretase cleavage of the Alzheimer amyloid protein precursor. *J Biol Chem*; 273(43):27765-7.

Caescu CI, Jeschke GR, Turk BE (2009) Active-site determinants of substrate recognition by the metalloproteinases TACE and ADAM10. *Biochem J*; 424(1):79-88.

Canault M, Peiretti F, Kopp F, Bonardo B, Bonzi MF, Coudeyre JC, Alessi MC, Juhan-Vague I, Nalbone G (2006) The TNF alpha converting enzyme (TACE/ADAM17) is expressed in the atherosclerotic lesions of apolipoprotein E-deficient mice: possible contribution to elevated plasma levels of soluble TNF alpha receptors. *Atherosclerosis*; 187(1):82-91.

Canty EG and Kadler KE (2005) Procollagen trafficking, processing and fibrillogenesis. *J Cell Sci*; 118(Pt 7):1341–1353.

Castagna M, Takai Y, Kaibuchi K, Sano K, Kikkawa U, Nishizuka Y (1982) Direct activation of calcium-activated, phospholipid-dependent protein kinase by tumor-promoting phorbol esters. *J Biol Chem*; 257(13):7847-51.

Cavallo-Medved D, Dosesescu J, Linebaugh BE, Sameni M, Rudy D, Sloane BF (2003) Mutant K-ras regulates cathepsin B localization on the surface of human colorectal carcinoma cells. *Neoplasia*; 5(6):507-19.

Cesaro A, Abakar-Mahamat A, Brest P, Lassalle S, Selva E, Filippi J, Hébuterne X, Hugot JP, Doglio A, Galland F, Naquet P, Vouret-Craviari V, Mograbi B, Hofman PM (2009) Differential expression and regulation of ADAM17 and TIMP3 in acute inflamed intestinal epithelia. *Am J Physiol Gastrointest Liver Physiol*; 296(6):G1332-43

Chai X, Förster E, Zhao S, Bock HH, Frotscher M (2009) Reelin stabilizes the actin cytoskeleton of neuronal processes by inducing n-cofilin phosphorylation at serine3. *J Neurosci*; 29(1):288-99.

Chalaris A, Adam N, Sina C, Rosenstiel P, Lehmann-Koch J, Schirmacher P, Hartmann D, Cichy J, Gavrilova O, Schreiber S, Jostock T, Matthews V, Häslér R, Becker C, Neurath MF, Reiss K, Saftig P, Scheller J, Rose-John S (2010) Critical role of the disintegrin metalloprotease ADAM17 for intestinal inflammation and regeneration in mice. *J Exp Med*; 207(8):1617-24.

Chalaris A, Rabe B, Paliga K, Lange H, Laskay T, Fielding CA, Jones SA, Rose-John S, Scheller J (2007) Apoptosis is a natural stimulus of IL6R shedding and contributes to the proinflammatory trans-signaling function of neutrophils. *Blood*; 110(6):1748-55.

Chaly Y, Blair HC, Smith SM, Bushnell DS, Marinov AD, Campfield BT, Hirsch R (2014) Follistatin-like protein 1 regulates chondrocyte proliferation and chondrogenic differentiation of mesenchymal stem cells. *Ann Rheum Dis*

Chan YH and Boxer SG (2007) Model membrane systems and their applications. *Curr Opin Chem Biol*; 11(6):581-7.

Charbonneau M, Harper K, Grondin F, Pelmus M, McDonald PP, Dubois CM (2007) Hypoxia-inducible factor mediates hypoxic and tumor necrosis factor alpha-induced increases in tumor necrosis factor-alpha converting enzyme/ADAM17 expression by synovial cells. *J Biol Chem*; 282(46):33714-24.

Chen A, Engel P, Tedder TF (1995) Structural requirements regulate endoproteolytic release of the L-selectin (CD62L) adhesion receptor from the cell surface of leukocytes. *J Exp Med*; 182(2):519-30.

Chen CD, Podvin S, Gillespie E, Leeman SE, Abraham CR (2007) Insulin stimulates the cleavage and release of the extracellular domain of Klotho by ADAM10 and ADAM17. *Proc Natl Acad Sci USA*; 104(50):19796-801.

Chevalier F (2010) Highlights on the capacities of "Gel-based" proteomics. *Proteome Sci.*, 8:23

Cho RW, Park JM, Wolff SB, Xu D, Hopf C, Kim JA, Reddy RC, Petralia RS, Perin MS, Linden DJ, Worley PF (2008) mGluR1/5-dependent long-term depression requires the regulated ectodomain cleavage of neuronal pentraxin NPR by TACE. *Neuron*; 57(6):858-71.

Chow JP, Fujikawa A, Shimizu H, Suzuki R, Noda M (2008) Metalloproteinase- and gamma-secretase-mediated cleavage of protein-tyrosine phosphatase receptor type Z. *J Biol Chem*; 283(45):30879-89.

Coles CA, Wadeson J, Knight MI, Cafe LM, Johns WH, White JD, Greenwood PL, McDonagh MB. (2014) A disintegrin and metalloprotease-12 is type I myofiber specific in *Bos taurus* and *Bos indicus* cattle. *J Anim Sci*; 92(4):1473-83.

Colige A, Vandenberghe I, Thiry M, Lambert CA, Van Beeumen J, Li SW, Prockop DJ, Lapiere CM, Nusgens BV (2002) Cloning and characterization of ADAMTS-14, a novel ADAMTS displaying high homology with ADAMTS-2 and ADAMTS-3. *J Biol Chem*; 277(8): 5756–5766.

Condon TP, Flournoy S, Sawyer GJ, Baker BF, Kishimoto TK, Bennett CF (2001) ADAM17 but not ADAM10 mediates tumor necrosis factor-alpha and L-selectin shedding from leukocyte membranes. *Antisense Nucleic Acid Drug Dev*; 11(2):107-16.

Contin C, Pitard V, Itai T, Nagata S, Moreau JF, Déchanet-Merville J (2003) Membrane-anchored CD40 is processed by the tumor necrosis factor-alpha-converting enzyme. Implications for CD40 signaling. *J Biol Chem*; 278(35):32801-9.

Cox TR and Erler JT (2011) Remodeling and homeostasis of the extracellular matrix: implications for fibrotic diseases and cancer. *Dis Model Mech*; 4(2):165-78.

Cukierman E, Pankov R, Stevens DR, Yamada KM (2001) Taking cell-matrix adhesions to the third dimension. *Science*; 294(5547):1708-12.

d'Ortho MP, Will H, Atkinson S, Butler G, Messent A, Gavrilovic J, Smith B, Timpl R, Zardi L, Murphy G (1997) Membrane-type matrix metalloproteinases 1 and 2 exhibit broad-spectrum proteolytic capacities comparable to many matrix metalloproteinases. *Eur J Biochem*; (250) 751–757.

Dang M, Armbruster N, Miller MA, Cermeno E, Hartmann M, Bell GW, Root DE, Lauffenburger DA, Lodish HF, Herrlich A (2013) Regulated ADAM17-dependent EGF family ligand release by substrate-selecting signaling pathways. *Proc Natl Acad Sci USA*; 110(24):9776-81.

David A (1998) "Catalytic mechanisms for metalloproteinases" in Handbook of Proteolytic Enzymes (editors Barrett AJ, Rawlings ND, Woessner JF), pp. 268–289, Academic Press, San Diego, Calif, USA, 2nd edition, 1998.

De Strooper B, Annaert W, Cupers P, Saftig P, Craessaerts K, Mumm JS, Schroeter EH, Schrijvers V, Wolfe MS, Ray WJ, Goate A, Kopan R (1999) A presenilin-1-dependent gamma-secretase-like protease mediates release of Notch intracellular domain. *Nature*; 398(6727):518-22.

Dean RA and Overall CM (2007) Proteomics Discovery of Metalloproteinase Substrates in the Cellular Context by iTRAQ Labeling Reveals a Diverse MMP-2 Substrate Degradome. *Mol Cell Proteomics*; 6:611–623.

Dean RA, Butler GS, Hamma-Kourbali Y, Delbe J, Brigstock DR, Courty J, Overall CM (2007) Identification of candidate angiogenic inhibitors processed by matrix metalloproteinase 2 (MMP-2) in cell-based proteomic screens: disruption of vascular endothelial growth factor (VEGF)/heparin affinity regulatory peptide (pleiotrophin) and VEGF/Connective tissue growth factor angiogenic inhibitory complexes by MMP2 proteolysis. *Mol Cell Biol*; 27:8454–8465.

Dell KM, Nemo R, Sweeney WE Jr, Levin JJ, Frost P, Avner ED (2001) A novel inhibitor of tumor necrosis factor-alpha converting enzyme ameliorates polycystic kidney disease. *Kidney Int*; 60(4):1240-8.

Deryugina EI, Ratnikov B, Monosov E, Postnova TI, DiScipio R, Smith JW, Strongin AY (2001) MT1-MMP initiates activation of pro-MMP-2 and integrin alpha5beta3 promotes maturation of MMP-2 in breast carcinoma cells. *Exp Cell Res*; 263:209-223.

Díaz-Rodríguez E, Cabrera N, Esparís-Ogando A, Montero JC, Pandiella A (1999) Cleavage of the TrkA neurotrophin receptor by multiple metalloproteases generates signalling-competent truncated forms. *Eur J Neurosci*; 11(4):1421-30.

- Díaz-Rodríguez E**, Cabrera N, Esparís-Ogando A, Montero JC, Pandiella A (1999) Cleavage of the TrkA neurotrophin receptor by multiple metalloproteases generates signalling-competent truncated forms. *Eur J Neurosci*; 11(4):1421-30.
- Dolnik O**, Volchkova V, Garten W, Carbonnelle C, Becker S, Kahnt J, Ströher U, Klenk HD, Volchkov V (2004) Ectodomain shedding of the glycoprotein GP of Ebola virus. *EMBO J*; 23(10):2175-84.
- Doucet A**, Butler GS, Rodriguez D, Prudova A, Overall CM (2008) Metadegradomics: Toward in vivo quantitative degradation of proteolytic post-translational modifications of the cancer proteome. *Mol Cell Proteomics*; 7: 1925–1951.
- Dreymueller D**, Pruessmeyer J, Groth E, Ludwig A (2012) The role of ADAM-mediated shedding in vascular biology. *Eur J Cell Biol*; 91(6-7):472-85.
- Düsterhöft S**, Jung S, Hung CW, Tholey A, Sönnichsen FD, Grötzinger J, Lorenzen I (2013) Membrane-proximal domain of a disintegrin and metalloprotease-17 represents the putative molecular switch of its shedding activity operated by protein-disulfide isomerase. *J Am Chem Soc*; 135(15):5776-81.
- Dyczynska E**, Sun D, Yi H, Sehara-Fujisawa A, Blobel CP, Zolkiewska A (2007) Proteolytic processing of delta-like 1 by ADAM proteases. *J Biol Chem*; 282(1):436-44.
- Ebsen H**, Schröder A, Kabelitz D, Janssen O (2013) Differential surface expression of ADAM10 and ADAM17 on human T lymphocytes and tumor cells. *PLoS One*; 8(10):e76853.
- Edwards DR**, Handsley MM, Pennington CJ (2008) The ADAM metalloproteinases. *Mol Aspects Med*; 29(5):258-89.
- Endres K**, Anders A, Kojro E, Gilbert S, Fahrenholz F, Postina R (2003) Tumor necrosis factor-alpha converting enzyme is processed by proprotein-convertases to its mature form which is degraded upon phorbol ester stimulation. *Eur J Biochem*; 270(11):2386-93.
- Esselens CW**, Malapeira J, Colomé N, Moss M, Canals F, Arribas J (2008) Metastasis-associated C4.4A, a GPI-anchored protein cleaved by ADAM10 and ADAM17. *Biol Chem*; 389(8):1075-84.
- Etzerodt A**, Maniecki MB, Møller K, Møller HJ, Moestrup SK (2010) Tumor necrosis factor α -converting enzyme (TACE/ADAM17) mediates ectodomain shedding of the scavenger receptor CD163. *J Leukoc Biol*; 88(6):1201-5.
- Fabre-Lafay S**, Garrido-Urbani S, Reymond N, Gonçalves A, Dubreuil P, Lopez M (2005) Nectin-4, a new serological breast cancer marker, is a substrate for tumor necrosis factor-alpha-converting enzyme (TACE)/ADAM-17. *J Biol Chem*; 280(20):19543-50.
- Fisher GJ**, Quan T, Purohit T, Shao Y, Cho MK, He T, Varani J, Kang S, Voorhees JJ (2009) Collagen Fragmentation Promotes Oxidative Stress and Elevates Matrix Metalloproteinase-1 in Fibroblasts in Aged Human Skin. *Am J Pathol*; 174(1): 101–114.
- Fong KP**, Barry C, Tran AN, Traxler EA, Wannemacher KM, Tang HY, Speicher KD, Blair IA, Speicher DW, Grosser T, Brass LF (2011) Deciphering the human platelet sheddome. *Blood*; 117(1):e15-26.
- Fortelny N, Cox JH, Kappelhoff R, Starr AE, Lange PF, Pavlidis P, Overall CM (2014) Network analyses reveal pervasive functional regulation between proteases in the human protease web. *PLoS Biol*; 12(5):e1001869.
- Franzke CW**, Tasanen K, Borradori L, Huotari V, Bruckner-Tuderman L (2004) Shedding of collagen XVII/BP180: structural motifs influence cleavage from cell surface. *J Biol Chem*; 279(23):24521-9.
- Fujimoto N**, Terlizzi J, Aho S, Brittingham R, Fertala A, Oyama N, McGrath JA, Uitto J (2006) Extracellular matrix protein 1 inhibits the activity of matrix metalloproteinase 9 through high-affinity protein/protein interactions. *Exp Dermatol*; 15(4):300-7.
- Funderburgh JL**, Corpuz LM, Roth MR, Funderburgh ML, Tasheva ES, Conrad GW (1997) Mimecan, the 25-kDa corneal keratan sulfate proteoglycan, is a product of the gene producing osteoglycin. *J Biol Chem*; 272(44):28089-95.
- Gade D**, Thiermann J, Markowsky D, Rabus R (2003) Evaluation of two-dimensional difference gel electrophoresis for protein profiling. *Journal of Molecular Microbiology and Biotechnology* 2003, 5:240-251.

- Gál P, Ambrus G, Závodszy P (2002)** C1s, the protease messenger of C1. Structure, function and physiological significance. *Immunobiology*; 205(4-5):383-94.
- Gallatin WM, Weissman IL, Butcher EC (1983)** A cell-surface molecule involved in organ-specific homing of lymphocytes. *Nature*; 304(5921):30-4.
- Garton KJ, Gough PJ, Blobel CP, Murphy G, Greaves DR, Dempsey PJ, Raines EW (2001)** Tumor necrosis factor-alpha-converting enzyme (ADAM17) mediates the cleavage and shedding of fractalkine (CX3CL1). *J Biol Chem*; 276(41):37993-8001.
- Garton KJ, Gough PJ, Philalay J, Wille PT, Blobel CP, Whitehead RH, Dempsey PJ, Raines EW (2003)** Stimulated shedding of vascular cell adhesion molecule 1 (VCAM-1) is mediated by tumor necrosis factor-alpha-converting enzyme (ADAM 17). *J Biol Chem*; 278(39):37459-64.
- Garton KJ, Gough PJ, Philalay J, Wille PT, Blobel CP, Whitehead RH, Dempsey PJ, Raines EW (2003)** Stimulated shedding of vascular cell adhesion molecule 1 (VCAM-1) is mediated by tumor necrosis factor-alpha-converting enzyme (ADAM 17). *J Biol Chem*; 278(39):37459-64.
- Gechtman Z, Alonso JL, Raab G, Ingber DE, Klagsbrun M (1999)** The shedding of membrane-anchored heparin-binding epidermal-like growth factor is regulated by the Raf/mitogen-activated protein kinase cascade and by cell adhesion and spreading. *J Biol Chem*; 274(40):28828-35.
- Gerke V and Moss SE (2002)** Annexins: from structure to function. *Physiol Rev*; 82(2):331-71.
- Gonzales PE, Galli JD, Milla ME (2008)** Identification of key sequence determinants for the inhibitory function of the prodomain of TACE. *Biochemistry*; 47(37):9911-9.
- Gonzales PE, Solomon A, Miller AB, Leesnitzer MA, Sagi I, Milla ME (2004)** Inhibition of the tumor necrosis factor-alpha-converting enzyme by its pro domain. *J Biol Chem*; 279(30):31638-45.
- Gonzalez EM, Reed CC, Bix G, Fu J, Zhang Y, Gopalakrishnan B, Greenspan DS, Iozzo RV (2005)** BMP1/Tolloid-like metalloproteases process endorepellin, the angiostatic C-terminal fragment of perlecan. *J Biol Chem*; (280) 7080-7087
- Goos M (2010)** ADAM-17: the enzyme that does it all. *Crit Rev Biochem Mol Biol*; 45(2):146-69.
- Goulet B, Baruch A, Moon N-S, Poirier M, Sansregret LL (2004)** A cathepsin L isoform that is devoid of a signal peptide localizes to the nucleus in S phase and processes the CDP/Cux transcription factor. *Molecular Cell*; 14: 207– 219.
- Grindel BJ, Martinez JR, Pennington CL, Muldoon M, Stave J, Chung LW, Farach-Carson MC (2014)** Matrilysin/matrix metalloproteinase-7 (MMP7) cleavage of perlecan/HSPG2 creates a molecular switch to alter prostate cancer cell behavior. *Matrix Biol*; Epub ahead of print
- Guinea-Viniegra J, Zenz R, Scheuch H, Hnisz D, Holcman M, Bakiri L, Schonhaler HB, Sibilina M, Wagner EF (2009)** TNFalpha shedding and epidermal inflammation are controlled by Jun proteins. *Genes Dev*; 23(22):2663-74.
- Guo J, He L, Yuan P, Wang P, Lu Y, Tong F, Wang Y, Yin Y, Tian J, Sun J (2012)** ADAM10 overexpression in human non-small cell lung cancer correlates with cell migration and invasion through the activation of the Notch1 signaling pathway. *col Rep*; 28(5):1709-18.
- Guo L, Eisenman JR, Mahimkar RM, Peschon JJ, Paxton RJ, Black RA, Johnson RS (2002)** A proteomic approach for the identification of cell-surface proteins shed by metalloproteases. *Mol Cell Proteomics*; 1(1):30-6.
- Hagner-McWhirter A, Winkvist M, Bourin S, Marouga R (2008)** Selective labelling of cell-surface proteins using CyDye DIGE Fluor minimal dyes. *J Vis Exp*; (21).
- Hahn D, Pischitzis A, Roesmann S, Hansen MK, Leuenberger B, Luginbuehl U, Sterchi EE (2003)** Phorbol 12-myristate 13-acetate-induced ectodomain shedding and phosphorylation of the human meprinbeta metalloprotease. *J Biol Chem*; 278(44):42829-39.
- Hansen HP, Dietrich S, Kisseleva T, Mokros T, Mentlein R, Lange HH, Murphy G, Lemke H (2000)** CD30 shedding from Karpas 299 lymphoma cells is mediated by TNF-alpha-converting enzyme. *J Immunol*; 165(12):6703-9.

- Hansen HP**, Recke A, Reineke U, Von Tresckow B, Borchmann P, Von Strandmann EP, Lange H, Lemke H, Engert A (2004) The ectodomain shedding of CD30 is specifically regulated by peptide motifs in its cysteine-rich domains 2 and 5. *FASEB J*; 18(7):893-5.
- Harteringer J**, Stenius K, Högemann D, Jahn R (1996) 16-BAC/SDS-PAGE: a two-dimensional gel electrophoresis system suitable for the separation of integral membrane proteins. *Anal Biochem*; 240(1):126-33.
- He HT**, Barbet J, Chaix JC, Goridis C (1986) Phosphatidylinositol is involved in the membrane attachment of NCAM-120, the smallest component of the neural cell adhesion molecule. *EMBO J*, 2489–2494.
- Hehlgans T and Pfeffer K (2005)** The intriguing biology of the tumour necrosis factor/tumour necrosis factor receptor superfamily: players, rules and the games. *Immunology*; 115(1):1-20.
- Hermey G**, Sjøgaard SS, Petersen CM, Nykjaer A, Gliemann J (2006) Tumour necrosis factor alpha-converting enzyme mediates ectodomain shedding of Vps10p-domain receptor family members. *Biochem J*; 395(2):285-93.
- Hoettecke N**, Ludwig A, Foro S, Schmidt B (2010) Improved synthesis of ADAM10 inhibitor GI254023X. *Neurodegener Dis*; 7(4):232-8.
- Holmbeck K**, Bianco P, Caterina J, Yamada S, Kromer M, Kuznetsov SA, Mankani M, Robey PG, Poole AR, Pidoux I, Ward JM, Birkedal-Hansen H (1999) MT1-MMP-deficient mice develop dwarfism, osteopenia, arthritis, and connective tissue disease due to inadequate collagen turnover. *Cell*; 99:81–92
- Hooper NM (1994)** Families of zinc metalloproteases. *FEBS Lett*; 354(1):1-6.
- Hopkins DR**, Keles S, Greenspan DS (2007) The bone morphogenetic protein 1/Tolloid-like metalloproteinases. *Matrix Biol*; 26(7):508–523.
- Horiuchi K**, Kimura T, Miyamoto T, Takaishi H, Okada Y, Toyama Y, Blobel CP (2007) Cutting edge: TNF-alpha-converting enzyme (TACE/ADAM17) inactivation in mouse myeloid cells prevents lethality from endotoxin shock. *J Immunol*; 179(5):2686-9.
- Horiuchi K**, Morioka H, Takaishi H, Akiyama H, Blobel CP, Toyama Y (2009) Ectodomain shedding of FLT3 ligand is mediated by TNF-alpha converting enzyme. *J Immunol*; 182(12):7408-14.
- Hulmes DJ (2002)** Building collagen molecules, fibrils, and suprafibrillar structures. *J Struct Biol*; 137(1-2):2–10.
- Hulmes DJ (2008)** Collagen diversity, synthesis and assembly. *Collagen: Structure and Mechanics*, ed Fratzl P (Springer, New York), pp 15–74.
- Huxley-Jones J**, Clarke TK, Beck C, Toubaris G, Robertson DL, Boot-Handford RP (2007) The evolution of the vertebrate metzincins; insights from *Ciona intestinalis* and *Danio rerio*. *BMC Evol Biol*; 7:63.
- Hwang IK**, Park SM, Kim SY, Lee ST (2004) A proteomic approach to identify substrates of matrix metalloproteinase-14 in human plasma. *Biochim Biophys Acta*; 1702:79–87.
- Iba K**, Albrechtsen R, Gilpin BJ, Loechel F, Wewer UM (1999) Cysteine-rich domain of human ADAM 12 (meltrin alpha) supports tumor cell adhesion. *Am J Pathol*; 154(5):1489-501.
- Ida-Yonemochi H (2013)** Role of perlecan, a basement membrane-type heparan sulfate proteoglycan, in enamel organ morphogenesis. *J Oral Biosc*; 55(1):23–28.
- Izzo RV (1998)** Matrix proteoglycans: from molecular design to cellular function. *Annu Rev Biochem*; (67) 609 – 652
- Izzo RV and San Antonio JD (2001)** Heparan sulfate proteoglycans: heavy hitters in the angiogenesis arena. *J Clin Invest*; (108) 349–355
- Jacobsen KT**, Adlerz L, Multhaup G, Iverfeldt K (2010) Insulin-like growth factor-1 (IGF-1)-induced processing of amyloid-beta precursor protein (APP) and APP-like protein 2 is mediated by different metalloproteinases. *J Biol Chem*; 285(14):10223-31.
- Janes PW**, Saha N, Barton WA, Kolev MV, Wimmer-Kleikamp SH, Nievergall E, Blobel CP, Himanen JP, Lackmann M, Nikolov DB (2005) Adam meets Eph: an ADAM substrate recognition module acts as a molecular switch for ephrin cleavage in trans. *Cell*; 123(2):291-304.

- Janicki JS (1995)** Collagen degradation in the heart. In: Eghbali-Webb M, editor. *Molecular biology of collagen matrix in the heart*. Austin: Landes; 1995. pp. 61–76.
- Jefferson T, Auf dem Keller U, Bellac C, Metz VV, Broder C, Hedrich J, Ohler A, Maier W, Magdolen V, Sterchi E, Bond JS, Jayakumar A, Traupe H, Chalaris A, Rose-John S, Pietrzik CU, Postina R, Overall CM, Becker-Pauly C (2012)** The substrate degradome of meprin metalloproteases reveals an unexpected proteolytic link between meprin β and ADAM10. *Cell Mol Life Sci*; 70(2):309-33.
- Jones ARC, Gleghorn JP, Hughes CE, Fitz LJ, Zollner R, Wainwright SD (2007)** Binding and localization of recombinant lubricin to articular cartilage surfaces. *J Orthop Res*; 25(3):283e92.
- Kadler KE, Holmes DF, Graham H, Starborg T (2000)** Tip-mediated fusion involving unipolar collagen fibrils accounts for rapid fibril elongation, the occurrence of fibrillar branched networks in skin and the paucity of collagen fibril ends in vertebrates. *Matrix Biol*; 19(4):359–365.
- Kalus I, Bormann U, Mzoughi M, Schachner M, Kleene R (2006)** Proteolytic cleavage of the neural cell adhesion molecule by ADAM17/TACE is involved in neurite outgrowth. *J Neurochem*; 98(1):78-88.
- Kalus L, Bormann U, Mzoughi M, Schachner M, Kleene R (2006)** Proteolytic cleavage of the neural cell adhesion molecule by ADAM17/TACE is involved in neurite outgrowth. *J Neurochem*; 98, 78–88.
- Kassiri Z, Oudit GY, Kandalam V, Awad A, Wang X, Ziou X, Maeda N, Herzenberg AM, Scholey JW (2009)** Loss of TIMP3 enhances interstitial nephritis and fibrosis. *J Am Soc Nephrol*; 20(6):1223-35.
- Kawaguchi M, Mitsuhashi Y, Kondo S (2005)** Overexpression of tumour necrosis factor-alpha-converting enzyme in psoriasis. *Br J Dermatol*; 152(5):915-9.
- Kenny PA and Bissell MJ (2007)** Targeting TACE-dependent EGFR ligand shedding in breast cancer. *J Clin Invest*; 117(2):337-45.
- Khawam K, Giron-Michel J, Gu Y, Perier A, Giuliani M, Caignard A, Devocelle A, Ferrini S, Fabbi M, Charpentier B, Ludwig A, Chouaib S, Azzarone B, Eid P (2009)** Human renal cancer cells express a novel membrane-bound interleukin-15 that induces, in response to the soluble interleukin-15 receptor alpha chain, epithelial-to-mesenchymal transition. *Cancer Res*; 69(4):1561-9.
- Kishimoto TK, Kahn J, Migaki G, Mainolfi E, Shirley F, Ingraham R, Rothlein R (1995)** Regulation of L-selectin expression by membrane proximal proteolysis. *Agents Actions Suppl*; 47:121-34.
- Kleifeld O, Doucet A, Auf dem Keller U, Schilling O, Kainthan RK, Foster L, Kizhakkedathu J, Overall CM (2009)** System-Wide Proteomic Identification of Protease Cleavage Products by Terminal Amine Isotopic Labeling of Substrates. *Protocol Exchange*
- Knäuper V, Reinke H, Tschesche H (1990)** Inactivation of human plasma α 1-proteinase inhibitor by human PMN leucocyte collagenase. *FEBS Lett*; 263: 355–357.
- Koenen RR, Pruessmeyer J, Soehnlein O, Fraemohs L, Zerneck A, Schwarz N, Reiss K, Sarabi A, Lindbom L, Hackeng TM, Weber C, Ludwig A (2009)** Regulated release and functional modulation of junctional adhesion molecule A by disintegrin metalloproteinases. *Blood*; 113(19):4799-809.
- Koenen RR, Pruessmeyer J, Soehnlein O, Fraemohs L, Zerneck A, Schwarz N, Reiss K, Sarabi A, Lindbom L, Hackeng TM, Weber C, Ludwig A (2009)** Regulated release and functional modulation of junctional adhesion molecule A by disintegrin metalloproteinases. *Blood*; 113(19):4799-809.
- Krüger A (2009)** Functional genetic mouse models: promising tools for investigation of the proteolytic internet. *Biol Chem*; 390: 91–97.
- Kumar S and Weaver VM (2009)** Mechanics, malignancy, and metastasis: the force journey of a tumor cell. *Cancer Metastasis Rev*; 28(1-2):113-27.
- Kummer MP, Maruyama H, Huelsmann C, Baches S, Weggen S, Koo EH (2009)** Formation of Pmel17 amyloid is regulated by juxtamembrane metalloproteinase cleavage, and the resulting C-terminal fragment is a substrate for gamma-secretase. *J Biol Chem*; 284(4):2296-306.

- Lambert DW**, Yarski M, Warner FJ, Thornhill P, Parkin ET, Smith AI, Hooper NM, Turner AJ (2005) Tumor necrosis factor-alpha convertase (ADAM17) mediates regulated ectodomain shedding of the severe-acute respiratory syndrome-coronavirus (SARS-CoV) receptor, angiotensin-converting enzyme-2 (ACE2). *J Biol Chem*; 280(34):30113-9.
- Lawrence MB**, Bainton DF, Springer TA (1994) Neutrophil tethering to and rolling on E-selectin are separable by requirement for L-selectin. *Immunity*; 1(2):137-45.
- Le Gall SM**, Bobé P, Reiss K, Horiuchi K, Niu XD, Lundell D, Gibb DR, Conrad D, Saftig P, Blobel CP (2009) ADAMs 10 and 17 represent differentially regulated components of a general shedding machinery for membrane proteins such as transforming growth factor alpha, L-selectin, and tumor necrosis factor alpha. *Mol Biol Cell*; 20(6):1785-94.
- Le Gall SM**, Maretzky T, Issuree PD, Niu XD, Reiss K, Saftig P, Khokha R, Lundell D, Blobel CP (2010) ADAM17 is regulated by a rapid and reversible mechanism that controls access to its catalytic site. *J Cell Sci*; 123(Pt 22):3913-22.
- Lee Y**, Block G, Chen H, Folch-Puy E, Foronjy R, Jalili R, Jendresen CB, Kimura M, Kraft E, Lindemose S, Lu J, McLain T, Nutt L, Ramon-Garcia S, Smith J, Spivak A, Wang ML, Zanic M, Lin S (2008) One-step isolation of plasma membrane proteins using magnetic beads with immobilized concanavalin A. *Protein Expr Purif*; 62(2): 223–229.
- Leksa V**, Loewe R, Binder B, Schiller HB, Eckerstorfer P, Forster F, Soler-Cardona A, Ondrovicová G, Kutejová E, Steinhuber E, Breuss J, Drach J, Petzelbauer P, Binder BR, Stockinger H (2011) Soluble M6P/IGF2R released by TACE controls angiogenesis via blocking plasminogen activation. *Circ Res*; 108(6):676-85.
- Leonard JD**, Lin F, Milla ME (2005) Chaperone-like properties of the prodomain of TNFalpha-converting enzyme (TACE) and the functional role of its cysteine switch. *Biochem J*; 387(Pt 3):797-805.
- Levental I**, Grzybek M, Simons K (2011) Raft domains of variable properties and compositions in plasma membrane vesicles. *Proc Natl Acad Sci USA*; 108(28):11411-6.
- Li N**, Wang Y, Forbes K, Vignali KM, Heale BS, Saftig P, Hartmann D, Black RA, Rossi JJ, Blobel CP, Dempsey PJ, Workman CJ, Vignali DA (2007) Metalloproteases regulate T-cell proliferation and effector function via LAG-3. *EMBO J*; 26(2):494-504.
- Li X**, Yan Y, Huang W, Yang Y (2009) The study of the inhibition of the recombinant TACE prodomain to endotoxemia in mice. *Int J Mol Sci*; 10(12):5442-54.
- Li Z**, Yasuda Y, Li W, Bogoyo M, Katz N (2004) Regulation of collagenase activities of human cathepsins by glycosaminoglycans. *J Biol Chem*; 279: 5470– 5479.
- Lichtenthaler SF (2012)** Cell biology. Sheddase gets guidance. *Science*; 335(6065):179-80.
- Lincz LF (1998)** Deciphering the apoptotic pathway: all roads lead to death. *Immunol Cell Biol*; 76: 1–19.
- Liu Q**, Zhang J, Tran H, Verbeek MM, Reiss K, Estus S, Bu G (2009) LRP1 shedding in human brain: roles of ADAM10 and ADAM17. *Mol Neurodegener*; 4:17.
- López B**, González A, Díez J (2010) Circulating biomarkers of collagen metabolism in cardiac diseases. *Circulation*; 121(14):1645-54.
- López-Otín C and Bond JS (2008)** Proteases: multifunctional enzymes in life and disease. *J Biol Chem*; 283(45):30433-7
- López-Otín, C., Bond, J.S. (2008)** Proteases: Multifunctional Enzymes in Life and Disease. *J. Biol. Chem.*, 283(45):30433-30497
- Lorenzen I**, Trad A, Grötzinger J (2011) Multimerisation of A disintegrin and metalloprotease protein-17 (ADAM17) is mediated by its EGF-like domain. *Biochem Biophys Res Commun*; 415(2):330-6.
- Lothrop AP**, Torres MP, Fuchs SM (2013) Deciphering post-translational modification codes. *FEBS Lett*; 587(8):1247-57

- Lovejoy B**, Cleasby A, Hassell AM, Luther MA, Weigl D, McGeehan G, Lambert MH, Jordan SR (1994) Structural analysis of the catalytic domain of human fibroblast collagenase. *Ann N Y Acad Sci*; 732:375-8.
- Luche S**, Santoni V, Rabilloud T (2003) Evaluation of nonionic and zwitterionic detergents as membrane protein solubilizers in two-dimensional electrophoresis. *Proteomics*; 3:249-253.
- Lum L**, Wong BR, Josien R, Becherer JD, Erdjument-Bromage H, Schlöndorff J, Tempst P, Choi Y, Blobel CP (1999) Evidence for a role of a tumor necrosis factor-alpha (TNF-alpha)-converting enzyme-like protease in shedding of TRANCE, a TNF family member involved in osteoclastogenesis and dendritic cell survival. *J Biol Chem*; 274(19):13613-8.
- Maetzel D**, Denzel S, Mack B, Canis M, Went P, Benk M, Kieu C, Papior P, Baeuerle PA, Munz M, Gires O (2009) Nuclear signalling by tumour-associated antigen EpCAM. *Nat Cell Biol*; 11(2):162-71.
- Mahmoodi M**, Sahebjam S, Smookler D, Khokha R, Mort JS (2005) Lack of tissue inhibitor of metalloproteinases-3 results in an enhanced inflammatory response in antigen-induced arthritis. *Am J Pathol*; 166(6):1733-40.
- Malapeira J**, Esselens C, Bech-Serra JJ, Canals F, Arribas J (2010) ADAM17 (TACE) regulates TGFβ signaling through the cleavage of vasorin. *Oncogene*; 30(16):1912-22.
- Malinverno M**, Carta M, Epis R, Marcello E, Verpelli C, Cattabeni F, Sala C, Mulle C, Di Luca M, Gardoni F (2010) Synaptic localization and activity of ADAM10 regulate excitatory synapses through N-cadherin cleavage. *J Neurosci*; 30(48):16343-55.
- Mann M** (2006) Functional and quantitative proteomics using SILAC. *Nat. Rev. Mol. Cell Biol*; 7:952–958.
- Maquart FX**, Pickart L, Laurent M, Gillery P, Monboisse JC, Borel JP (1988) Stimulation of collagen synthesis in fibroblast cultures by the tripeptide-copper complex glycyl-L-histidyl-L-lysine- Cu²⁺. *FEBS Lett*; 238:343–346.
- Maretzky T**, Schulte M, Ludwig A, Rose-John S, Blobel C, Hartmann D, Altevogt P, Saftig P, Reiss K (2005) L1 is sequentially processed by two differently activated metalloproteases and presenilin/gamma-secretase and regulates neural cell adhesion, cell migration, and neurite outgrowth. *Mol Cell Biol*; 25(20):9040-53.
- Marin V**, Montero-Julian F, Grès S, Bongrand P, Farnarier C, Kaplanski G (2002) Chemotactic agents induce IL-6Ralpha shedding from polymorphonuclear cells: involvement of a metalloproteinase of the TNF-alpha-converting enzyme (TACE) type. *Eur J Immunol*; 32(10):2965-70.
- Maruhashi T**, Kii I, Saito M, Kudo A (2010) Interaction between periostin and BMP-1 promotes proteolytic activation of lysyl oxidase. *J Biol Chem*; 285(17):13294-303.
- Mast AE**, Enghild JJ, Nagase H, Suzuki K, Pizzo SV, et al. (1991) Kinetics and physiologic relevance of the inactivation of alpha 1-proteinase inhibitor, alpha 1- antichymotrypsin, and antithrombin III by matrix metalloproteinases-1 (tissue collagenase), -2 (72-kDa gelatinase/type IV collagenase), and -3 (stromelysin). *J Biol Chem*; 266: 15810–15816.
- Matthews V**, Schuster B, Schütze S, Bussmeyer I, Ludwig A, Hundhausen C, Sadowski T, Saftig P, Hartmann D, Kallen KJ, Rose-John S (2003) Cellular cholesterol depletion triggers shedding of the human interleukin-6 receptor by ADAM10 and ADAM17 (TACE). *J Biol Chem*; 278(40):38829-39.
- McGeehan GM**, Becherer JD, Bast RC Jr, Boyer CM, Champion B, Connolly KM, Conway JG, Furdon P, Karp S, Kidao S (1994) Regulation of tumour necrosis factor-alpha processing by a metalloproteinase inhibitor. *Nature*; 370(6490):558-61.
- McGowan PM**, McKiernan E, Bolster F, Ryan BM, Hill AD, McDermott EW, Evoy D, O'Higgins N, Crown J, Duffy MJ (2008) ADAM-17 predicts adverse outcome in patients with breast cancer. *Ann Oncol*; 19(6):1075-81.
- McIlwain DR**, Lang PA, Maretzky T, Hamada K, Ohishi K, Maney SK, Berger T, Murthy A, Duncan G, Xu HC, Lang KS, Häussinger D, Wakeham A, Itie-Youten A, Khokha R, Ohashi PS, Blobel CP, Mak TW (2012) iRhom2 regulation of TACE controls TNF-mediated protection against *Listeria* and responses to LPS. *Science*; 335(6065):229-32.

- Meissner F**, Scheltema RA, Mollenkopf HJ, Mann M (2013) Direct proteomic quantification of the secretome of activated immune cells. *Science*; 340(6131):475-8.
- Merlos-Suárez A**, Ruiz-Paz S, Baselga J, Arribas J (2001) Metalloprotease-dependent protransforming growth factor- α ectodomain shedding in the absence of tumor necrosis factor- α -converting enzyme. *J Biol Chem*; 276(51):48510-7.
- Millar AW**, Brown PD, Moore J, Galloway WA, Cornish AG, Lenehan TJ, Lynch KP (1998) Results of single and repeat dose studies of the oral matrix metalloproteinase inhibitor marimastat in healthy male volunteers. *Br J Clin Pharmacol*; 45(1):21-6.
- Mizuno M**, Fujisawa R, Kuboki Y (2000) Carboxyl-terminal propeptide of type I collagen (c-propeptide) modulates the action of TGF- β on MC3T3-E1 osteoblastic cells. *FEBS Letters*; 479(3):123-126
- Moali C and Hulmes DJS (2012)** Extracellular Matrix: Pathobiology and Signaling. Roles and Regulation of BMP-1/Tolloid-Like Proteinases: Collagen/Matrix Assembly, Growth Factor Activation and Beyond, ed Karamanos M (De Gruyter, Berlin).
- Moali C**, Font B, Ruggiero F, Eichenberger D, Rousselle P, François V, Oldberg A, Bruckner-Tuderman L, Hulmes DJ (2005) Substrate-specific modulation of a multisubstrate proteinase: C-terminal processing of fibrillar procollagens is the only BMP-1-dependent activity to be enhanced by PCPE-1. *J Biol Chem*; 280(25):24188–24194.
- Mohler KM**, Sleath PR, Fitzner JN, Cerretti DP, Alderson M, Kerwar SS, Torrance DS, Otten-Evans C, Greenstreet T, Weerawarna K (1994) Protection against a lethal dose of endotoxin by an inhibitor of tumour necrosis factor processing. *Nature*; 370(6486):218-20.
- Montero JC**, Yuste L, Díaz-Rodríguez E, Esparís-Ogando A, Pandiella A (2000) Differential shedding of transmembrane neuregulin isoforms by the tumor necrosis factor- α -converting enzyme. *Mol Cell Neurosci*; 16(5):631-48.
- Moon A and Drubin DG (1995)** The ADF/cofilin proteins: stimulus-responsive modulators of actin dynamics. *Mol Biol Cell*; 6: 1423–1431.
- Moriyama H**, Tsukida T, Inoue Y, Yokota K, Yoshino K, Kondo H, Miura N, Nishimura S (2004) Azasugar-based MMP/ADAM inhibitors as antipsoriatic agents. *J Med Chem*; 47(8):1930-8.
- Moriyama K**, Iida K, Yahara I (1996) Phosphorylation of Ser-3 of cofilin regulates its essential function on actin. *Genes Cells*; 1: 73–86.
- Morrison VL**, Barr TA, Brown S, Gray D (2010) TLR-mediated loss of CD62L focuses B cell traffic to the spleen during Salmonella typhimurium infection. *J Immunol*; 185(5):2737-46.
- Moss ML**, Bartsch JW (2004) Therapeutic benefits from targeting of ADAM family members. *Biochemistry*; 43(23):7227-35.
- Moss ML**, Bomar M, Liu Q, Sage H, Dempsey P, Lenhart PM, Gillispie PA, Stoeck A, Wildeboer D, Bartsch JW, Palmisano R, Zhou P (2007) The ADAM10 prodomain is a specific inhibitor of ADAM10 proteolytic activity and inhibits cellular shedding events. *J Biol Chem*; 282(49):35712-21.
- Moss ML**, Jin SL, Becherer JD, Bickett DM, Burkhart W, Chen WJ, Hassler D, Leesnitzer MT, McGeehan G, Milla M, Moyer M, Rocque W, Seaton T, Schoenen F, Warner J, Willard D (1997b) Structural features and biochemical properties of TNF- α converting enzyme (TACE). *J Neuroimmunol*; 72(2):127-9.
- Moss ML**, Jin SL, Milla ME, Bickett DM, Burkhart W, Carter HL, Chen WJ, Clay WC, Didsbury JR, Hassler D, Hoffman CR, Kost TA, Lambert MH, Leesnitzer MA, McCauley P, McGeehan G, Mitchell J, Moyer M, Pahel G, Rocque W, Overton LK, Schoenen F, Seaton T, Su JL, Becherer JD (1997a) Cloning of a disintegrin metalloproteinase that processes precursor tumour-necrosis factor- α . *Nature*; 385(6618):733-6.
- Müller-Eberhard HJ (1988)** Molecular organization and function of the complement system. *Annu Rev Biochem*; 57: 321–347.
- Murphy G (2008)** The ADAMs: signalling scissors in the tumour microenvironment. *Nat Rev Cancer*; 8(12):929-41.

- Myers MA**, McPhail LC, Snyderman R (1985) Redistribution of protein kinase C activity in human monocytes: correlation with activation of the respiratory burst. *J Immunol*; 135(5):3411-6.
- Myhre GM**, Toruner M, Abraham S, Egan LJ (2004) Metalloprotease disintegrin-mediated ectodomain shedding of EGFR ligands promotes intestinal epithelial restitution. *Am J Physiol Gastrointest Liver Physiol*; 287(6):1213-9.
- Naba A**, Clauser KR, Hoersch S, Liu H, Carr SA, Hynes RO (2012) The matrisome: in silico definition and in vivo characterization by proteomics of normal and tumor extracellular matrices. *Mol Cell Proteomics*; 11(4)
- Nakamura T**, Abe H, Hirata A, Shimoda C (2004) ADAM family protein Mde10 is essential for development of spore envelopes in the fission yeast *Schizosaccharomyces pombe*. *Eukaryot Cell*; 3(1):27-39.
- Nakayama H**, Fukuda S, Inoue H, Nishida-Fukuda H, Shirakata Y, Hashimoto K, Higashiyama S (2012) Cell surface annexins regulate ADAM-mediated ectodomain shedding of proamphiregulin. *Mol Biol Cell*; 23(10):1964-75.
- Nelson KK**, Schlöndorff J, Blobel CP (1999) Evidence for an interaction of the metalloprotease-disintegrin tumour necrosis factor alpha convertase (TACE) with mitotic arrest deficient 2 (MAD2), and of the metalloprotease-disintegrin MDC9 with a novel MAD2-related protein, MAD2beta. *Biochem J*; 343 Pt 3:673-80.
- Nemo R**, Murcia N, Dell KM (2005) Transforming growth factor alpha (TGF-alpha) and other targets of tumor necrosis factor-alpha converting enzyme (TACE) in murine polycystic kidney disease. *Pediatr Res*; 57(5 Pt 1):732-7.
- Niehage C**, Steenblock C, Pursche T, Bornhäuser M, Corbeil D, Hoflack B (2011) The cell surface proteome of human mesenchymal stromal cells. *PLoS One*; 6(5):e20399.
- Numomura K**, Nagano K, Itagaki C, Taoka M, Okamura N, Yamauchi Y, Sugano S, Takahashi N, Izumi T, Isobe T (2005) Cell surface labeling and mass spectrometry reveal diversity of cell surface markers and signaling molecules expressed in undifferentiated mouse embryonic stem cells. *Mol Cell Proteomics*; 4(12):1968-76.
- Ohta S**, Harigai M, Tanaka M, Kawaguchi Y, Sugiura T, Takagi K, Fukasawa C, Hara M, Kamatani N (2001) Tumor necrosis factor-alpha (TNF-alpha) converting enzyme contributes to production of TNF-alpha in synovial tissues from patients with rheumatoid arthritis. *J Rheumatol*; 28(8):1756-63.
- Ozawa M and Kemler R** (1990) Correct proteolytic cleavage is required for the cell adhesive function of uvomorulin. *J Cell Biol*; 111; 1645-1650
- Parr-Sturgess CA**, Rushton DJ, Parkin ET (2010) Ectodomain shedding of the Notch ligand Jagged1 is mediated by ADAM17, but is not a lipid-raft-associated event. *Biochem J*; 432(2):283-94.
- Patel IR**, Attur MG, Patel RN, Stuchin SA, Abagyan RA, Abramson SB, Amin AR (1998) TNF-alpha convertase enzyme from human arthritis-affected cartilage: isolation of cDNA by differential display, expression of the active enzyme, and regulation of TNF-alpha. *J Immunol*; 160(9):4570-9.
- Patton WF** (2002) Detection technologies in proteome analysis. *Journal of Chromatography B-Analytical Technologies in the Biomedical and Life Sciences*, 771:3-31.
- Peiretti F**, Canault M, Deprez-Beauclair P, Berthet V, Bonardo B, Juhan-Vague I, Nalbone G (2003a) Intracellular maturation and transport of tumor necrosis factor alpha converting enzyme. *Exp Cell Res*; 285(2):278-85.
- Peiretti F**, Deprez-Beauclair P, Bonardo B, Aubert H, Juhan-Vague I, Nalbone G (2003b) Identification of SAP97 as an intracellular binding partner of TACE. *J Cell Sci*; 116(Pt 10):1949-57.
- Peng M**, Guo S, Yin N, Xue J, Shen L, Zhao Q, Zhang W (2010) Ectodomain shedding of Fcalpha receptor is mediated by ADAM10 and ADAM17. *Immunology*; 130(1):83-91.
- Peschon JJ**, Slack JL, Reddy P, Stocking KL, Sunnarborg SW, Lee DC, Russell WE, Castner BJ, Johnson RS, Fitzner JN, Boyce RW, Nelson N, Kozlosky CJ, Wolfson MF, Rauch CT, Cerretti DP, Paxton RJ, March CJ, Black RA (1998) An essential role for ectodomain shedding in mammalian development. *Science*; 282(5392):1281-4.
- Philipp S**, Jakoby T, Tholey A, Janssen O, Leippe M, Gelhaus C (2012) Cationic detergents enable the separation of membrane proteins of *Plasmodium falciparum* infected erythrocytes by 2D gel electrophoresis. *Electrophoresis*; 33(7):1120-8.

- Plumb J**, McQuaid S, Cross AK, Surr J, Haddock G, Bunning RA, Woodroffe MN (2006) Upregulation of ADAM-17 expression in active lesions in multiple sclerosis. *Mult Scler*; 12(4):375-85.
- Poth AG**, Deeth HC, Alewood PF, Holland JW (2008) Analysis of the Human Casein Phosphoproteome by 2-D Electrophoresis and MALDI-TOF/TOF MS Reveals New Phosphoforms. *Journal of Proteome Research*; 7:5017-5027.
- Prudova A**, auf dem Keller U, Butler GS, Overall CM (2010) Multiplex N-terminome analysis of MMP-2 and MMP-9 substrate degradomes by iTRAQ-TAILS quantitative proteomics. *Mol Cell Proteomics*;9(5):894-911.
- Prudova A**, Keller U auf dem, Butler GS, Overall CM (2010) Multiplex N- terminome analysis of MMP-2 and MMP-9 substrate degradomes by iTRAQ- TAILS quantitative proteomics. *Mol Cell Proteomics*; 9: 894–911.
- Pruessmeyer J**, Ludwig A (2009) The good, the bad and the ugly substrates for ADAM10 and ADAM17 in brain pathology, inflammation and cancer. *Semin Cell Dev Biol*; 20(2):164-74.
- Pruessmeyer J**, Martin C, Hess FM, Schwarz N, Schmidt S, Kogel T, Hoettecke N, Schmidt B, Sechi A, Uhlig S, Ludwig A (2010) A disintegrin and metalloproteinase 17 (ADAM17) mediates inflammation-induced shedding of syndecan-1 and -4 by lung epithelial cells. *J Biol Chem*; 285(1):555-64.
- Puente XS**, Sánchez LM, Overall CM, López-Otín C (2003) Human and mouse proteases: a comparative genomic approach. *Nat Rev Genet*. 2003 Jul;4(7):544-58.
- Qu D**, Wang Y, Esmon NL, Esmon CT (2007) Regulated endothelial protein C receptor shedding is mediated by tumor necrosis factor-alpha converting enzyme/ADAM17. *Thromb Haemost*; 5(2):395-402.
- Rabie T**, Strehl A, Ludwig A, Nieswandt B (2005) Evidence for a role of ADAM17 (TACE) in the regulation of platelet glycoprotein V. *J Biol Chem*; 280(15):14462-8.
- Rawlings ND**, Barret AJ, Woessner JF (2004) Introduction: metallopeptidases and their clans. *Handbook of Proteolytic Enzymes, Academic Press, 2nd Edition*, pp. 231-268
- Reddy P**, Slack JL, Davis R, Cerretti DP, Kozlosky CJ, Blanton RA, Shows D, Peschon JJ, Black RA (2000) Functional analysis of the domain structure of tumor necrosis factor-alpha converting enzyme. *J Biol Chem*; 275(19):14608-14.
- Reiss K**, Maretzky T, Ludwig A, Tousseyn T, de Strooper B, Hartmann D, Saftig P (2005) ADAM10 cleavage of N-cadherin and regulation of cell-cell adhesion and beta-catenin nuclear signalling. *EMBO J*; 24(4):742-52.
- Rhee DK**, Marcelino J, Al-Mayouf S, Schelling DK, Bartels CF, Cui Y, Laxer R, Goldbach-Mansky R, Warman ML (2005) Consequences of disease-causing mutations on lubricin protein synthesis, secretion, and post-translational processing. *J Biol Chem*; 280(35):31325-32.
- Richards FM**, Tape CJ, Jodrell DI, Murphy G (2012) Anti-tumour effects of a specific anti-ADAM17 antibody in an ovarian cancer model in vivo. *PLoS One*; 7(7):e40597.
- Rio C**, Buxbaum JD, Peschon JJ, Corfas G (2000) Tumor necrosis factor-alpha-converting enzyme is required for cleavage of erbB4/HER4. *Biol Chem*; 275(14):10379-87.
- Rivera S**, Khrestchatskiy M, Kaczmarek L, Rosenberg GA, Jaworski DM (2010) Metzincin proteases and their inhibitors: foes or friends in nervous system physiology? *J Neurosci*; 30(46):15337-57
- Roghani M**, Becherer JD, Moss ML, Atherton RE, Erdjument-Bromage H, Arribas J, Blackburn RK, Weskamp G, Tempst P, Blobel CP (1999) Metalloprotease-disintegrin MDC9: intracellular maturation and catalytic activity. *J Biol Chem*. 1999 Feb 5;274(6):3531-40.
- Roshy S**, Sloane BF, Moin K (2003) Pericellular cathepsin B and malignant progression. *Cancer Metastasis Rev*; 22(2-3):271-86.
- Ross PL**, Huang YN, Marchese JN, Williamson B, Parker K, Hattan S, Khainovski N, Pillai S, Dey S, Daniels S, Purkayastha S, Juhasz P, Martin S, Bartlet-Jones M, He F, Jacobson A and Pappin DJ (2004) Multiplexed protein quantitation in *Saccharomyces cerevisiae* using amine-reactive isobaric tagging reagents. *Mol. Cell. Proteomics*; 3:1154–1169.

- Rössler U**, Thomassen E, Hültner L, Baier S, Danescu J, Werenskiold AK (1995) Secreted and membrane-bound isoforms of T1, an orphan receptor related to IL-1-binding proteins, are differently expressed in vivo. *Dev Biol*; 168(1):86-97.
- Rovida E**, Paccagnini A, Del Rosso M, Peschon J, Dello Sbarba P (2001) TNF-alpha-converting enzyme cleaves the macrophage colony-stimulating factor receptor in macrophages undergoing activation. *J Immunol*; 166(3):1583-9.
- Ruhe JE**, Streit S, Hart S, Ullrich A (2006) EGFR signaling leads to downregulation of PTP-LAR via TACE-mediated proteolytic processing. *Cell Signal*; 18(9):1515-27.
- Rundhaug JE** (2006) Matrix metalloproteinases and angiogenesis. *Cell Mol Med*; 9(2):267-85.
- Sadoul K**, Meyer A, Low MG, Schachner M (1986) Release of the 120 kDa component of the mouse neural cell adhesion molecule N-CAM from cell surfaces by phosphatidylinositol-specific phospholipase C. *Neurosci Lett*, (72) 341-346.
- Sahebjam S**, Khokha R, Mort JS (2007) Increased collagen and aggrecan degradation with age in the joints of Timp3(-/-) mice. *Arthritis Rheum*; 56(3):905-9.
- Sahin U and Blobel CP** (2007) Ectodomain shedding of the EGF-receptor ligand epigen is mediated by ADAM17. *FEBS Lett*; 581(1):41-4.
- Sahin U**, Weskamp G, Kelly K, Zhou HM, Higashiyama S, Peschon J, Hartmann D, Saftig P, Blobel CP (2004) Distinct roles for ADAM10 and ADAM17 in ectodomain shedding of six EGFR ligands. *J Cell Bio*; 164(5):769-79.
- Santiago-Josefat B**, Esselens C, Bech-Serra JJ, Arribas J (2007) Post-transcriptional up-regulation of ADAM17 upon epidermal growth factor receptor activation and in breast tumors. *J Biol Chem*; 282(11):8325-31.
- Santoni V**, Kieffer S, Desclaux D, Masson F, Rabilloud T (2000) Membrane proteomics: Use of additive main effects with multiplicative interaction model to classify plasma membrane proteins according to their solubility and electrophoretic properties. *Electrophoresis*; 21:3329-3344.
- Sarras MP, Jr.** (1996) BMP-1 and the astacin family of metalloproteinases: A potential link between the extracellular matrix, growth factors and pattern formation. *Bio-essays*; 18(6):439-442.
- Schlöndorff J**, Becherer JD, Blobel CP (2000) Intracellular maturation and localization of the tumour necrosis factor alpha convertase (TACE). *Biochem J*; 347 Pt 1:131-8.
- Schroeter EH**, Kisslinger JA, Kopan R (1998) Notch-1 signalling requires ligand-induced proteolytic release of intracellular domain. *Nature*; 393(6683):382-6.
- Schwarz J**, Schmidt S, Will O, Koudelka T, Köhler K, Boss M, Rabe B, Tholey A, Scheller J, Schmidt-Arras D, Schwake M, Rose-John S, Chalaris A (2013) Polo-like kinase 2, a novel ADAM17 signaling component, regulates tumor necrosis factor α ectodomain shedding. *J Biol Chem*; 289(5):3080-93.
- Seals DF and Courtneidge SA** (2003) The ADAMs family of metalloproteases: multidomain proteins with multiple functions. *Genes Dev*; 17(1):7-30.
- Seifert T**, Kieseier BC, Ropele S, Strasser-Fuchs S, Quehenberger F, Fazekas F, Hartung HP (2002) TACE mRNA expression in peripheral mononuclear cells precedes new lesions on MRI in multiple sclerosis. *Mult Scler*; 8(6):447-51.
- Sezgin E**, Kaiser HJ, Baumgart T, Schwille P, Simons K, Levental I (2012) Elucidating membrane structure and protein behavior using giant plasma membrane vesicles. *Nat Protoc*; 7(6):1042-51.
- Shiio Y and Aebersold R** (2006) Quantitative proteome analysis using isotope-coded affinity tags and mass spectrometry. *Nat Protoc*; 1:139-145.
- Sim RB and Laich A** (2000) Innate Immunity. Serine proteases of the complement system. *Biochem Soc Trans*; 28: 545.
- Siméon A**, Emonard H, Hornebeck W, Maquart FX (2000) The tripeptide-copper complex glycyl-L-histidyl-L-lysine-Cu²⁺ stimulates matrix metalloproteinase-2 expression by fibroblast cultures. *Life Sci*; 67:2257-2265.

- Smith KM**, Gaultier A, Cousin H, Alfandari D, White JM, DeSimone DW (2002) The cysteine-rich domain regulates ADAM protease function in vivo. *J Cell Biol*; 159(5):893-902.
- Smookler DS**, Mohammed FF, Kassiri Z, Duncan GS, Mak TW, Khokha R (2006) Tissue inhibitor of metalloproteinase 3 regulates TNF-dependent systemic inflammation. *Immunol*; 176(2):721-5.
- Snel B**, Lehmann G, Bork P, Huynen MA (2000) STRING: a web-server to retrieve and display the repeatedly occurring neighbourhood of a gene. *Nucleic Acids Res*; 28(18):3442-4.
- Soond SM**, Everson B, Riches DW, Murphy G (2005) ERK-mediated phosphorylation of Thr735 in TNF α -converting enzyme and its potential role in TACE protein trafficking. *J Cell Sci*; 118(Pt 11):2371-80.
- Sounni NE and Noel A (2005)** Membrane type-matrix metalloproteinases and tumor progression. *Biochimie*; 87:329–342
- Springer TA** (1994) Traffic signals for lymphocyte recirculation and leukocyte emigration: the multistep paradigm. *Cell*; 76(2):301-14.
- Srouf N**, Lebel A, McMahon S, Fournier I, Fugère M, Day R, Dubois CM (2003) TACE/ADAM-17 maturation and activation of sheddase activity require proprotein convertase activity. *FEBS Lett*; 554(3):275-83.
- Stawikowska R**, Cudic M, Giulianotti M, Houghten RA, Fields GB, Minond D (2013) Activity of ADAM17 (a disintegrin and metalloprotease 17) is regulated by its noncatalytic domains and secondary structure of its substrates. *J Biol Chem*; 288(31):22871-9.
- Steinman DH**, Curtin ML, Garland RB, Davidsen SK, Heyman HR, Holms JH, Albert DH, Magoc TJ, Nagy IB, Marcotte PA, Li J, Morgan DW, Hutchins C, Summers JB (1998) The design, synthesis, and structure-activity relationships of a series of macrocyclic MMP inhibitors. *Bioorg Med Chem Lett*; 8(16):2087-92.
- Sterchi EE. (2008)** Special issue: metzincin metalloproteinases. *Mol Aspects Med*; 29(5):255-7.
- Sterchie E.E. (2008)** Special issue: metzincin metalloproteinases. *Mol. Aspects Med.*, 29(5):255-257
- Stetler-Stevenson WG**, Brown PD, Onisto M, Levy AT, Liotta LA (1990) Tissue inhibitor of metalloproteinases-2 (TIMP-2) mRNA expression in tumor cell lines and human tumor tissues. *J Biol Chem*; 265:13933-13938.
- Stevanović M (2013)** Analysis of A Disintegrin and Metalloprotease 17 (ADAM17) in the metastatic niche of the lung. (PhD Thesis; http://eldiss.uni-kiel.de/macau/receive/dissertation_diss_00014334)
- Stöcker W**, Grams F, Baumann U, Reinemer P, Gomis-Rüth FX, McKay DB, Bode W (1995) The metzincins--topological and sequential relations between the astacins, adamalysins, serralysins, and matrixins (collagenases) define a superfamily of zinc-peptidases. *Protein Sci*; 4(5):823-40.
- Stöcker, W.**, Grams, F., Baumann, U., Reinemer, P., Gomis-Rüth, F.X. (1995) The metzincins – topological and sequential relations between the astacins, adamalysins, serralysins and matrixins (collagenases) define a superfamily of zinc-peptidases. *Protein Sci.*, 4(5):823-840
- Stöcker, W.**, Grams, F., Baumann, U., Reinemer, P., Gomis-Rüth, F.X. (1995) The metzincins – topological and sequential relations between the astacins, adamalysins, serralysins and matrixins (collagenases) define a superfamily of zinc-peptidases. *Protein Sci.*, 4(5):823-840
- Stoeck A**, Keller S, Riedle S, Sanderson MP, Runz S, Le Naour F, Gutwein P, Ludwig A, Rubinstein E, Altevogt P (2006) A role for exosomes in the constitutive and stimulus-induced ectodomain cleavage of L1 and CD44. *Biochem J*; 393(Pt 3):609-18.
- Sunnarborg SW**, Hinkle CL, Stevenson M, Russell WE, Raska CS, Peschon JJ, Castner BJ, Gerhart MJ, Paxton RJ, Black RA, Lee DC (2004) Tumor necrosis factor- α converting enzyme (TACE) regulates epidermal growth factor receptor ligand availability. *J Biol Chem*; 277(15):12838-45.
- Swendeman S**, Mendelson K, Weskamp G, Horiuchi K, Deutsch U, Scherle P, Hooper A, Rafii S, Blobel CP (2008) VEGF-A stimulates ADAM17-dependent shedding of VEGFR2 and crosstalk between VEGFR2 and ERK signaling. *Circ Res*; 103(9):916-8.

- Tellier E**, Canault M, Rebsomen L, Bonardo B, Juhan-Vague I, Nalbhone G, Peiretti F (2006) The shedding activity of ADAM17 is sequestered in lipid rafts. *Exp Cell Res*; 312(20):3969-80.
- Thathiah A**, Blobel CP, Carson DD (2003) Tumor necrosis factor-alpha converting enzyme/ADAM 17 mediates MUC1 shedding. *J Biol Chem*; 278(5):3386-94.
- Thornberry NA and Lazebnik Y (1998)** Caspases: enemies within. *Science*; 281:1312-1316. doi:10.1126/science.281.5381.1312.
- Togashi N**, Ura N, Higashiura K, Murakami H, Shimamoto K (2002) Effect of TNF-alpha--converting enzyme inhibitor on insulin resistance in fructose-fed rats. *Hypertension*; 39(2 Pt 2):578-80.
- Tsakadze NL**, Sithu SD, Sen U, English WR, Murphy G, D'Souza SE (2006) Tumor necrosis factor-alpha-converting enzyme (TACE/ADAM-17) mediates the ectodomain cleavage of intercellular adhesion molecule-1 (ICAM-1). *J Biol Chem*; 281(6):3157-64.
- Tsakadze NL**, Sithu SD, Sen U, English WR, Murphy G, D'Souza SE (2006) Tumor necrosis factor-alpha-converting enzyme (TACE/ADAM-17) mediates the ectodomain cleavage of intercellular adhesion molecule-1 (ICAM-1). *J Biol Chem*; 281(6):3157-64.
- Tsukamoto H**, Tanida S, Ozeki K, Ebi M, Mizoshita T, Shimura T, Mori Y, Kataoka H, Kamiya T, Fukuda S, Higashiyama S, Joh T. (2013) Annexin A2 regulates a disintegrin and metalloproteinase 17-mediated ectodomain shedding of pro-tumor necrosis factor- α in monocytes and colon epithelial cells. *Inflamm Bowel Dis*; 19(7):1365-73.
- Tucher J**, Linke D, Koudelka T, Cassidy L, Tredup C, Wichert R, Pietrzik C, Becker-Pauly C, Tholey A (2014) LC-MS based cleavage site profiling of the proteases ADAM10 and ADAM17 using proteome-derived peptide libraries. *J Proteome Res*; 13(4):2205-14.
- Tziakas DN**, Chalikias GK, Papanas N, Stakos DA, Chatzikyriakou SV, Maltezos E (2007) Circulating levels of collagen type I degradation marker depend on the type of atrial fibrillation. *Europace*; 9(8):589-96.
- Uría JA**, Ferrando AA, Velasco G, Freije JM, López-Otín C (1994) Structure and expression in breast tumors of human TIMP-3, a new member of the metalloproteinase inhibitor family. *Cancer Res*; 54(8):2091-4.
- Vadon-Le Goff S**, Kronenberg D, Bourhis JM, Bijakowski C, Raynal N, Ruggiero F, Farndale RW, Stöcker W, Hulmes DJ, Moali C (2011) Procollagen C-proteinase enhancer stimulates procollagen processing by binding to the C-propeptide region only. *J Biol Chem*; 286(45):38932-8.
- Vaisar T**, Kassim SY, Gomez IG, Green PS, Hargarten S, Gough PJ, Parks WC, Wilson CL, Raines EW, Heinecke KW (2009) MMP-9 sheds the β 2 integrin subunit (CD18) from macrophages. *Mol Cell Proteomics*; 8:1044-1060.
- Vincent B**, Paitel E, Saftig P, Frobert Y, Hartmann D, De Strooper B, Grassi J, Lopez-Perez E, Checler F (2001) The disintegrins ADAM10 and TACE contribute to the constitutive and phorbol ester-regulated normal cleavage of the cellular prion protein. *J Biol Chem*; 276(41):37743-6.
- Walcheck B**, Kahn J, Fisher JM, Wang BB, Fisk RS, Payan DG, Feehan C, Betageri R, Darlak K, Spatola AF, Kishimoto TK (1996) Neutrophil rolling altered by inhibition of L-selectin shedding in vitro. *Nature*; 380(6576):720-3.
- Waldhauer I**, Goehlsdorf D, Gieseke F, Weinschenk T, Wittenbrink M, Ludwig A, Stevanovic S, Rammensee HG, Steinle A (2008) Tumor-associated MICA is shed by ADAM proteases. *Cancer Res*; 68(15):6368-76.
- Wang X**, He K, Gerhart M, Huang Y, Jiang J, Paxton RJ, Yang S, Lu C, Menon RK, Black RA, Baumann G, Frank SJ (2002) Metalloprotease-mediated GH receptor proteolysis and GHBP shedding. Determination of extracellular domain stem region cleavage site. *J Biol Chem*; 277(52):50510-9.
- Wang Y**, Zhang AC, Ni Z, Herrera A, Walcheck B (2010) ADAM17 activity and other mechanisms of soluble L-selectin production during death receptor-induced leukocyte apoptosis. *J Immunol*; 184(8):4447-54.
- Wasinger VC**, Zeng M, Yau Y (2013) Current status and advances in quantitative proteomic mass spectrometry. *Int J Proteomics*; 2013:180605.

- Weskamp G**, Schlöndorff J, Lum L, Becherer JD, Kim TW, Saftig P, Hartmann D, Murphy G, Blobel CP (2004) Evidence for a critical role of the tumor necrosis factor alpha convertase (TACE) in ectodomain shedding of the p75 neurotrophin receptor (p75NTR). *Biol Chem*; 279(6):4241-9.
- White JM (2003)** ADAMs: modulators of cell-cell and cell-matrix interactions. *Curr Opin Cell Biol*; 15(5):598-606.
- Whitelock JM**, Murdoch AD, Iozzo RV, Underwood PA (1996) The degradation of human endothelial cell-derived perlecan and release of bound basic fibroblast growth factor by stromelysin, collagenase, plasmin, and heparanases. *J Biol Chem*; (271) 10079–10086.
- Wiley HS**, Woolf MF, Opresko LK, Burke PM, Will B, Morgan JR, Lauffenburger DA (1998) Removal of the membrane-anchoring domain of epidermal growth factor leads to intracrine signaling and disruption of mammary epithelial cell organization. *J Cell Biol*; 143(5):1317-28.
- Willems SH**, Tape CJ, Stanley PL, Taylor NA, Mills IG, Neal DE, McCafferty J, Murphy G (2010) Thiol isomerases negatively regulate the cellular shedding activity of ADAM17. *Biochem J*; 428(3):439-50.
- Wolfsberg TG**, Primakoff P, Myles DG, White JM (1995b) ADAM, a novel family of membrane proteins containing A Disintegrin And Metalloprotease domain: multipotential functions in cell-cell and cell-matrix interactions. *J Cell Biol*; 131(2):275-8.
- Wolfsberg TG**, Straight PD, Gerena RL, Huovila AP, Primakoff P, Myles DG, White JM (1995a) ADAM, a widely distributed and developmentally regulated gene family encoding membrane proteins with a disintegrin and metalloprotease domain. *Dev Biol*; 169(1):378-83.
- Worley JR**, Hughes DA, Dozio N, Gavrilovic J, Sampson MJ (2007) Low density lipoprotein from patients with Type 2 diabetes increases expression of monocyte matrix metalloproteinase and ADAM metalloproteinase genes. *Cardiovasc Diabetol*; 6:21.
- Xiao LJ**, Lin P, Lin F, Liu X, Qin W, Zou HF, Guo L, Liu W, Wang S, Yu XG (2012) ADAM17 targets MMP-2 and MMP-9 via EGFR-MEK-ERK pathway activation to promote prostate cancer cell invasion. *Int J Oncol*; 40, 1714–24.
- Xu P**, Derynck R (2010) Direct activation of TACE-mediated ectodomain shedding by p38 MAP kinase regulates EGF receptor-dependent cell proliferation. *Mol Cell*; 37(4):551-66.
- Yamada M**, Murakami K, Wallingford JC, Yuki Y (2002) Identification of low- abundance proteins of bovine colostrum and mature milk using two- dimensional electrophoresis followed by microsequencing and mass spectrometry. *Electrophoresis*, 23:1153-1160.
- Yamazaki K**, Mizui Y, Sagane K, Tanaka I (1998) Genetic mapping of mouse tumor necrosis factor-alpha converting enzyme (TACE) to chromosome 12. *Genomics*; 49(2):336-7.
- Yang N**, Higuchi O, Ohashi K, Nagata K, Wada A, Kangawa K, Nishida E, Mizuno K (1998) Cofilin phosphorylation by LIM-kinase 1 and its role in Rac-mediated actin reorganization. *Nature*; 393(6687):809-12.
- Yang P**, Baker KA, Hagg T (2006) The ADAMs family: coordinators of nervous system development, plasticity and repair. *Prog Neurobiol*; 79(2):73-94.
- Yokoyama R**, Iwafune Y, Kawasaki H, Hirano H (2009) Isoelectric focusing of high-molecular-weight protein complex under native conditions using agarose gel. *Analytical Biochemistry*; 387:60-63.
- Young J**, Yu X, Wolslegel K, Nguyen A, Kung C, Chiang E, Kolumam G, Wei N, Wong WL, DeForge L, Townsend MJ, Grogan JL (2010) Lymphotoxin-alpha-beta heterotrimers are cleaved by metalloproteinases and contribute to synovitis in rheumatoid arthritis. *Cytokine*; 51(1):78-86.
- Yu M**, Lam J, Rada B, Leto TL, Levine SJ (2011) Double-stranded RNA induces shedding of the 34-kDa soluble TNFR1 from human airway epithelial cells via TLR3-TRIF-RIP1-dependent signaling: roles for dual oxidase 2- and caspase-dependent pathways. *J Immunol*; 186(2):1180-8.
- Zatovicova M**, Sedlakova O, Svastova E, Ohradanova A, Ciampor F, Arribas J, Pastorek J, Pastorekova S (2005) Ectodomain shedding of the hypoxia-induced carbonic anhydrase IX is a metalloprotease-dependent process regulated by TACE/ADAM17. *Br J Cancer*; 93(11):1267-76.

Zheng Y, Schlondorff J, Blobel CP (2002) Evidence for regulation of the tumor necrosis factor alpha-converterase (TACE) by protein-tyrosine phosphatase PTPH1. *J Biol Chem*; 277(45):42463-70.

Zhou Z, Wang J, Cao R, Morita H, Soininen R, Chan KM, Liu B, Cao Y, and Tryggvason K (2004) Impaired angiogenesis, delayed wound healing and retarded tumor growth in perlecan heparan sulfate-deficient mice. *Cancer Res*; (64) 4699–4702.

Zhu L, Bergmeier W, Wu J, Jiang H, Stalker TJ, Cieslak M, Fan R, Boumsell L, Kumanogoh A, Kikutani H, Tamagnone L, Wagner DD, Milla ME, Brass LF (2007) Regulated surface expression and shedding support a dual role for semaphorin 4D in platelet responses to vascular injury. *Proc Natl Acad Sci USA*; 104(5):1621-6.

10 Addendum

This section summarizes all images of performed 2D-DiGE analyses, presented in this thesis. In addition, all protein spots that were selected for protein identification are indicated. Please note that corresponding protein information including protein fold-change values and MALDI-ToF/ToF-derived protein data can be found on the enclosed compact disk.

10.1 DIGE145 – Supernatant analysis

2D-DiGE analysis of wild-type (MEF 1#3) and ADAM17^{ex/ex} (MEF1#1) MEF cell supernatants enriched by centrifugal filter units.

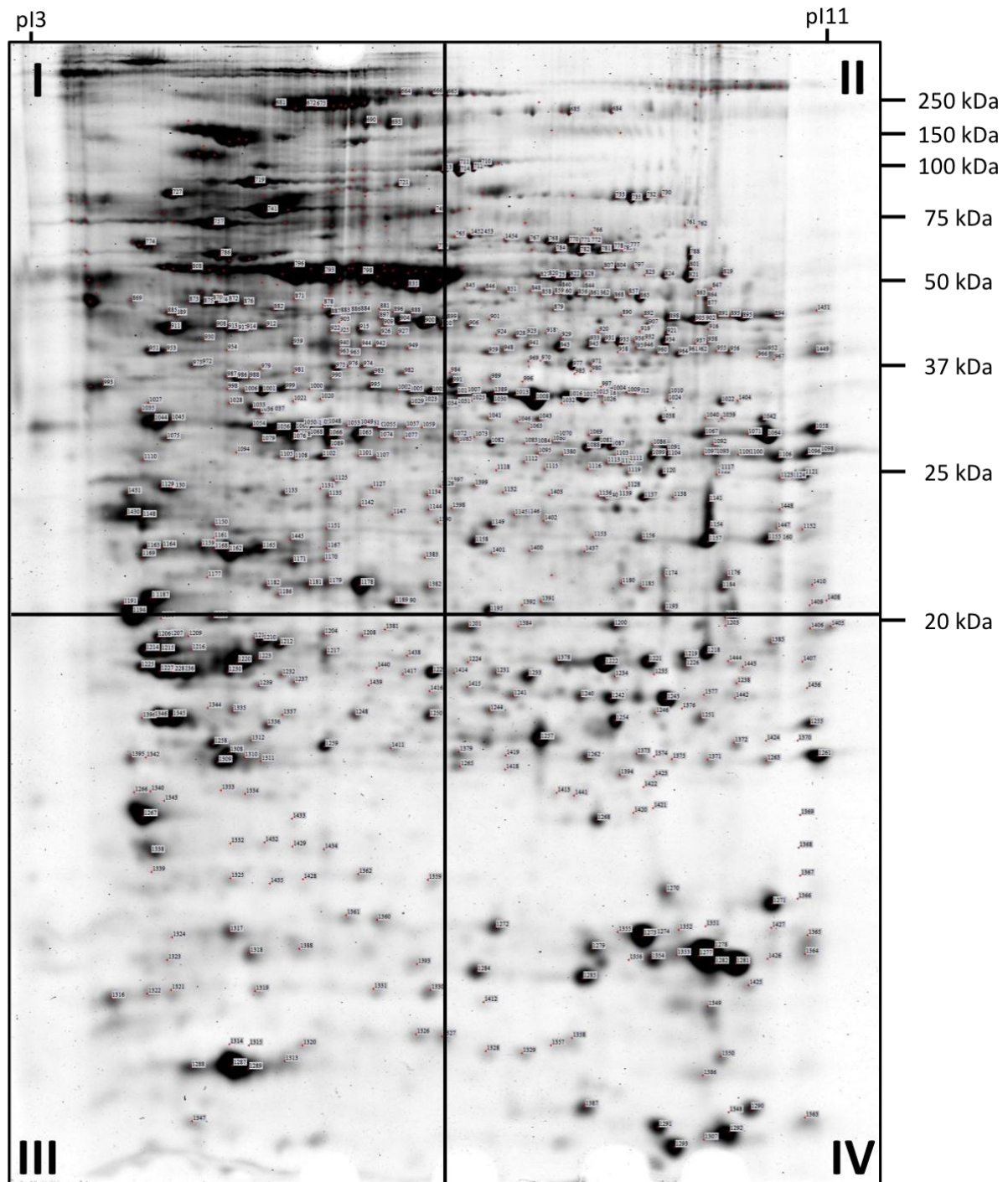


Fig. 10.1: Supernatant analysis DIGE145. Cell culture supernatant proteins of wild-type (MEF 1#3) and ADAM17^{ex/ex} (MEF 1#1) MEF cells were enriched by centrifugal filter units, differentially labelled and separated by 2D-DiGE. Two-dimensional gel was post-stained with Flamingo™ and imaged using the TyphoonTRIO. Numbers indicate protein spots picked for protein identification by MALDI-ToF/ToF. Corresponding data are enclosed on the compact disc (File: A10.1 – DIGE145).

10.2 DIGE150 – Supernatant analysis

Two independent 2D-DiGE analysis of TNF α -overexpressing wild-type (MEF 1#3^{TNF α}) and ADAM17^{ex/ex} (MEF1#1^{TNF α}) MEF cell supernatants enriched by centrifugal filter units.

10.2.1 Gel 12595 (DIGE150a)

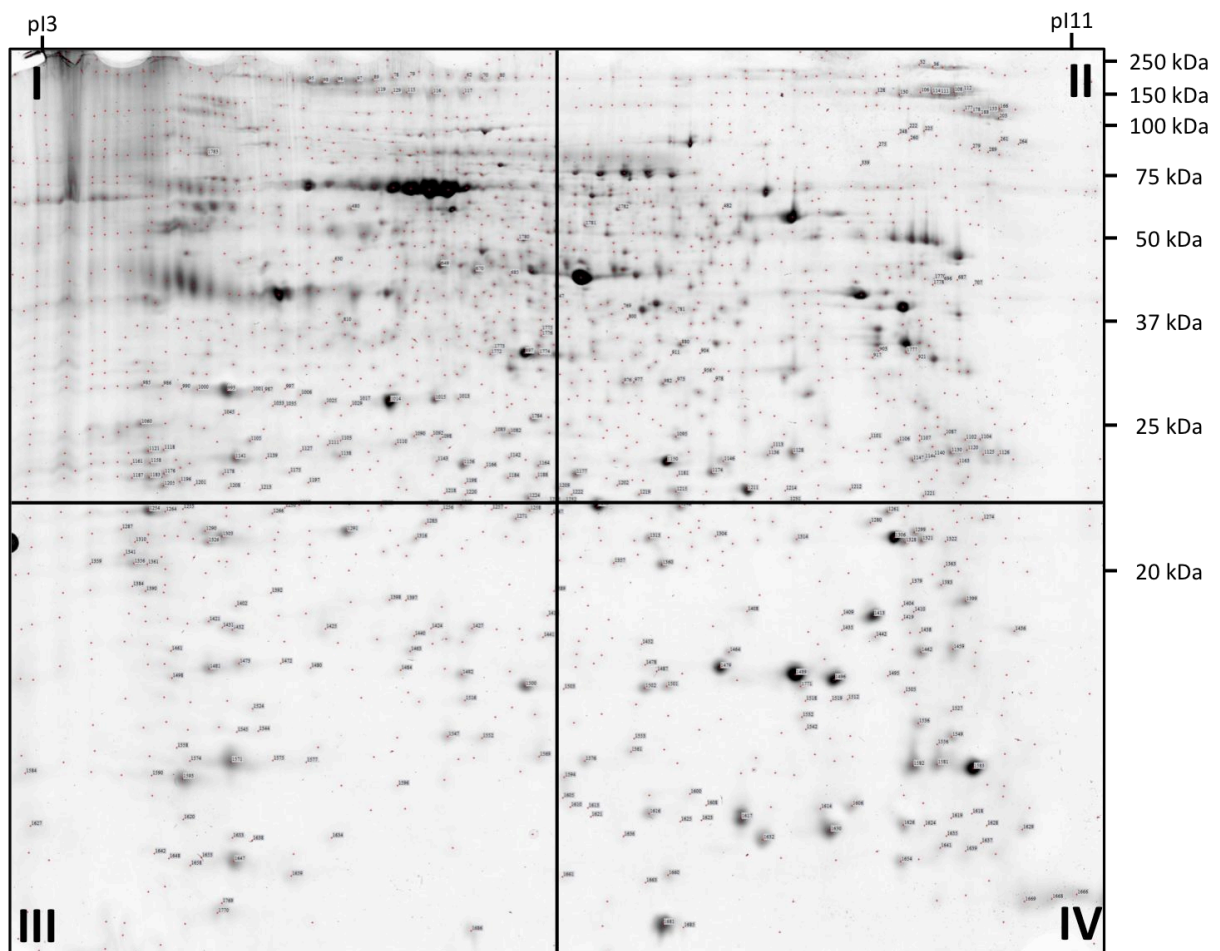


Fig. 10.2: Supernatant analysis DIGE150_12595. Cell culture supernatant proteins of TNF α -overexpressing wild-type (MEF 1#3^{TNF α}) and ADAM17^{ex/ex} (MEF 1#1^{TNF α}) MEF cells were enriched by centrifugal filter units, differentially labelled and separated by 2D-DiGE. Two-dimensional gel was post-stained with FlamingoTM and imaged using the TyphoonTRIO. Numbers indicate protein spots picked for protein identification by MALDI-ToF/ToF. Corresponding data are enclosed on the compact disc (File: A10.2 – DIGE150_12595).

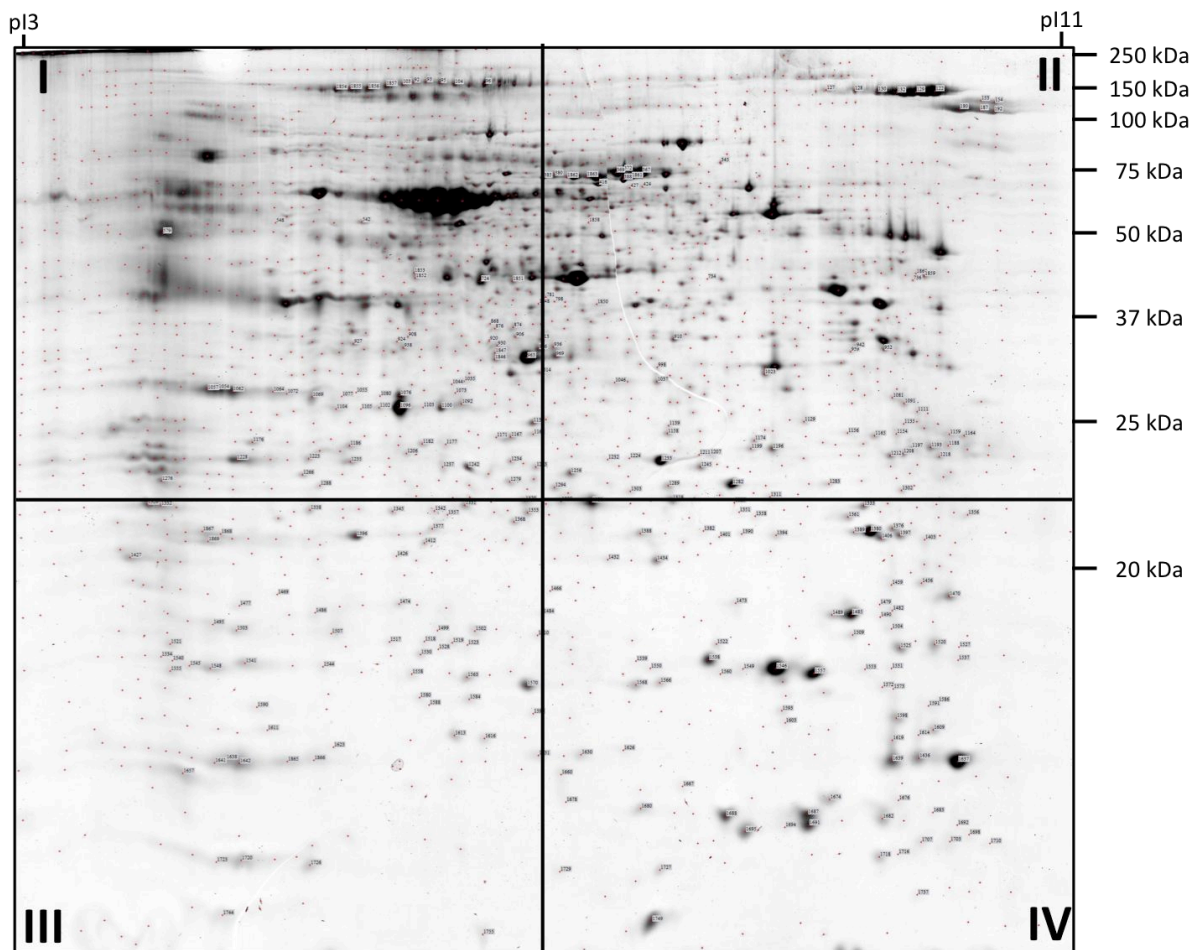
10.2.2 Gel 12722 (DIGE150b)

Fig. 10.3: Supernatant analysis DIGE150_12722. Cell culture supernatant proteins of TNF α -overexpressing wild-type (MEF 1#3^{TNF α}) and ADAM17^{ex/ex} (MEF 1#1^{TNF α}) MEF cells were enriched by centrifugal filter units, differentially labelled and separated by 2D-DiGE. Two-dimensional gel was post-stained with FlamingoTM and imaged using the TyphoonTRIO. Numbers indicate protein spots picked for protein identification by MALDI-ToF/ToF. Corresponding data are enclosed on the compact disc (File: A10.2 – DIGE150_12722).

10.3 DIGE153 – Supernatant analysis

2D-DiGE analysis of wild-type (MEF 1#3) and ADAM17^{ex/ex} (MEF1#1) MEF cell supernatants enriched by WGA-mediated precipitation.

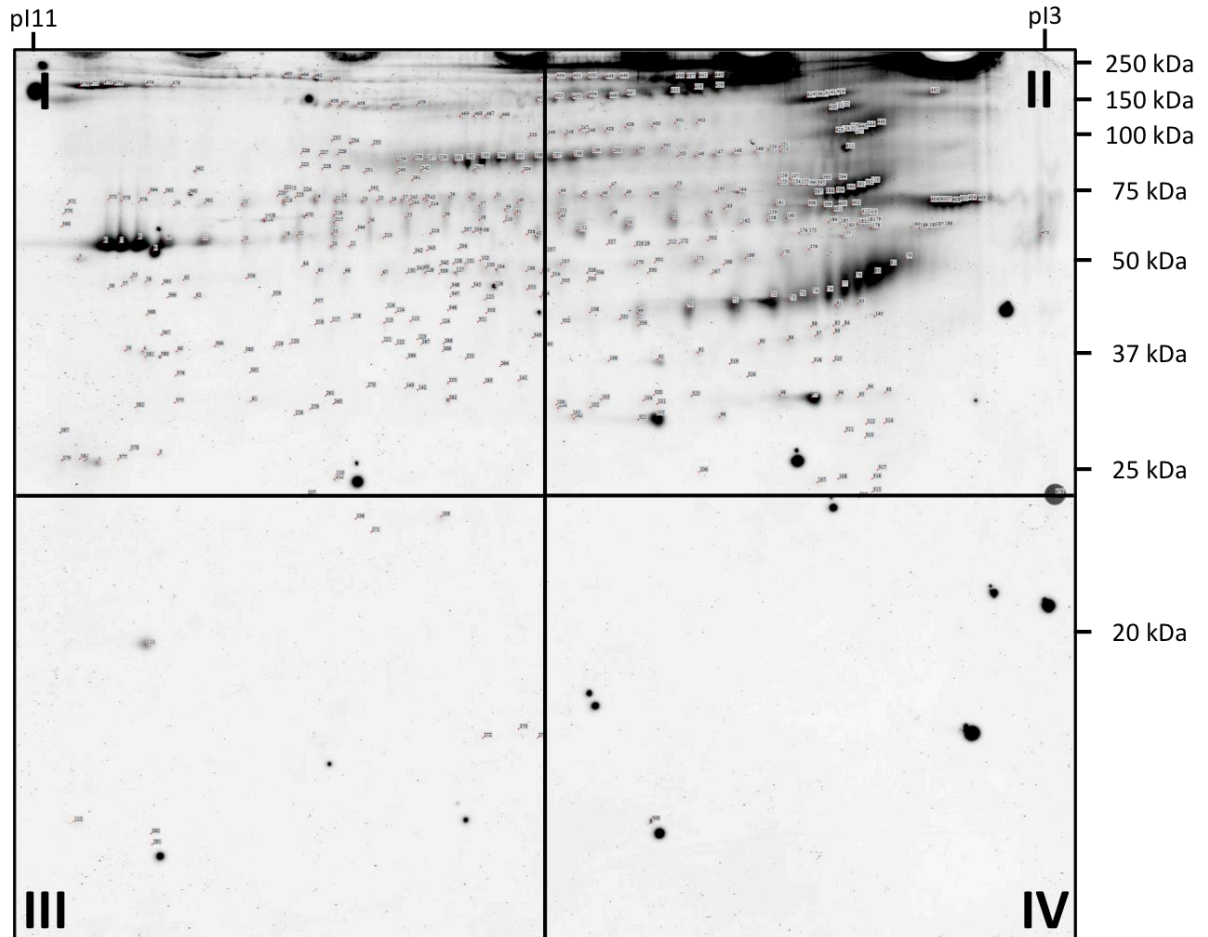


Fig. 10.4: Supernatant analysis DIGE153. Cell culture supernatant proteins of wild-type (MEF 1#3) and ADAM17^{ex/ex} (MEF 1#1) MEF cells were enriched by centrifugal filter units, differentially labelled and separated by 2D-DiGE. Two-dimensional gel was post-stained with FlamingoTM and imaged using the TyphoonTRIO. Numbers indicate protein spots picked for protein identification by MALDI-ToF/ToF. Corresponding data are enclosed on the compact disc (File: A10.3 – DIGE153).

10.4.2 Gel 68573

2D-DiGE analysis of wild-type (MEF 1#7) and ADAM17^{ex/ex} (MEF1#8) MEF cell supernatants enriched by WGA-mediated precipitation.

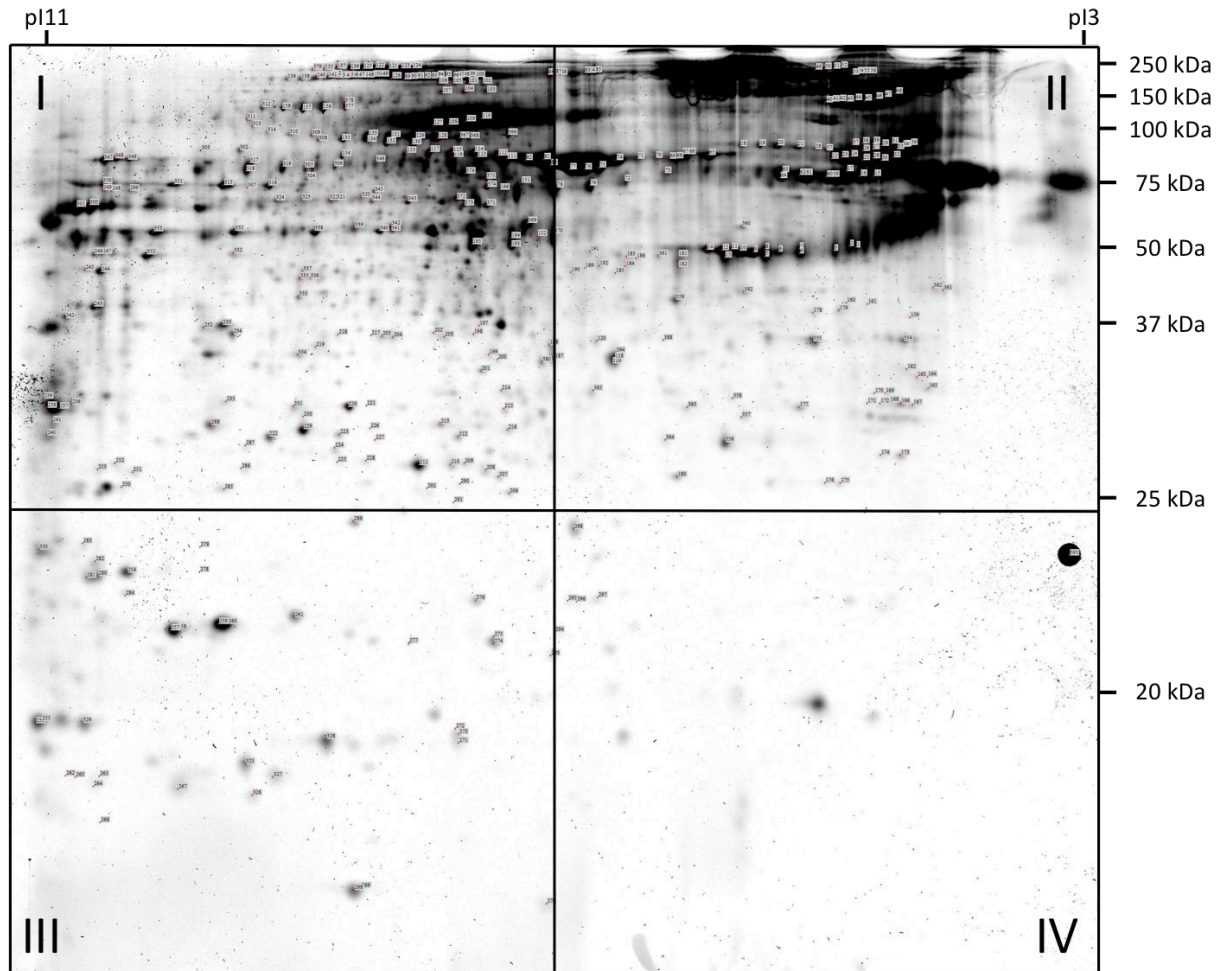


Fig. 10.6: Supernatant analysis DIGE169_68573. Cell culture supernatant proteins of wild-type (MEF 1#7) and ADAM17^{ex/ex} (MEF 1#8) MEF cells were enriched by WGA, differentially labelled and separated by 2D-DiGE. Two-dimensional gel was post-stained with Flamingo™ and imaged using the TyphoonTRIO. Numbers indicate protein spots picked for protein identification by MALDI-ToF/ToF. Corresponding data are enclosed on the compact disc (File: A10.4 – DIGE169_68573).

10.4.3 Gel 68574

2D-DiGE analysis of wild-type (MEF 2#1) and ADAM17^{ex/ex} (MEF2#8) MEF cell supernatants enriched by WGA-mediated precipitation.

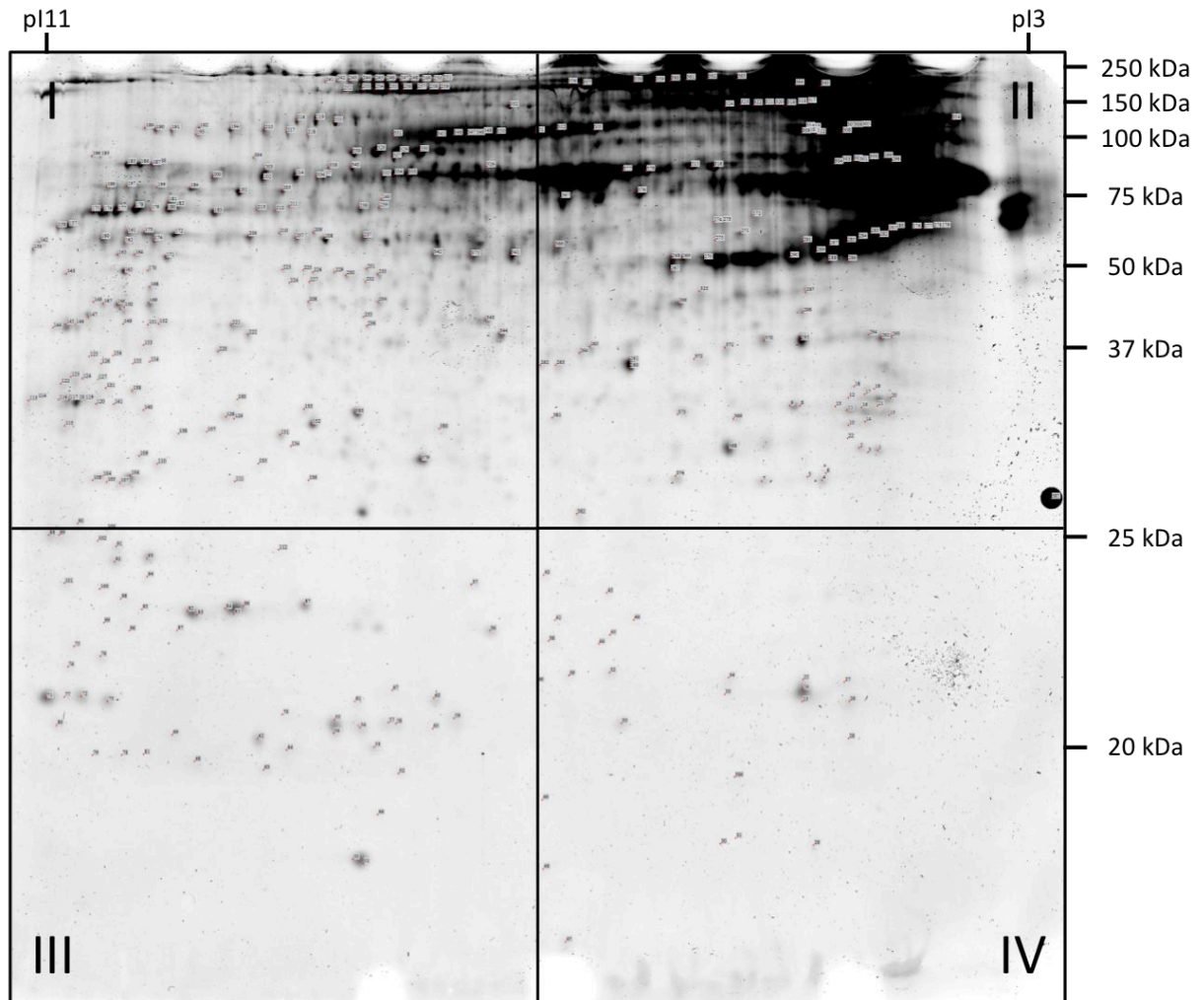


Fig. 10.7: Supernatant analysis DIGE169_68574. Cell culture supernatant proteins of wild-type (MEF 2#1) and ADAM17^{ex/ex} (MEF 2#8) MEF cells were enriched by WGA, differentially labelled and separated by 2D-DiGE. Two-dimensional gel was post-stained with FlamingoTM and imaged using the TyphoonTRIO. Numbers indicate protein spots picked for protein identification by MALDI-ToF/ToF. Corresponding data are enclosed on the compact disc (File: A10.4 – DIGE169_68574).

10.5 DIGE172 – Supernatant analysis

Independent 2D-DiGE analyses of different sets of wild-type and ADAM17^{ex/ex} MEF cell supernatants enriched by WGA-mediated precipitation.

10.5.1 Gel 68917

2D-DiGE analysis of wild-type (MEF 1#3) and ADAM17^{ex/ex} (MEF1#1) MEF cell supernatants enriched by WGA-mediated precipitation.

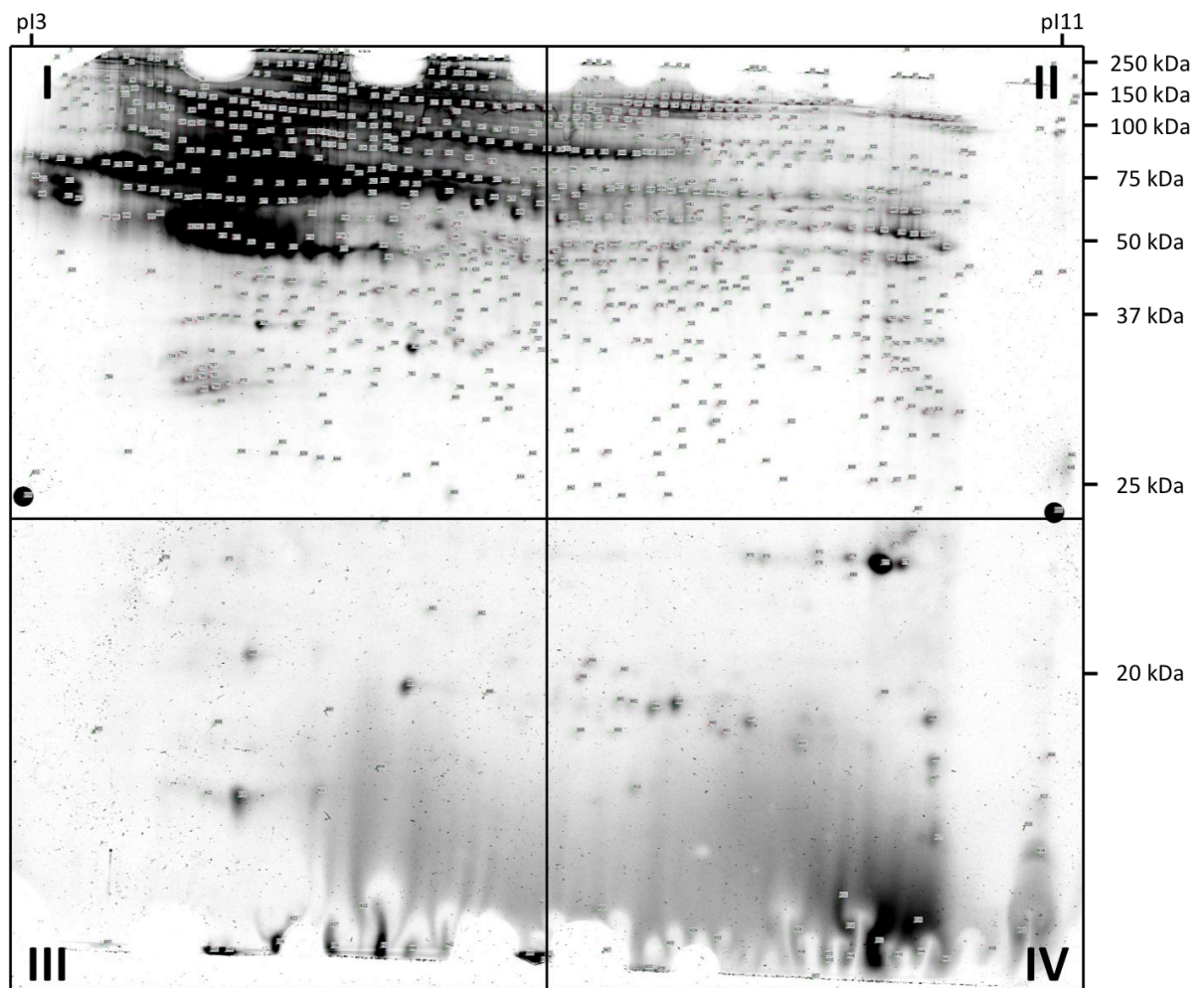


Fig. 10.8: Supernatant analysis DIGE172_68917. Cell culture supernatant proteins of wild-type (MEF 1#3) and ADAM17^{ex/ex} (MEF 1#1) MEF cells were enriched by WGA, differentially labelled and separated by 2D-DiGE. Two-dimensional gel was post-stained with FlamingoTM and imaged using the TyphoonTRIO. Numbers indicate protein spots picked for protein identification by MALDI-ToF/ToF. Corresponding data are enclosed on the compact disc (File: A10.5 – DIGE172_68917).

10.5.2 Gel 68918

2D-DiGE analysis of wild-type (MEF 1#7) and ADAM17^{ex/ex} (MEF1#8) MEF cell supernatants enriched by WGA-mediated precipitation.

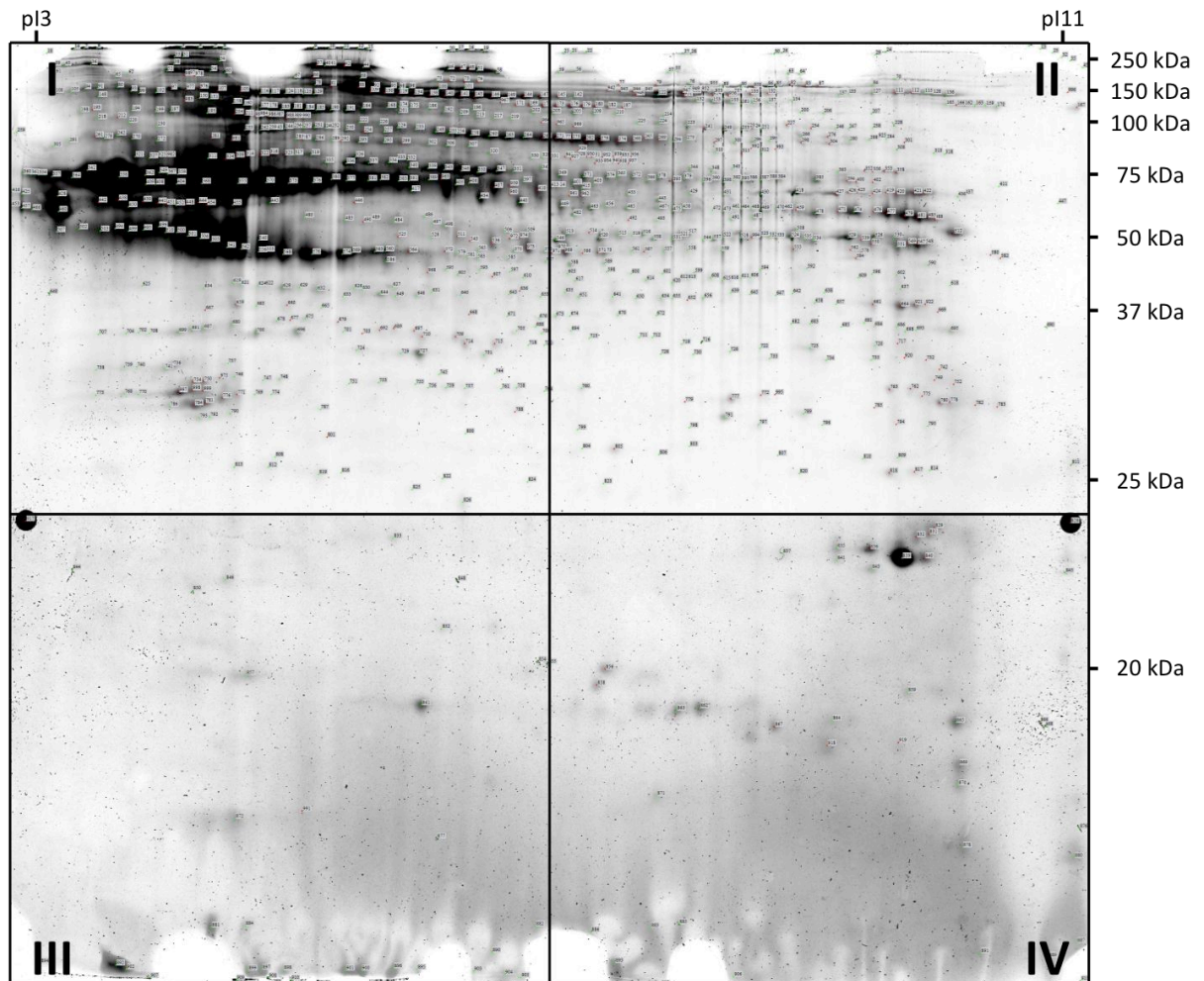


Fig. 10.9: Supernatant analysis DIGE172_68918. Cell culture supernatant proteins of wild-type (MEF 1#7) and ADAM17^{ex/ex} (MEF 1#8) MEF cells were enriched by WGA, differentially labelled and separated by 2D-DiGE. Two-dimensional gel was post-stained with FlamingoTM and imaged using the TyphoonTRIO. Numbers indicate protein spots picked for protein identification by MALDI-ToF/ToF. Corresponding data are enclosed on the compact disc (File: A10.5 – DIGE172_68918).

10.5.3 Gel 68919

2D-DiGE analysis of wild-type (MEF 2#1) and ADAM17^{ex/ex} (MEF2#8) MEF cell supernatants enriched by WGA-mediated precipitation.

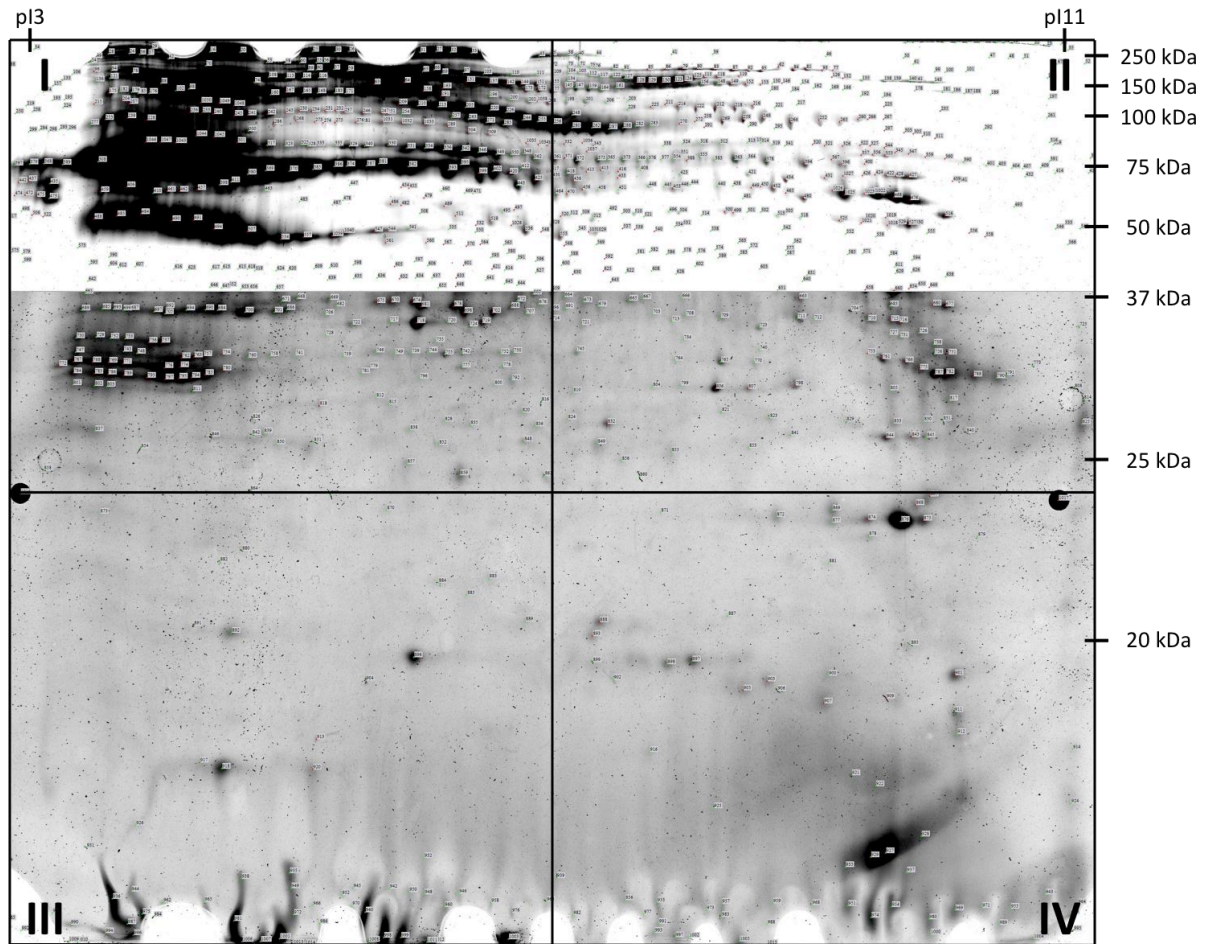


Fig. 10.10: Supernatant analysis DIGE172_68919. Cell culture supernatant proteins of wild-type (MEF 2#1) and ADAM17^{ex/ex} (MEF 2#8) MEF cells were enriched by WGA, differentially labelled and separated by 2D-DiGE. Two-dimensional gel was post-stained with FlamingoTM and imaged using the TyphoonTRIO. Numbers indicate protein spots picked for protein identification by MALDI-ToF/ToF. Corresponding data are enclosed on the compact disc (File: A10.5 – DIGE172_68919).

10.6 DIGE182 – Supernatant analysis

2D-DiGE analysis of deglycosylated wild-type (MEF 1#3) and ADAM17^{ex/ex} (MEF1#1) MEF cell culture supernatant proteins enriched by WGA-mediated precipitation.

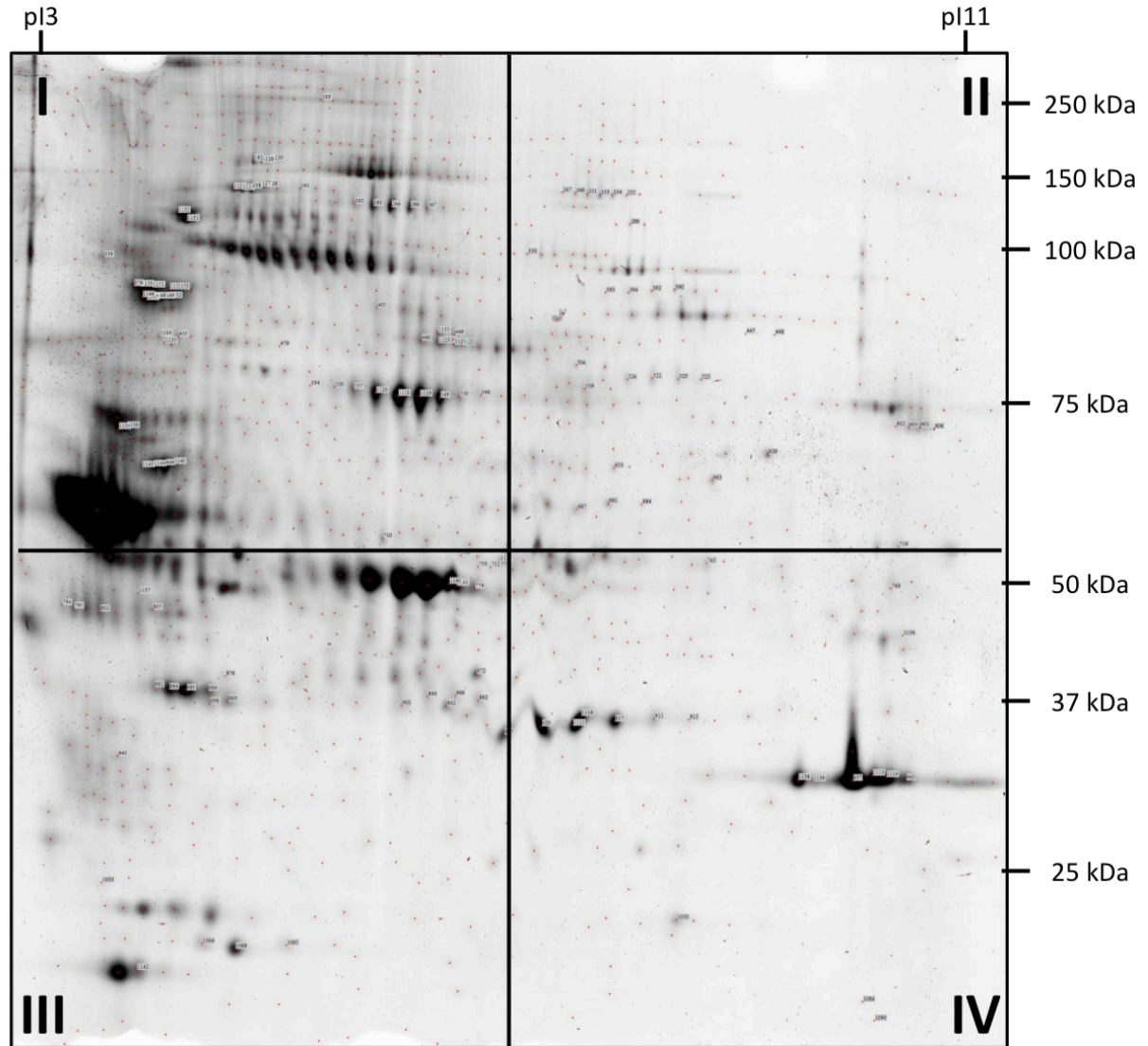


Fig. 10.11: Supernatant analysis DIGE182. Cell culture supernatant proteins of wild-type (MEF 1#3) and ADAM17^{ex/ex} (MEF 1#1) MEF cells were enriched by WGA, deglycosylated, differentially labelled and separated by 2D-DiGE. Two-dimensional gel was post-stained with FlamingoTM and imaged using the TyphoonTRIO. Numbers indicate protein spots picked for protein identification by MALDI-ToF/ToF. Corresponding data are enclosed on the compact disc (File: A10.6 – DIGE182).

10.7 DIGE158 – Analysis of whole-cell lysates

Independent 2D-DiGE analyses of wild-type (MEF 1#3) and ADAM17^{ex/ex} MEF whole-cell lysates.

10.7.1 Gel 76295

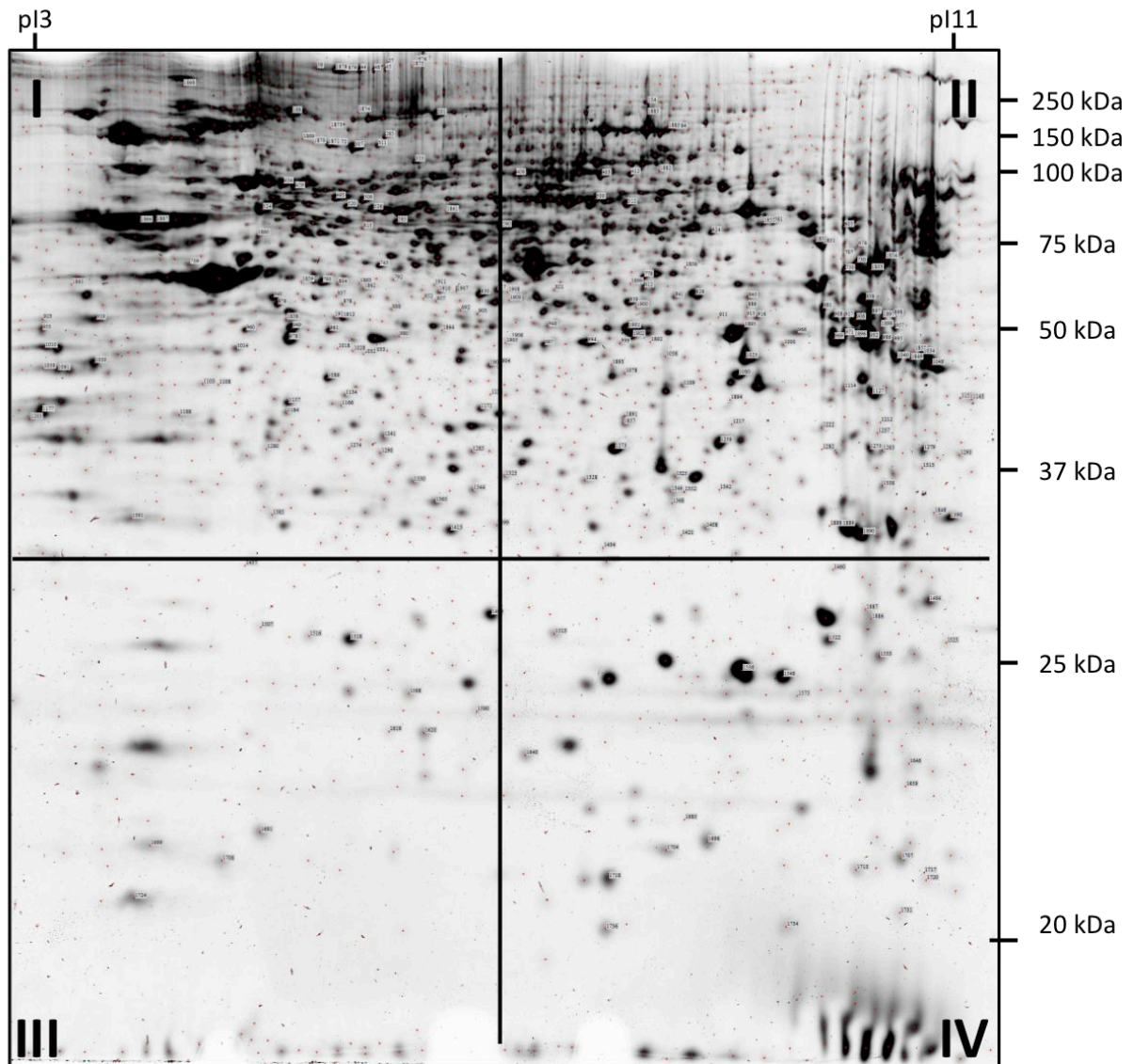


Fig. 10.12: Whole-cell lysate analysis DIGE158_76295. Whole-cell lysates of TPA-treated wild-type (MEF 1#3) and ADAM17^{ex/ex} (MEF 1#1) MEF cells were enriched by WGA, differentially labelled and separated by 2D-DiGE. Two-dimensional gel was post-stained with FlamingoTM and imaged using the TyphoonTRIO. Numbers indicate protein spots picked for protein identification by MALDI-ToF/ToF. Corresponding data are enclosed on the compact disc (File: A10.7 – DIGE158_76295).

10.7.2 Gel 76296

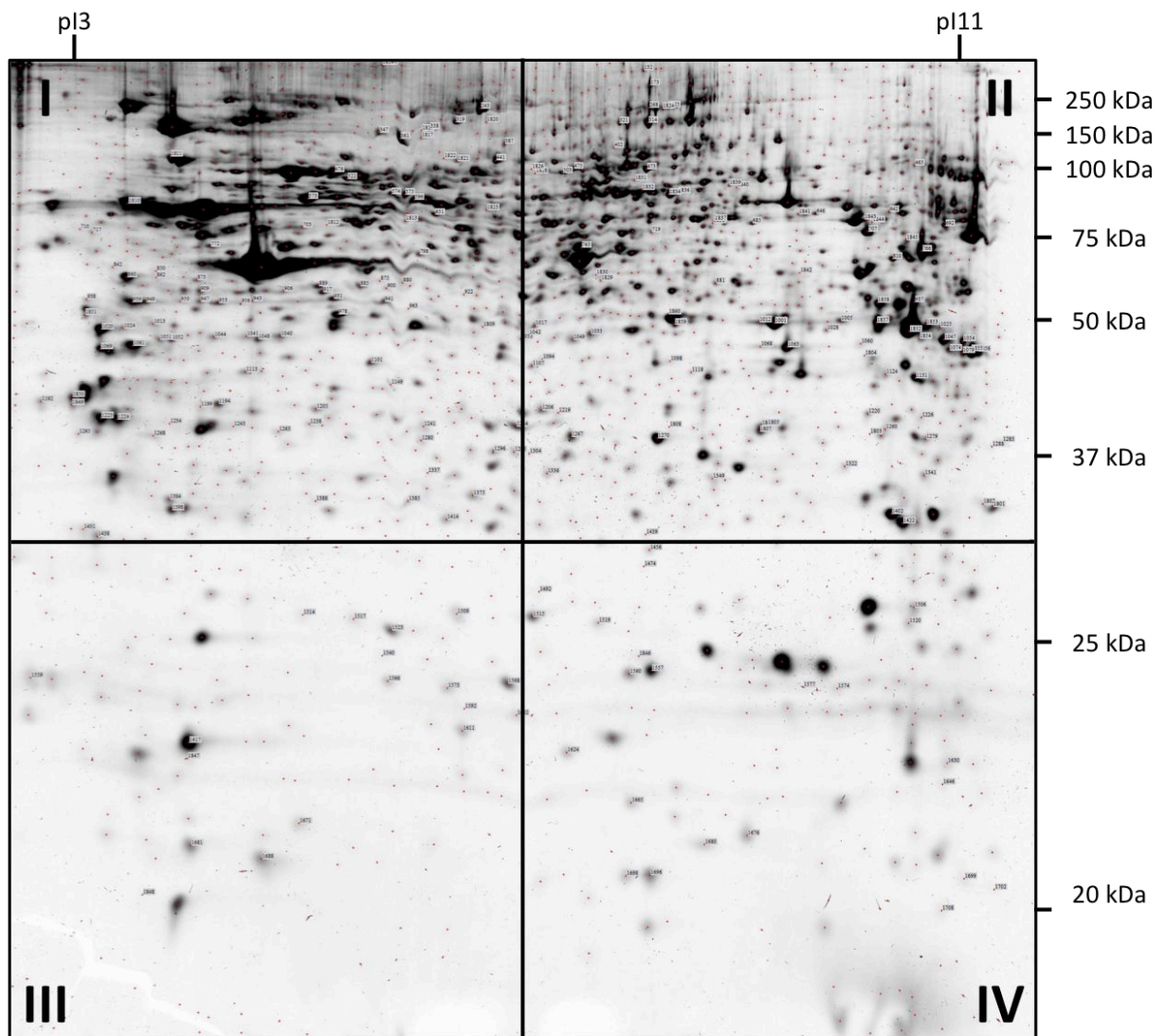


Fig. 10.13: Whole-cell lysate analysis DIGE158_76296. Whole-cell lysates of TPA-treated wild-type (MEF 1#3) and ADAM17^{ex/ex} (MEF 1#1) MEF cells were enriched by WGA, differentially labelled and separated by 2D-DiGE. Two-dimensional gel was post-stained with Flamingo™ and imaged using the TyphoonTRIO. Numbers indicate protein spots picked for protein identification by MALDI-ToF/ToF. Corresponding data are enclosed on the compact disc (File: A10.7 – DIGE158_76296).

10.7.3 Gel 76297

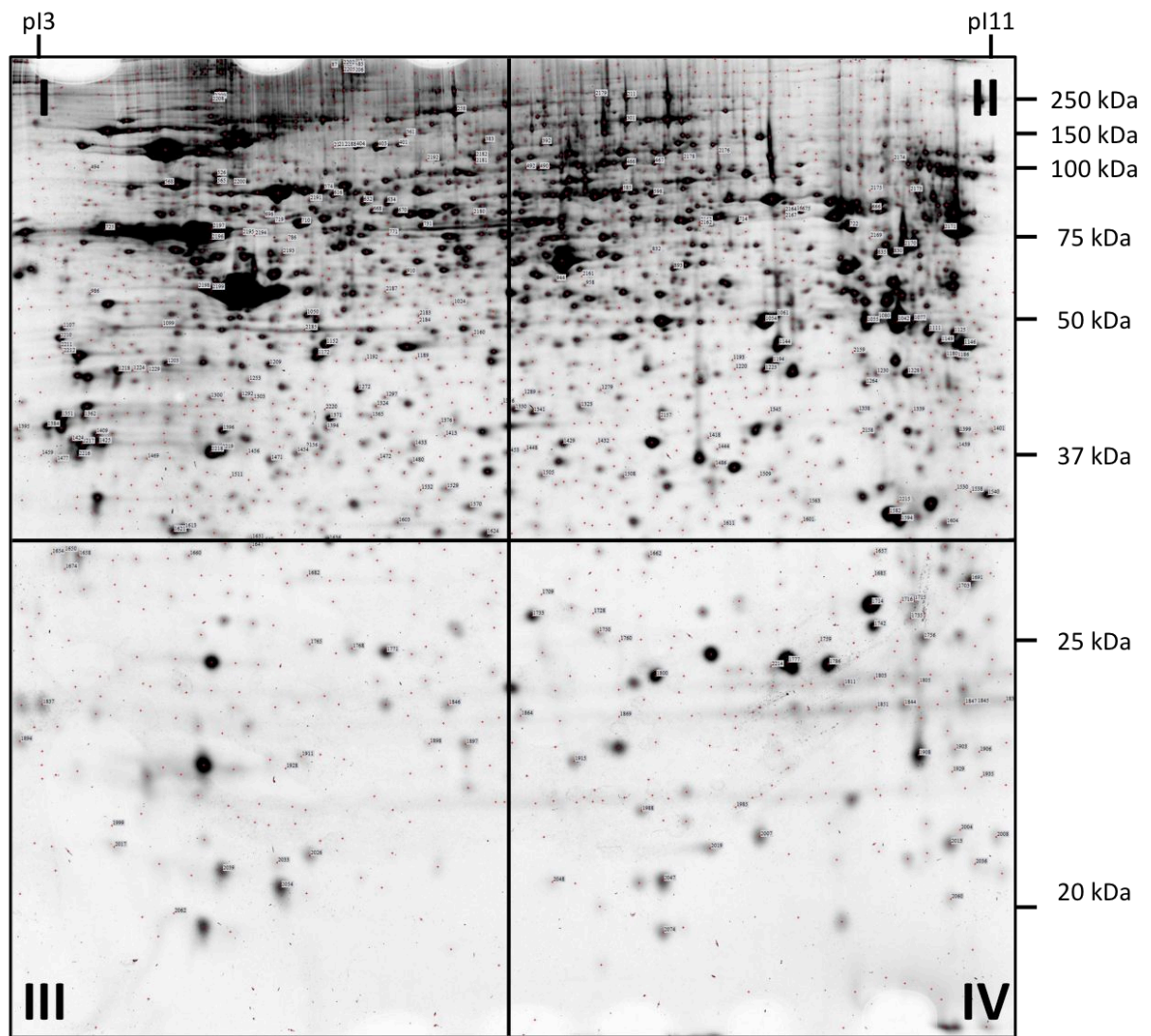


Fig. 10.14: Whole-cell lysate analysis DIGE158_76297. Whole-cell lysates of TPA-treated wild-type (MEF 1#3) and ADAM17^{ex/ex} (MEF 1#1) MEF cells were enriched by WGA, differentially labelled and separated by 2D-DiGE. Two-dimensional gel was post-stained with FlamingoTM and imaged using the TyphoonTRIO. Numbers indicate protein spots picked for protein identification by MALDI-ToF/ToF. Corresponding data are enclosed on the compact disc (File: A10.7 – DIGE158_76297).

10.8 DIGE160 – Analysis of whole-cell lysates

Independent 2D-DiGE analyses of wild-type (MEF 1#3) and ADAM17^{ex/ex} MEF whole-cell lysates.

10.8.1 Gel 76300

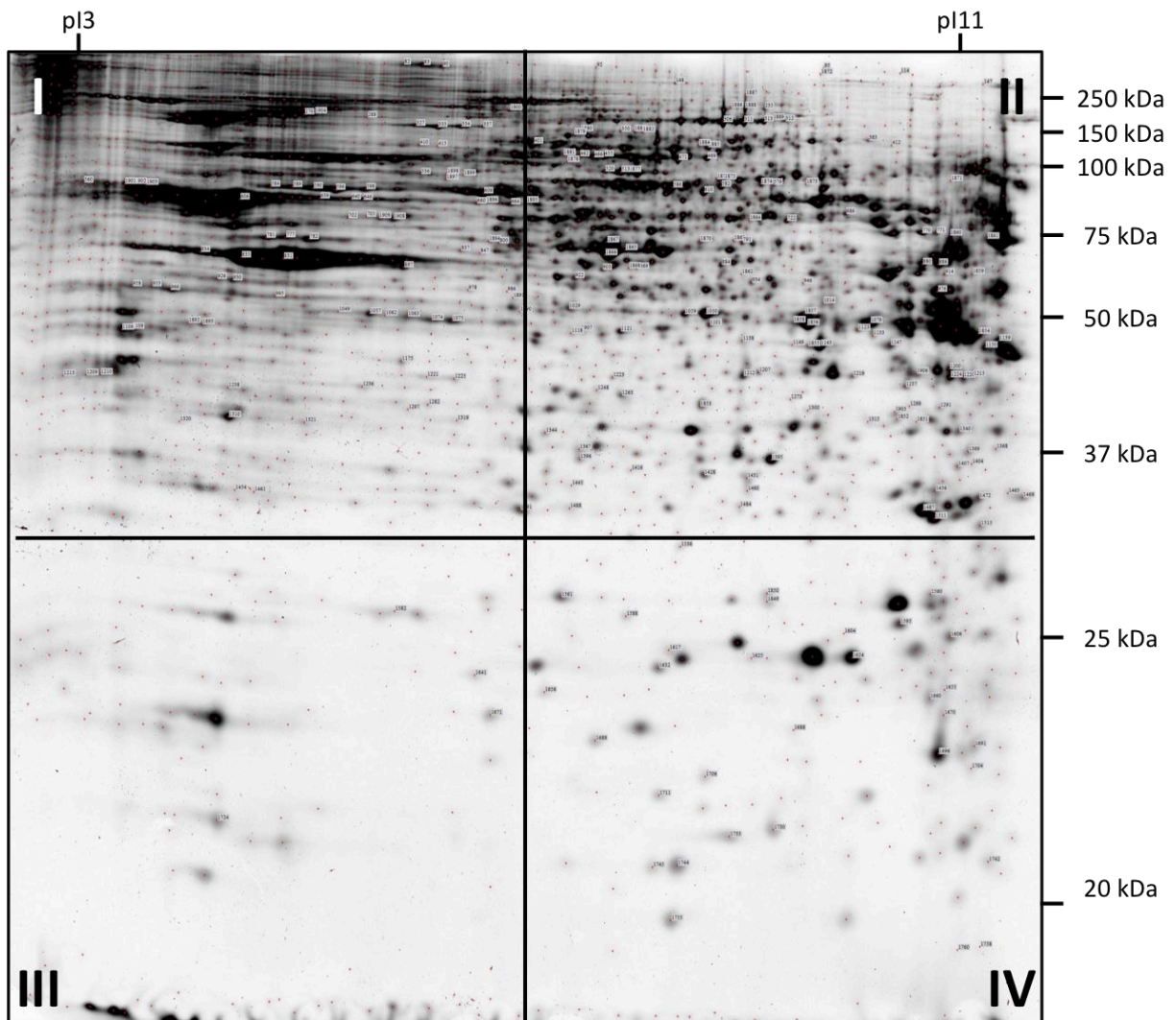


Fig. 10.15: Whole-cell lysate analysis DIGE160_76300. Whole-cell lysates of TPA-treated wild-type (MEF 1#3) and ADAM17^{ex/ex} (MEF 1#1) MEF cells were enriched by WGA, differentially labelled and separated by 2D-DiGE. Two-dimensional gel was post-stained with FlamingoTM and imaged using the TyphoonTRIO. Numbers indicate protein spots picked for protein identification by MALDI-ToF/ToF. Corresponding data are enclosed on the compact disc (File: A10.8 – DIGE160_76300).

10.8.2 Gel 76301

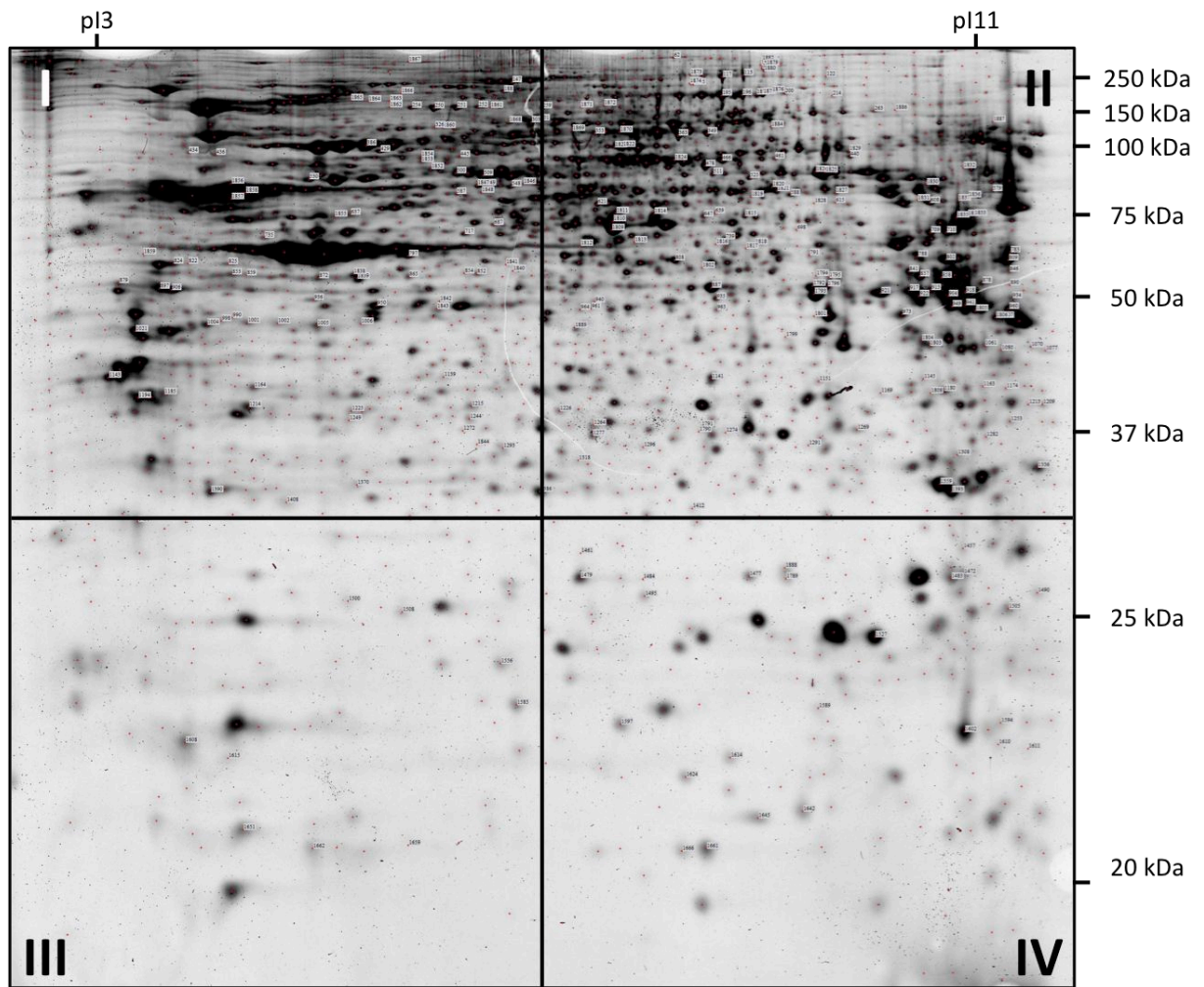


Fig. 10.16: Whole-cell lysate analysis DIGE160_76301. Whole-cell lysates of TPA-treated wild-type (MEF 1#3) and ADAM17^{ex/ex} (MEF 1#1) MEF cells were enriched by WGA, differentially labelled and separated by 2D-DiGE. Two-dimensional gel was post-stained with FlamingoTM and imaged using the TyphoonTRIO. Numbers indicate protein spots picked for protein identification by MALDI-ToF/ToF. Corresponding data are enclosed on the compact disc (File: A10.8 – DIGE160_76301).

10.9 DIGE184 – Analysis of ECM from cultured MEF cells

2D-DiGE analysis of extracellular matrix proteins derived from cultured wild-type (MEF 1#3) and ADAM17^{ex/ex} MEF cells by decellularization.

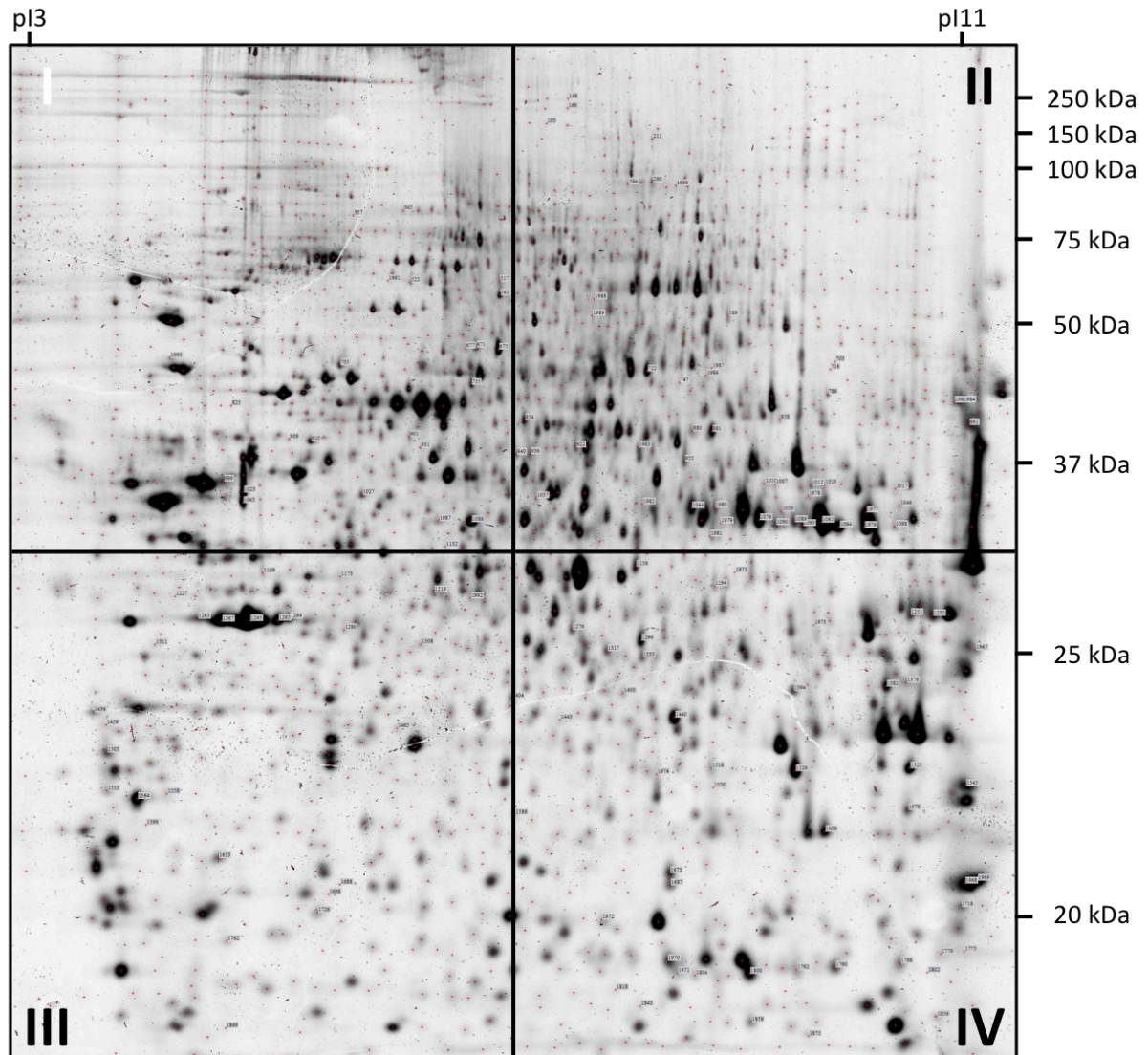


Fig. 10.17: Cellular ECM analysis DIGE184. Extracellular matrix of TPA-treated wild-type (MEF 1#3) and ADAM17^{ex/ex} (MEF 1#1) MEF cells was enriched by decellularization. Samples were differentially labelled and separated by 2D-DiGE. Two-dimensional gel was post-stained with FlamingoTM and imaged using the TyphoonTRIO. Numbers indicate protein spots picked for protein identification by MALDI-ToF/ToF. Corresponding data are enclosed on the compact disc (File: A10.9 – DIGE184).

10.10 CTAB-DIGE: Two-Phase system

2D-CTAB/SDS-DiGE analysis of plasma membrane proteins from wild-type (MEF 1#3) and ADAM17^{ex/ex} (MEF 1#1) MEF cells enriched using a commercially available two-phase system.

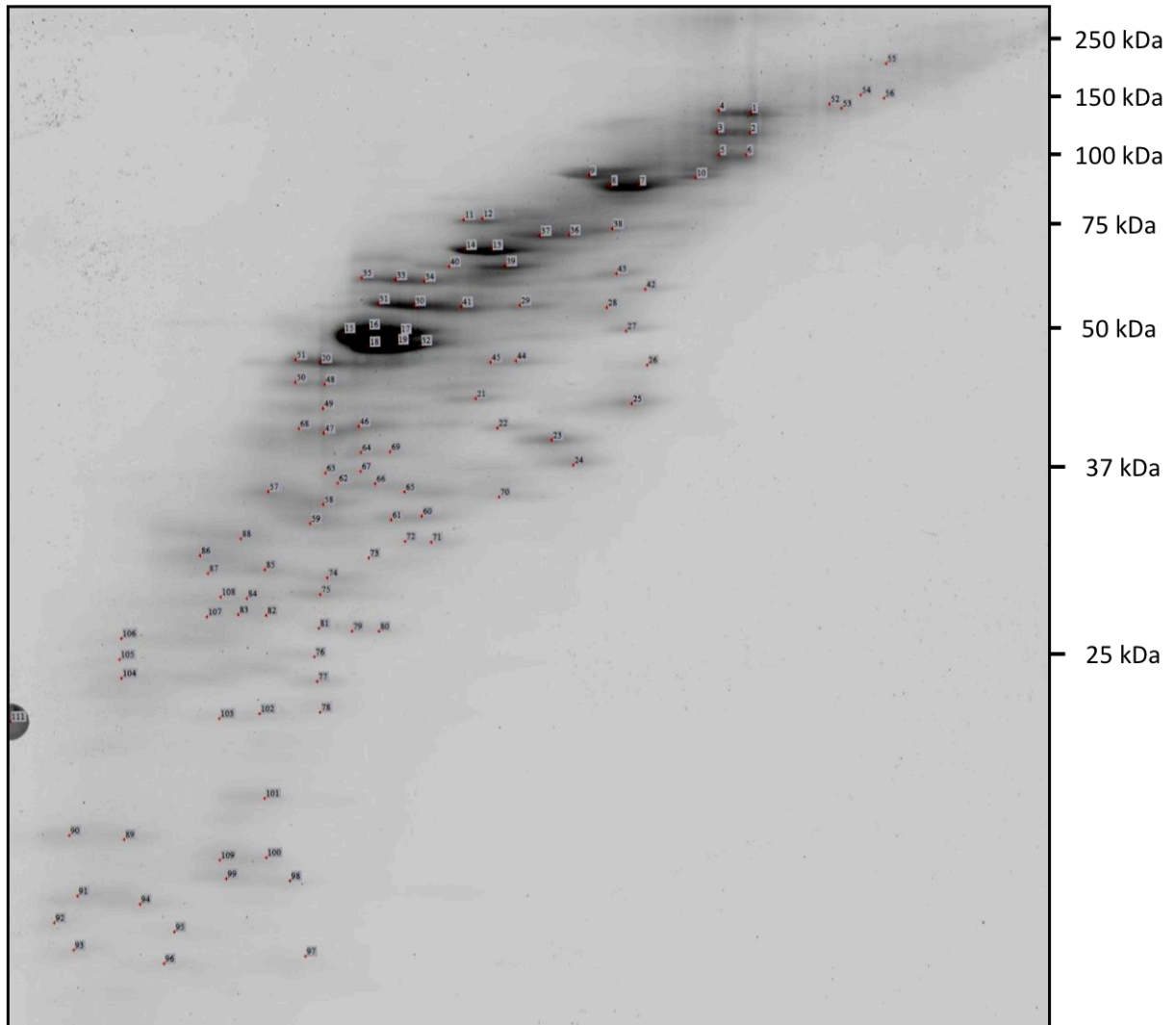


Fig. 10.18: CTAB-DIGE analysis of MEF membrane fractions enriched using a two-phase system. Putative membrane proteins of TPA-treated wild-type (MEF 1#3) and ADAM17^{ex/ex} (MEF 1#1) MEF cells were differentially labelled and separated by 2D-CTAB/SDS-DiGE. Two-dimensional gel was post-stained with FlamingoTM and imaged using the TyphoonTRIO. Numbers indicate protein spots picked for protein identification by MALDI-ToF/ToF. Corresponding data are enclosed on the compact disc (File: A10.10 – CTAB-DIGE-1).

10.11 CTAB-DIGE: Giant Plasma Membrane Vesicles

2D-CTAB/SDS-DiGE analysis of wild-type (MEF 1#3) and ADAM17^{ex/ex} (MEF 1#1) MEF cell-derived giant plasma membrane vesicles.

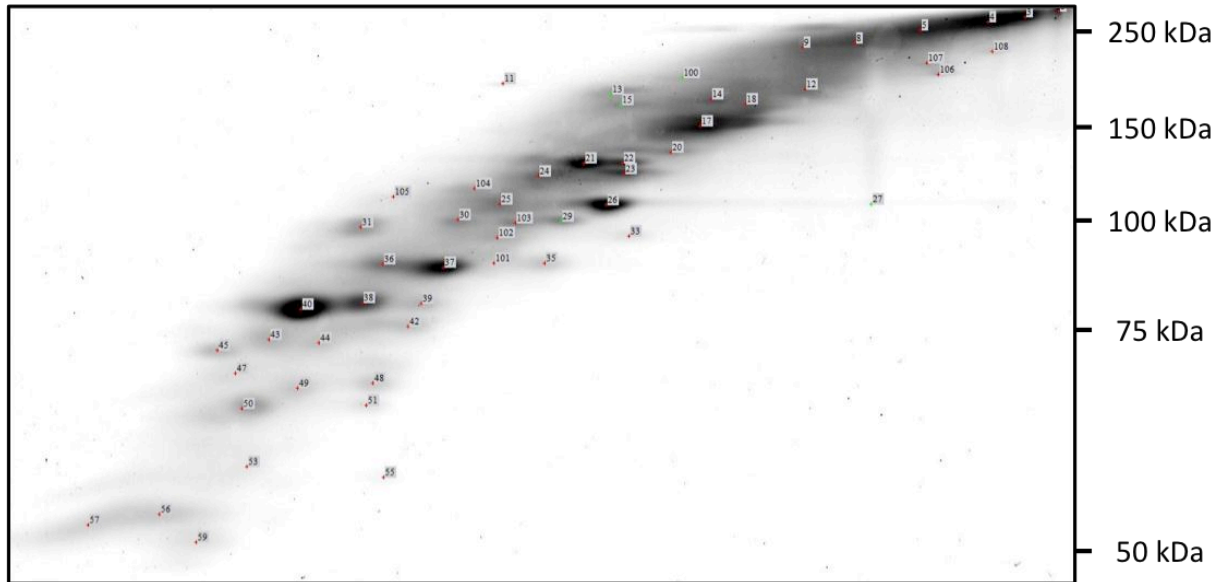


Fig. 10.19: CTAB-DIGE analysis of Giant Plasma Membrane Vesicles (GPMVs). GPMV-derived proteins of TPA-treated wild-type (MEF 1#3) and ADAM17^{ex/ex} (MEF 1#1) MEF cells were differentially labelled and separated by 2D-CTAB/SDS-DiGE. Two-dimensional gel was post-stained with FlamingoTM and imaged using the TyphoonTRIO. Numbers indicate protein spots picked for protein identification by MALDI-ToF/ToF. Corresponding data are enclosed on the compact disc (File: A10.11 – CTAB-DIGE-2).

10.12 CTAB-DIGE: Two-Phase system and Concanavalin A

2D-CTAB/SDS-DiGE analysis of wild-type (MEF 1#3) and ADAM17^{ex/ex} MEF cell membrane proteins enriched by combination of a commercial two-phase system and ConA-mediated precipitation.

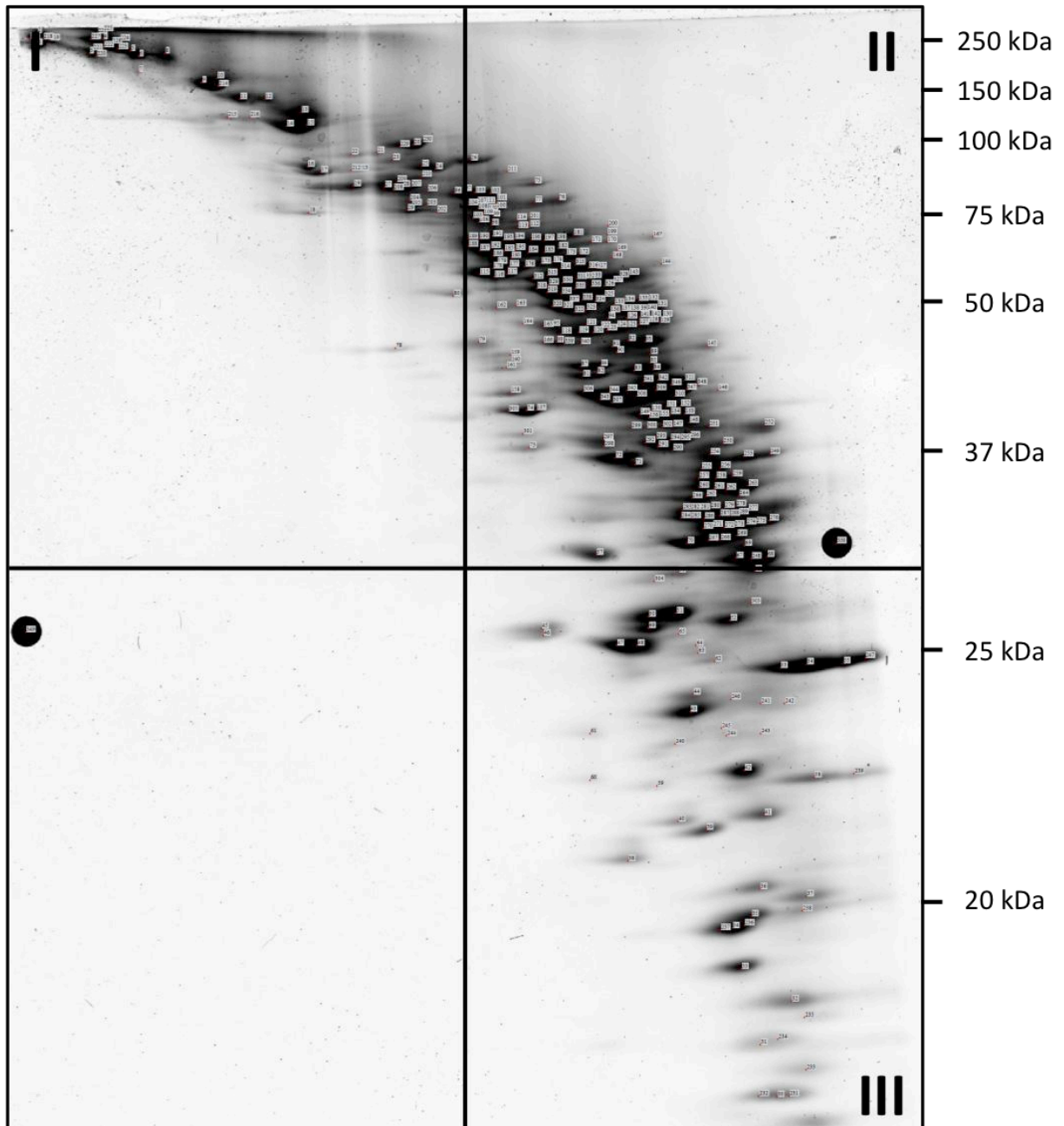


Fig. 10.20: CTAB-DIGE analysis of MEF membrane fractions enriched using a two-phase system and Concanavalin A. Putative membrane proteins of TPA-treated wild-type (MEF 1#3) and ADAM17^{ex/ex} (MEF 1#1) MEF cells were differentially labelled and separated by 2D-CTAB/SDS-DiGE. Two-dimensional gel was post-stained with FlamingoTM and imaged using the TyphoonTRIO. Numbers indicate protein spots picked for protein identification by MALDI-ToF/ToF. Corresponding data are enclosed on the compact disc (File: A10.12 – CTAB-DIGE-3).

11 Acknowledgement

This presented work has been conducted between September 2010 and June 2014 as part of the Collaborative Research Center 877 (SFB877) “Proteolysis as a Regulatory Event in Pathophysiology” in the group of Prof. Dr. Ottmar Janßen.

In particular, I would like to express gratitude to my supervisor Prof. Dr. Ottmar Janßen who gave me the chance to join his group and the proteomics platform of the SFB877. I am grateful for the experiences in this lab especially regarding the independent work on the adaption of new approaches that might help to elucidate the role of ADAM17 and for motivating words.

For representing this work in front of the faculty for mathematics and natural sciences, I would like to thank Prof. Dr. Dr. Thomas Bosch. In addition, I would like to express my gratitude for his support during my studies.

In place of all members of the Institute for Immunology, I would also want to thank Prof. Dr. Dietrich Kabelitz for the possibility to join the Institute for Immunology with its warm and social community that I will miss and that is not usual in other institutes.

Special thanks go to Melanie Nebendahl for excellent technical assistance in the lab and beyond during this project. In addition I want to thank Henriette Ebsen, Dr. Jürgen Fritsch and Dr. Markus Lettau for scientific discussions and support. Jaydeep Bhat I want to thank for interesting ideas and discussions and for becoming a good friend. Notably, I especially have to thank Melanie Nebendahl and Signe Valentin as they were able to cure my frustration at so many occasions.

For providing wild-type and ADAM17^{ex/ex} MEF cells, anti-ADAM17 antibodies ELISA kits and ADAM17^{ex/ex} mice and for being a post-doc for me during the initial stages of this project, I have to thank Dr. Athena Chalaris. For answering my questions and needs regarding collagens and anti-collagen antibodies I hereby thank Prof. Dr. Christoph Becker-Pauly.

For numerous protein identifications by mass spectrometry and discussions I would like to thank Prof. Dr. Andreas Tholey and especially his post-docs Tomas Koudelka and Bart van den Berg.

Finally, I want to thank my family who always supported me during my studies and my life. Thus, I would like to use this acknowledgement to especially thank my grandparents and my grand-grand mother, whom I owe so much as they made me the person I am today. Moreover, I would never have overcome the bad times of this project without escaping to the beautiful places of this world. Thus, I thank my love May for joining me in my life and on these amazing journeys.

12 Curriculum Vitae

PERSONAL DATA

Name: Benjamin John Schönbeck
 Address: Wrangelstr. 60
 24105 Kiel
 Phone: +49-176-82155936
 Day of birth: June 15th, 1984
 Place of birth: Preetz
 Martial status: single
 Nationality: german

SCIENTIFIC EMPLOYMENT

03/2011 – 09/2014 **Research Associate** (PhD student)
 University Hospital Schleswig-Holstein, Campus Kiel
 Institute for Immunology (Prof. Dr. Janssen)
 “Proteome analyses for the characterization of the ADAM17^{ex/ex}
 hypomorphic mouse model “

EDUCATION

since 09/2012 **Bachelor studies** of Business Administration (ONLINE)
 University of Applied Sciences Kiel

10/2008 – 07/2010 **Master of Science in Biology at the University of Kiel**
 major subjects: Cell and Developmental Biology
 Microbiology and Genetics
 minor subjects: Immunology
 Molecular Virology
 Master’s thesis:
 “Molecular characterization of the defensome in *Hydra*“

10/2005 – 09/2008 **Bachelor of Science in Biology at the University of Kiel**
 major subjects: Cell and Developmental Biology
 Microbiology and Genetics
 minor subjects: Immunology
 Molecular Virology
 Bachelor’s thesis:
 „Molekularbiologische Untersuchungen an *C. intestinalis*“

SECONDARY EDUCATION

- 08/1997 – 05/2004 **Abitur at the Gymnasium Wellingdorf (Kiel, Germany)**
focus subjects: Biology and Mathematics
additional subject: Research project at GEOMAR Kiel
- 08/1995 – 07/1997 Thor-Heyerdahl Gymnasiums (Kiel, Germany)

AWARDS

- 11/2011 **GBM Innovation Award**
Membrane Proteomics by protein enrichment from Giant Plasma Membrane Vesicles (GPMVs) and subsequent analysis by 2D-CTAB/SDS-DiGE.

13 List of Publication

13.1 Affiliated Works

Onkes W, Frederik R, Micci F, **Schönbeck BJ**, Martin-Subero JI, Ullmann R, Hilpert F, Bräutigam K, Janssen O, Maass N, Siebert R, Heim S, Arnold N and Weimer J (2013) Breakpoint characterization of the der(19)t(11;19)(q13;p13) in the ovarian cancer cell line SKOV-3. *Genes Chromosomes Cancer*; 52(5): 512-522

13.2 Meeting contributions

Schönbeck BJ, Augustin R, Bosch TCG (2010) Molecular Characterization of the defensome of *Hydra*. 14th STS Meeting in Weimar, GER.

Schönbeck BJ, Chalaris A, van den Berg B, Nebendahl M, Tholey A, Janssen O (2011) Proteomic Analysis of the sheddomes of the metalloproteases ADAM 10 and 17 in mice and man. 15th STS Meeting in Weimar, GER.

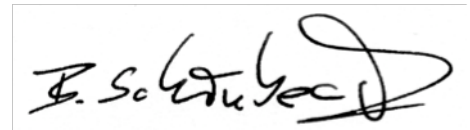
Schönbeck BJ, Chalaris A, Oberdoerster H, Koudelka T, Nebendahl M, Tholey A, Janssen O (2012) Characterization of substrates and regulatory proteins of the A Disintegrin And Metalloprotease 17 (ADAM17). 16th STS Meeting in Weimar, GER.

Schönbeck BJ, Chalaris A, Koudelka T, Nebendahl M, Tholey A, Janssen O (2013) A Disintegrin And Metalloprotease 17 – Putative Substrates, regulated and regulatory proteins within the protease web. 17th STS Meeting in Weimar, GER.

14 Eidesstattliche Erklärung

Hiermit erkläre ich, Benjamin John Schönbeck, an Eides statt, dass ich die vorliegende Arbeit mit dem Titel „*Proteome analyses for the characterization of the ADAM17^{ex/ex} hypomorphic mouse model*“ selbstständig und nur unter zu Hilfenahme der angegebenen Hilfsmittel und Quellen unter Anleitung meiner akademischen Mentoren angefertigt habe. Die Arbeit erfolgte unter Einhaltung der Regeln guter wissenschaftlicher Praxis der Deutschen Forschungsgemeinschaft (DFG). Ich versichere ferner, dass diese Dissertation bisher an keiner anderen Universität oder Fakultät vorgelegt wurde. Des Weiteren erkläre ich, kein anderes Promotionsverfahren ohne Erfolg beendet zu haben und dass keine Aberkennung eines bereits erworbenen Doktorgrades vorliegt.

Kiel, den 26. August 2014



Benjamin John Schönbeck